AMERICAN UNIVERSITY OF BEIRUT

ANTI-INFLAMMATORY APPROACHES TO MITIGATE ENDOTHELIAL DYSFUNCTION IN EARLY METABOLIC IMPAIRMENT

by
RANA ALI ALAAEDDINE

A thesis
submitted in partial fulfillment of the requirements
for the degree of Doctor of Philosophy
to the Department of Pharmacology and Toxicology
of the Faculty of Medicine
at the American University of Beirut

Beirut, Lebanon
August 2021

AMERICAN UNIVERSITY OF BEIRUT

ANTI-INFLAMMATORY APPROACHES TO MITIGATE ENDOTHELIAL DYSFUNCTION IN EARLY METABOLIC IMPAIRMENT

by
RANA ALI ALAAEDDINE

Approved by:

A. Elyazbi

Dr. Ahmed El-Yazbi, Assistant Professor — Advisor
Department of Pharmacology and Toxicology

Ahmed S.F. Belal

Dr. Ahmed Belal, Associate Professor — Co-Advisor
Department of Pharmaceutical Chemistry, Faculty of Pharmacy, Alexandria University

Nadine Darwiche

Dr. Nadine Darwiche, Professor — Chair of Committee
Department of Biochemistry and Molecular Genetics

Dr. Marwan El-Sabban, Professor — Member of Committee
Department of Anatomy, Cell Biology and Physiological Sciences

Dr. Wassim Abou kheir, Associate Professor — Member of Committee
Department of Anatomy, Cell Biology and Physiological Sciences

Dr. Ali Eid, Associate Professor — Member of Committee
Department of Basic Medical Sciences, College of Medicine, Qatar University

F. Plane

Dr. Frances Plane, Associate Professor — Member of Committee
Department of Pharmacology, Faculty of Medicine and Dentistry, University of Alberta

27 Jan 2022

Dr. Richard Schulz, Professor — Member of Committee
Department of Pharmacology, Faculty of Medicine and Dentistry, University of Alberta

Date of dissertation defense: August 23, 2021

AMERICAN UNIVERSITY OF BEIRUT

THESIS RELEASE FORM

Student Name: ____Alaaeddine_____________Rana_________________Ali______________

Last First Middle

I authorize the American University of Beirut, to: (a) reproduce hard or electronic copies of my thesis; (b) include such copies in the archives and digital repositories of the University; and (c) make freely available such copies to third parties for research or educational purposes:

☐ As of the date of submission

☐ One year from the date of submission of my thesis.

☐ Two years from the date of submission of my thesis.

☒ Three years from the date of submission of my thesis.

Rana Alaeddine 07/02/2022

Signature Date

ACKNOWLEDGEMENTS

It is a pleasure to thank those who made this work possible.

Foremost, I owe my deepest gratitude to my advisor, Dr. Ahmed El-Yazbi. His knowledge, experience and patience have guided me during my PhD journey and daily life. My sincere gratitude also goes to my co-advisor, Dr. Ahmed Bilal, for his advice and support.

My special thanks also go to the members of my thesis committee; Dr. Nadine Darwiche, as the chairperson of my committee and the PhD program coordinator, for her huge support. I would also like to thank Dr. Frances Plane and Dr. Richard Schulz for their valuable comments and suggestions. My gratitude is extended to Dr. Marwan Sabban for his precious contribution in our projects. I would also like to thank Dr. Wassim Abou kheir, whom I had the chance to work closely with, for his time and dedication. I was also delighted to have Dr. Ali Eid as a member of my PhD committee. I am sincerely grateful not only for his valuable contribution, but also for his guidance throughout my PhD journey. My gratitude is also extended to the Pharmacology and Toxicology department.

I was extremely fortunate to be part of Dr. El-Yazbi's lab team. I would like to thank Mrs. Nahed Mougharbel, the lab manager, for always being ready to help. I would also like to thank Dr. Ibrahim AlZaim, for his helpfulness and support on every level. Special thanks go to my colleague, Dr. Haneen Dwaib, for being there in every step. Many thanks go to each member of Dr. El-Yazbi team for making the lab feel like home.

Finally, my family deserves the deepest gratitude for their unconditional love and continuous support. I owe them every milestone in my life, this also being one.

ABSTRACT
OF THE DISSERTATION OF

Rana Ali Alaaeddine for Doctor of Philosophy
Major: Biomedical Sciences

Title: Anti-inflammatory approaches to mitigate endothelial dysfunction in early metabolic impairment

Endothelial dysfunction is a hallmark of diabetic vasculopathies. Although hyperglycemia is believed to be the culprit causing endothelial damage, the mechanism underlying early endothelial insult in prediabetes remains obscure. The majority of studies attributed early endothelial damage to an impairment in nitric oxide (NO)-mediated vasodilation in isolation of other endothelial mechanisms. Nevertheless, the low-grade inflammation process and the associated imbalances in lipid assimilation implicated in the pathogenesis of metabolic disease are known to affect the molecular effectors of endothelium-dependent hyperpolarization (EDH). Indeed, such an early deterioration in the interplay between EDH and NO pathways, culminating in endothelial dysfunction, might be triggered by a lipid mediator. Yet, whether the contribution of EDH-type relaxation to the integrative endothelial response is altered in the prediabetic stage remains unclear. To address this issue, we used a non-obese high-calorie-fed rat model with hyperinsulinemia, hyperlipidemia, and delayed development of hyperglycemia. Compared with aortic rings from control rats, HC-fed rat rings displayed attenuated acetylcholine-mediated relaxation. While sensitive to nitric oxide synthase (NOS) inhibition, aortic relaxation in HC-rat tissues was not affected by blocking the inward-rectifier potassium (Kir) channels using $BaCl_2$. Although Kir channel expression was reduced in HC-rat aorta, Kir expression, endothelium-dependent relaxation, and the $BaCl_2$-sensitive component improved in HC rats treated with atorvastatin to reduce serum lipid. Remarkably, HC tissues demonstrated increased reactive species (ROS) in smooth muscle cells, which was reversed in rats receiving atorvastatin. *In vitro* ROS reduction, with superoxide dismutase, improved endothelium-dependent relaxation in HC-rat tissues. Significantly, connexin-43 expression increased in HC aortic tissues, possibly allowing ROS movement into the endothelium and reduction of eNOS activity. In this context, gap junction blockade with 18-β-glycyrrhetinic acid reduced vascular tone in HC rat tissues but not in controls. This reduction was sensitive to NOS inhibition and SOD treatment, possibly as an outcome of reduced ROS influence, and emerged in $BaCl_2$-treated control tissues. Such vascular alterations in HC-fed rats were accompanied by a localized perivascular adipose tissue (PVAT) inflammation, as manifested by an increase in macrophage infiltration and inflammatory markers exclusively in PVAT depot. In this context, custom-designed novel

multi-targeting drug ligands (MTDLs), targeting COX-2, 15-LOX, and/or PPARγ, were developed in an attempt to halt inflammation. *In vitro, in silico* and biological screening of these compounds demonstrated selective but moderate COX-2/15-LOX inhibitory activity as well as partial PPARγ agonistic actions. Given that the pro-inflammatory phenotype of PVAT is thought to drive FFA spill-over possibly underlying the observed endothelial derangements, we tested whether the modulation of different inflammatory targets will ameliorate the observed endothelial insults at this stage. Therefore, endothelial dysfunction was studied in rat thoracic aortic rings resulting from *ex vivo* exposure to increased concentrations of saturated fatty acids. Only treatment with anti-inflammatory triple targeting MTDLs affecting COX-2, 15-LOX, and PPARγ restored endothelium-dependent relaxation. Whereas the impact of the triple-targeting MTDLs appeared to be similar to the single targeting pioglitazone in acute *ex vivo* exposure, it was more effective on aortic tissues isolated from prediabetic rats with chronic vascular inflammation. Importantly, treatment with the triple targeting MTDL restored Kir channel expression in tissues exposed to palmitic acid. Altogether, these results suggest that early metabolic challenge, associated with local PVAT inflammation, leads to reduced Kir-mediated EDH, increased vascular ROS potentially impairing NO synthesis and highlight these channels as a possible target for early intervention with vascular dysfunction in metabolic disease. Also, our results provide insights on the potential efficacy of using novel anti-inflammatory agents to alleviate vascular dysfunction in metabolic disease.

TABLE OF CONTENTS

ILLUSTRATIONS

Figure

TABLES

CHAPTER I

INTRODUCTION

A. Diabetes mellitus

1. Definition

Diabetes is a heterogeneous metabolic disease defined by constant hyperglycemia (American Diabetes Association, 2020). The most common forms of diabetes are types 1 and 2. Type 1 diabetes, formerly referred to as juvenile-onset or insulin-dependent diabetes, results from autoimmune destruction of β-cells of the pancreas and causes absolute insulin deficiency (American Diabetes Association, 2020). Previously known as adult-onset or non-insulin dependent diabetes, type 2 diabetes is mainly characterized by a progressive loss of pancreatic beta cell secretory function on a background of insulin resistance, and accounts for majority (90-95%) of diabetes cases (American Diabetes Association, 2020). The pathophysiology of this heterogeneous type is less characterized than that of type 1, yet various contributors, including chronic inflammation, metabolic stress, and genetic factors, may promote the progression of type 2 diabetes (American Diabetes Association, 2020).

2. Global Burden

Diabetes is a growing epidemic with a global prevalence of 463 million individuals in 2019 (Saeedi et al., 2019). In the Middle East and North Africa (MENA) region, it's estimated that 1 in 8 people have diabetes (Saeedi et al., 2019). Globally, the highest number of deaths attributable to diabetes were reported in 60-69 age group (Saeedi et al., 2019). However, nearly 50% of deaths due to diabetes were in people under 60 in the MENA region (Saeedi et al., 2019). This region is expected to witness a 96% increase in the number of diabetic cases by the year 2045, which is the second highest increase among the IDF Regions (Saeedi et al., 2019). Interestingly, such a steep rise in diabetes is attributed to the accelerated shift towards energy-dense Western Diets, rich in saturated fats and refined sugars (Kuhnlein & Receveur, 1996).

3. Atherosclerotic Cardiovascular Disease

Diabetic complications, whether microvascular or macrovascular, are a major contributor to the rise in diabetes morbidity and mortality (Ahlqvist, van Zuydam, Groop, & McCarthy, 2015). Microvascular complications –due to damage at the level of microvessels– include chronic kidney disease (CKD), neuropathy and retinopathy, whereas macrovascular complications –due to damage at the level of arteries– comprise hypertension and dyslipidemia (American Diabetes, 2017; Forbes & Cooper, 2013). However, the leading cause of death in diabetes is atherosclerotic cardiovascular disease (ASCVD), defined as cardiovascular events that are attributed to atherosclerosis (American Diabetes Association, 2020). Established risk factors for ASCVD encompass hypertension and dyslipidemia, the two major diabetic macrovascular complications, in addition to diabetes itself (American Diabetes, 2017). Risk of cardiovascular complications is not only limited to individuals with established hyperglycemia, but also extends to prediabetic patients who have worse cardiovascular outcomes compared to normoglycemic individuals

(Giraldez-Garcia et al., 2015; Huang, Cai, Mai, Li, & Hu, 2016). Endothelial dysfunction (ED), which is defined as a shift of the endothelium towards a non-adaptive phenotype, is regarded as an independent predictor of ASCVD that is involved in the pathogenesis of the different stages of vascular diseases (Gimbrone & Garcia-Cardena, 2016; Mudau, Genis, Lochner, & Strijdom, 2012).

B. Physiology of endothelium-dependent relaxation

The endothelium was once thought of as a passive layer separating circulating blood from the smooth muscle cells that make up the majority of the blood vessels wall but is now recognized to control a broad range of homeostatic functions. Metabolic disorders such as hyperlipidemia and hyperglycemia cause deleterious changes in endothelial function associated with increased risk of cardiovascular disease. Release of nitric oxide (NO) and electrotonic spread of charge from endothelial to smooth muscle cells (SMCs), termed endothelium-dependent hyperpolarization (EDH), are the two major mechanisms by which the endothelium regulates arterial diameter, and thus blood flow and pressure (Vanhoutte, Boulanger, & Mombouli, 1995; Vanhoutte, Shimokawa, Feletou, & Tang, 2017). To date, these two pathways have been generally regarded as acting independently to mediate endothelium-dependent vasodilation. The endothelium releases a wide range of vasoactive factors but herein, we will focus on the two major mediators of endothelium-dependent vasorelaxation, NO and EDH (Vanhoutte et al., 1995; Vanhoutte et al., 2017).

1. NO-dependent vasorelaxation

NO was the first endothelium-dependent relaxing factor to be identified. It is synthesized in endothelial cells through the enzymatic conversion of L-arginine by endothelial NO synthase (eNOS), an enzyme that can be activated via both calcium-dependent and -independent mechanisms(Vanhoutte et al., 2017). NO activates soluble guanylate cyclase (sGC) in vascular smooth muscle cells (VSMCs) leading to increased cyclic guanylyl monophosphate (cGMP), activation of cGMP-dependent kinase (cGK), and consequent relaxation (Katsuki, Arnold, Mittal, & Murad, 1977). Insulin is an example of calcium independent eNOS activators. It promotes eNOS activation through protein kinase B (Akt)-phosphorylation(Muniyappa, Montagnani, Koh, & Quon, 2007). The subsequent NO-mediated vasodilation increases microvascular perfusion to facilitate glucose uptake by skeletal muscles, thereby augmenting the metabolic actions of insulin(Muniyappa et al., 2007).

2. EDH-mediated vasorelaxation

Reports of endothelium-dependent vasorelaxation persisting in the presence of inhibitors of eNOS and accompanied by hyperpolarization of the vascular SMC membrane potential, led to identification of the EDH pathway. Hyperpolarization of SMCs decreases the open probability of voltage-dependent Ca^{2+} channels to reduce Ca^{2+} influx, and thus, cause relaxation. A number of endothelium-derived molecules such as epoxyeicosatrienoic acids, produced by metabolism of arachidonic acid by cytochrome P450 enzymes, H_2O_2, and carbon monoxide can activate K^+ channels to cause SMC hyperpolarization. However, it is now widely accepted that rather than a diffusible factor, EDH is largely mediated by direct electrical coupling between endothelial and smooth muscle cells via myoendothelial gap junctions (reviewed in(Edwards, Feletou, & Weston, 2010)).

EDH-mediated relaxation is initiated by an increase in endothelial Ca^{2+} levels activating small (SK_{Ca}) and intermediate (IK_{Ca}) conductance Ca^{2+}-dependent K^+ channels to hyperpolarize the endothelial cell membrane potential(Billaud et al., 2014; Feletou & Vanhoutte, 2009). This hyperpolarization spreads electrotonically to surrounding SMCs via myoendothelial gap junctions, consequently recruiting Na^+/K^+ATPase and/or inwardly rectifying potassium (Kir) channels(Edwards G, 1998). Inhibition of Kir channels by $BaCl_2$ or knockout of Kir2.1 channels reduced the response to endothelium-dependent vasodilators in rat mesenteric arteries(Sonkusare, Dalsgaard, Bonev, & Nelson, 2016). Thus, Kir channels, whether present on the endothelium or SMCs, are regarded as “end-stage amplifiers” of EDH(Johnson, Marrelli, Steenberg, Childres, & Bryan, 1998; Sonkusare et al., 2016).

Myoendothelial gap junctions conduct charges between endothelial and SMC layer. Vascular gap junctions are made up of sub-units belonging to one or more isoforms called connexins (Cxs): Cx37, 40, 43 and 45(Abed, Dussaule, Boffa, Chatziantoniou, & Chadjichristos, 2014; Figueroa & Duling, 2009). Cx40 is involved in both radial and longitudinal transmission of signals amongst and along ECs and SMCs(de Wit et al., 2000). Cx43 is of particular interest as it is abundant in both SMC and ECs, and plays an important role in vascular-endothelial communication. In the context of radial communication, myoendothelial gap junctions permit transit of signaling molecules (Ca^{2+} and inositol triphosphate (IP_3)) and charge. Such a tight coupling of the two cell types allows for control of vascular tone not only through active relaxation, but by opposing vasoconstriction(Xavier F. Figueroa, 2004). For example, in rat basilar and mesenteric arteries, agonist-evoked depolarization was opposed by endothelial hyperpolarization; IP3 produced in SMCs in response to the α_1-adrenoceptor agonist phenylephrine passes through myoendothelial gap junctions, leading to calcium release, activation of endothelial IK_{Ca} channels, and hyperpolarization opposing depolarization and SMC contraction(Kerr et al., 2015).

3. Interactions between NO and EDH pathways

NO and EDH pathways co-exist amongst all vascular beds. However, the density of myoendothelial gap junctions is inversely proportional to arterial size and directly proportional to the contribution of EDH to vasorelaxation(Sandow & Hill, 2000; Hiroaki Shimokawa et al., 1996). Both components have widely been viewed as separate mechanisms of endothelium-dependent relaxation (EDR). However, several lines of evidence support a more complex relationship between NO and EDH whereby activation of endothelial K_{Ca} channels may enhance NO production/availability, and in turn, NO may play a role in EDH. Data from experiments employing small molecule modulators of endothelial SK_{Ca} and IK_{Ca} channels indicate that NO production/release may be modulated by changes in endothelial membrane potential. An IK_{Ca}/SK_{Ca} channel opener enhanced ATP-evoked membrane hyperpolarization and NO synthesis in cultured human umbilical vein endothelial cells and rat cremaster arterioles(Sheng & Braun, 2007; Sheng, Ella, Davis, Hill, & Braun, 2009), and elicited NO-dependent increases in coronary blood flow in anesthetized dogs(Kurian, Berwick, & Tune, 2011). IK_{Ca} channel activity was shown to underpin NO-mediated myoendothelial feedback in rat basilar and mesenteric arteries(Kerr et al., 2015) and loss of SK_{Ca} channels impaired NO-mediated dilation to both acetylcholine and shear stress in mouse carotid and skeletal muscle arterioles *in vivo*(Brahler et al., 2009).

Conversely, block of EDH by eNOS inhibitors points to the possibility that endothelium-derived NO itself may be a mediator of EDH(Cohen et al., 1997; Plane & Garland, 1993; Rand & Garland, 1992; Tare, Parkington, Coleman, Neild, & Dusting, 1990). Indeed, a rich body of literature shows that NO produces SMC hyperpolarization contributing to endothelium-dependent relaxation of a variety of vascular beds *e.g.* rabbit aorta, carotid and mesenteric arteries, rat aorta, tail and middle cerebral arteries as well as in guinea-pigs uterine and mesenteric vessels(Bolotina, Najibi, Palacino, Pagano, & Cohen, 1994; Cohen et al., 1997; Mistry & Garland, 1998; Tare et al., 1990; Vanheel, Van de Voorde, & Leusen, 1994). Some studies implicated K^+-channels in this effect including K_{Ca} channels(Bolotina et al., 1994; Brakemeier et al., 2003; Mistry & Garland, 1998; Pickkers, Dorresteijn, Bouw, van der Hoeven, & Smits, 2006), and ATP-activated K channels(Musser et al., 2004) However, NO is not able to cause SMC hyperpolarization in all arteries, and an alternative explanation for the sensitivity of EDH-mediated responses to eNOS, which has yet to be fully explored, is that endothelium-derived NO may play a permissive or fascilitatory role in the EDH response. In support of this idea, rat mesenteric and basilar arteries, in which NO failed to elicit SMC hyperpolarization(Garland & McPherson, 1992), block of eNOS inhibited both relaxation and EDH to acetylcholine(Waldron & Garland, 1994; Wei R., 2014).

C. Abnormalities in endothelium-dependent relaxation in metabolic disorders

1. NO-dependent pathways in metabolic disorders

a. Insulin Resistance

Insulin resistance is accompanied by ED that is partly due to a shift in endothelial signaling in favor of the production of the vasoconstrictor endothelin-1 rather than NO. This can be attributed to the selective impairment of the phosphoinositide 3-kinase (PI3K)/Akt pathway with preserved activity of mitogen-activated protein kinase (MAPK)-dependent signaling. Thereby, components of PI3K-dependent pathway, such as insulin receptor substrate-1, PI3k and Akt are downregulated while components of the opposing pathway remain unaltered(Sowers, 2013; Wheatcroft, Williams, Shah, & Kearney, 2003).

b. eNOS Uncoupling

Accumulating evidence indicate that the impairment of the eNOS/NO pathway, leading to decreased NO bioavailability, might be an early predictor of ED(Z. Yang & Ming, 2006). Although it is well-established in the literature that increased NO production is protective against atherosclerosis(van Haperen et al., 2002), another line of evidence supports an opposing point of view and documents that overexpression of eNOS accelerates atherosclerosis progression in hypercholesterolemia(Ozaki et al., 2002). Such controversy can be attributed to "eNOS uncoupling"(H. Li, Horke, & Förstermann, 2014). Under physiological conditions, the catalytic function of eNOS is dependent on enzyme dimerization followed by binding of the cofactor tetrahydrobiopterin and substrate L-arginine. The phenomenon of “eNOS uncoupling” occurs when eNOS monomers do not couple to their cofactors/substrates and instead produce superoxide anions (O_2^-)(J. Lee, Bae, Ma, & Kim, 2016). O_2^- production, in turn, promotes impairment of endothelial function and mediates vasoconstriction(Lawson, Mehta, Nichols, Mehta, & Donnelly, 1990). Despite the fact that SMCs and adventitial cells can produce reactive oxygen species, endothelium-derived O_2^- has been shown to be the main contributor to cardiovascular disease linked to metabolic disorders such as hyperlipidemia(Sohn et al., 2000).

2. Abnormalities in EDH in metabolic disorders

Studies examining EDH abnormalities in metabolic disorders have largely focused on the contribution of EDH abnormalities to ED in type II diabetes(Matsumoto et al., 2017; Schach, Resch, Schmid, Riegger, & Endemann, 2014). Although ED might occur in the absence of hyperglycemia in prediabetic patients(Wasserman David, Wang Thomas, & Brown Nancy, 2018), few studies have investigated the changes in EDH at the early stages of metabolic disease. In mesenteric arteries from a fructose-fed rat model of insulin resistance, impairment of EDRs to acetylcholine was primarily due to loss of EDH(Miller, Hoenig, & Ujhelyi, 1998). Despite these observations, our knowledge regarding the mechanism underlying impairment of EDH is not complete, and extensive efforts are required to characterize the pathophysiological changes underlying the early loss of EDH.

An outline of the possible aberrations leading to EDH dysfunction in metabolic diseases is provided below.

a. Channelopathies

i. SK_{Ca}/IK_{Ca} channels

Alterations in these two channels are associated with ED in various cardiovascular diseases, such as hypertension(Kohler, Olivan-Viguera, & Wulff, 2016). A recent study showed that in rats, diet-induced hypertension is associated with reduced function and expression of SK_{Ca}/IK_{Ca} channels(Gradel, Salomonsson, Sorensen, Holstein-Rathlou, & Jensen, 2018). Significantly, coronary microvessels of diabetic patients also displayed reductions in endothelial SK_{Ca}/IK_{Ca} channel activity without changes in expression or distribution(Y. Liu et al., 2015). This decrease in K_{Ca} channel function could be attributed to advanced glycation end products that are formed in diabetes(Zhao et al., 2014). Changes in K_{Ca} channel function but not expression support the potential therapeutic use of small molecules that modulate these channels in metabolic diseases. However, it is noteworthy that both studies described above examined arteries at relatively advanced stages of the disease where hypertension and diabetic hyperglycemia were established, and so time course of such changes remains to be established.

ii. Kir channels

Kir channels play an essential role in amplifying EDH responses, and act as “end-stage boosters of endothelium-dependent vasodilation”(Sonkusare et al., 2016). The negative slope conductance of Kir2.1-containing channels leads to increased activity as a function of membrane potential hyperpolarization(Jantzi et al., 2006). In a rat model of early stages of metabolic disease prior to overt glycemic or hemodynamic impairment, the primary changes in EDH were attributed to defective Kir2.1 channel expression/function(R. Alaaeddine et al., 2018). In a similar model, a longer duration of exposure to high fat/ high fructose led to a hypertensive phenotype, in which not only Kir2.1 channel expression/function was reduced, but also SK_{Ca}/IK_{Ca} channels were affected(Gradel et al., 2018). These results indicate that EDH alteration may be of an insidious onset, where various channels could be affected at different stages. Significantly, an inverse relationship between Kir channel activity and high cholesterol levels in the channel microenvironment was described. One study showed that exposing human endothelial cells to a cholesterol-rich environment suppressed Kir currents and inhibited flow-induced hyperpolarization(Fang et al., 2006). These results were verified by *ex vivo* experiments conducted on aortae from a pig model of hypercholesterolemia, that showed a reduction in Kir channel activity and a shift to a more depolarized state(Fang et al., 2006). Moreover, electrophysiology and biochemical data suggest a negative effect of hypercholesterolemia on the activity of Kir2 series subunits in both the endothelial and muscular layers in mouse cerebral arteries(Maria Sancho & Welsh, 2018). These observations provide a framework for functional alteration of Kir channel activity and EDH impairment with slight cholesterol changes early in metabolic diseases.

b. Alterations in Gap Junctions/ Cxs

Changes in Cx expression have been shown to be associated with the different macro- and micro-vascular complications of diabetes, ranging from atherosclerosis, hypertension, dyslipidemia to peripheral vascular disease(Josephine A. Wright, 2011). However, discrepancies in vascular expression levels of different Cx isoforms were observed in these conditions. Cx40 downregulation is implicated in ED in coronary arteries from streptozotocin-induced type I diabetic mice(Makino A1, 2008). Similarly, in long-term dyslipidemia, a reduction in endothelial Cx37 and 40 expression levels was detected in mouse aorta(Yeh et al., 2003). On the other hand, Cx43 was upregulated in smooth muscle cells in early stages of atherosclerotic plaque formation and was also identified in the endothelial cells covering the shoulder of the atherosclerotic lesion(Kwak, Mulhaupt, Veillard, Gros, & Mach, 2002). Furthermore, Cx43 is increased in the endothelium and tunica media of the aorta in hereditary hypertriglyceridemic rats, an effect reversed by treatment with the antihyperlipidemic drug atorvastatin or omega-3 fatty acids(Dlugosova et al., 2009). This apparent discrepancy could be reconciled upon examining some of the molecular mechanisms regulating the expression patterns of different Cx isoforms. Whereas GATA4, which is down-regulated in endothelial cells by hyperglycemia (Xu, Wang, Sun, Ni, & Zheng, 2018), was shown to be an important mediator of Cx40 expression(Oyamada, Oyamada, & Takamatsu, 2005), Cx43 was the only isoform whose expression was driven by factors that are upregulated in metabolic disease including the Wnt and Ras/Map kinase pathways(Oyamada et al., 2005).

While the downregulation of Cx37 and Cx40 is in line with reduction of EDH conduction expected as a part of the ED in metabolic disorders, changes in Cx43 appear to be paradoxical. Yet, this has to be viewed in the context of overall vascular activity, where flow-mediated EDR occurs simultaneously with increased SMC depolarization leading to myogenic contractility in response to increased intravascular pressure(Eid et al., 2018; El-Yazbi & Abd-Elrahman, 2017). Under these circumstances, facilitated myoendothelial conduction could lead to a situation whereby depolarization originating in SMCs may overwhelm the compromised hyperpolarization in the endothelium. Under such conditions, a reduction in Cx43 expression may afford protection against ED and exaggerated vasoconstriction.

3. Endothelial Dysfunction and Perivascular Adipose Tissue

The cross-talk between the vasculature and surrounding adipose tissue is integral for proper vascular function, whereby the perivascular adipose tissue (PVAT) layer releases a number of vasoactive factors that modulate the contractility of the vascular layer (Y. J. Gao, Lu, Su, Sharma, & Lee, 2007). However, adipose remodeling and inflammation was shown to be implicated in the pathogenesis of cardiovascular dysfunction in the early course of metabolic disease, prior to hyperglycemia (Choe, Huh, Hwang, Kim, & Kim, 2016; M. A. W. Elkhatib et al., 2019), whereby PVAT acquires proinflammatory and proatherogenic properties that culminate in vascular remodeling (Chang, Milton, Eitzman, & Chen, 2013). As such, a state of insulin resistance creates an imbalance in the nature of secreted substances, favoring the production of pro-inflammatory cytokines and NADPH oxidase-derived reactive oxygen species, which contribute to the aggravation of endothelial dysfunction (Gil-Ortega et al., 2014; Ketonen, Shi, Martonen, & Mervaala, 2010).

D. Adipose tissue Inflammation

Our view of the adipose tissue has advanced from being a simple energy storage depot to a dynamic organ with multiple immunological and endocrine functions. Chronic, low grade adipose tissue inflammation has been linked to the progression of type 2 diabetes and vascular dysfunction (AlZaim et al., 2020). With excess energy intake associated with metabolic challenge, adipose tissue undergoes expansion to meet the enhanced metabolic demand in one of two mechanisms, either through increasing the number of cells, known as hyperplasia, or enhancing the size of adipocytes, referred to as hypertrophy (Jo et al., 2009). While hyperplasia of adipocytes is a more physiologically-relevant mechanism that occurs as a function of enhanced adipogenesis to accommodate surplus energy, hypertrophy is rather observed in obesity and insulin resistance, and even aggravated in the presence of high levels of inflammatory mediators (Arner et al., 2010; Tchkonia et al., 2013). Interestingly, a saturated free fatty acid (SFA)-rich high fat diet was shown to favor the hypertrophic phenotype of adipose tissue (Finucane et al., 2015).

In the absence of sufficient vascularization, hypertrophied adipose tissue creates a hypoxic environment that drives the accumulation of macrophages, hence triggering adipose tissue inflammation (AlZaim et al., 2020). Given that adipocyte hypertrophy is associated with adipose tissue necrosis, the early infiltration of macrophages into adipose tissue may be viewed as a mechanism that is intended to be protective, aiming at sequestering adipocyte debris and residual lipid droplets (Cinti et al., 2005). However, the continuous recruitment of these macrophages into adipose tissue results in a state of chronic, low-grade inflammation that precipitates cardiometabolic manifestations of metabolic disease (Xu et al., 2003). Given that insulin inhibits lipolysis, insulin resistance drives a surge in free fatty acids (FFAs) originating from adipose tissue depots (Guilherme, Virbasius, Puri, & Czech, 2008). Not only does this rise in FFAs trigger inflammation and insulin resistance to neighboring tissues, but also it can exacerbate adipose tissue inflammation in an autocrine manner (mechanisms discussed below). Under such circumstances, macrophages and adipocytes become involved in a cross-talk loop, further accentuating adipose tissue inflammation.

E. Free Fatty Acids

FFAs are carboxylic acids with long aliphatic chains, with a methyl group at one end and a carboxylic group at the other end (Thijssen & Mensink, 2005). They can be categorized into three groups depending on the presence of double bonds: saturated fatty acid (SFAs) containing no double bonds, monounsaturated fatty acids (MUFAs) having only one double bond, and polyunsaturated fatty acids (PUFA) with two or more double bonds (Thijssen & Mensink, 2005). FFAs are further classified according to the length of their aliphatic chain into short-chain fatty acids (less than 6 carbons), medium-chain fatty acids (6-12 carbons), and long-chain fatty acids (more than 12 carbons) (Miyamoto et al., 2016).

These different types of FFAs exert various functions in health and disease. For example, MUFA-rich diets were linked to a reduction in cardiovascular risk and found beneficial in hypertension and diabetes (Schwingshackl & Hoffmann, 2012). However, palmitic acid, which is a saturated FFA most commonly found in western diet, is the predominant contributing element to atherosclerosis progression, according to a metabolomics study (X. Chen et al., 2010). In fact, metabolic challenge results in "FFA spill-over", accumulation in metabolic tissues, and triggering a pro-inflammatory phenotype that culminates in disease progression (van Herpen & Schrauwen-Hinderling, 2008). As such, FFAs have emerged as an important link between metabolic disease, insulin resistance and development of cardiovascular diseases (Boden, 2008). Circulating levels of palmitic acid were also found to exhibit increased levels in diabetic patients (Prescott, Owens, Collins, Johnson, & Tomkin, 1999).

Previously labeled as an orphan class of G-protein coupled receptors, FFA-sensing receptors (FFARs) are now known to be important mediators of certain FFA functions (Briscoe et al., 2003). There are four well-characterized FFARs, including FFAR1/GPR40, FFAR2/GPR43, FFAR3/GPR41, and FFAR4/GPR120, and are distributed among different tissues (Secor, Fligor, Tsikis, Yu, & Puder, 2021). More importantly, FFAs were also shown to exhibit the ability to bind to other types of receptors, such as toll-like receptors, and elicit their corresponding immune actions (Shi et al., 2006). Due to the presence of these receptors on the surface of immune cells, FFAs are thought to possess an immune-regulatory role, especially in metabolic inflammation (Hidalgo, Carretta, & Burgos, 2021).

As a matter of fact, infiltration of immune cells to adipose tissue depots represents the initial stage of metabolic inflammation.

1. FFAs as Immune Modulators of Adipose Tissue Inflammation

Toll-like receptor (TLR)-4 signaling plays a crucial role in the FFA-induced upregulation of pro-inflammatory mediators in macrophages, through downstream Myd88- (Kochumon et al., 2018; Sindhu, Al-Roub, Koshy, Thomas, & Ahmad, 2016) or TRIF-dependent (Hasan et al., 2019) downstream pathways. As such, SFAs promote the expression of chemotactic cytokines, such as IL-8, and macrophages inflammatory proteins (MIPs), in addition to nuclear factor kappa B (NF-κB), all which were previously reported to be implicated in the pathogenesis of metabolic inflammation (Hasan et al., 2019; Kochumon et al., 2018; Suganami et al., 2007). Moreover, SFAs induce the formation of matrix metalloproteinase (MMP)-9, which is important in adipose tissue remodeling in obesity-related inflammation and insulin resistance (Sindhu et al., 2016).

In the presence of FFA-induced pro-inflammatory milieu, palmitate can cooperate with TNF-α, to induce the expression of MIP1α/CCL3 and MIP1β/CCL4, which further amplify the immune response in metabolic disease. The synergistic effect of palmitate and TNF-α on promoting MIP1α secretion was found to be mediated by TLR4-IRF3 pathway and signaling that involves c-Jun/NF-κB, a mechanism which is exacerbated by the presence of oxidative stress in metabolic inflammation (Sindhu et al., 2020). Similarly, palmitate and TNF-α together can trigger the expression of CCL4/MIP-1β chemokine via the activation of TLR4-MyD88 axis and MAPK/NF-κB pathways (Sindhu et al., 2019). Furthermore, the synergy between palmitate and TNF-α plays an important role in upregulating the chemokine CCL2 or monocyte chemoattractant protein (MCP)-1 via the TLR4/TRIF/IRF3 signaling cascade (Ahmad et al., 2018). Furthermore, elevated levels of FFAs, in the presence of hyperinsulinemia observed in metabolic disease, can favor adipose tissue inflammation progression in a feed forward loop. This is evident in a study demonstrating that palmitate, cooperatively with insulin, instigates the synthesis of PGE_2 in macrophages, which further enhances IL-8 formation, known to promote insulin resistance and inflammation (Henkel et al., 2021). Not only does SFAs enhance the production of inflammatory mediators, but also it can downregulate the expression of players with an anti-inflammatory role, including peroxisome proliferator-activated receptor-gamma (PPARγ) (Engin, 2017).

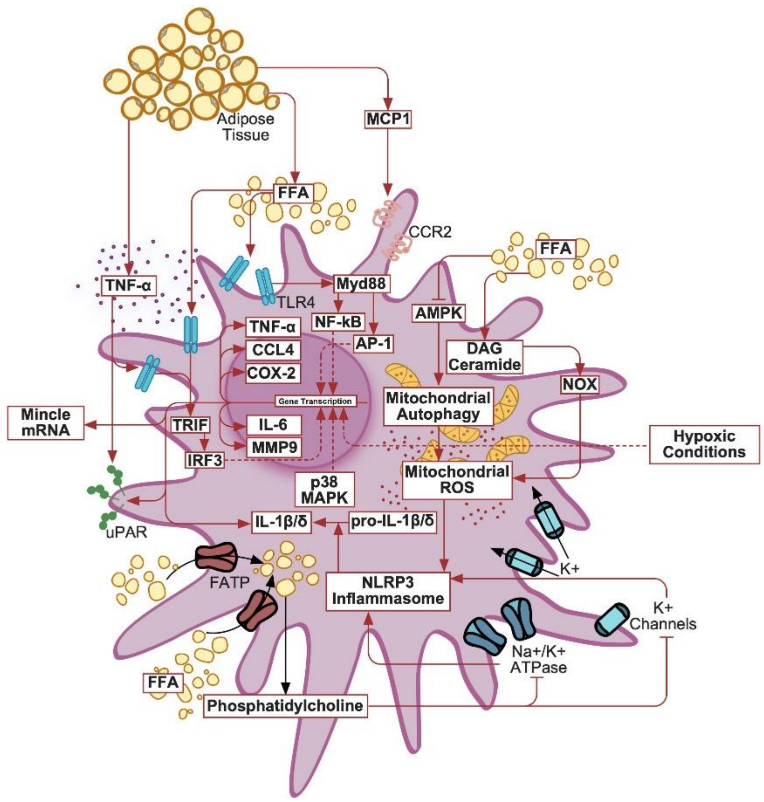

Figure 1. **Proposed mechanisms for monocyte/macrophage activation and upregulation of pro-inflammatory markers as a function of FFA exposure**. A FFA flux, possibly through the fatty acid transporter protein (FATP), induces saturation of phosphatidylcholine that impairs the cell membrane fluidity and disrupts Na/K ATPase, which then triggers a potassium efflux sufficient to activate NLRP3 inflammasome, leading to the production of IL-1β and IL-8. NLRP3 inflammasome can be also be activated as a function of an increase in mitochondrial reactive oxygen species (ROS) production, resulting from FFA-induced suppression of AMP-activated protein kinase (AMPK) signaling and subsequent mitochondrial autophagy. Moreover, the lipid metabolites of FFAs, ceramide and diacylglycerol (DAG) may also activate NLRP3 inflammasome, via stimulating NADPH oxidase and enhancing ROS production. Furthermore, Toll-like receptor (TLR)-4 signaling plays a crucial role in the FFA-induced upregulation of pro-inflammatory mediators in macrophages, through downstream Myd88- or TRIF- dependent downstream pathways. The activation of TLR4/Myd88/NF-κB pathway by FFAs can lead to the upregulation of macrophage-inducible C-type lectin (mincle), which is a type II transmembrane C-type lectin triggered in macrophages specifically upon interaction with adipose tissue. As well, FFAs modifies the expression of urokinase-type plasminogen activator receptor (uPAR) through p38 MAPK-dependent mechanisms. The combination of FFAs and tumor necrosis factor (TNF-α), potentially originating from adipose tissue, can enhance the expression of CCL4 (Chemokine (C-C motif) ligand 4), which contributes to the recruitment of monocytes into adipose tissue.

NLRP (NOD-, LRR- and pyrin domain-containing protein)-3 inflammasome plays an important role in modulating western-diet induced inflammation, mainly by responding to changes in metabolic intermediates, such as free fatty acids, ceramide, and glucose (Donath, Dalmas, Sauter, & Boni-Schnetzler, 2013; Legrand-Poels et al., 2014). In fact, metabolically unhealthy patients exhibited enhanced activation of NLRP3 inflammasome in macrophages resident in visceral adipose tissue, in line with the low-grade inflammation observed in this fat depot in metabolic disease (Esser et al., 2013). More recent evidence demonstrated that SFAs promotes the activation of NLRP3 inflammasome, via impairing cell membrane fluidity and disrupting Na/K ATPase, which then triggers a potassium efflux sufficient to activate NLRP3 inflammasome, leading to the production of IL-1β and IL-8 (Gianfrancesco et al., 2019). In another study, FFA-induced activation of NLRP3 inflammasome was shown to be mediated by suppressing the signaling of AMP-activated protein kinase (AMPK), a pleiotropic metabolic sensor, and subsequent accumulation of mitochondrial reactive oxygen species (ROS) production, which impairs insulin signaling in certain target tissues (H. Wen et al., 2011). Such activation of NLRP3 is not only restricted to SFAs, but also the lipid metabolites of FFAs, ceramide and diacylglycerol (DAG), can in turn activate NLRP3, via stimulating NADPH oxidase and enhancing ROS production (Brookheart, Michel, & Schaffer, 2009).

Adipose tissue macrophages are directly influenced by an increase in FFAs associated with metabolic inflammation. This subpopulation of macrophages was shown undergo a phenotypic switch from an anti-inflammatory alternative M2 to a pro-inflammatory M1 phenotype with insulin desensitizing actions as a function of SFAs, palmitate in particular (K. L. Chan et al., 2015). Interestingly, such an enhancement in M1/M2 macrophages polarization is not only restricted to patients with metabolic syndrome, but it was also demonstrated that the polarization towards M1 proinflammatory macrophages resident in adipose tissue was positively related to the proportion of palmitate in the cell membrane in healthy individuals (Poledne et al., 2019). The cross-talk between adipose tissue-resident macrophages and adipocytes was illustrated by an *in vitro* co-culture model, composed of 3T3-L1 adipocytes and RAW264 cell line of macrophages (Suganami, Nishida, & Ogawa, 2005). This study showed that macrophage-derived TNF-α is induced by palmitate, released in large quantities from hypertrophised adipocytes, as a result of macrophage-induced adipocyte lipolysis (Suganami et al., 2005). Thereby, TNF-α and palmitate are involved in “paracrine loop” that exacerbates the inflammatory phenotype of adipose tissue. In an attempt to further characterize this interaction, cDNA microarray analyses revealed an upregulation in macrophage-inducible C-type lectin (Mincle), which is a type II transmembrane C-type lectin suggested to play a role in pathogenesis of obesity-related metabolic derangements (Ichioka et al., 2011). In fact, palmitate was shown to promote the upregulation of Mincle, through the activation of TLR4/Myd88/NF-κB signaling pathway (Ichioka et al., 2011).

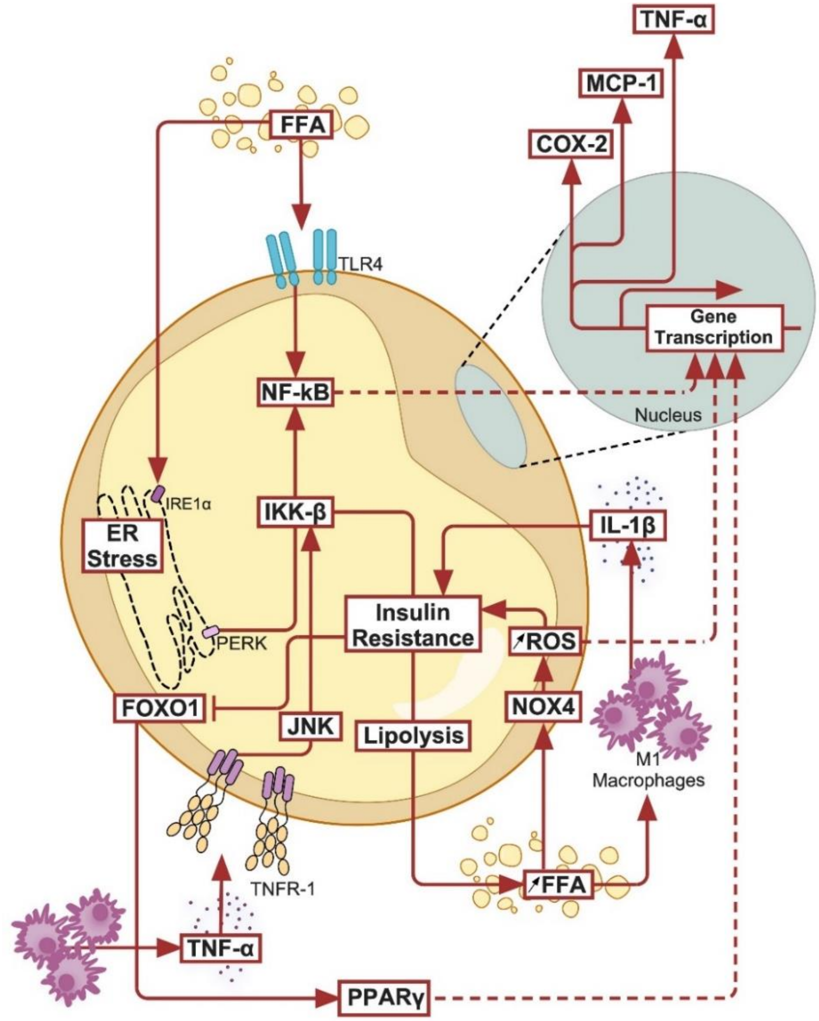

Figure 2. **Possible mechanisms for FFA-induced adipose tissue inflammation**. FFAs can upregulated the expression of pro-inflammatory mediators via TLR4/NF-κB signaling. FFA-induced ER stress also results in activation of IKKβ, a master kinase for regulating expression of inflammatory gene. Moreover, FFAs can increase the expression of NAPDH oxidase, hence leading to an enhanced production of ROS, with its deleterious consequences on insulin signaling pathway. The inflammatory phenotype of adipose tissue is exacerbated by the actions of proinflammatory cytokines originating from macrophages, especially TNF-α, which activates downstream JNK/IKKβ. The expression of peroxisome proliferator-activated receptor-gamma (PPARγ), a transcription factor with known anti-inflammatory properties, is reduced in response to FFAs. In the presence of insulin resistance, the enhanced lipolysis ensures the continuous mobilization of FFAs from adipocytes, thus causing further recruitment and activation of macrophages. In conclusion, adipocytes and macrophages are involved in a vicious self-exacerbating cycle that leads to an upregulation of the inflammatory phenotype of adipose tissue. Adipose tissue hypertrophy and subsequent hypoxia drive the accumulation of macrophages, hence exacerbating the effects of FFA-induced adipose tissue inflammation.

2. FFAs and Endothelial Dysfunction

A significant body of evidence has suggested a role for SFAs as key drivers of metabolic stress-evoked endothelial dysfunction. In fact, elevated circulating levels of FFAs were directly associated with an impairment of endothelium-dependent relaxation (Steinberg et al., 1997). Previous studies investigating FFA-induced endothelial dysfunction demonstrated NO as the principal compromised relaxing component, whereby shear-stress mediated NO production was shown to be impaired in insulin-sensitive individuals upon infusion with FFAs (Steinberg et al., 2000). Thus, by inducing a state of insulin resistance in the endothelium, FFAs can contribute to the derangements in endothelial function. These inhibitory effects of FFAs on endothelial NO were mainly attributed to a palmitate-induced reduction of phosphorylation of IRS-1, which interrupts PI3K/Akt/eNOS insulin signaling pathway (Fratantonio et al., 2017).

Oxidative stress is another mechanism by which FFAs can impair NO-mediated responses in the endothelium. FFAs can enhance the production of ROS through PKC-dependent activation of NADPH oxidase (Inoguchi et al., 2000). Furthermore, palmitate, via the activation of ER stress pathways, was shown to increase the formation of ROS and trigger the apoptosis of endothelial cells (Y. Lu et al., 2013). In addition, the role of FFA-evoked oxidative stress in impairing endothelial function is further illustrated by the findings a study demonstrating that NF-κB-dependent COX-2 upregulation of ROS may underlie palmitate-induced endothelial dysfunction (Z. Gao et al., 2014). In this study, *ex vivo* treatment of aortic rings with palmitate attenuated acetylcholine-mediated relaxation in a concentration-dependent manner, which was improved upon superoxide scavenging and

COX-2 inhibition/knockout (Z. Gao et al., 2014). However, the observed profile of endothelium-dependent relaxation was not altered in *COX-1*$^{-/-}$ mice (Z. Gao et al., 2014). Interestingly, these effects were shown to be mediated by the actions of thromboxane, downstream of COX-2 (Z. Gao et al., 2014).

The pro-inflammatory phenotype triggered by FFAs is also proposed as a possible mechanism that may cause insulin resistance and impair endothelial function. In fact, the FFA-induced pro-inflammatory microenvironment in vascular walls is aggravated by two main factors: (1) the upregulation of cytokines and adhesion molecules in endothelial that attracts macrophages, (2) the close proximity of PVAT layer, that also acts a continuous source of FFAs. The activation of IKKβ by SFAs, and the consequent NF-κB p65 phosphorylation and increase in IL-6 and TNF-α, was found to play an integral role in decreasing IRS-1 tyrosine phosphorylation, hence altering IRS-1/Akt/eNOS pathway (Kim et al., 2005; K. Liu et al., 2012). The insulin-signaling pathway is also impaired by FFA-induced activation of NLRP3 inflammasome in endothelial cells, that culminates in the formation of IL-1β (Xing et al., 2019). These effects were found to be mediated by palmitate through the inactivation of AMPKα (Xing et al., 2019). Activated NLRP3 inflammasome in endothelial cells in response to FFAs was also associated FFAs with a reduction in inter-endothelial tight junction proteins zona occludens (ZO)-1/ZO-2 in microvascular endothelial cells (MVECs), hence enhancing endothelial permeability (L. Wang et al., 2016). As such, FFA-induced endothelial dysfunction was also reported in adipose microvasculature, where palmitate was shown to enhance monocyte transmigration and impair insulin transport in primary endothelial cells from human adipose tissue microvasculature (HAMEC), through TLR4/NF-κB signaling (Pillon et al., 2015). Another study conducted on human aortic endothelial cells proposed that palmitate-induced mitochondrial damage is a possible mechanism behind endothelial inflammation, where the consequent leakage of mitochondrial DNA, sensed by cyclic GMP-AMP synthase, triggers the activation of the stimulator of interferon genes protein (STING). Hence, this critical signaling molecule promotes the phosphorylation of interferon regulatory factor 3 (IRF3), which in turn, upregulates the expression of intercellular adhesion molecule 1 (ICAM-1) and facilitate monocyte-endothelial cell adhesion (Mao et al., 2017).

Despite the interaction between the two endothelial mechanisms, the effect of FFAs on EDH responses is poorly investigated in the literature. Up to our knowledge, only one study conducted on human subjects has provided evidence on the impairment of NO-independent vasodilation in response to infusion with FFAs, mainly through suppression of Kir channels (de Kreutzenberg et al., 2003). Interestingly, FFAs is able to induce an upregulation of gap junction connexin 43, a common pathological alteration previously reported to exist in vascular diseases (Kiec-Wilk et al., 2012).

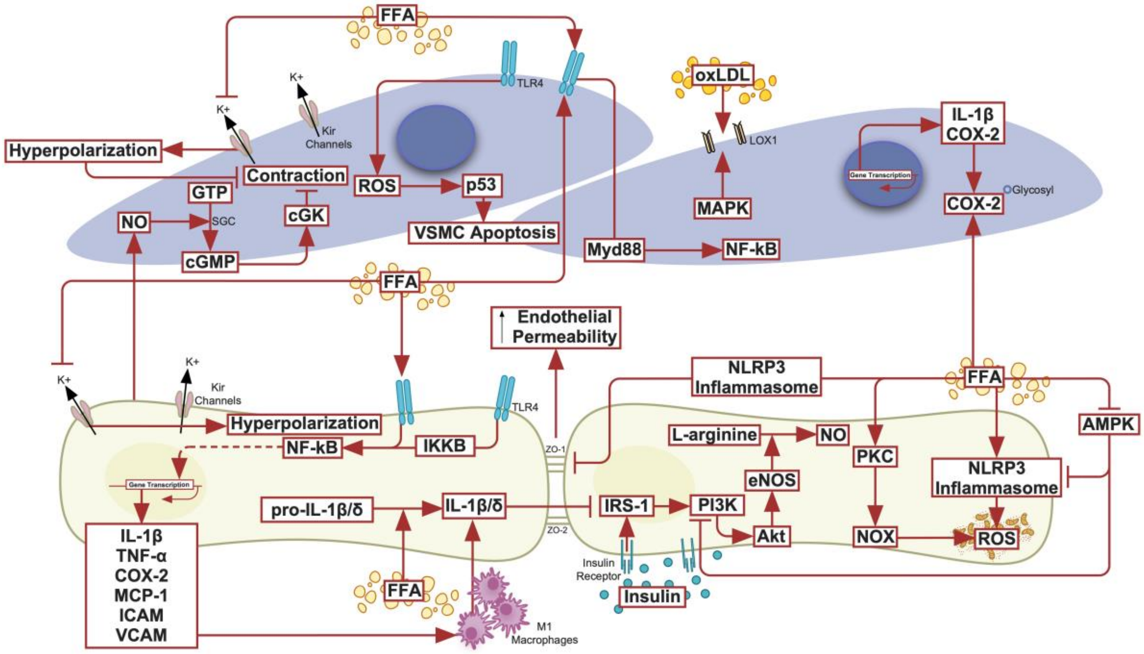

Figure 3. **Potential mechanisms by which FFAs trigger endothelial dysfunction**. In endothelial cells, FFAs upregulate the expression of different pro-inflammatory mediators and adhesion molecules via activation of TLR4/NF-κB or IKKβ/NF-κB. The production of IL-1β can be further enhanced through the actions of FFAs on NLRP3 inflammasome, which is mediated by the FFA-induced inactivation of AMPKα. This will cause a disruption of the insulin-signaling pathway, leading to the reduction in the generation of the vasorelaxing component NO. Another mechanism by which NO is reduced is in the presence of oxidative stress. FFAs can enhance the production of reactive oxygen species through the induction of NADPH oxidase and NLRP3 inflammasome. FFAs can also impair endothelial relaxation mechanisms by suppressing inward rectifier potassium (Kir) channels and reducing EDH responses. Furthermore, FFAs can promote endothelial permeability, through targeting zona occludens and impairing endothelial tight junctions. FFAs is able to induce an upregulation of gap junction connexin 43, which ensures proper endothelial-smooth muscle cross-talk for efficient control of vascular tone. In vascular smooth muscle cells, inflammatory markers are also upregulated as a function of FFA/TLR4/Myd88/NF-κB signaling. Besides enhancing the expression of COX-2, FFAs is responsible for the glycosylation of this enzyme, as a form of posttranslational modification. FFAs also upregulates lectin-like oxidized low-density lipoprotein receptor 1 (LOX-1), thus favoring ox-LDL uptake. TLR4/ROS/p53 pathway activation by FFA may lead to the apoptosis of vascular smooth muscle.

F. Multi-targeting Drug Ligands

Designing highly selective single-target ligands for specific diseases has been the predominating paradigm in drug discovery programs in the 20th century (Ramsay, Popovic-Nikolic, Nikolic, Uliassi, & Bolognesi, 2018; Zhou et al., 2019). Indeed, this paradigm was very effective in many instances, yet it did not show the same success in complex diseases such as cancer, neurodegenerative diseases, metabolic diseases and inflammatory disorders (Ramsay et al., 2018; Zhou et al., 2019). These diseases are under the control of several biochemical processes and hence display complexities and redundancies that frequently compensate for the action of single-targeted therapies making them more prone to adaptive resistance mechanisms (Proschak, Stark, & Merk, 2019; Ramsay et al., 2018). Hence, the pharmaceutical pipeline has now perceived the notion that "Simple Drugs Do Not Cure Complex Diseases", which called for "The Need for Multi-Targeted Drugs". In this regard, multi-targeting affinity profiles have established themselves to be the rule rather than the exception in drug discovery campaigns and among clinically useful drugs for complex multifactorial diseases (Shahid et al., 2012). This is quite evident as multi-target drugs represent 21% of the drugs approved by the Food and Drug Administration (FDA) in the period from 2015 to 2017 (Sanchez-Tejeda, Sanchez-Ruiz, Salazar, & Loza-Mejia, 2020).

In this context, inflammation emerges as a major predisposing factor for many complex diseases. Of particular interest, metabolic disorders, such as insulin resistance, type 2 diabetes, obesity, and their relevant cardiovascular complications, are thought to be driven by a chronic state of inflammation (Hotamisligil, 2006). The multifaceted nature of these diseases requires intervention via targeting multiple underlying inflammatory pathways. In the complexity of the inflammatory response, arachidonic acid (AA) metabolites play a significant role in mediating inflammation besides their homeostatic function. AA metabolism is mainly mediated by two key enzymes: lipoxygenase (LOX) and cyclooxygenase (COX). On one hand, LOX enzymes (5-, -12 or 15-LOX) catalyze the dioxygenation of polyunsaturated fatty acids (PUFA), linoleic acid and AA, producing different oxygenated lipid mediators (Mashima & Okuyama, 2015). On the other hand, the action of COX enzymes (COX-1 or COX-2) on AA leads to the generation of a number of metabolites, including prostaglandin $F_{2\alpha}$ ($PGF_{2\alpha}$), prostaglandin D_2 (PGD_2), prostaglandin E_2 (PGE_2), prostacyclin (PGI_2), and thromboxane A_2 (TxA_2), collectively known as prostanoids (Schauberger, Peinhaupt, Cazares, & Lindsley, 2016). Although, LOXs, COXs, and their corresponding metabolites showcase a physiological and homeostatic importance, a body of research highlighted the involvement of LOX and COX pathways in metabolic diseases (Singh & Rao, 2019; D. Wang & Dubois, 2010). In this context, LOX and COX AA metabolites modulate the activity of a major molecular switch of metabolic and inflammatory processes, peroxisome proliferator-activated receptor gamma (PPARγ)(Mateu, Ramudo, Manso, & De Dios, 2015; Sun et al., 2015), that is intimately intertwined in the complex pathology of these disorders. In the below sections, we highlight the contribution of 15-LOX, COX-2, and PPARγ targets in the etiology of metabolic diseases. More importantly, we present our novel multi-targeting drug ligands (MTDLs), that were designed based on COX-2 and 15-LOX inhibition as well as PPARγ agonism.

1. 15-LOX as a potential target in metabolic disease

a. 15-LOX pathway in inflammation

Lipoxygenases are dioxygenase enzymes that are responsible for the catalysis of dioxygenation of polyenoic fatty acids, such as AA and linoleic acid, yielding peroxidase derivatives (Kuhn, Banthiya, & van Leyen, 2015). The nomenclature of LOXs depends on the location of the carbon in the AA chain on which a hydroxyperoxy- moiety is added (Brash, 1999). Thus, the family of LOXs include 5-, 8-, platelet-type 12(*S*)-, epidermal-type 12(*R*)-, and 15-LOXs (Kuhn, Walther, & Kuban, 2002). 15-LOX is also sub-classified into two isoforms: 15-LOX-1 and 15-LOX-2, whose genes are referred to as *ALOX15* and *ALOX15B* respectively (Kuhn et al., 2002). The LOX pathway generates a plethora of bioactive metabolic products that include leukotrienes, lipoxins, eoxins, resolvins, and others (Kuhn et al., 2015). LOX enzymes metabolize AA into 5-, 8-, 12- and 15-hydroperoxyeicosatetraenoic acids (HPETEs), which are readily transformed to their corresponding hydroxy fatty acids, hydroxyeicosatetraenoic acids (HETEs) (C. Schneider & Pozzi, 2011). Primarily, both 15-LOX-1 and 15-LOX-2 generate 15-HPETE upon metabolism of AA. Yet, 15-LOX-1 can additionally metabolize ω-3 and ω-6 PUFA obtained from food, such as Docosahexaenoic acid (DHA) and linoleic acid, thus forming 17-HPDHA and 13-hydroxyoctadecadienoic acid (13-HODE) respectively (C. Schneider & Pozzi, 2011). Similar metabolites can be produced by both the human reticulocyte-type 15-LOX-1 and leukocyte-type 12-LOX, thus they can be alternatively referred to as 12/15-LOXs (Dobrian et al., 2011). There is a remarkable interspecies variability in the products formed by 12/15-LOX enzymes (Singh & Rao, 2019). The human *ALOX15* mainly yields

15(S)-HETE and small amounts of 12(S)-HETE, whereas its murine orthologue produces both 12(S)-HETE and 15(S)-HETE in 3:1 ratio (Singh & Rao, 2019). Therefore, these differences limit the translational potential of data obtained from animal studies.

b. <u>15-LOX and Vascular Dysfunction</u>

Various studies proved the involvement of 12/15-LOX enzyme in the phenotypic alterations of the endothelial layer under inflammatory conditions, which is characterized by a disruption of endothelial barrier function and enhanced interaction with leucocytes (Pober & Sessa, 2007). Early stages of endothelial dysfunction, also referred to as type I activation of endothelial cells, include the opening of intracellular tight junctions and increased vascular permeability (Pober & Sessa, 2007). *In vivo* and *ex vivo* evidence demonstrated that the major 15-LOX metabolite, 15-(S)HETE, is involved in HFD-induced endothelial tight junction disruption via Src and Pyk2-induced zonula occludens-2 tyrosine phosphorylation and its detachment from the tight junction complexes (Kundumani-Sridharan, Dyukova, Hansen, & Rao, 2013). Moreover, 15-(S)HETE can also induce tight junction opening via PKCε-dependent zonula occludens-1 phosphorylation (R. Chattopadhyay et al., 2014). In more advanced stages of endothelial dysfunction, changes that comprise regulation of gene expression lead to the upregulation of adhesion molecules, hence permitting leucocyte-endothelial interaction. 15(S)-HPETE was shown to induce the upregulation of adhesion molecules in human umbilical vein endothelial cells (HUVECs), thus allowing the transendothelial migration of monocyte-like HL-60 cells (Sultana, Shen, Rattan, & Kalra, 1996). The expression of the intercellular adhesion molecule 1 (ICAM-1) was also elevated in the aortic endothelial cells isolated from 12/15-LO transgenic mice, through RhoA/protein kinase C-dependent activation of the transcription factor NF-kB (Bolick et al., 2005). Such a signaling pathway leading to enhanced monocyte-endothelial interactions was found in the aortic endothelium of atherosclerotic apo$E^{-/-}$ mice (Bolick, Srinivasan, Whetzel, Fuller, & Hedrick, 2006). Selective inhibition of 12/15-LOX prevented monocyte adhesion to aortic endothelium (Bolick et al., 2006). Moreover, the increase in 12/15-LOX-derived eicosanoids, especially 13(S)-HODE, facilitated monocyte-endothelial cell interaction in db/db diabetic mice (Hatley, Srinivasan, Reilly, Bolick, & Hedrick, 2003). It is worth mentioning that the pleiotropic effects of the antihypercholesterolemic drug atorvastatin on endothelial dysfunction was found to be mediated by modulation of *ALOX15* expression in endothelial cells (P. Zhang et al., 2016).

c. <u>15-LOX and Adipose Tissue Inflammation</u>

Given that adipose tissue inflammation is regarded as a hallmark of metabolic diseases, the contribution of *ALOX15* was extensively investigated in inflammation-mediated metabolic alterations. The murine orthologue of *ALOX15* was found to be upregulated in white epididymal fat of high-fat diet (HFD) fed mice (Chakrabarti, Cole, Wen, Keller, & Nadler, 2009). These observations were confirmed by *in vitro* evidence, where fully differentiated murine 3T3-L1 adipocytes exhibited elevated levels of 12/15-LOX in response to treatment with palmitic acid (Chakrabarti et al., 2009). This upregulation of 12/15-LOX in adipose tissue was shown to be implicated in adipose tissue macrophage infiltration and inflammatory cytokine expression in HFD-fed rats (Nunemaker et al., 2008; Sears et al., 2009). Furthermore, 12/15-LOX knock out was also found to be protective against HFD-induced whole body insulin resistance, as confirmed by hyperinsulinemic euglycemic clamp technique (Sears et al., 2009). The notion that adipose 12/15-LOX is responsible for insulin resistance and inflammation was supported by a study, where adipose tissue-specific deletion of 12/15-LOX reduced serum insulin levels and macrophage infiltration respectively (Cole, Morris, Grzesik, Leone, & Nadler, 2012). Recent findings have described a possible role for 12/15-LOX enzyme in mediating ER stress in the adipocytes of HFD-fed mice (Cole, Kuhn, et al., 2012), a mechanism that has been implicated in insulin resistance and diabetes mellitus (Boden, 2009; Boden et al., 2008). Such pro-inflammatory effects of 12/15-LOX was shown to be at least partly mediated by its product 15-(S)HETE. Investigation of adipose tissue of db/db pre-diabetic mice demonstrated an enhanced expression of both 12/15-LOX and 15-(S)HETE (Dobrian et al., 2018). Also, 15-(S)HETE was shown to promote adipogenesis in human bone marrow mesenchymal stem cells (hBMSCs) (Y. S. Song et al., 2016). Human 15-LOX isoforms were reported to have differential expression in the visceral fat of morbidly obese patients (Dobrian et al., 2010).While 15-LOX-2 was detected in both subcutaneous and omental visceral fat, 15-LOX-1 was exclusively found in omental adipose tissue (Dobrian et al., 2010). This selective increase in 15-LOX-1 expression in omental fat may provide a possible mechanism behind the cardiometabolic risk associated with the increase of visceral adipose tissue in obese patients (Dobrian et al., 2010).

2. COX-2 as a potential target in metabolic disease

a. COX-2 pathway in Inflammation

The synthesis of prostanoids is catalyzed by the two isoforms of the COX enzyme: COX-1 and COX-2. Although these two enzymes demonstrate analogy in structure and kinetics, COX-1 and COX-2 exhibit distinctive tissue distribution and regulation mechanisms, which is reflected on the pharmacological and biological level (W. L. Smith, DeWitt, & Garavito, 2000). COX-1, constitutively expressed in most tissues, is the major source of prostanoids that serve homeostatic functions. On the contrary, COX-2, known as the inducible isoform, is responsible for the increased production of prostanoids in inflammatory conditions and proliferative diseases, as in cancer (P. C. Chan, Liao, & Hsieh, 2019; S. G. Harris, Padilla, Koumas, Ray, & Phipps, 2002; Ricciotti & FitzGerald, 2011).

b. COX-2 and Vascular Dysfunction

Although clinical observations report cardiotoxic effects for selective COX-2 inhibitors, these findings are still a subject of controversy. It has been suggested that COX-2 inhibition may still be beneficial in the case of active inflammation within patients with unstable atherosclerotic plaques, where PGE_2 is the predominant prostaglandin (Cipollone & Fazia, 2006). However, this is not the case in patients with a low inflammatory profile, where the use of COX-2 inhibition may be harmful as it inhibits the predominant endothelial PGI_2 (Cipollone & Fazia, 2006). Such a dual role of selective COX-2 inhibition was supported by the results of a study investigating the effect of selective COX-2 inhibitors on atherosclerosis progression in apoE-deficient mice, where coxibs exhibited anti-atherogenic effects in advanced stages while enhancing atherosclerosis progression in early stages (Metzner et al., 2007).

Several lines of evidence support a possible beneficial effect of COX-2 blockade in the context of atherosclerotic vascular dysfunction in metabolic disorders. As demonstrated by the Diabetes Heart Study, elevated levels of COX-2 mRNA expression were found in atherosclerotic plaques of patients with type 2 diabetes (Baldan et al., 2014). COX-2 expression was elevated in arteries of HFD-induced metabolically obese and normal weight rabbits (Alarcon et al., 2018) and was shown to be implicated in the pathogenesis of atherosclerotic lesions in the aortas of apoE$^{-/-}$ mice, partly through facilitating monocyte recruitment by upregulating endothelial adhesion molecules (Jacob, Laury-Kleintop, & Lanza-Jacoby, 2008). Treatment with celecoxib in combination with atorvastatin attenuated the size of atherosclerotic lesions and the expression of adhesion molecules, such as VCAM and MCP-1, in the vessels of apoE$^{-/-}$ mice fed a western diet (Raval, Frank, Laury-Kleintop, Yan, & Lanza-Jacoby, 2010). Linoleic acid was shown to induce monocyte chemotaxis and binding in a COX-2-dependent manner (Matesanz et al., 2012). High dose irbesartan and celecoxib exhibited anti-atherosclerotic properties by inhibition of NF-KB-dependent activation of COX-2 and MMP-9 in in the atherosclerotic aortas obtained from HFD-fed rabbits (L. Li, Li, Yi, Liu, & Lei, 2018).

Moreover, TNF-α- and angiotensin II-induced COX-2 activation is implicated in vascular smooth muscle proliferation (Young, Mahboubi, Haider, Li, & Ferreri, 2000).

Anti-atherosclerotic properties of certain nuclear receptor activators were attributed to their ability to inhibit COX-2 in smooth muscle cells (Rival et al., 2009). COX-2-derived PGD_2 is responsible for phenotypic switching of VSMCs from the contractile to synthetic phenotype, a phenomenon observed in vascular injury and atherosclerosis leading to neointima formation (H. S. Lee et al., 2019). Celecoxib exhibited remarkable inhibitory effects on neointimal hyperplasia, through blocking of Akt activation (H. M. Yang et al., 2004). The enhanced expression of PGE_2 from lipopolysaccharide-stimulated monocytes obtained from 291 subjects was associated with higher mean carotid intima-media thickness, suggesting PGE2 as a potential biomarker in subclinical atherosclerosis (Beloqui et al., 2005). Production of PGE2 might lead to plaque instability and rupture, via induction of matrix metalloproteinase by macrophages (Gargiulo et al., 2018).

c. <u>COX-2 and Adipose Tissue Inflammation</u>

Substantial evidence from human and animal studies has illustrated that COX-2 and COX-derived prostanoids, mainly PGE_2, are responsible for the etiology of obesity-induced adipose tissue inflammation and insulin resistance. This was evident in a HFD-fed rodent model, where selective inhibition of COX-2 by using celecoxib led to an attenuation in adipose tissue infiltration and inflammation, as well as insulin resistance indices (Hsieh et al., 2009; C. H. Lu, Hung, & Hsieh, 2016). Consistent findings were recorded in human adipocytes isolated from obese patients, where both COX-2 and its receptor prostaglandin E receptor 3 (EP3) expression were correlated with higher body mass index values (P. C. Chan, Hsiao, Chang, Wabitsch, & Hsieh, 2016). A recent study proposed that COX-

2/PGE_2/EP3 signaling axis is implicated in the progression of adipose tissue inflammation and insulin resistance (P. C. Chan et al., 2016). As suggested by this study, activation of this pathway enhanced pro-inflammatory adipokine expression, such as monocyte chemoattractant protein 1 (MCP-1) and RANTES, while inhibiting the production of adiponectin, via a NF-κB-mediated mechanism (P. C. Chan et al., 2016). As such, this increase in pro-inflammatory molecules was responsible for driving the recruitment of immune cells, which exacerbates adipocyte inflammation and insulin resistance (P. C. Chan et al., 2016). Furthermore, LC-MS/MS lipidomic analysis of human omental white adipose tissue obtained from obese patients detected elevated PGE_2 levels, attributed to significantly enhanced COX-2 expression in the absence of overexpression of prostaglandin E synthases (Garcia-Alonso et al., 2016). Moreover, there is a growing interest in the role of adipose tissue macrophages (ATMs) in insulin resistance. The amount of ATM accumulating in adipose tissue was found to positively correlated with insulin resistance markers (Weisberg et al., 2003). In fact, HFD feeding in mice promoted a phenotypic switch of ATMs from the anti-inflammatory, protective M2 state towards a pro-inflammatory M1 (Lumeng, Bodzin, & Saltiel, 2007). It has been suggested that COX-2-dependent macrophage migration inhibitory factor (MIF) secretion from hypertrophic and hypoxic adipocytes may underlie the observed phenotypic switch of ATMs through CD74, a transmembrane protein that is part of the MIF receptor complex (P. C. Chan et al., 2018).

3. PPARγ as a potential target

Peroxisome Proliferator-Activated Receptors (PPARs) are members of the nuclear hormone receptor superfamily of ligand-activated transcription factors that regulate various genes implicated in cellular metabolism, proliferation and function (Marx, Duez, Fruchart, & Staels, 2004). After interaction with specific PPAR ligands, PPARs heterodimerize with the retinoid X receptor (RXR), translocate to the nucleus where they undergo a conformational change and consequently transactivate transcription (Berger, Akiyama, & Meinke, 2005). In addition, PPARs can repress the transcription of genes by negatively interfering with other transcription factors independent from DNA binding. PPAR family comprises three members PPARα, PPARβ/δ and PPARγ (Holm, Mønsted, Haupt-Jorgensen, & Buschard, 2020). PPARγ is highly expressed in the adipose tissue where it regulates adipogenesis, lipid metabolism and insulin sensitivity but also in endothelial cells, VSMCs and various immune-related cell types such as macrophages, dendritic cells and microglia (L. Han, Shen, Bittner, Kraemer, & Azhar, 2017). Genetic polymorphisms in PPARγ have been associated with the development of metabolic syndrome, partial lipodystrophy, essential hypertension and insulin resistance (Petrosino et al., 2017; R. M. Rocha et al., 2015). PPARγ agonism with thiazolidinediones (TZDs) has emerged as a therapeutic approach in the treatment of type 2 diabetes (T2D). Nevertheless, PPARγ expression in various cell types and the pleiotropic effects of TZDs suggest a role played by PPARγ in metabolic diseases, inflammation, atherosclerosis, insulin resistance and diabetes.

a. <u>PPARγ in inflammation</u>

PPARγ plays a major role in the regulation of inflammatory pathways in several organ systems. PPARγ drives the alternative activation of macrophages in a myriad of inflammatory diseases thus conferring an anti-inflammatory and pro-resolving response (Chinetti et al., 1998; Linares et al., 2018; Tokutome et al., 2019). The administration of rosiglitazone, a PPARγ agonist ameliorated HFD-induced hepatic steatosis by reducing hepatic TLR4/NF-κB expression and M1-polarized Kupffer cells whereby suggesting an ameliorative role of PPARγ agonism in non-alcoholic fatty liver disease (NAFLD) (Luo, Xu, Wang, Wu, & Hua, 2017; Wu et al., 2020). PPARγ deletion in mouse primary macrophages reduced IL-1 release in response to lipotoxic stimulation by transcriptionally inhibiting the expression of multiple activators of the NLRP3 inflammasome. Conversely, PPARγ activation selectively suppressed IFN-β expression in activated macrophages (Weber et al., 2018). In addition to TZDs, several other molecules have been shown to mediate macrophage alternative activation through PPARγ agonism including statins (Q. Wang et al., 2017; T. Zhang, Shao, & Liu, 2017). Furthermore, PPARγ was also shown to reverse microglial polarization and thus play a neuroprotective effect in inflammatory neurological disorders such as epilepsy, traumatic brain injury, ischemic stroke and Parkinson's disease (Bonato, Bassani, Milani, Vital, & de Oliveira, 2018; He et al., 2018; Hussein, Moghimi, & Roohbakhsh, 2019; Kinouchi et al., 2018; R. Liu et al., 2018; Meng et al., 2019; Peng et al., 2019; Yuan et al., 2017).

b. PPARγ and Vascular Dysfunction

Impaired endothelial PPARγ activity results in excessive oxidative stress, promotes the emergence of a pro-inflammatory phenotype, and enhances the development of atherosclerosis. Age-related vascular dysfunction and inflammation was attributed in part to a perturbed PPARγ function in vascular endothelial cells (De Silva, Li, Kinzenbaw, Sigmund, & Faraci, 2018). In addition, it was found that HFD-induced obesity is associated with a reduction of vascular endothelial PPARγ which resulted in exaggerated inflammation in response to chronic intermittent hypoxia (Y. Zhang, Zhang, Li, & Hou, 2017). PPARγ was found to protect endothelial cells against IL-1β-mediated dysfunction by reducing oxidative stress (Mukohda et al., 2016). Indeed, PPARγ agonism was shown to convey endothelial cell protection against tumor necrosis factor (TNF)-α in humans with an increased cardiovascular risk due to type 2 diabetes (Martens, Rabelink, op 't Roodt, de Koning, & Visseren, 2006). Endothelial PPARγ agonism with TZDs was shown to ameliorate endothelial insulin resistance, protect against high-glucose-mediated endothelial dysfunction and lipopolysaccharide (LPS)-mediated endothelial inflammation (C. Chen et al., 2017; Ji, Ji, Li, Lu, & Luo, 2018; Y. Zhang et al., 2015). Moreover, PPARγ agonism with TZDs enhanced endothelial migration and tube formation (Rudnicki et al., 2016).

c. PPARγ and Adipose Tissue Inflammation

Immune cell infiltration into the hypoxic adipose tissue environment and the subsequent production of proinflammatory cytokines play a pivotal role in driving chronic adipose tissue inflammation. In addition to its roles in adipogenesis and energy metabolism, PPARγ plays a pivotal role in regulating the function of adipose tissue-infiltrating immune cells. In fact, obesity results in a hypermethylation at the PPARγ promoter region promoting the proinflammatory activation of macrophages (X. Wang et al., 2016; X. Yang et al., 2014). Moreover, the deficiency of PPARγ in macrophages favors the predominance of M1 markers in white adipose tissue (Bassaganya-Riera, Misyak, Guri, & Hontecillas, 2009). Resident alternatively activated macrophages were shown to maintain a homeostatic state and were proposed as a useful strategy in the treatment of T2D (Dai et al., 2017; Odegaard et al., 2007). Natural, synthetic and exercise-induced upregulation of PPARγ promoted an anti-inflammatory state either through promoting macrophages alternative activation or through inhibiting the expression of pro-inflammatory genes (Ricote, Li, Willson, Kelly, & Glass, 1998; Ruffino et al., 2016). Indeed, dual PPARα/γ agonism reduced adipose tissue inflammation and dysfunction (D. Kumar et al., 2018). In HFD-fed 129SV mice, rosiglitazone increased the number of adipose tissue-infiltrating alternatively activated macrophages and it was suggested that these macrophages mediated the effects of PPARγ on the expansion and remodeling of the adipose tissue (Stienstra et al., 2008).

It was shown that the perivascular adipose tissue (PVAT) possesses a heightened proinflammatory state in comparison to other fat depots (Chatterjee et al., 2009). HFD-induced PVAT dysfunction exacerbated vascular derangements and interventions targeting PVAT inflammation are emerging as valuable therapeutic approaches in the treatment of vascular complications of metabolic diseases (R. Rafeh, A. Viveiros, Gavin Y. Oudit, & Ahmed F. El-Yazbi, 2020). In addition, Pioglitazone ameliorated PVAT inflammation-mediated arterial stiffness (Chang, Zhao, Garcia-Barrio, Zhang, & Eugene Chen, 2018). We have recently reported that the administration of pioglitazone in a non-obese prediabetic rat model devoid of systemic inflammation, ameliorated PVAT inflammation and vascular dysfunction (M. A. W. Elkhatib et al., 2019).

4. Introducing Multi-targeting Drug Ligands

The underpinning concept of simultaneous targeting of multiple pathways stems from the peculiarities of traditional Chinese medicine (TCM) that have been developed and used for centuries to treat complex diseases (Tang, Zhang, Nie, Yao, & Chen, 2009). TCMs are designed based on the principle of "syndrome differentiation" allowing a match of the pharmacological properties of multiple compounds with the symptoms exhibited by patients (Shao, 2009). Great efforts have been made towards the extraction and isolation of newly identified compounds that have been pivotal to drug discovery and development (Q.-W. Zhang, Lin, & Ye, 2018). Several approaches have been adopted to establish the multiple target network of these compounds taking into consideration the available known drug-target network information to construct complex predictive models to predict ligands and targets (W. Zhang, Huai, Miao, Qian, & Wang, 2019). Indeed, systems pharmacology provided strategies for efficient combination of novel compounds for the treatment of complex diseases (W.-Y. Lee, Lee, Kim, & Kim, 2019). Nevertheless, and in contrast to Western medicine, several issues halt the extensive use of TCMs including the purity of the extract, the overall efficacy, the pharmacokinetic profile of the compounds and their underlying mechanisms of action.

The phenomenon of modulating multiple biomolecular targets was first described by the immensely broad term “Polypharmacology”. Polypharmacology entails either a single agent acting on multiple targets of a specific disease pathway, or a single entity modulating various targets related to multiple disease pathways (Reddy & Zhang, 2013). Moreover, polypharmacology for intricate diseases involves multiple drugs acting on distinct targets, that are implicated in the complex networks regulating several physiological responses (Reddy & Zhang, 2013). Combination and multicomponent therapies also come under the umbrella of this term (Morphy & Rankovic, 2005). As a matter of fact, many drugs possess multi-targeting activities and represent the polypharmacological approach despite not being designed on purpose. For example, Aspirin, is an analgesic, antipyretic and anti-inflammatory medication. Additionally, it has been reported to be used in the prophylaxis of transient ischemic attacks, strokes, pregnancy loss and cancer (Reddy & Zhang, 2013). Also, Sildenafil, the phosphodiesterase inhibitor, was initially intended for hypertension and ischemic heart disease. Nonetheless, it is currently used to treat erectile dysfunction (Reddy & Zhang, 2013).

Evans et al. in 1988 described the concept of privileged structures from a chemistry point of view, which paved the way for the evolution of both the concept and terminology of multi-targeting (Evans et al., 1988; Shahid et al., 2012). By the first decade of this century, Morphy et al. used “designed multiple ligands “ to describe the phenomenon of multi-targeting (Morphy & Rankovic, 2005). However, and according to SCOPUS and PubMed, the term “multi-target directed ligands” and the acronym “MTDLs” were first introduced in 2007 by Bolognesi et al., reporting some quinone-bearing polyamines for the treatment of Alzheimer's disease (Bolognesi et al., 2007). Since then, it is not surprising that most (if not all) Alzheimer's medicinal chemistry papers contain this term or that acronym. In 2010, Metz and Hajduk provided a more comprehensive description of 'multi-targeted' drug design or MTDD as the ability to modulate the activity of multiple protein targets. In essence, this designation can also refer to 'treating complex, heterogeneous diseases that tend to result from multiple molecular abnormalities (such as cancer, cardiovascular, and psychiatric disorders) with a highly specific drug that concertedly modulates two or more targets (Metz & Hajduk, 2010).

In brief, regardless of all the terms used to describe the phenomenon of multi-targeting by a single ligand, the term "multi-target directed ligands or the acronym MTDLs gained much popularity within medicinal chemistry literature and their use have extended from Alzheimer's disease to all other complex disorders. We also envisage setting up a sharp boundary, especially from a medicinal chemistry viewpoint, by reserving the term multi-target designed ligands to single chemical agents modulating multiple (and closely related) targets of a specific disease pathway or distinct targets implicated in highly networked disorders. Moreover, they have to be rationally or purposefully designed and not serendipity based. Simultaneous Modulation of multiple targets that are distantly related or of two or more diseases does not fall under the definition of MTDLs, but still can be included under the umbrella of the broader term "polypharmacology".

The process of rational design and development of MTDLs is definitely a challenging task both in terms of selecting the "right" combination of targets for a certain disease and small molecule discovery (Ramsay et al., 2018). Concerning the former issue, an in-depth understanding of pathway-target-drug-disease relationships (also known as network pharmacology (Hopkins, 2008)), target-disease associations and adverse effects profiling is essential (Ramsay et al., 2018). This will not only result in the identification of compounds with enhanced efficacy and/or safety, but also the introduction of novel target combinations that can lead to synergistic (if targets exist in complementary pathway), additive (if targets are located in the same pathway) or beneficial (such as evading drug resistance) effects (Rastelli & Pinzi, 2015) (Ramsay et al., 2018). In this context, partial inhibition of a specific number of targets can be more rewarding than the total inhibition of a single target, especially when dealing with complex and multifactorial diseases (Rastelli & Pinzi, 2015). Moreover, prediction of the activity profile of ligands on a number of targets is facilitated by computational approaches such as statistical data analysis and bioinformatics, structure-based (docking) and ligand-based (pharmacophore) approaches (Rastelli & Pinzi, 2015).

As for generation of chemical libraries of multi-target ligands, this is classically accomplished by hybridization of more than one pharmacophoric scaffolds, from previously reported compounds or well-known drugs acting on targets of interest, into a single framework. These elements can be combined together either by conjugation, fusion or merging (Ramsay et al., 2018). The former separates the essential pharmacophoric elements for each target, by distinct linker group (cleavable or not) that is absent in either of the selective ligands. In this particular type, some physicochemical limitations may arise. MTDLs can be regarded as “fused” if the pharmacophoric elements are directly connected to each other. The frameworks can be “merged” by overlapping commonalities in the structures of the starting ligands. These result in smaller and simpler molecules (Morphy & Rankovic, 2005; Zhou et al., 2019). Owing to the scope of this review, we refer the reader to the recent review article by Zhou et al to have a deeper perspective about the exact details of each type (Zhou et al., 2019). Proper structure-activity relationship studies should be established for the ligands in order to ensure a balanced degree of modulation for different intended targets while, at the same time, designing-out off-target interactions as much as possible (Ramsay et al., 2018). The latter aspect is of particular relevance when dealing with targets that belong to the same family of proteins (such as multi-target kinase inhibitors) and also with structurally distinct targets but bearing local binding site similarities (Ramsay et al., 2018). In addition, if the targets are unrelated or distantly related to each other, this might necessitate extensive rounds of optimization to identify the best hits (Ramsay et al., 2018). Thus, the successful design of MTDLs is the resultant of many factors, the most important of which is adopting an effective target combination and its balanced modulation in addition to preserving the drug-like characters of the designed compounds. Accordingly, in the context of our interest in the intertwining roles of COX-2, 15-LOX, and PPARγ in inflammatory changes encompassing metabolic disorders and their interaction with vascular dysfunction and diabetic complications, we present the design, synthesis and pharmacological evaluation of COX-2/15-LOX dual-targeting and COX-2/15-LOX/PPARγ triple-targeting compounds.

G. Mild Hyper-Caloric Animal Model

The mild hyper-caloric (MHC) fed animal model that is adopted in our study is a modified form of the high-fat diet (HFD) animal model. HFD, first introduced by Surwett et al.in 1988, is used to study metabolic syndrome and impaired glucose tolerance (Surwit, Kuhn, Cochrane, McCubbin, & Feinglos, 1988; Winzell & Ahren, 2004). In contrast to other animal models, the HFD model permits the investigation of molecular mechanisms during the early stages of diabetes (Winzell & Ahren, 2004). Increased fat intake (20-60% energy as fat) results in weight gain, hyperinsulinemia and eventually hyperglycemia (Buettner, Scholmerich, & Bollheimer, 2007). Since the increased prevalence of type II diabetes has been attributed to the accelerated changes in dietary habits, it is pivotal to select a dietary composition that reflects the western diet rich in refined sugars and saturated fats. Fructose is one component that is enriched in the western diet, particularly present in carbohydrate beverages, syrup additives, and prepared foods (Elliott, Keim, Stern, Teff, & Havel, 2002). The high fat, high fructose fed rat model has been used by many to study vascular and metabolic dysfunction (Balakumar et al., 2016; Hazarika, Kalita, Chandra Boruah, Chandra Kalita, & Devi, 2016; Lozano et al., 2016a; Poudyal et al., 2017). Unlike HFD fed rat model where fasting hyperglycemia was not maintained, long-term (8 months) animal feeding with the combination of high fat and high fructose led to the progression of a more robust phenotype of type II diabetes with stable fasting and postprandial hyperglycemia and increased insulin resistance (Lozano et al., 2016a). The ADA recommends the ideal daily fat intake to range between 20-35 % of energy for management of diabetes and its cardiovascular complication in adults (Evert et al., 2013).

The fat composition of the MHC fed rat model is 38% of energy, that is slightly higher than that recommended by the ADA, however is still within the low range of HFD composition in the literature, thereby minimizing weight again and permitting a longer timeframe for studying the vascular and metabolic pathogenesis before the achievement of diabetes. The body weight gain in this rat model was not significant in comparison to the normal fed rats, thus omitting the interference of obesity. The stable hyperglycemia and impaired glucose tolerance were not observed, and MHC rats responded to glucose intake in the same manner as normal rats after 12 weeks of feeding. This rat model develops stable fasting hyperglycemia after 16 weeks of MHC feeding, thus allowing proper development of pathological mechanisms of cardiovascular complications (M. A. W. Elkhatib et al., 2019). Details of the dietary composition and biometric and biochemical characterization of these rats will be provided in the methods and results section.

CHAPTER II

HYPOTHESIS AND AIMS OF THE STUDY

While ED and ASCVD were thought to initiate after the onset of diabetes, recent studies indicated that ED could occur before hyperglycemia manifests. Despite the cross-talk between NO and EDH mechanisms, studies focused on derangements in NO-dependent pathway in the context of metabolic disease development, and little emphasis was given to alteration in EDH in response to caloric excess. Under such circumstances, adipose tissue inflammation and insulin resistance might contribute to vascular derangement. Thus, we hypothesize that early metabolic impairment, associated with adipose inflammation and insulin resistance, will trigger a lipid-mediated endothelial dysfunction, likely resulting from an inflammation-evoked perturbation of the Nitric Oxide/Endothelium-dependent Hyperpolarization interplay. Amelioration of the potential inflammatory processes via modulation of targets such as COX-2, 15-LOX, PPARγ will result in the improvement of endothelial function in this early stage of metabolic impairment.

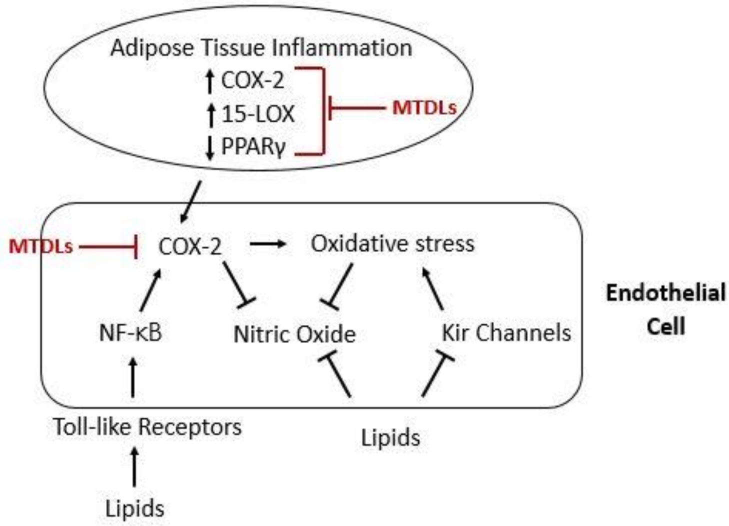

Figure 4**. A schematic representation of the proposed hypothesis**

Our specific aims are:

1. **Investigate the mechanism underlying the early endothelial dysfunction in metabolic disease**
   - Investigate the changes in Kir channels as the main contributors EDH-type relaxation
   - Elucidate the changes in myoendothelial gap junctions in response to metabolic stress
   - Examine the role of oxidative stress in NO pathway impairment following altered EDH and myoendothelial coupling
2. **Elucidate the mechanism underlying the lipid-induced endothelial dysfunction in early metabolic impairment**
   - Assess the effect of lipid-lowering agents on the impaired endothelial phenotype

- Evaluate the effect of free fatty acids on endothelium-dependent relaxation mechanisms *ex vivo*

3. **Assess the impact of anti-inflammatory approaches on the observed pathological alterations *ex vivo***

    - Evaluate the effect of MTDLs on free fatty acid-induced impairment of endothelium-dependent mechanisms *ex vivo*

CHAPTER III

METHODS

A. Ethical Approval

All animal experiments were conducted according to an experimental protocol approved by the Institutional Animal Care and Use Committee at the American University of Beirut in compliance with the Guide for Care and Use of Laboratory Animals of the Institute for Laboratory Animal Research of the National Academy of Sciences, USA.

B. Rationale for Drug Design and Synthesis

1. COX-2/15-LOX Dual-targeting compounds

The design of the dual COX-2/15-LOX targeting compounds were based on five main lead structures: 1) phenolic arylidene thiazolidinones darbufelone (Structure I, Figure 5) (Y. Song et al., 1999), 2) CI-987 (Structure II, Figure 5) (Mullican et al., 1993) that showed low ulcerogenicity and potent COX/LOX inhibitory activity, 3) morpholinoethyl thiazolidin-4-ones (Structure III, Figure 5), which reduced ear oedema in mice and possessed COX inhibitory activity (Pires Gouvea et al., 2016), 4) the pyrazoline derivative (Structure IV, Figure 5) reported by Abdellal et al., which showed more selectivity than celecoxib towards COX-2 and more potency than meclofenamate sodium towards 15-LOX (Abdelall & Kamel, 2016), and 5) the pyrazole-containing hydroxamic acid COX/LOX inhibitor, tepoxalin (Structure V, Figure 5), which was authorized for use in veterinary settings in the European Union and the United States under the brand name Zubrin® for the relief of pain associated with musculoskeletal disorders (Curry, Cogar, & Cook, 2005). In view of the above facts, we envisioned that a hybrid design that combines both pyrazolyl and thiazolyl privileged scaffolds might be a good candidate for a dual COX-2/LOX inhibitor. In addition, we reasoned that adding a cyclized secondary amine moiety (such as; morpholine, piperidine and piperazine) might enhance the anti-inflammatory activity as indicated by several reports (Kaur, Devi, Kumari, Devi, & Banerjee, 2018; Pires Gouvea et al., 2016; Shaquiquzzaman et al., 2015).

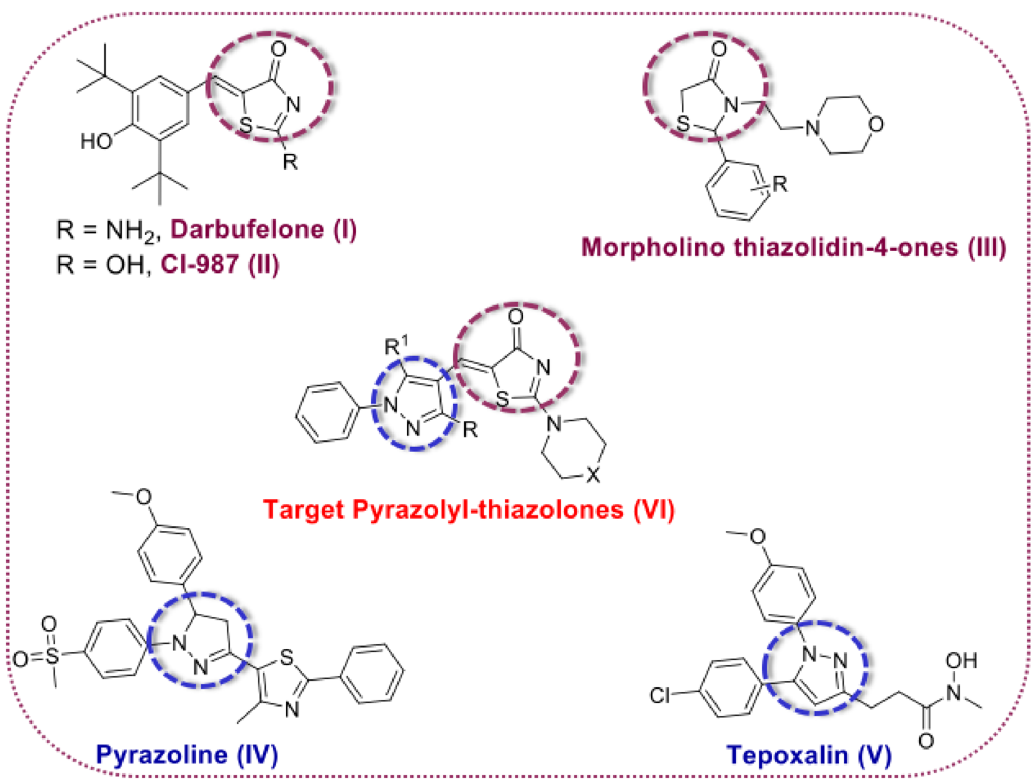

Figure 5. Rationale for the design of COX-2/15-LOX dual-targeting compounds

2. COX-2/15-LOX/PPAR Triple-Targeting Compounds

Thiazolidine-2,4-diones (TZDs)/rhodanines constitute diverse scaffolds that are known to exert a vast array of pleiotropic benefits, including insulin-sensitizing, anti-inflammatory and antiproliferative activities (Chadha, Bahia, Kaur, & Silakari, 2015; Kaminskyy, Kryshchyshyn, & Lesyk, 2017; Naim et al., 2017). They were also reported to prevent the progression of atherosclerotic lesions in patients with type 2 diabetes (B. R. Kumar et al., 2011). Over and above, telmisartan-rosiglitazone hybrid molecules were evaluated as dual PPARγ agonists/angiotensin II antagonists for management of metabolic syndrome (Chittiboyina et al., 2009). In particular, TZDs, known as high-affinity PPARγ agonists, have been introduced into clinical practice for the treatment of type 2 diabetes (B. R. Kumar et al., 2011). Thus, in our search for multi-target anti-inflammatory leads with potential efficacy in metabolic disorders, and based on the structural features of four pleiotropic lead compounds; LYSO-7 (**A**) (Rudnicki et al., 2016; Santin et al., 2013), pioglitazone (**B**), a reported LOX-inhibiting thiazolidinedione (**C**) (Choi et al., 2011) and a dual COX-2 / 15-LOX inhibitor (**D**) (Moussa et al., 2018) recently reported by our laboratory, we adopted a pharmacophoric molecular hybridization approach to design and synthesize some novel triazolyl-thiazolidinedione/rhodanine hybrids as potential simultaneous COX-2/LOX inhibitors and PPARγ agonists. It is worth mentioning that developing a small molecule modulating these three targets was not encountered before. Over and above, the designed assembly has its pharmacophoric parts rooted from pioglitazone. It comprises the essential pharmacophore TZD or its rhodanine bioisostere. This pharmacophore is decorated with a methoxybenzylidene group like compounds A and

C (Figure 6), which in turn is connected to the 1,2,3-triazole moiety. This should retain the 3-carbon atom spacer between the oxygen of the phenoxy- linker and nitrogen atom of the pyridine ring (as in pioglitazone) or N-1 of the triazole nucleus (in our designed compounds). Substitution pattern at N-1 of the triazole ring with various aryl and aralkyl groups is attempted to grant variable electronic and lipophilic environments to investigate their effect on the anticipated biological activity and with the hope of achieving better binding interactions with the potential biological targets. In addition, our design agrees with the three-module framework proposed by Pirat *et al.* to represent PPARγ agonist glitazones (Pirat et al., 2012). It is composed of an acidic polar head group, TZD or rhodanine, joined to a hydrophobic tail through an aromatic linker (Pirat et al., 2012). We altered the tail group to afford chemical and biological uniqueness while conserving the polar head and the linker regions (Pirat et al., 2012). Our tail moiety was carefully chosen to be 1,4-disubstituted-1,2,3-triazole which is a pharmacophore we recently reported to show dual COX-2 and LOX inhibitory activity (Structure D, Figure 6) (Moussa et al., 2018). Furthermore, target compounds were mapped out with a benzylidene attachment between the polar head and the linker instead of the usual benzyl, which is one distinct difference from pioglitazone. We thought that this would be more convenient since recent reports indicated benzylidene TZD derivatives are endowed with partial PPARγ agonistic properties, which retain the desired pharmacological actions while avoiding the untoward adverse effects (Silva et al., 2016; Yasmin et al., 2017). To the best of our knowledge, the click chemistry-derived 1,4-disubstituted-1,2,3-triazoles have not been explored before for their synchronous PPARγ agonistic and COX-2/LOX inhibitory activities. Together with their wide-ranging biological activities, bioorthogonal nature, being non-classical bioisosteres of the amide group and their propensity to be involved in hydrogen bond and π-π stacking interactions with potential targets (Silva et al., 2016), it would be tempting to employ this easily accessible structural motif into the aforementioned framework.

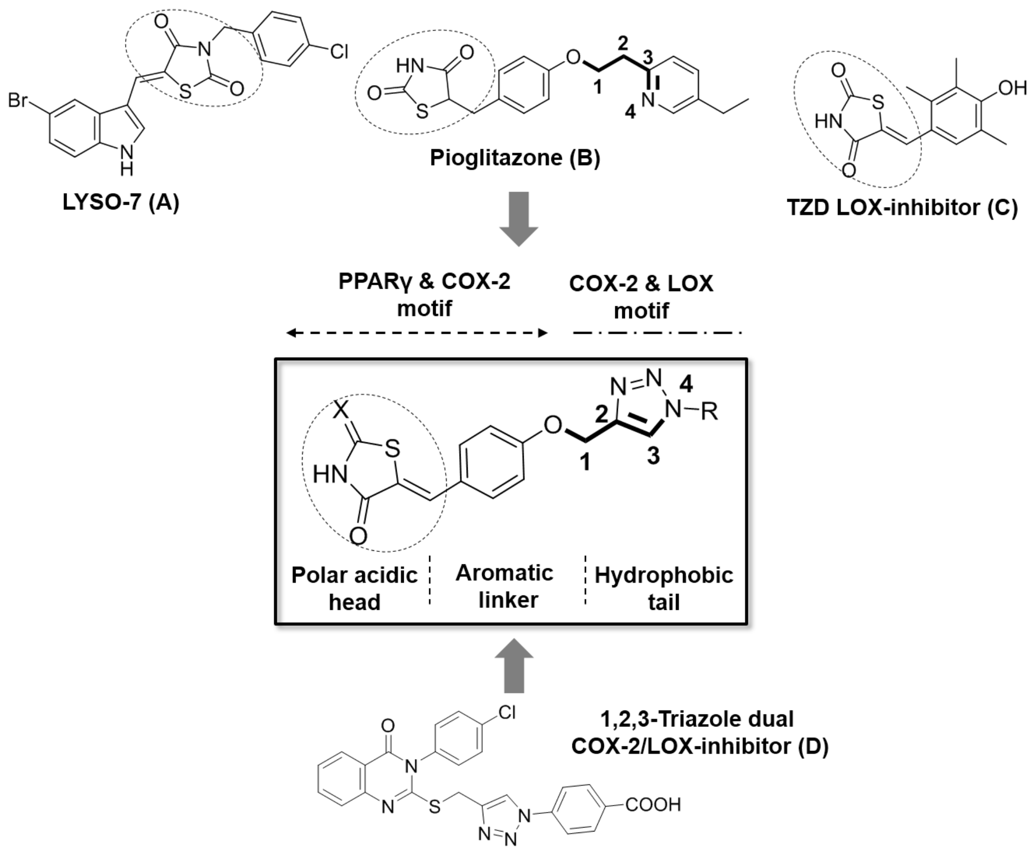

Figure 6**. Rationale for the design of the triple-targeting compounds.**

C. Experimental Design

Male Sprague-Dawley rats (5-6 weeks of age; 150 g) were randomly divided into three groups (7 rats per group): (1) rats fed with normal chow (control, 3 Kcal/g), (2) rats fed with mild hypercaloric diet (HC, 4.035 Kcal/g) for 12 weeks (3) rats fed with mild hypercaloric diet for 12 weeks and treated with 20 mg/kg atorvastatin once daily at week 8. All rats had free access of food and water throughout the 12-week period. Rats were kept in a temperature- and humidity-controlled room, in a 12-hour light/dark cycle. Body weight was measure weekly. The treatment group received atorvastatin incorporated with the HC chow. The calculated dose was geometrically mixed with a 5 g HC diet pellet. The drug-containing food pellet was administered once daily starting week 8 and continued for four weeks till the end of the twelve-week feeding period. Ad libitum access to HC diet resumed after the drug-containing 5 g pellet was consumed. HC diet was administered to the HC-fed group in the same manner during that period.

D. Food Preparation and macronutrient composition

HC diet was prepared as described previously (Al-Assi et al., 2018; Mohammed A. W. Elkhatib et al., 2019). Normal chow diet (ENVIGO) was obtained from Teklad Rodent Diets (Madison, WI). This diet offers 3 Kcal/g divided as follows: 54% from carbohydrates, 32% from protein, and 14% from fat (0.9% saturated fat by weight). The HC diet was prepared in-house and consists of food grade fructose (20% by weight, Santiveri foods, Spain) and hydrogenated vegetable oil (Mazola®, 15% by weight, BFSA) added to the normal chow diet. Major electrolytes and vitamins were supplemented to match the concentration in ENVIGO diet and as recommended by the American Institute of Nutrition (Reeves, Nielsen, & Fahey, 1993). The final composition of the HC diet was confirmed by bomb calorimetry and found to be: by weight (calorie content) 18.06% fat

(38.68%, 5% saturated fat by weight), 15.8% protein (15.66%) and 46.13% carbohydrates (45.73%).

E. Blood Chemistry

Total serum cholesterol, serum insulin, random blood glucose levels, and glucose tolerance were assessed in all groups. Rats were fasted in metabolic cages with free access to drinking water for either 6-8 hours prior to glucose tolerance testing or 12 hours for cholesterol measurement. Blood samples (0.7 ml) were taken by retro-orbital bleeding and centrifuged at 4000 rpm for 10 minutes. The supernatant serum was isolated and stored at -80°C till the time of analysis. Total serum cholesterol was measured using electrochemiluminescence on a Cobas 6000 reader (Roche Diagnostics, Basel, Switzerland). Measurement of rat insulin in serum was carried out using a rat insulin ELISA kit (Thermo-Fisher Scientific, Waltham, MA) according to manufacturer's protocol. Intraperitoneal glucose tolerance was evaluated in fasting rats as described previously (Lozano et al., 2016b) following a 2 g/Kg intraperitoneal glucose load. Glucose was measured in blood droplets collected by a tail prick at baseline, 15, 30, and 60 minutes using Accu-check Performa glucometer (Roche Diagnostics, Rotkreuz, Switzerland).

F. Non-invasive blood pressure measurement:

Non-invasive blood pressure measurement was done by tail-cuff using CODA High Throughput Monitor (Kent Scientific, Torrington, CT) (Y. Wang, Thatcher, & Cassis, 2017). Blood pressure data were collected at the end of week 11 of feeding. Any irregular or unacceptable recording noted as a false recording by the system was excluded. The parameters obtained are: systolic, diastolic, mean arterial blood pressure, and heart rate.

G. *In Vitro* Aortic Vessel Reactivity

At the end of the 12-week period, the rats were anesthetized by isoflurane and sacrificed by decapitation. The thoracic cavity was exposed and the thoracic aorta was isolated for tension measurements as outlined in previous studies (El-Mas et al., 2011; Kimmoun et al., 2015; Plane et al., 2005). Specifically, thoracic aorta was excised from beneath the aortic arch to immediately above the diaphragm and dissected free of connective tissue. Aortic rings 0.3-0.5 cm in length were used for contractility experiments. The rings were assigned to experiments in the same given order among all groups in such a way that rings from equivalent positions were used to perform the same assay across all groups. The rest of the rings were flash frozen in liquid nitrogen and stored at -80˚C. Aortic rings were mounted in a multichannel organ bath system (World Precision Instrument, Inc.). Each ring was suspended in a 15-ml oxygenated Krebs solution organ bath (NaCl 118 mM, KCl 4.7 mM, $MgSO_4.7H_2O$ 1.2 mM, $NaHCO_3$ 25 mM, $CaCl_2.2H_2O$ 2.5 mM, KH_2PO_4 1.2 mM, Glucose 11.1 mM; pH 7.4 upon aeration with 95%O_2/5%CO_2 gas mixture). The bath was constantly aerated with 95% O_2 / 5% CO_2 gas mixture and temperature was maintained at 37˚C. Digital recording of changes in aortic tissue tension was performed using Transbridge TBM4M force transducer (World Precision Instrument, Inc.) and an Acqknowledge 3.9.1 data acquisition system (World Precision Instrument, Inc.). The aortic rings were exposed to a resting tension of 2 grams and allowed to stabilize for 1 hour, during which rings were washed with Krebs solution and tension was adjusted.

Our recent findings in this rat model (Mohammed A. W. Elkhatib et al., 2019) indicated signaling changes in the aortic smooth muscle layer in response to phenylephrine stimulation and increased ROS production, possibly interfering with endothelial function. Thus, we opted to use a fixed concentration of the contractile agonist to expose the tissue to the same stimulus to be better able to assess the myoendothelial feedback. This approach was used previously despite changes in the initial contractile tone (Fleischhacker et al., 1999; Keegan, Walbank, Cotter, & Cameron, 1995; McNally et al., 1994; Oyama, Kawasaki, Hattori, & Kanno, 1986; Pieper & Gross, 1988; Shaligram et al., 2018; Taylor, McCarthy, Thomas, & Poston, 1992). Aortic tissues were constricted with phenylephrine (30 μM) or U-46619 (0.5 μM) (Plane & Garland, 1996). The concentration of PE used to constrict the aortic rings was selected within the upper submaximal range obtained from PE concentration-response curves conducted in preliminary experiments to accentuate the difference between control and HC-fed rats allowing dissection of the role of individual endothelial pathways. Nevertheless, to confirm the findings in experiments with different initial contractile tone, an additional set of experiments were conducted using equi-effective concentrations of phenylephrine (10^{-6}-10^{-5} M to produce ~1 g tension) and a reduced concentration of U46619 (0.1 μM to produce ~ 3g tension). Aortic endothelial vasoreactivity was assessed by response to acetylcholine (ACh, $1x10^{-9}$-$1x10^{-4}$ M) (Grizelj et al., 2015), or diazoxide (100 μM). Several concentrations of diazoxide, within the range of $1x10^{-7}$ -$1x10^{-4}$ M were tested and a concentration of $1x10^{-4}$ M was selected as it produced reproducible relaxations of a considerable magnitude. The sensitivity of ACh-mediated relaxation to a number of blockers (Table 1) was assessed. Effect of ACh was represented as percentage of residual constriction calculated based on 100% contraction of PE/U-46619.

In order investigate the effect of FFAs on endothelium-dependent mechanisms, aortic rings obtained from twelve-week old control male rats were incubated with 800 μM of the free fatty acid palmitic acid (PA) for 4 hours. Afterwards, rings were constricted with phenylephrine (30 μM). Aortic endothelial vasoreactivity was assessed by response to acetylcholine (ACh, $1x10^{-9}$-$1x10^{-4}$ M). Corresponding treatment with MTDLs, reference compounds, or blockers (Table 1) were added 30 min prior to constriction with PE.

Table 1: Concentrations of different agents used in vascular reactivity experiments.

Name	Supplier	Concentration	Vehicle
Phenylephrine	ICN Biochemicals	30 μM	Water
U46619	Sigma (St. Louis, MO)	0.5 μM (Plane & Garland, 1996)	DMSO
Acetylcholine (ACh)	ICN Biomedicals	$1x10^{-9}$-$1x10^{-4}$ M (Grizelj et al., 2015)	Water
Diazoxide	Sigma (St. Louis, MO)	100 μM	DMSO

L-NAME	Sigma (St. Louis, MO)	100 μM (Grizelj et al., 2015)	Water
Apamin	Tocris Bioscience	1 μM (Martinez-Orgado, Gonzalez, Alonso, & Marin, 1999)	Water
Tram-34	Sigma (St. Louis, MO)	1 μM (Wei et al., 2018)	DMSO
$BaCl_2$	Mallinckrodt chemical works	30 μM (Subramaniam, Achike, & Mustafa, 2009)	Water
Indomethacin	Sigma (St. Louis, MO)	10 μM (Roghani-Dehkordi & Roghani, 2016)	DMSO
Atrasentan	Sigma (St. Louis, MO)	10 nM (Thakali, Galligan, Fink, Gariepy, & Watts, 2008)	DMSO
18-β-glycyrrhetinic acid (18-β-GA)	ICN Biomedicals	100 μM (M. L. Rocha et al., 2008)	DMSO

SOD	Sigma (St. Louis, MO)	200U/ml (Tep-areenan, Wetchasit, & Sawasdee, 2015)	Water
4b (Triple targeting compound, COX-2/15-LOX inhibitor, PPARγ partial agonist)	-	10 μM	DMSO
7 (Dual targeting compound, COX-2/15-LOX inhibitor)	-	10 μM	DMSO
Pioglitazone (PPARγ full agonist)	-	10 μM	DMSO
Celecoxib (selective COX-2 inhibitor)	-	0.1 μM	DMSO

H. Cerebral Arterial Pressure Myography

After decapitation, the brain was immediately removed and placed in an ice-cold buffer solution containing (NaCl 130 mM, KCl 4 Mm, $MgSO_4.7H_2O$ 1.2 mM, $NaHCO_3$ 4 mM, $CaCl_2.2H_2O$ 1.8 mM, HEPES 10 mM, KH_2PO_4 1.18 Mm, Glucose 6 mM, EDTA 0.03 Mm, pH 7.4). Rat middle cerebral artery was isolated from surrounding connective tissue and dissected into segments of 2-3 mm of length. Cerebral artery segments were mounted in a chamber attached to a pressure myograph (DMT, Hinnerup, Denmark) for measurement of arterial diameter. Arteries were allowed to warm up to 37˚C and equilibrate for 15-20 min at 10 mm Hg. The vessels were then pressurized to 60 mmHg and allowed to develop a stable myogenic tone over 30 min. Pressure was then dropped to 20 mmHg and then increased again to 80 mmHg in a series of pressure steps until a reproducible myogenic response is obtained. Endothelial function was evaluated using ACh (10 μM) in the presence or absence of potassium channel blocker $BaCl_2$ (30 μM) at 80 mm Hg. The vasodilatory effect of ACh was estimated as a percentage of the active tone produced at 80 mm Hg defined as the difference in the vessel diameter in normal and calcium-free buffer solution with 2 mM EGTA.

I. Quantitative Polymerase Chain Reaction (Q-PCR):

Q-PCR was performed as described previously (Al-Assi et al., 2018). Total RNA was extracted from aortic tissue using RNeasy Mini kit with DNase treatment (Qiagen, Hilden, Germany) and first strand cDNA was produced with the Sensiscript RT kit (Qiagen, Hilden, Germany) with oligo d(T) primer. Primer pairs for rat Kir2.1, Kir2.2, Cx37, Cx40, Cx43, and Cx45, and GAPDH were designed and obtained from Sigma (St. Louis, MO). Primer sequence was Kir2.1 (KCNJ2), forward AAAGCGTGTGTGTCTGAGGT, reverse ATCGGGCACTCGTCTGTAAC; Kir2.2 (KCNJ12), forward CCACTGACCGAGAAGTGCCC, reverse ATCGTAGCCCGTAGCCAATG; Cx37 (Gja4) forward

TTGACCACCGAGGAGAGACT, reverse AGCCCCAGAGCCCTATACAT; Cx40 (Gja5) forward CCAGTCTCCAACACTTGGCA, reverse GCGGAAAATGAACAGGACGG; Cx43 (Gja1) forward TTCATTGGGGGAAAGGCGTG, reverse CTGGGCACCTCTCTTTCACTT; Cx45 (Gjc) forward GTTAACAGGGCAAACCAATTCCA, reverse AGATGGACTCTCCTCCTACCG and GAPDH forward AGACAGCCGCATCTTCTTGT and, reverse CTTGCCGTGGGTAGAGTCAT. Q-PCR was carried out with SYBR-Green and threshold cycle was established using Bio-Rad iCycler (Hercules, CA). Transcript abundance was computed by the $2^{-\Delta\Delta Ct}$ method with GAPDH as a reference.

J. Western Blotting

Western blotting was carried out as described in our previous studies (Al-Assi et al., 2018; El-Yazbi, Abd-Elrahman, & Moreno-Dominguez, 2015; Moreno-Dominguez et al., 2014). Briefly, aortic tissue samples stored at -80˚C were crushed under liquid nitrogen. 50 mg of aortic tissue were added to a 1 ml protein extraction buffer composed of 100 mM dithiothreitol, 1% sodium dodecyl sulphate (SDS), 0.9% NaCl, and 80 mM Tris hydrochloride (pH 6.8). Preliminary experiments were done to optimize tissue amounts needed for protein extraction. Samples were heated at 95˚C for 10 min and left overnight on a rocking shaker at 4˚C. Aliquots of equal protein content were loaded on a 10% sodium dodecyl sulphate polyacrylamide gel electrophoresis, and the separated proteins were transferred and fixed on a nitrocellulose membrane. Membranes were then blocked with 5% skimmed milk and TBST (Tris-buffered saline with 0.1% Tween 20) for 2 hours at room temperature (RT). The membranes were then incubated with a dilution of the primary antibody in 1% skim milk and 0.1% TBST (1:200 for rabbit polyclonal anti-Kir2.1, 1:500 for anti-phospho-Akt Thr308, 1:1000 for rabbit polyclonal anti-Akt, and 1:1000 for rabbit polyclonal anti-caspase 3, Abcam, Cambridge, UK; 1:1000 for rabbit polyclonal anti-Cx43, Sigma-Aldrich, St. Louis, MO; 1:1000 for rabbit polyclonal anti-phospho-eNOS Ser1177, rabbit polyclonal anti-eNOS, 1:500 for rabbit polyclonal anti-IL-1β and 1:1000 for rabbit monoclonal anti-GAPDH, Cell Signaling, Danvers, MA) overnight at 4˚C. Afterwards, the membranes were washed with 0.02% TBST (4 x 5min) and incubated with 1:40,000 biotinylated goat anti-rabbit Ig secondary antibody (Abcam, Cambridge, UK) in 0.1% TBST for one hour at RT. Membranes are then washed with 0.02% TBST (4 x 5min) and incubated with 1:200,000 HRP-conjugated streptavidin (Abcam, Cambridge, UK) in 0.1% TBST for 30 min at RT. After washing with 0.02% TBST (2 x 5min) and TBS (2 x 5 min), membranes were developed using Clarity Western ECL substrate for 5 min prior to image detection by Chemidoc imaging system (BioRad, Hercules, CA). ImageJ software was used to measure optical density of protein bands. A ratio of arbitrary density units was obtained for the protein band of interest and the density of the band representing total protein for p-eNOS and p-AKt after stripping and re-probing, while eNOS, Cx43, and Kir2.1 bands were normalized to GAPDH. Membrane stripping was done using freshly prepared mild stripping buffer (15 g glycine, 1 g SDS and 10 ml Tween in 1 L of ultrapure water, pH 2.2). Membranes were inserted in enough volume of the buffer to be covered at RT for 5-10 min. Buffer was discarded and another volume was added for 5-10 min. Afterwards, membranes were washed with 0.5% TBST (2 x 5min) and then with TBS (2 x 5 min), and used for re-probing.

K. Histopathological and fluorescent microscopy

1. DHE Staining

Aortic tissue sectioning and staining was done as described previously (Al-Assi et al., 2018). Dihydroethidium (DHE) staining was performed on cryosections to demonstrate reactive oxygen species (ROS) load. Fluorescent images were obtained using a Zeiss Axio inverted microscope (Carl Zeiss, Germany) through the Alexa Fluor 568 filter for the DHE red fluorescence and measured against the green collagen autofluorescence obtained through the Alexa Fluor 488 filter. Images were taken from three sections for each animal. The obtained images were analyzed using Zen software.

2. Hematoxylin & Eosin (H&E) staining

Serial sectioning and staining of formalin-fixed PVAT segments were performed simultaneously for accurate comparison as previously described (Al-Assi et al., 2018). Hematoxylin & Eosin staining was used for gross examination of tissue structure.

L. Flow Cytometry

Stromal vascular cells were isolated from freshly dissected PVAT as described previously (Cho, Morris, & Lumeng, 2014). CD45/CD68/CD86 staining was used to identify M1 polarized macrophages, while M2 macrophages were identified by CD45/CD68/CD163 staining (Rubio-Navarro et al., 2016). An aliquot of the stromal fraction containing cells was incubated in FACS buffer with DAPI (1:100), 1:50 APC-

Cy780-conjugated anti-CD45, 1:10 PEconjugated anti-CD68, 1:125 FITC-conjugated anti-CD86 (Thermo Fisher Scientific, Waltham, MA), and 1:200 APC647-conjugated anti-CD163 (Bioss Antibodies, Woburn, MA) on ice for 30 minutes in the dark. Cells were gently washed for three times and resuspended in FACS buffer. Stained cells were counted using a BD FACS Aria Cell Sorter (BD Biosciences, San Jose, CA) and M1/M2 ratio was determined. Antibody-beads mixtures, fluorophore-conjugated isotypes, and unstained cells were used to set compensation and gating. Cellular Debris were removed and alive singlet cells were selected from the acquired events based on the height and area of the forward and side scatters and negativity for the DAPI stain. Thereafter, the subsequent identification of leukocytes (CD45+), macrophages (CD45+,CD68+), M1 macrophages (CD45+,CD68+,CD86+), and M2 macrophages (CD45+,CD68+,CD163+) was done according to the gating strategy depicted in figure 18 and 19.

M. *In vitro* COX-1/2 inhibition assay

All synthesized compounds were subjected to an in vitro COX-1/COX-2 inhibition assay using an ovine COX-1/human recombinant COX-2 assay kit (Catalog no. 560131; Cayman Chemicals Inc. Ann Arbor, MI, USA). The half maximal inhibitor concentrations (IC50 µM) were determined and the selectivity index (SI) values were calculated as IC50 (COX-1)/ IC50 (COX-2). Celecoxib (selective COX-2 inhibitor), diclofenac and indomethacin (non-selective COX inhibitors) were used as references for COX inhibition assay.

N. *In vitro* 15-LOX inhibition assay

Synthesized compounds were subjected to *in vitro* lipoxygenase inhibition assay using soybean 15-LOX assay kit (Catalog no. 760700; Cayman Chemicals Inc. Ann Arbor, MI, USA). Both soybean LOX and human 15-LOX are structurally similar in terms of the presence of both C-terminal catalytic domain and N-terminal membrane binding domain (Sadeghian & Jabbari, 2016). Also, their catalytic domains display a high level of conservation. More specifically, within 10 Angstrom of the catalytic binding site they show more than 50 % identity (Sadeghian & Jabbari, 2016). Hence, soybean LOX has been used by a lot of research groups as a valid model to gauge the ability of many novel compounds to inhibit human 15-LOX (Sadeghian & Jabbari, 2016). *In vitro* 15-LOX enzymatic inhibitory activities are expressed as IC_{50} values of the tested compounds. The universal LOX inhibitor, nordihydroguaiaretic acid (NDGA) (Q. H. Chen, Rao, & Knaus, 2006; Meyers et al., 2009) and selective 12/15-LOX inhibitor quercetin (Sadik, Sies, & Schewe, 2003; I. Schneider & Bucar, 2005), and the LOX inhibitory drug meclofenamate were used as positive controls for LOX inhibition assay.

O. *In vivo* inflammatory models

The *in vivo* anti-inflammatory activity of compounds was assessed both in acute and chronic inflammatory models by using the formalin-induced paw edema (Subramanium, 2015) and cotton pellet-induced granuloma screening protocols (Mishra et al., 2011), respectively. Diclofenac sodium (5 mg/kg) and celecoxib (5 mg/kg) were used as references. Animals were randomly split into six groups, where each group consisted of six rats, and was treated with different test compounds. Sets treated with celecoxib and diclofenac sodium acted as reference and those given the vehicle only (DMSO) were used as control.

1. Formalin-induced paw edema test (acute inflammation model)

A freshly prepared 5% formalin solution (prepared from 37% formaldehyde and saline (Merck, Germany)) was used as a phlogistic agent. Test and reference compounds (5 mg/kg body weight) were dissolved in DMSO and given orally with gastric gavage once per day for seven consecutive days, whereas DMSO was administered to the control group. On the 8th day, the initial paw volume was determined by a Vernier caliper. Then, a subcutaneous injection of 40 μl formalin was introduced into the right hind paw of all groups under light ether anesthesia. The paw volume was measured 4 h after the formalin injection and the edema volume was calculated by the difference in paw volume before and 4 h after the formalin injection. The percentage inhibition of edema (or % protection against inflammation) was calculated for each compound as previously reported (Subramanium, 2015).

2. Cotton pellet-induced granuloma assay (chronic inflammation model)

The rat abdomen was prepared by shaving and swabbing with 70% ethanol then two sterilized cotton pellets (each weighing 20 ± 1 mg) were subcutaneously implanted, on both sides of the abdomen under xylazine/ketamine anesthesia (intraperitoneally, 9 mg/kg and 50 mg/kg, respectively). Intramuscular gentamycin injection (4 mg/kg) was used for three days after the experiment to guard against post-operative infection. Test compounds, celecoxib, diclofenac sodium or vehicle (DMSO) were administered orally as before. On the 8th day after implantation, rats were subjected to light ether anesthesia. The pellets were excised, dried at 60^{0}C for 24 h and weighed after cooling. The mean weights of the dried cotton pellets of all groups were calculated then % granuloma inhibition of all compounds was calculated relative to control (Mishra et al., 2011).

P. Monocyte-to-macrophage differentiation assay

Monocytes were cultured and differentiated as described previously (Vasamsetti et al., 2015). THP-1 cells (human acute monocytic leukaemia lineage, American Type Culture Collection, Manassas, VA) were seeded at a density of 20x10^{5} cells/ml. A set of cells were exposed to 25 nM of phorbol myristate-acetate (PMA, Calbiochem, Darmstadt, Germany) for 24 hours to drive differentiation. Another set was similarly treated with PMA followed by 100 ng/ml of lipopolysaccharide (LPS, invivogen, San Diego, CA, USA) for 72 hours. After incubation, the supernatant was aspirated and the density of the adherent cells was estimated using MTS colorimetric cell viability kit (Abcam, Cambridge, UK). The inhibitory actions of different compounds on the differentiation process were evaluated by pre-incubation with different concentrations of each compound for 6 h. Cell viability after treatment was normalized to the reading after PMA exposure following a 6-hour incubation with DMSO. All experiments were conducted in triplicates. A positive control for the effect of COX1/COX2 inhibition on monocyte-to-macrophage differentiation was obtained by treatment with diclofenac. IC_{50} values for each compound were determined by non-linear regression as the best fit values of the log [inhibitor] vs. response curve using GraphPad Prism software.

Q. Cytotoxicity assay

To confirm that the previous observations were a consequence of interference of the compounds with the differentiation process rather than a reduction in monocyte viability, THP-1 monocytes were incubated with different concentrations of the compound for 30 hours. No difference in cell viability was detected. Moreover, the cytotoxic effects of the drugs on differentiated macrophages were evaluated. Following the incubation of THP-1 cells with 25 nM PMA for 24 hours and 100 ng/ml LPS for 24 hours, the differentiated macrophages were treated with different concentrations of the compounds for 24 hours. Cell viability was assessed using MTS colorimetric cell viability kit (Abcam, Cambridge, UK).

R. Caspase-3 activity determination

THP-1 cells were activated with 25 nM PMA for 24 hours, followed by 100 ng/ml LPS for 4 hours. For treatment, cells were exposed to 100 μM of the test compounds. Afterwards, adherent macrophages were detached using 2.5% trypsin in PBS (abcam, Cambridge, UK). Caspase activity was assessed using the Caspase-3 Assay Kit (Abcam, Cambridge, UK). Measured activity was normalized to sample protein concentration determined by Bradford protein assay.

S. *In vitro* glucose uptake using rat hemi-diaphragm model

Reagent preparation and testing procedures for glucose uptake using in vitro rat hemi-diaphragm model of the tested compounds were carried out following the instructions in accordance with a previously reported method. In brief, rats weighing 150-250 g were used. The animals were euthanized under ether anesthesia and diaphragms were taken out swiftly avoiding trauma and divided into two halves and weight was noted. The hemi-diaphragms were then rinsed in cold Tyrode solution (without glucose) to remove any blood clots and used accordingly. The glucose content of the working solutions was measured by GOD/POD enzymatic method using VITRO SCIENT glucose kit. The working solutions (n=3) were categorized as follows:

- A negative control that was provided by 2 ml of Tyrode solution with 2000 mg/l glucose with and without regular insulin (Novo Nordisk, 40 IU/ml) 5 µl containing 0.2 units of insulin.
- Test solutions which contained 2 ml of Tyrode solution with 2000 mg/l glucose and 2 mg of the test compound with and without regular insulin (Novo Nordisk, 40 IU/ml) 5 µl containing 0.2 units of insulin.
- A positive control which contained: 2 ml of Tyrode solution with 2000 mg/l glucose and 2 mg of pioglitazone (standard) with and without regular insulin

(Novo Nordisk, 40 IU/ml) 5 μl containing 0.2 units of insulin.

The glucose content of the working solution was measured, and the glucose uptake was calculated as the difference between the initial and final glucose content at 2 mg of optimized drug concentration. The glucose uptake by rat hemi-diaphragm was measured in mg/dl/45 min.

T. Immunohistochemical analysis of ligand-stimulated PPARγ nuclear localization

Primary rat adipocytes were isolated from perivascular adipose tissue and differentially cultured as described previously (Fernyhough et al., 2004). Adipocytes were seeded on sterile coverslips in a 12-well plate at a density of 3000 cells/well. Cells were cultured in DMEM F-12 (Lonza, Basel, Switzerland) containing 10% fetal bovine serum (FBS, Sigma, St. Louis, MO), penicillin (100 U/mL), and streptomycin (100μg/mL); and incubated at 37°C in a humidified atmosphere with 5% CO2 and 95% O_2. Forty-eight hours post seeding, cells were incubated with 10 μM concentration of either pioglitazone, 4b, 5b, 5e, or 5g; or the equivalent amount of the vehicle (DMSO) in triplicates. Following a three-hour exposure interval, treatment media were discarded, cells were washed with phosphate-buffered saline (PBS) and fixed with 2% formaldehyde in PBS for 20 minutes at room temperature. After rinsing with PBS, cells were permeabilized by 0.1% Triton X-100 for 30 minutes at room temperature. Cells were then blocked with 3% normal goat serum (Abcam, Cambridge, UK) in PBS for one hour at room temperature followed by incubation in 1:200 rabbit polyclonal anti-PPARγ (Abcam, Cambridge, UK) in PBS containing 1% normal goat serum overnight at 4°C. Cells were rinsed three times with PBS followed by incubation with 1:100 FITC-conjugated goat anti-rabbit Ig (Abcam, Cambridge, UK) in PBS containing 1% normal goat serum in a light-proof container for one hour at room temperature. Afterwards, cells were rinsed with PBS and mounted on microscopic slides with Fluoroshield anti-fade mounting medium containing DAPI (Abcam, Cambridge, UK). Negative control slides were prepared by omission of either the primary or the secondary antibodies. Slides were left at 4°C overnight. FITC green fluorescence representing PPARγ staining and DAPI nuclear staining were recorded on an Axiovert Observer Z1 High Resolution Fluorescent Imaging Microscope (Zeiss, Oberkochen, Germany). Fluorescence distribution profiles along line scans in both the FITC and DAPI channels was generated using ImageJ software (National Institutes of Health, Bethesda, MD) to show cellular localization of PPARγ relative to the nucleus.

U. PPARγ functional reporter gene assay

HEK293T cells were transiently co-transfected with a hybrid receptor comprising the N-terminal Gal4 DNA binding domain fused to the ligand binding domain of Human PPARγ. The reporter vectors comprise the Renilla luciferase gene functionally linked to the Gal4 upstream activation sequence. Cells were treated with vehicle (DMSO), pioglitazone or test compounds for 24 h. Following the incubation period, treatment media were discarded and luciferase activity was measured using reporter luciferase assay kit according to the manufacturer’s instructions and as reported earlier (Kojo et al., 2003). Luciferase activity was normalized to Renilla luciferase activity and reported as fold induction compared to vehicle. Each experiment was performed in triplicate and repeated at least three times.

V. X-ray Crystallography

The PPARγ LBB was expressed in *E. coli*, purified, and concentrated as described previously (Rajapaksha, Bhatia, Wegener, Petrovsky, & Bruning, 2017). Apo crystals of PPARγ were created by using the hanging drop vapour diffusion method with 500 μL well solution comprising 0.8-1.2M sodium citrate and 0.1M Tris 8.0. The hanging drop was made using 1μL protein plus 1μL well solution. Crystals were cubic, approximately 400microns in each dimension, and formed within 3 days at 16 ^{o}C. Crystals were soaked with a final concentration of 2mM **4b** in the crystallization well for 2 weeks. Crystals were harvested and transferred to well solution containing 15% ethylene glycol as a cryo-protectant. Crystals were flash cooled by direct submersion into liquid nitrogen and data collection was carried out at beamline MX2 of the Australian Synchrotron. 0.1 degree oscillations were collected using the Eiger 16M detector. Data was processed in XDS (Kabsch, 2010). Molecular replacement using Phaser (McCoy, 2007), PDB ID: 5U5L (Rajapaksha et al., 2017) as a search model, with ligands and water molecules removed), electron density for **4b** was visible initial difference density maps. Two subunits were found per asymmetric unit. Phenix.refine (Afonine et al., 2012) and Coot (Emsley, Lohkamp, Scott, & Cowtan, 2010) were used for refinement and multiple rounds of manual rebuilding. MolProbity was used for structure validation (Williams et al., 2018). A Feature

Enhanced Map (FEM) $2F_o - F_c$ electron density map was calculated using Phenix to help reduce model bias and improve map quality (Afonine et al., 2015). Coordinates and structure factors were deposited in the Protein Data Bank under accession code 6E5A.

W. Chemicals

All chemicals were obtained from Sigma (St. Luis, MO) unless otherwise indicated. Pharmaceutical grade atorvastatin was obtained as a kind gift from a regional pharmaceutical manufacturer (PharoPharma).

X. Statistics

Data were expressed as mean ±SEM. Comparisons between groups were done using Student's *t*-test, one-way ANOVA followed by Tukey *post hoc* test, as well as two-way ANOVA followed by Sidak's multiple comparisons test in comparing the effect of different concentrations among groups using Graphpad Prism software. The specific test used is mentioned in the corresponding figure legend. P value < 0.05 was considered statistically significant.

CHAPTER IV

RESULTS

A. Metabolic consequences of a twelve-week mild hypercaloric feeding

Full metabolic and hemodynamic profiling of the HC rat model was done previously (Al-Assi et al., 2018; Mohammed A. W. Elkhatib et al., 2019). To confirm the metabolic characteristics in the cohort used in the present study, body weight, blood glucose, glucose tolerance, serum insulin, triglycerides and cholesterol were assessed at the end of the twelve-week feeding period. Similar to previous observations, no differences were detected in body weight (Fig. 7A), random blood glucose levels (Fig. 7B), glucose tolerance (Fig. 7C), and hemodynamic parameters including systolic blood pressure (Fig. 7G), diastolic blood pressure, and heart rate (data not shown) between control and HC-fed rats. However, as expected, HC-fed rats exhibited elevated plasma insulin (Fig. 7D), total serum cholesterol levels (Fig. 7E) and total serum triglyceride levels (Fig. 7F) compared to the control group.

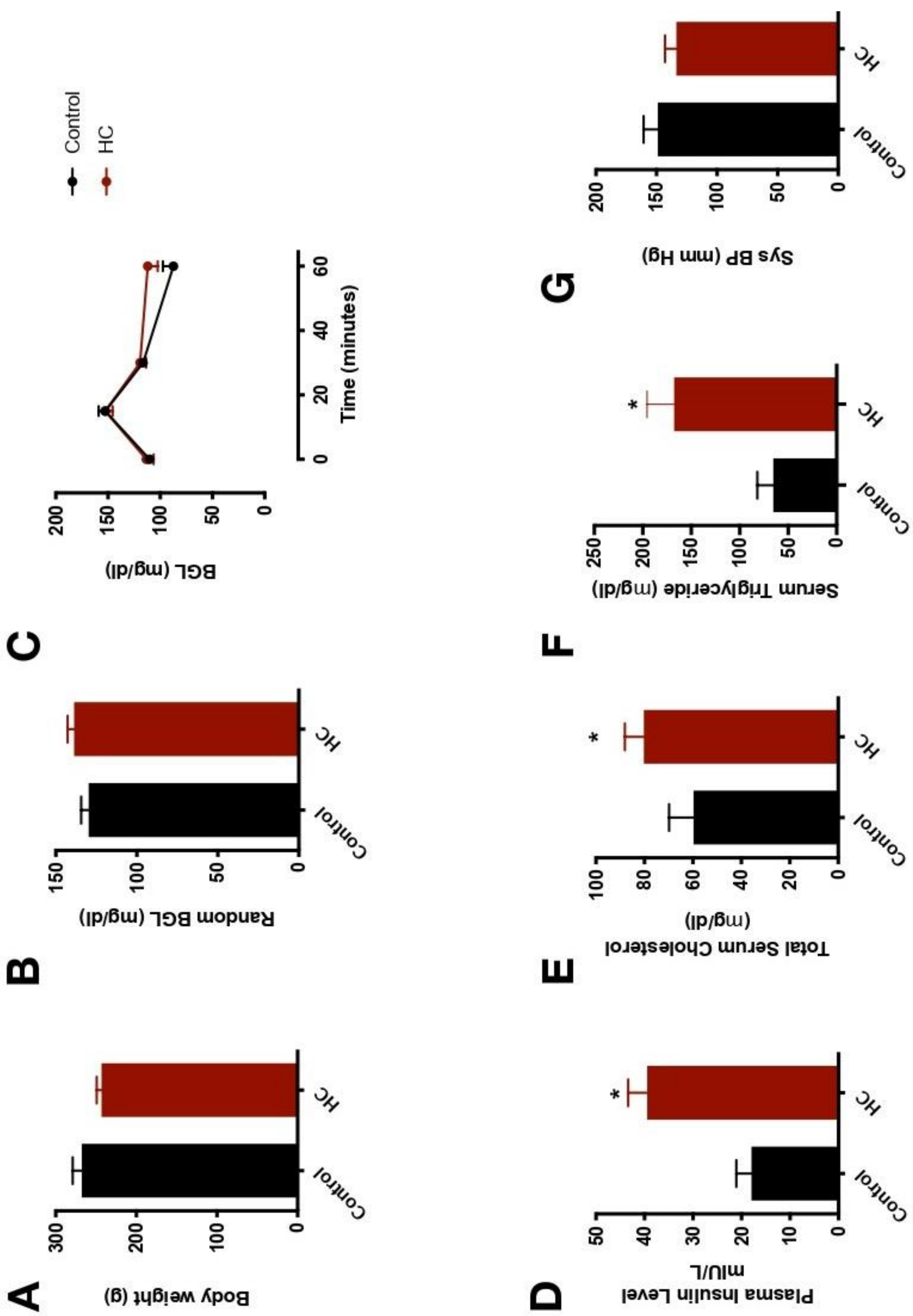

Figure 7. Metabolic and hemodynamic properties of HC-fed rats following 12-week mild hypercaloric feeding. A, body weight after 12 weeks of feeding compared to control; B, Random blood glucose level on sacrifice day; C, intra-peritoneal glucose tolerance test; D, Fasting plasma insulin level; E, Fasting total serum cholesterol; F, serum triglyceride; and G, systolic blood pressure measurement. Data presented are mean ± SEM of seven separate observations. Statistical significance was assessed by unpaired Student's *t*-test for A, B, and D-F and by two-way ANOVA for C. * denotes $P < 0.05$ vs. the corresponding value in control rats.

B. Endothelium-dependent relaxation is impaired in HC-fed rats with an intact SNP-mediated relaxation

In order to examine endothelium-dependent relaxation (EDR), *in vitro* contractility experiments were conducted on thoracic aortas obtained from control and HC-fed rats at the end of the twelve-week feeding duration. Fig. 8A depicts representative tracings of the relaxation of pre-constricted aortic rings to increasing concentrations of ACh. A progressive relaxation was observed in rings from control rats that reached a maximum of ~75% of the initial PE tone. On the other hand, aortic rings from HC-fed rats demonstrated an impaired ACh-mediated relaxation (~25% of the PE tone) which levelled off at a lower ACh concentration (1 μM, Fig. 8B). Whereas the aortic rings from HC-fed rats exhibited an exaggerated contractile response upon exposure to PE (Fig. 8C, left), the maximal absolute tension reduction in response to ACh was less in rings from HC-fed rats confirming the endothelial deficit (Fig. 8C, right). The NO donor SNP produced similar relaxation patterns in both groups (Fig. 8D). Further, to investigate the possibility of release of the contractile endothelial mediator, endothelin-1 as the underlying cause for the observed dysfunction in aortic rings from HC-fed rats, ACh-mediated relaxation was assessed in these rings in the presence of endothelin-1 receptor antagonist atrasentan (Fig. 8). However, this intervention did not alter the aortic response to ACh observed in the HC group. Atrasentan was also without effect in preliminary experiments conducted on control tissue.

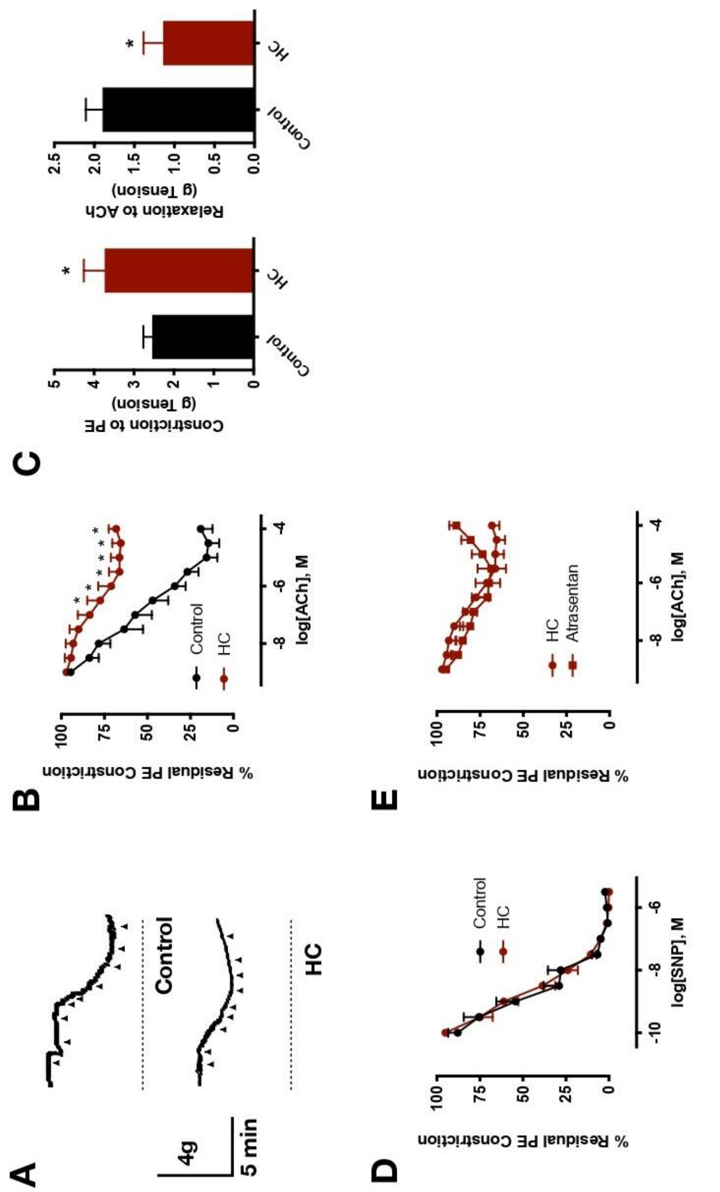

Figure 8. Impaired ACh-mediated endothelium dependent relaxation in HC-fed rats' aortic segments. A, representative tracings of the relaxation response to increasing ACh concentrations. The dotted line represents the basal tension level before constriction with PE. Time points where ACh was added are marked by arrow heads; B, Summary of the ACh-evoked relaxation in aortic rings from 7 control and 7 HC rats; C, Absolute tension increase (left) and decrease (right) in response to PE and ACh, respectively, in experiments summarized in B; D, Relaxant response to SNP in control (5 rats) vs. HC-fed (5 rats) aortic rings; E, ACh-mediated relaxation in HC-fed rat aortic rings in presence (5 rats) and absence (7 rats) of 10 nM atrasentan. Data presented are mean ± SEM. Statistical significance was assessed by unpaired Student's *t*-test for C and by two-way ANOVA for A, B, D, and E. * denotes $P < 0.05$ vs. the corresponding value in control rats in B, C, and D; and the corresponding values in absence of atrasentan in E.

C. Impaired endothelial function in aorta of HC-fed rats is related to an altered endothelial relaxing mediator profile

We examined the relative contribution of different endothelial relaxing mediators in rat aorta and the differential impact of HC-feeding on them. On the one hand, blockade of endothelial NO production by L-NAME significantly reduced ACh-mediated relaxation in aortic rings from both rat groups (Fig. 9A). Yet a residual relaxation that gradually increased to ~25% at higher ACh concentrations was observed only in aortic rings from control rats. To address the role of EDH-type relaxation, the effect of blockade of SK/IK with apamin and Tram-34 (Fig. 9B) and Kir channels with $BaCl_2$ (Fig. 9B) was assessed. SK/IK channel blockers appeared to attenuate ACh-mediated relaxations in either group, albeit more effectively in aortic rings from control rats. Interestingly, while $BaCl_2$ attenuated the ACh-mediated relaxation in rings from control rats, particularly towards the higher ACh concentrations, aortic rings obtained from HC-fed rats were not sensitive (Fig. 9C).

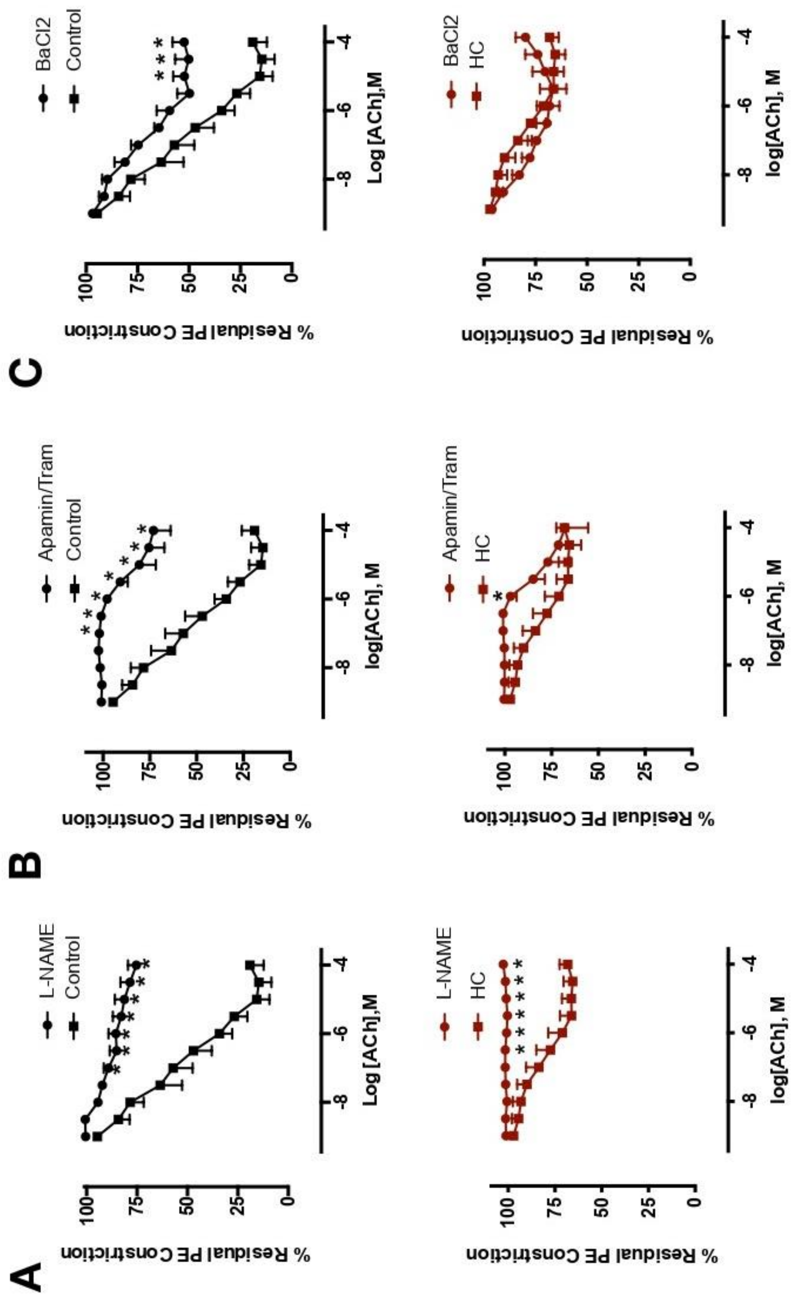

Figure 9. The effect of blockade of different endothelium-relaxing pathways on ACh-evoked relaxation in aortic rings from control (top panels) and HC-fed (bottom panels) rats. A, ACh-evoked relaxation in presence (5 rats) and absence (7 rats) of 100 μM L-NAME; B, ACh-evoked relaxation in presence (5 rats) and absence (7 rats) of 1 μM apamin and Tram-34; C, ACh-evoked relaxation in presence (5 rats) and absence (7 rats) of 30 μM $BaCl_2$. Data presented are mean ± SEM. Statistical significance was assessed by two-way ANOVA. * denotes $P < 0.05$ vs. the corresponding value in absence of the different blockers.

D. Impairment of endothelial function is likely attributed to the loss of endothelium-dependent hyperpolarization-type relaxation

In order to confirm the potential impairment of EDH-type relaxation, ACh-mediated relaxation profile of aortic rings was examined following pre-constriction with the thromboxane analogue, U46619. This contractile agent produces vasoconstriction mainly through calcium sensitization (Plane & Garland, 1993), likely ruling out the potential vasodilatory effect of EDH. As predicted, aortic rings from both control and HC-fed rats produced equal contractions to U46619 and relaxed similarly to ACh (Fig. 10 A & B). Inhibition of NO production by L-NAME attenuated the relaxation response to ACh equally in aortic rings from both control and HC-fed rats (Fig. 10C), while $BaCl_2$ was without effect on ACh-mediated relaxation (Fig. 10D).

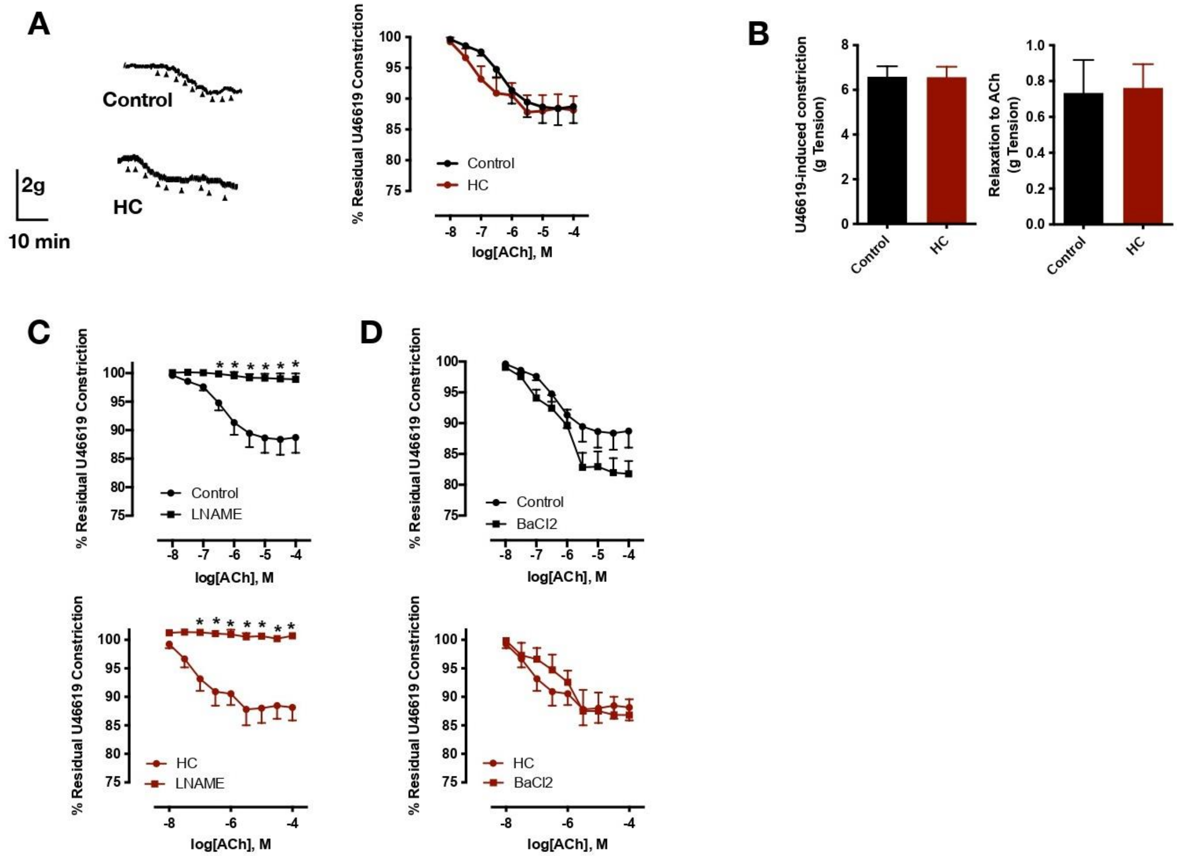

Figure 10. ACh-evoked relaxation in aortic rings pre-constricted with the thromboxane analogue, U46619. A, representative tracings of the relaxation response to increasing ACh concentrations (left). Time points where ACh was added are marked by arrow heads, and summary of the ACh-evoked relaxation in aortic rings from control and HC rats (right, five rats per group); B, Absolute tension increase (left) and decrease (right) in response to U46619 and ACh, respectively, in experiments summarized in A; C, ACh-evoked relaxation in presence and absence of 100 μM L-NAME in control (top) and HC-fed (bottom) rat aortic rings pre-constricted with U46619 (5 rats per group); D, ACh-evoked relaxation in presence and absence of 30 μM $BaCl_2$ in control (top) and HC-fed (bottom) rat aortic rings pre-constricted with U46619 (5 rats per group). Data presented are mean ± SEM. Statistical significance was assessed by unpaired Student's *t*-test for B and by two-way ANOVA for A, C and D. * denotes $P < 0.05$ vs. the corresponding control value in A and B and the corresponding value in absence of the blockers in C and D.

E. The observed endothelial impairment in HC-fed rats is likely due to Kir channel dysfunction

Given the previous observations indicating the likelihood of Kir channel dysfunction in HC-fed rat aortic rings, we further examined their role as "end-stage amplifiers" of hyperpolarization (Sonkusare et al., 2016). We assessed the aortic response to the potassium channel opener, diazoxide (Fig. 11A). Diazoxide produced an 80% tone reduction in control aortic rings pre-constricted with PE; a response that was much attenuated in aortic rings from HC-fed rats. Interestingly, blockade of Kir channels with $BaCl_2$ lacked any effect in HC-fed rat aortic rings, but brought the diazoxide-evoked relaxation in control rats to a level similar to that seen in the HC-fed group. Recent studies implicated Kir2.1 and 2.2 subunits as the molecular carrier of the inward rectifier potassium current in rat vasculature (M. Sancho et al., 2019). We examined the relative expression of both channel subunits in our vessel preparation using Q-PCR revealing that Kir2.1 was the predominant subunit expressed (Fig. 11B). Western blotting showed a reduction of Kir2.1 subunit expression in aortic tissues of HC-fed rats compared to control rats (Fig. 11C).

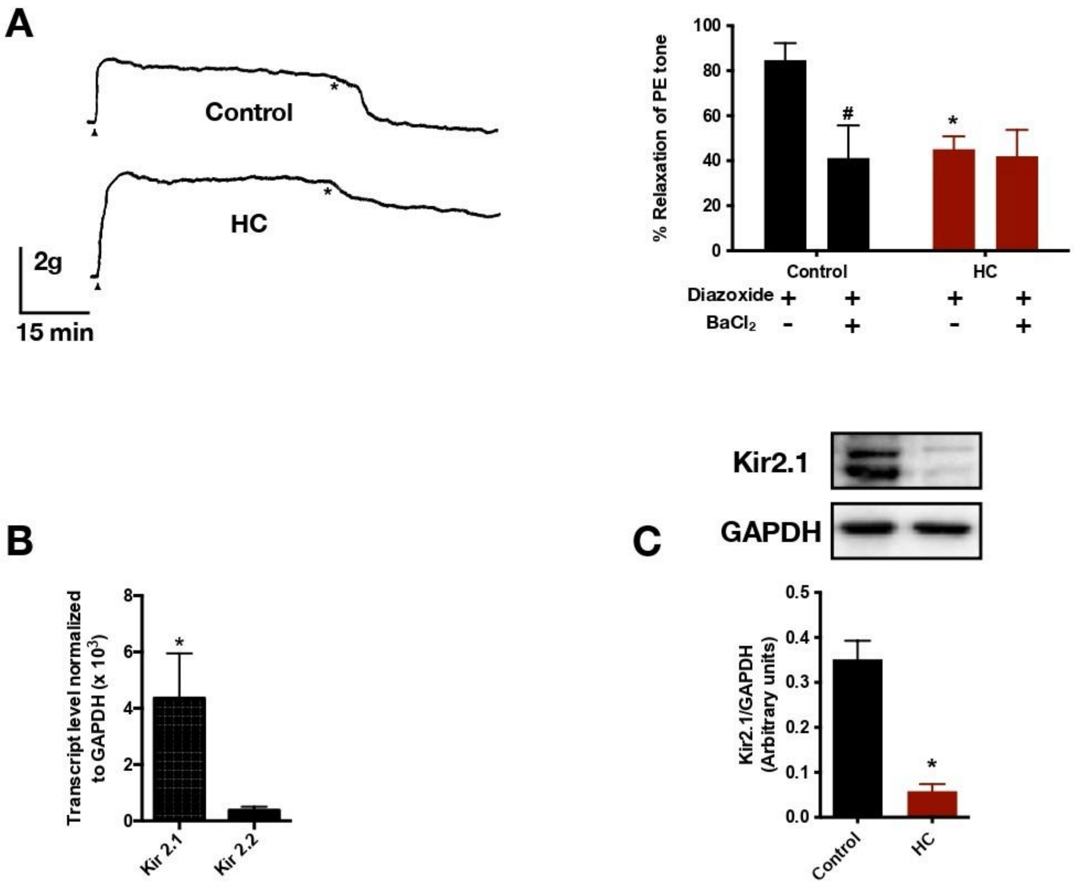

Figure 11. Dysfunctional Kir channels in HC-fed rat aortic rings. A, representative tracings for the diazoxide-mediated relaxations in control and HC-fed rat aortic rings (left). Arrow heads indicate the time point PE was added, while asterisks indicate the points where diazoxide was added; and average magnitude of these relaxations in presence and absence of 30 μM $BaCl_2$ (right, rings from five rats in each experiment); B, mRNA expression levels of Kir2.1 and Kir2.2 in control rat aortic tissue (data from four rats); C, Kir2.1 protein expression level in aortic tissue of control vs. HC-fed rats (data from four rats). Data presented are mean ± SEM. Statistical significance was assessed by two-way ANOVA for A and unpaired Student's *t*-test for B and C. * denotes $P < 0.05$ vs. the corresponding control value in A and C, and the Kir2.2 value in B; while # denotes $P < 0.05$ vs. the value in rings unexposed to $BaCl_2$.

F. Gap junction contribution to the observed endothelial dysfunction in HC-fed rat aorta

Since gap junctions are an essential element of myoendothelial feedback, we examined the effect of the gap junction blocker 18-β-GA on ACh-mediated relaxation (Fig. 12A). As expected, the gap junction blocker greatly attenuated the response to ACh in control aortic rings. Conversely, 18-β-GA did not alter the ACh-dependent relaxation in rings from HC-fed rats. Interestingly, the addition of 18-β-GA to the pre-constricted aortic rings produced disparate effects (Fig. 12B). Control rings exhibited an increase in contractile tone consistent with the interruption of EDH conduction and hence EDH-mediated relaxation. Surprisingly, rings from HC-fed rats demonstrated a decrease in vascular tone indicating that gap junctions might mediate the conduction of an entity impairing endothelial function. On the other hand, the examination of the relative expression of connexin subtypes in our vessel preparation showed that Cx43 is the most abundant (Fig. 12C). As such, we proceeded to examine the relative expression of Cx43 between control and HC-fed rat aortic tissues. Western blotting showed that Cx43 expression was higher in aortic tissues from HC-fed rats (Fig. 12D, left). Such a change was accompanied by an enhancement in phosphorylation of ERK1/2 in aortic rings from HC-fed rats, as demonstrated by western blotting (Fig. 12D, right).

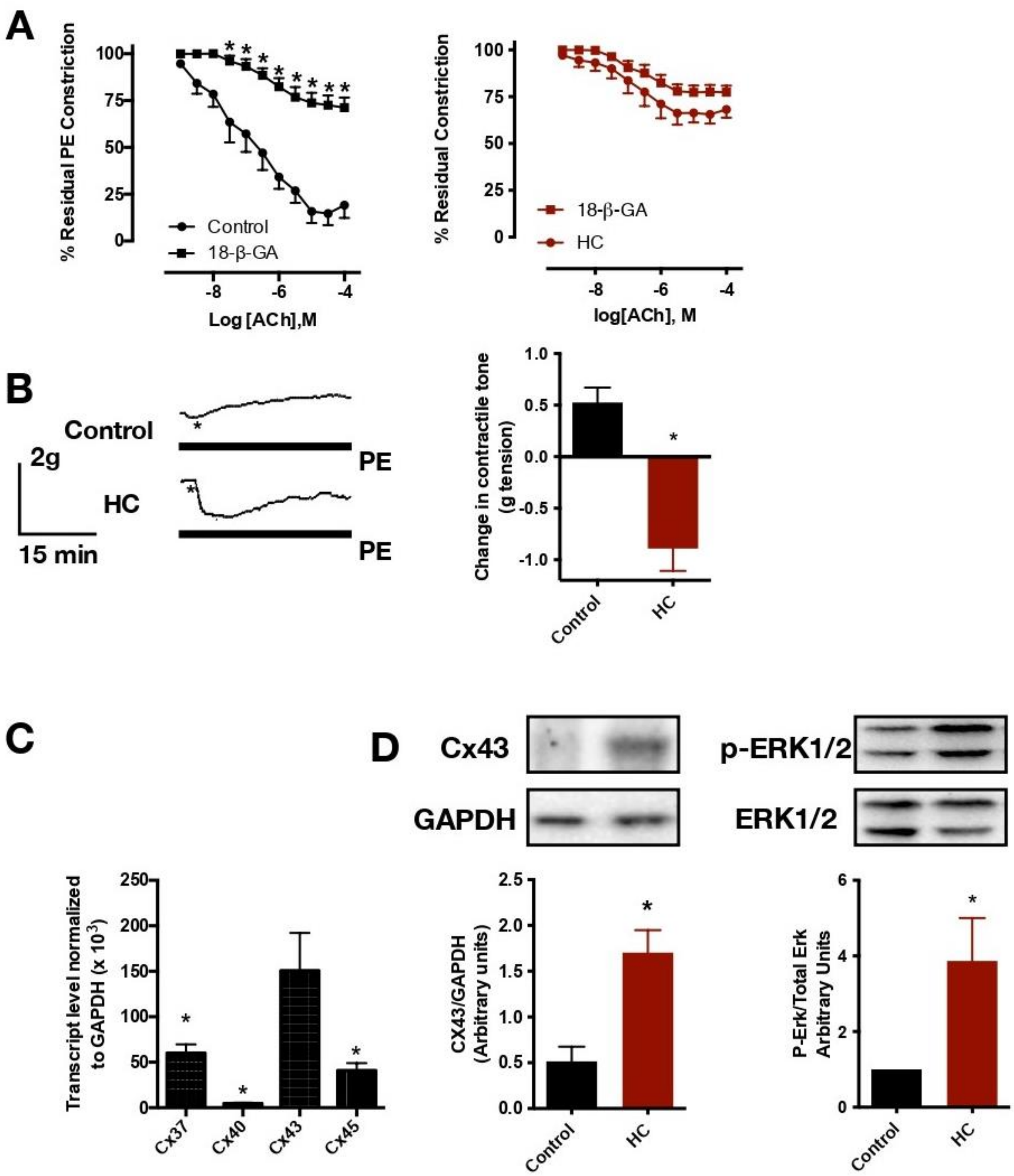

Figure 12. Effect of gap junction blockade on ACh-evoked relaxation and PE-induced constriction. A, ACh-evoked relaxation in presence (5 rats) and absence (7 rats) of 100 μM 18-β-GA in control (left) and HC-fed (right) rat aortic rings; B, representative tracings of the effect of 100 μM 18-β-GA on PE-induced tone in control and HC-fed rat aortic rings (left). Asterisks represent the time points where 18-β-GA was added in the continued presence of PE, and average absolute tension change in these experiments (rings from five rats per group, right); C, mRNA expression levels of Cx37, Cx40, Cx43, and Cx45 in control rat aortic tissue (data from four rats); D, Cx43 protein expression level in aortic tissue of control vs. HC-fed rats (data from four rats). Data presented are mean ± SEM. Statistical significance was

assessed by two-way ANOVA for A, one-way ANOVA for C, and unpaired Student's *t*-test for B and D. * denotes $P < 0.05$ vs. the corresponding value in absence of blocker in A, control rat value in B and D, and the Cx43 value in C.

G. Reactive oxygen species play a role in the impairment of endothelium-dependent relaxation in HC-fed rats

ROS examination using DHE staining showed a significant increase in aortic sections obtained from HC-fed rats (Fig. 13A). *In vitro* scavenging of ROS by incubating aortic rings from HC-fed rats with superoxide dismutase (SOD), not only reduced the ROS staining intensity, but also improved the ACh-mediated relaxation (Fig. 13B). SOD treatment was without effect on ACh-mediated relaxation in preliminary experiments done on control rat aortic rings. Since ROS was reported to spread across gap junctions among different vascular cell types (Feine, Pinkas, Salomon, & Scherz, 2012), and are known to inhibit eNOS activity (Ohara, Peterson, & Harrison, 1993b), we investigated whether the reduction in tone observed post-gap junction blockade in HC-fed rat tissues was because of an interruption of eNOS inhibition by ROS. First, inhibition of eNOS in HC-fed rat aortic rings by pre-incubation with LNAME precluded the loss of tone upon treatment with 18-β-GA (Fig. 13C). As well, ROS scavenging by SOD had a similar effect. In order to investigate whether the loss of Kir channel function was related to this observation, similar experiments were conducted in control rat aortic rings incubated with $BaCl_2$ to block Kir channels. Not only did incubation with $BaCl_2$ increase ROS upon DHE staining (Fig. 13D), $BaCl_2$-treated control aortic rings also exhibited a loss of tone upon treatment with 18-β-GA (Fig. 13E) similar to the observations in HC-fed rat tissues.

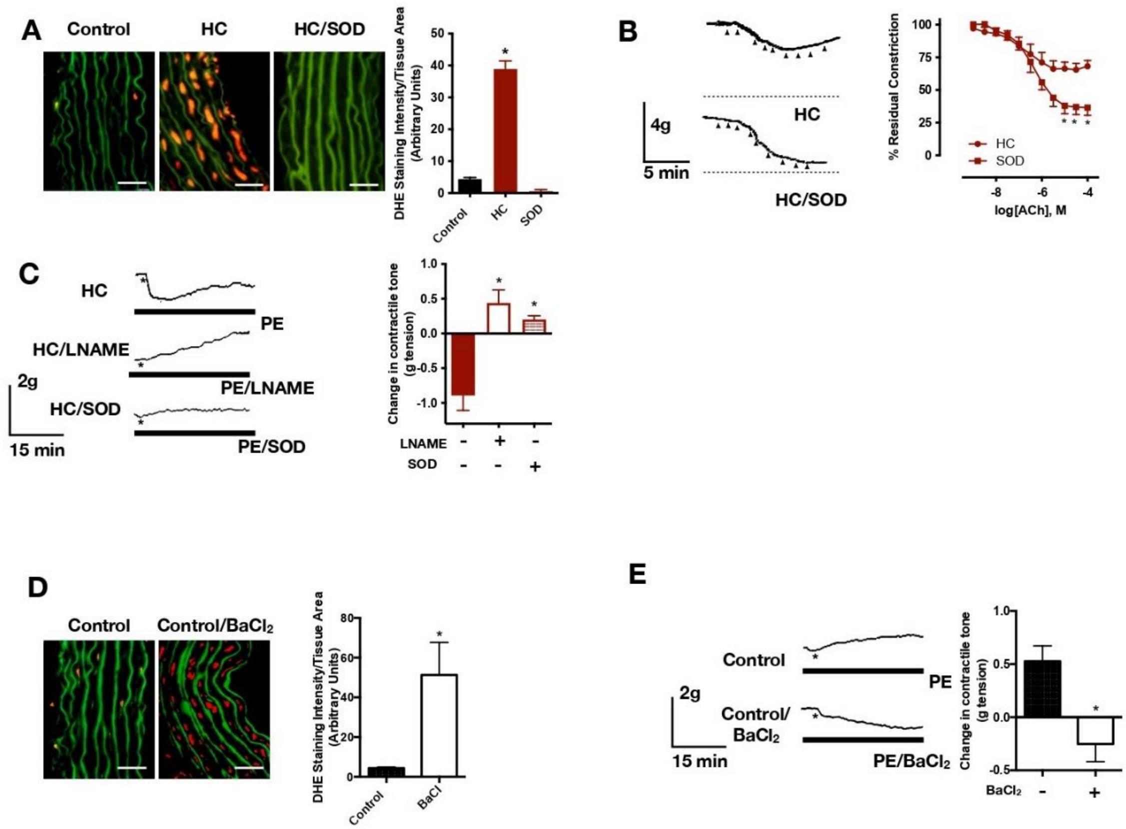

Figure 13. Aortic ROS levels and the effect of *in vitro* ROS modulation on endothelial function of rat aortic rings. A, representative micrographs of DHE staining of aortic tissues from control, HC-fed, and HC-fed rat aortic rings exposed to SOD *in vitro* (left), and average quantified data (right, data obtained from three sections per rat and four rats per group). DHE staining appears as red fluorescence on a background of green collagen autofluorescence. Scale bars are 40 μm; B, representative tracings of the relaxation response to increasing ACh concentrations in aortic rings from HC-rats in presence (5 rats) and absence (7 rats) of 200 U/ml SOD (left). Time points where ACh was added are indicated by arrowheads, and average responses at different concentrations (right); C, representative tracings of the effect of 100 μM 18-β-GA on PE-induced tone in HC-fed rat aortic rings in the continued presence of PE, PE/LNAME, or PE/SOD as indicated in the bar beneath the tracings (left). Asterisks represent the time points where 18-β-GA was added, and average absolute tension change in these experiments (rings from five rats per group, right). D, representative micrographs of DHE staining of aortic tissues from control rats with and without pre-incubation with $BaCl_2$ (left), and average quantified data (right, data obtained from three sections per rat and four rats per group). Scale bars are 40 μm; E, representative tracings of the effect of 100 μM 18-β-GA on PE-induced tone in control rat aortic rings in the continued presence of PE or PE/$BaCl_2$ as indicated in the bar beneath the tracings (left). Asterisks represent the time points where 18-β-GA was added, and average absolute tension change in these experiments (rings from five rats per group, right). Data presented are mean ± SEM. Statistical significance was assessed by one-way ANOVA for A and C, two-way ANOVA for B, and unpaired Student's

t-test for D and E. * denotes *P* < 0.05 vs. the control rat value in A and the corresponding HC-fed rat values in B and C.

H. Atorvastatin treatment improved endothelium-dependent hyperpolarization profile

Since hypercholesterolemia was shown previously to impair Kir channel function and reduce EDH (Fancher et al., 2018; M. Sancho et al., 2019), we examined the effect of blood cholesterol reduction in HC-fed rats on ACh-mediated relaxation in general, and the $BaCl_2$-sensitive component in particular. Four-week treatment of the HC-fed rats with the lipid-lowering agent atorvastatin restored their serum cholesterol levels to values comparable to that of the control group without affecting body weight, blood glucose, or serum insulin levels (Fig. 14A). This improvement was associated with an enhanced ACh-mediated relaxation compared to that of the HC-fed rat group (Fig. 14B). Significantly, $BaCl_2$ attenuated the ACh-mediated relaxation in aortic rings from atorvastatin-treated HC-fed rats in a pattern similar to that observed in rings from control rats (Fig. 14C). Similarly, further indication of the restoration of Kir channel function was demonstrated by the increased diazoxide-mediated relaxation in atorvastatin-treated HC-fed rat aortic rings compared to their untreated counterparts (Fig. 14D). Alongside, western blotting showed an increase of Kir2.1 subunit expression in the aorta of atorvastatin-treated rats (Fig. 14E). Moreover, DHE staining intensity indicative of ROS was also reduced by atorvastatin treatment (Fig. 14F).

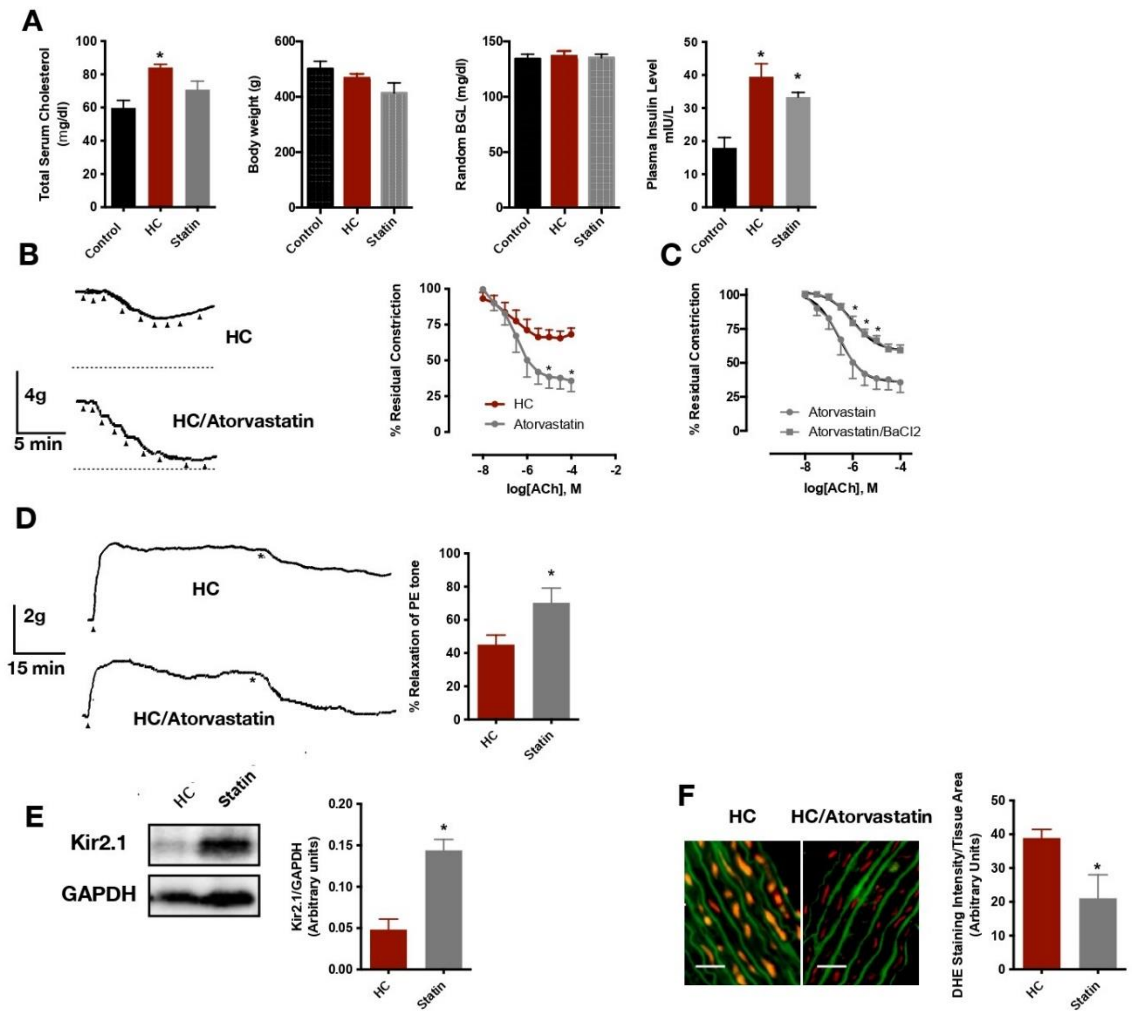

Figure 14. Serum cholesterol lowering improves ACh-evoked relaxations and restores Kir channel function. A, the effect of 4-week atorvastatin treatment in HC-fed rats on (left to right): total serum cholesterol, body weight, random blood glucose level, and plasma insulin level; B, Representative tracings of the ACh-mediated relaxation in untreated (7 rats) and atorvastatin-treated (5 rats) HC-fed rats (left). Arrowheads indicate time points where ACh was added, and average responses and different concentrations (right); C, the effect of $BaCl_2$ on ACh-mediated relaxation in atorvastatin-treated HC-fed rats (rings from 5 rats); D, Representative tracings for the diazoxide-induced relaxation of aortic rings from untreated and atorvastatin-treated HC-fed rats (left). Arrowheads indicate the time points where PE was added, while asterisks indicate the time points where diazoxide was added, and average vasorelaxant response (five rats, right); E, Kir2.1 protein expression in aortic tissues from untreated and atorvastatin-treated HC-fed rats (data for 4 rats); F, representative micrographs of DHE staining of aortic tissues from untreated and atorvastatin-treated HC-fed rats and average quantified data. Data are obtained from three sections per rat and four rats per group. DHE staining appears as red fluorescence on a background of green collagen autofluorescence. Scale bars are 40 μm. Data presented are mean ± SEM. Statistical significance was assessed by one-way ANOVA for A, two-way ANOVA for B and C, and

unpaired Student's *t*-test for D-F. * denotes $P < 0.05$ vs. the control rat value in A, the corresponding value in untreated HC-fed rats in B, E and F, and the corresponding value in absence of blocker in C.

I. Impairment of endothelium-dependent relaxation is not related to altered eNOS or Akt expression/phosphorylation

In order to rule out the potential contribution of insulin resistance to the observed endothelial impairment, we investigated whether eNOS and Akt phosphorylation were altered in aortic tissues from HC-fed rats. Western blotting was used to examine the phosphorylated and total forms of either protein. Neither eNOS expression (Fig. 15A), phosphorylation (Fig. 15B), nor Akt phosphorylation (Fig. 15C) levels were altered in aortic rings from HC-fed rats.

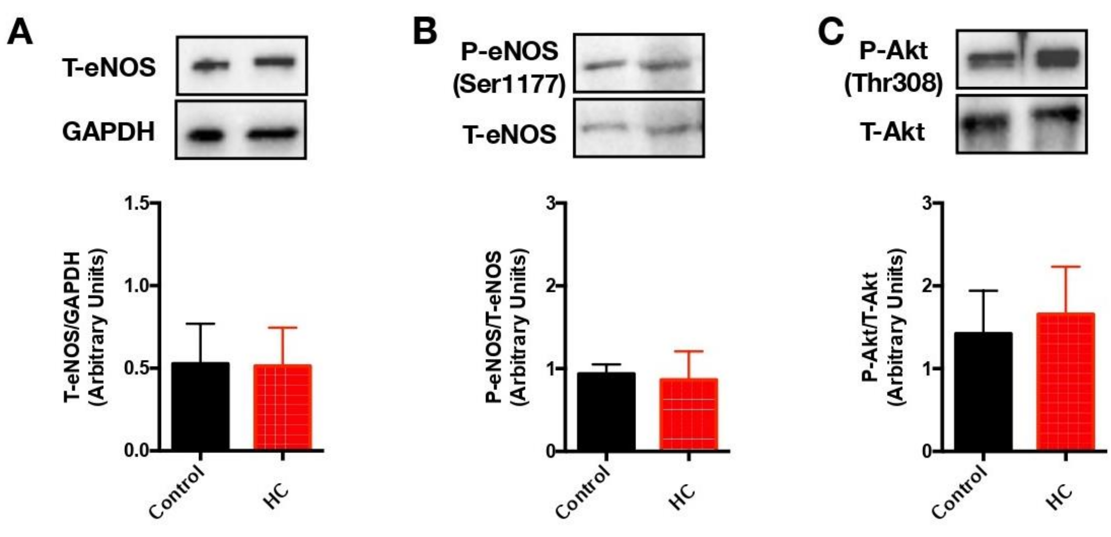

Figure 15. HC-feeding does not alter Akt or eNOS phosphorylation. A, representative blots for total eNOS in aortic tissues from control and HC-fed rats together with average quantified data normalized to GAPDH (three rats per group) B, representative blots for

phospho-eNOS Ser1177 and total eNOS in aortic tissues from control and HC-fed rats together with average quantified data (three rats per group); C, representative blots for phospho-Akt Thr308 and total eNOS in aortic tissues from control and HC-fed rats together with average quantified data (three rats per group). Data presented are mean ± SEM. Statistical significance was assessed by unpaired Student's *t*-test. * denotes $P < 0.05$ vs. the control rat value.

J. Endothelium-dependent hyperpolarization was attenuated in the microcirculation by HC-feeding and restored by atorvastatin

Given the increased relative contribution of EDH in the microvasculature (Garland & Dora, 2017), we examined the endothelium-dependent relaxation pattern in middle cerebral arterioles from HC-fed rats to confirm our findings regarding EDH impairment. In pressure myography experiments, middle cerebral arteriole segments produced spontaneous myogenic tone in response to increased intravascular pressure. The vasodilatory response to 10 μM ACh was assessed across different groups. Cerebral arteriole segments from control rats showed considerable dilation in response to 10 μM ACh accounting for ~40% of active tone generated by the vessel (Fig. 16A). Blocking Kir channels with 30 μM $BaCl_2$ attenuated the ACh-induced relaxation to ~10% of the active tone (Fig. 16D). Of note, addition of $BaCl_2$ produced a phasic constriction indicating an interference with an ongoing hyperpolarization (Fig. 16A & C). On the other hand, not only was ACh-mediated vasodilation much reduced in cerebral arteriole segments from HC-fed rats (~10%, Fig. 10A & B), but also this attenuated response was not affected by $BaCl_2$ treatment (Fig. 16D). Moreover, the phasic contraction in response to Kir channel blockade by $BaCl_2$ was blunted in vessel segments from HC-fed rats (Fig. 16C). Significantly, cerebral arterioles from atorvastatin-treated HC-fed rats demonstrated responses to ACh and $BaCl_2$ that were similar to those from control rats.

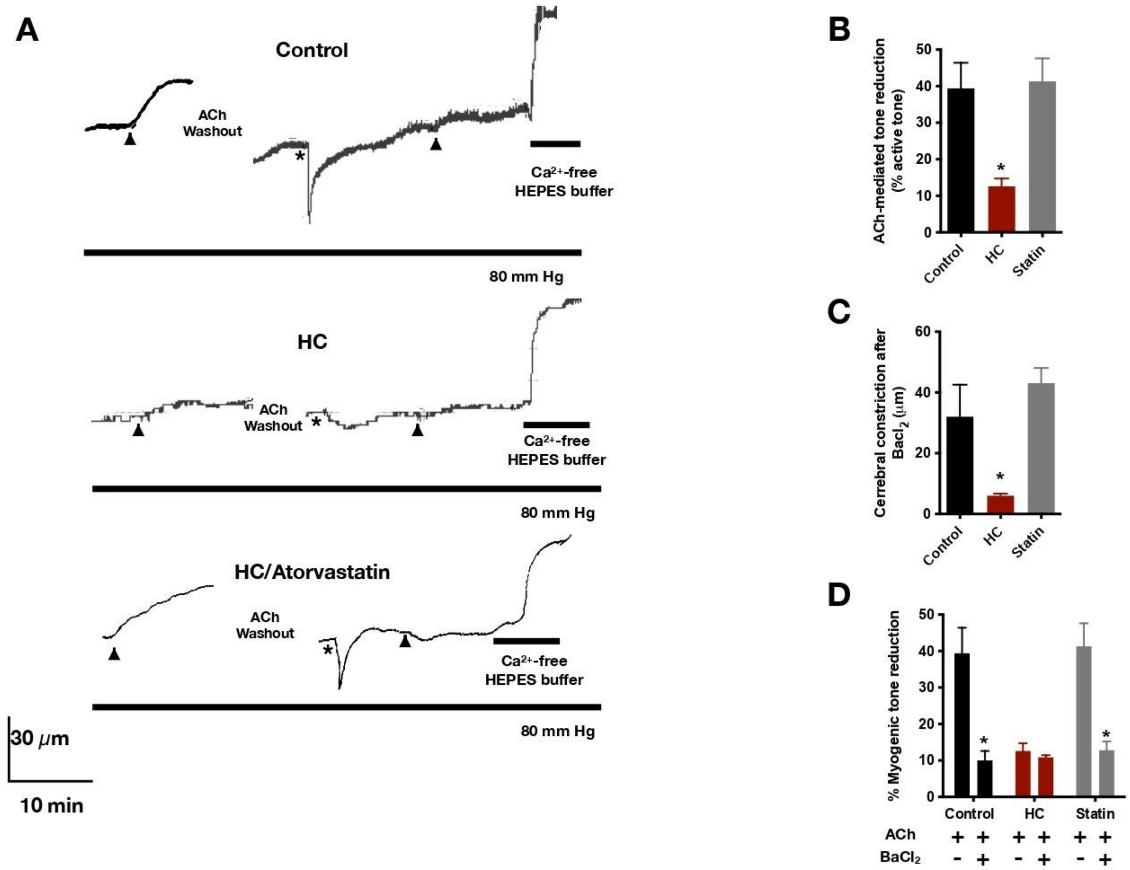

Figure 16. Impaired ACh-evoked cerebral artery dilation in HC-fed rats is ameliorated by atorvastatin treatment. A, Representative tracings of the cerebral arteriolar dilation to 10 μM ACh in presence and absence of 30 μM $BaCl_2$ in vessel segments from control, untreated and atorvastatin-treated HC-fed rats. Time points where ACh was added are indicated by heads, while time points were $BaCl_2$ was added are indicated by asterisks. Tracings were recorded during continuous pressurization to 80 mm Hg as indicated beneath them and Ca^{2+}-free buffer solution was added as indicated by the bar towards the end of the recording; B, average ACh-evoked relaxations (4 rats/group); C, average $BaCl_2$-induced constrictions (four rats/group); D, the effect of $BaCl_2$ on ACh-mediated vasodilation (four rats/group). Data presented are mean ± SEM. Statistical significance was assessed by one-way ANOVA for B and C, and two-way ANOVA for D. * denotes $P < 0.05$ vs. the control rat value in B and C, and the value in absence of $BaCl_2$ in D.

K. Twelve-week HC feeding was associated with localized PVAT inflammation

Given the aforementioned role of adipose tissue inflammation in exacerbating endothelial damage, the expression of markers of inflammation was assessed in perivascular and visceral white adipose tissue depots in HC-fed rats. As shown by western blotting, PVAT obtained from HC-fed rats exhibited elevated levels of UCP-1 and HIF-1α, indicative of increased adipose tissue browning and hypoxia respectively (Fig. 17A). Moreover, this adipose tissue pool manifested enhanced protein expression levels of inflammatory markers, including IL-1β and NF-κB as well as reduced PPARγ expression (Fig. 17A). In addition, H & E staining showed an increase in adipocyte size in PVAT from HC-fed rats compared to that of the control (Fig. 17B). On the other hand, white adipose tissue exhibited no differences in UCP-1, HIF-1α, or IL-1β protein expression between HC- and NC-fed rats (Fig. 17C), albeit a significant increase in adipocyte size in HC-fed rats (Fig. 17D).

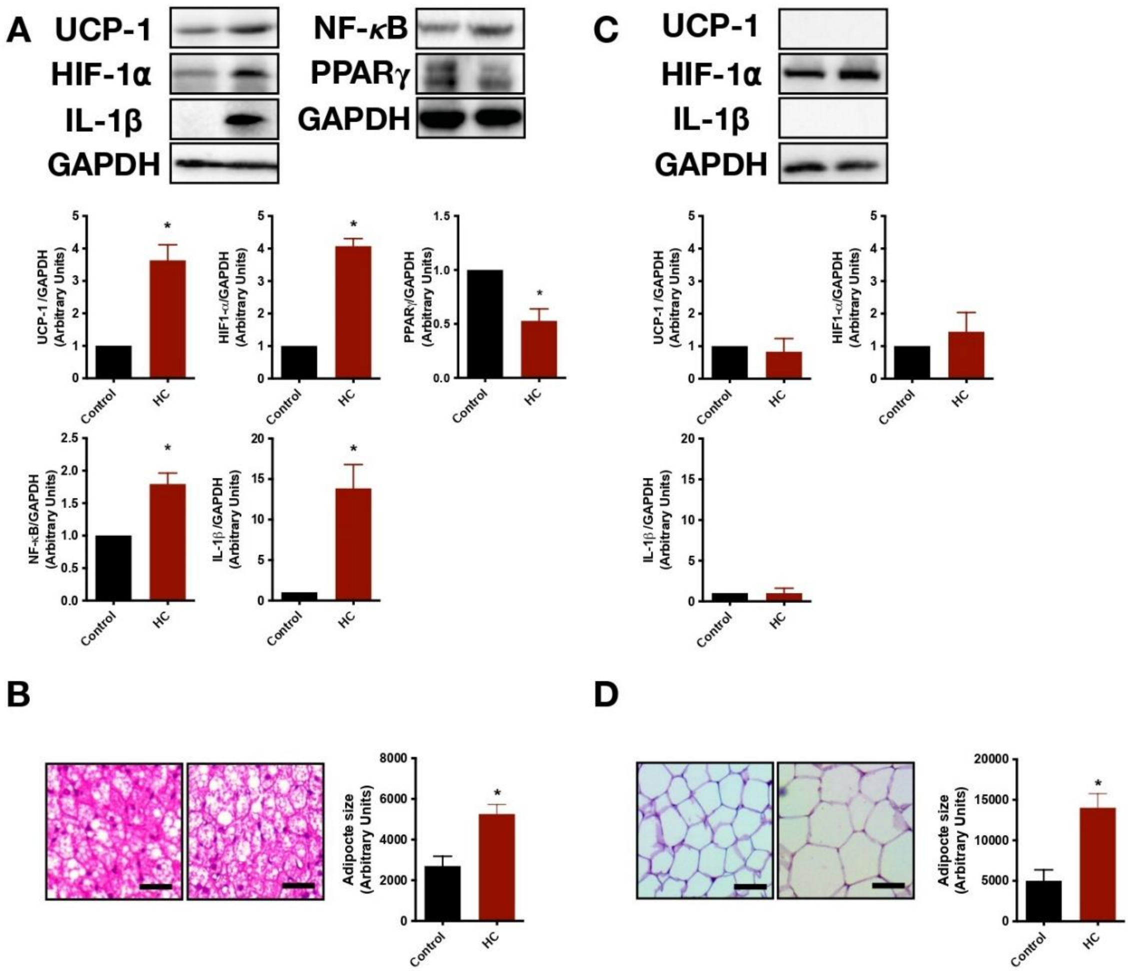

Figure 17. **HC-feeding is associated with perivascular, but not visceral adipose tissue inflammation. A,** Representative western blots of UCP-1, HIF-1α, IL-1β, NF-κB and PPARγ in PVAT from NC- and HC-fed rats, together with average quantified data normalized to GAPDH (three rats per group); B, Representative micrographs of serial sections of PVAT from control and HC-fed rats stained with H&E (bottom, scale bars are 50 μm), together with quantified average size of adipocytes (three rats per group); C, Representative western blots of UCP-1, HIF-1α and IL-1β in white visceral adipose tissue from NC- and HC-fed rats, together with average quantified data normalized to GAPDH (three rats per group); D, Representative micrographs of serial sections of white visceral adipose tissue from control and HC-fed rats stained with H&E (bottom, scale bars are 50 μm), together with quantified average size of adipocytes (three rats per group). Data presented are mean ± SEM. Statistical significance was assessed by unpaired Student's *t*-test. * denotes $P < 0.05$ vs. the control rat value.

L. HC feeding induces alteration of PVAT macrophage polarization

Resident macrophages contribute to adipose tissue homeostasis by adopting a wide range of activation phenotypes within the M1/M2 model of polarization. While M2 polarization is prevalent in a healthy adipose tissue, obesity and adipose expansion tend to alter the macrophages towards the M1 polarization concomitant with adipose tissue inflammation (Morris, Singer, & Lumeng, 2011). In line with the inflammatory changes, flow cytometric examination of the stromal vascular cell fraction of PVAT for macrophage markers showed that the ratio of CD45+/CD68+/CD86+ cells corresponding to M1 polarized macrophages to the CD45+/CD68+/CD163+ corresponding to M2 cells increased in animals receiving HC diet. Results of the FACS experiments are summarized in Fig. 19.

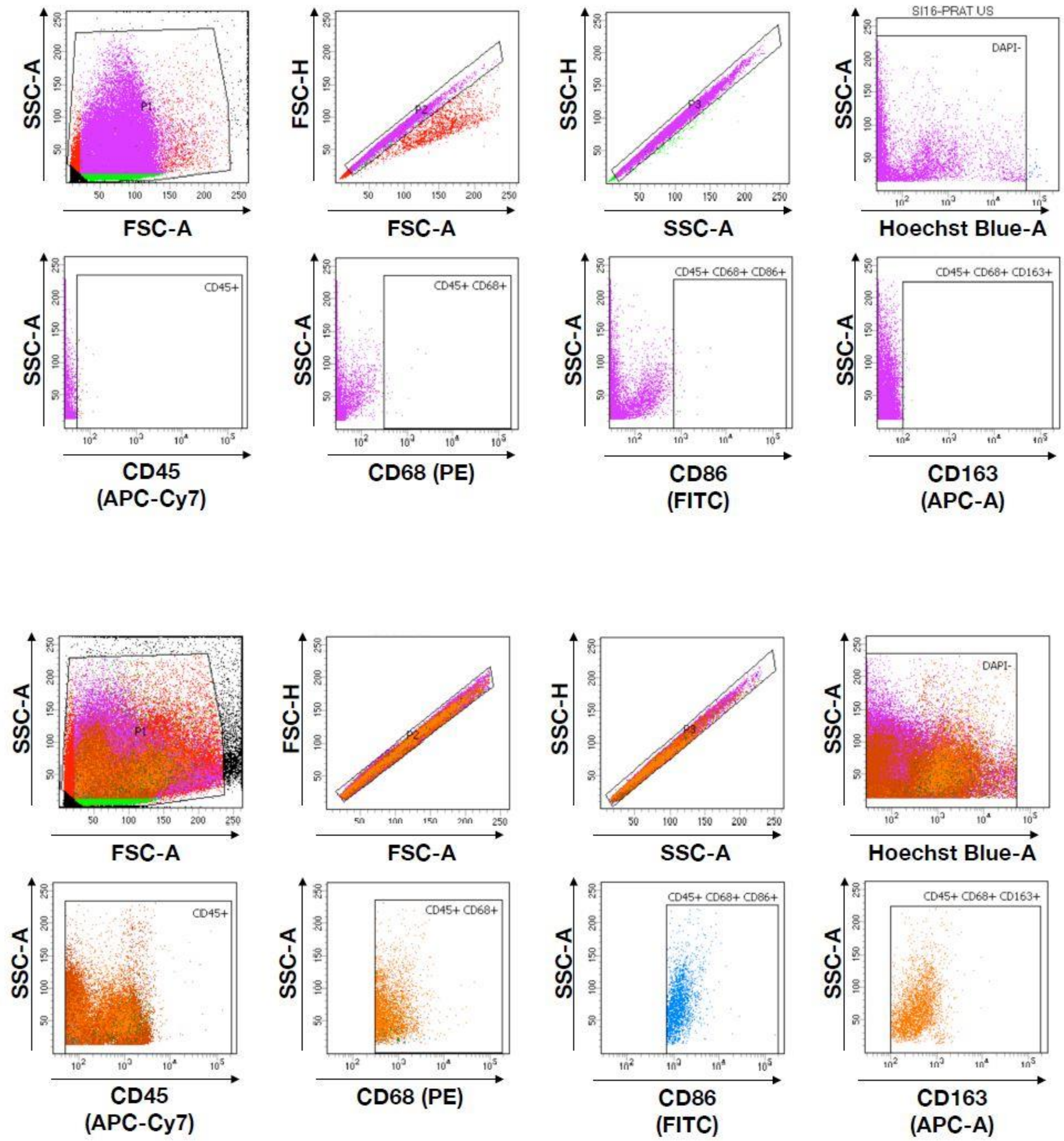

Figure 18. Representative gating strategy for flow cytometric analysis of macrophage polarization.

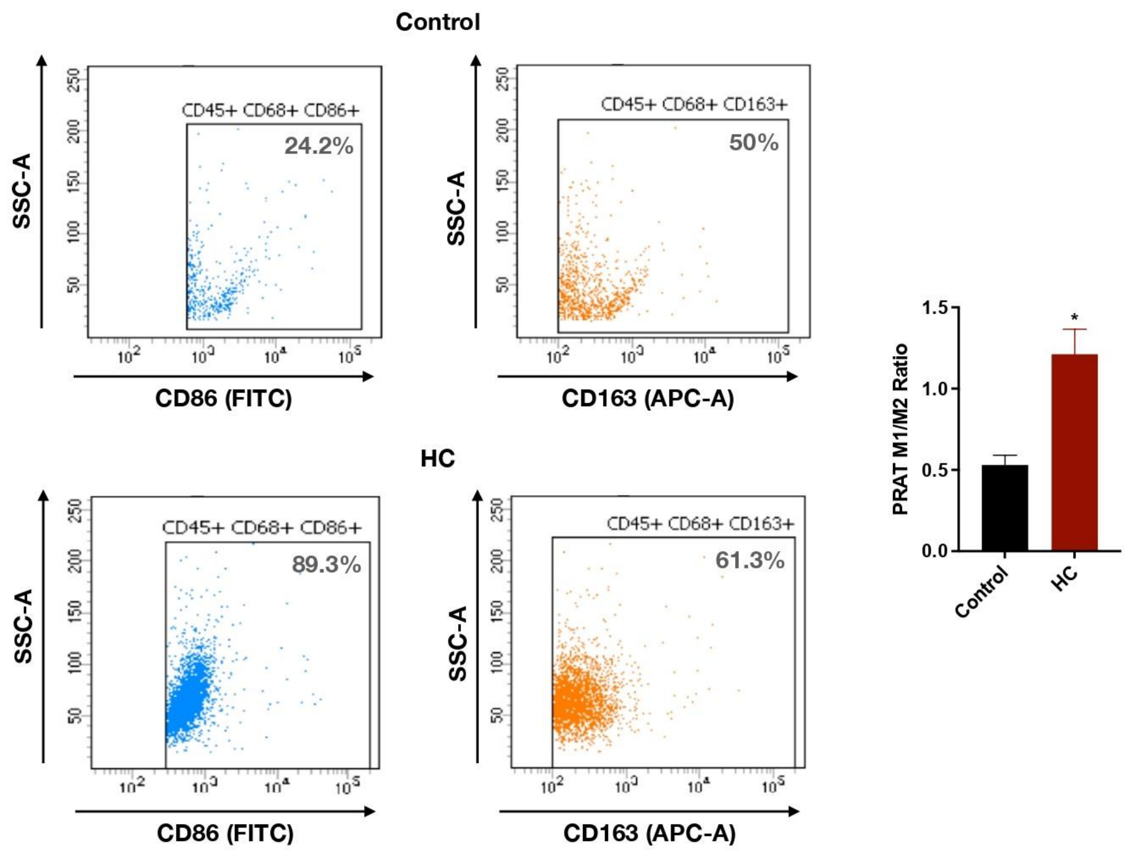

Figure 19. **Hypercaloric diet induced M1 macrophage polarization in PVAT.** Representative FACS scattergrams showing PVAT leukocytes expressing M1 vs. M2 macrophage polarization markers in rats fed NC or HC diet. Summary of the ratio of M1/M2 PVAT macrophages in controls vs HC-fed rats. Data presented are mean ± SEM. Statistical significance was assessed by unpaired Student's *t*-test. * denotes $P < 0.05$ vs. the control rat value.

M. *In vitro* and *in vivo* evaluation of COX-2/15-LOX dual-targeting compounds demonstrated potential anti-inflammatory properties

1. *In vitro COX-1/2 and 15-LOX inhibition assays*

Generally speaking, as depicted in Table 2, all compounds showed submicromolar IC50 values for COX-2 inhibition along with being one to two orders of magnitude lower than those for COX-1 inhibition. They were both more active and selective than the reference drugs diclofenac and indomethacin as COX-2 inhibitors. For 15-LOX inhibition, IC50 values for all compounds operated in the one-digit micromolar range and were more potent than both meclofenamate and NDGA. Additionally, compounds 1-3,6 and 7 were either more potent or equipotent to quercetin.

Regarding thiazolones (1 and 2) originating from 5-chloropyrazole-aldehyde (a), the piperidino-derivative 1 showed 1.7 times the activity of quercetin towards 15-LOX inhibition. Switching to the morpholino analog 2 slightly decreased 15-LOX inhibitory activity but still spanning within the same order of magnitude. Concerning thiazolones (3 and 4) derived from 1,3-diphenyl pyrazole-aldehyde (b), piperidine derivative 3 demonstrated higher 15-LOX inhibition that somewhat decreased upon replacement with morpholine moiety, yet, retaining the same one-digit micromolar range of inhibition. As for thiazolones (5 and 6) obtained from 1-phenyl-3-p-tolyl pyrazole-aldehyde (c), the lowest activity for 15-LOX inhibition was noticed with the piperidine derivative 5. Enhancement of activity occurred upon switching to the morpholino-analog 6, showing IC50 value of 2.85 μM for 15-LOX inhibition. While in case of the thiazolones (7 and 8) bearing an EDG methoxy group on the pyrazole-aldehyde moiety, the piperidine analog 7 was almost equipotent to quercetin for 15-LOX inhibition but the activity decreased upon shifting to the morpholine derivative 8. Finally, the thiazolones (9 and 10) carrying bromo substituent on the pyrazole-aldehyde moiety had 15-LOX inhibitory activities corresponding to 59% and 74% of the activity of quercetin, respectively.

As for COX-2 inhibition, careful inspection of the results revealed no appreciable differences in the IC50 values (0.09-0.19 μM) of the synthesized compounds, with the exception of compound 5 (IC50 value of 0.34 μM). This is in addition to some unique structural difference between the synthesized compounds, which impeded extracting sharper structure-activity relationships. However, the outcome of this study represents a good starting point to attempt a wider variety of substitution patterns that might aid in establishing decisive structure-activity relationships. However, and with regards to COX selectivity indices, it was clearly evident that thiazolones (7-10), bearing methoxy or bromo substitution, showed the highest selectivity (103-114). While for thiazolones (1-6), a decreased selectivity was generally observed with SI values ranging from 27-90. Among the latter, the morpholine derivatives 2, 4 and 6 demonstrated superior selectivity to the piperidine derivatives 1, 3 and 5.

Table 2: *In vitro* COX-1/2, 15-LOX inhibition IC_{50} values and COX selectivity indices of the newly synthesized compounds

Code	Structure	IC_{50} (μM)[a]			SI[b]
		15-LOX	**COX-1**	**COX-2**	(COX-1/ COX-2)
Celecoxib	---	nd[c]	14.8	0.05	296
Diclofenac Na	---	nd	3.9	0.8	4
Indomethacin	---	nd	0.039	0.49	0.08

Meclofenamate Na	---	5.64	nd	nd	nd
Quercetin	---	3.34	nd	nd	nd
NDGA	---	10.56	nd	nd	nd
1	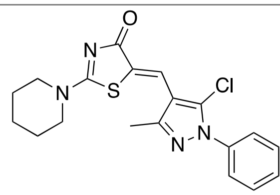	1.96	6.56	0.11	59
2	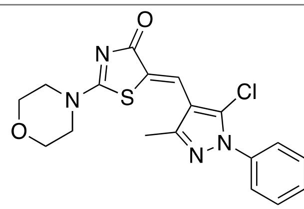	2.42	8.14	0.09	90
3	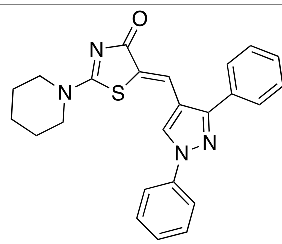	2.54	7.86	0.19	41
4	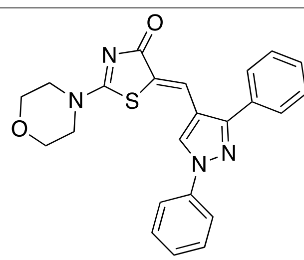	4.63	11.32	0.14	80
5	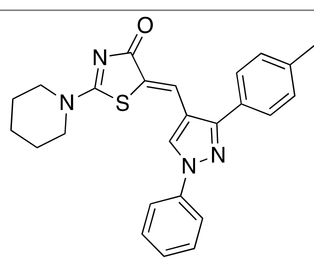	4.23	9.23	0.34	27

6	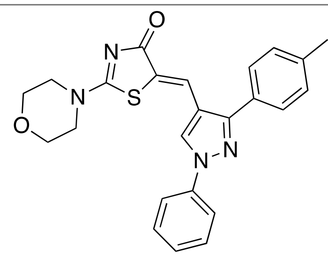	2.85	12.54	0.18	69
7	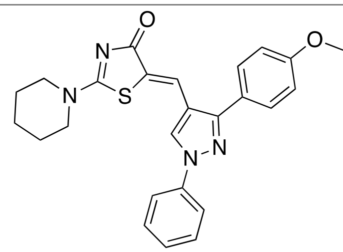	3.52	10.34	0.09	114
8	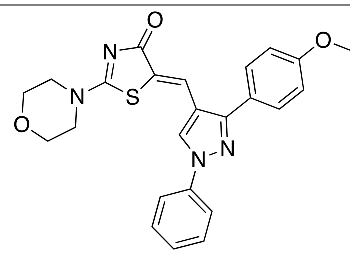	4.64	12.45	0.11	113
9	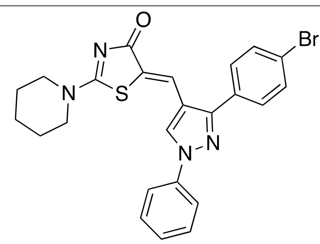	5.64	14.02	0.13	107
10	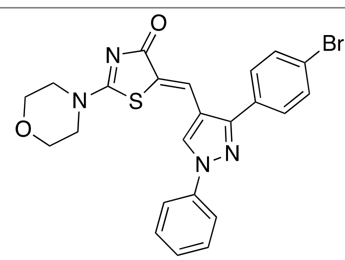	4.52	11.33	0.11	103

2. In vivo anti-inflammatory activity

Following *in vitro* COX and LOX inhibition assays, the three most active compounds were challenged using the acute inflammation model formalin-induced rat paw edema bioassay. Inflammation was stimulated by subcutaneous injection of formalin and the test compounds were administered as an oral dose of 5 mg/kg body weight. The % inhibition of edema after 4 h was measured to determine potencies of the test compounds in comparison to the control. The positive controls used were celecoxib and diclofenac sodium. Results indicated that compounds (4,7,8) were as effective as either diclofenac or celecoxib in suppressing acute inflammation measured by reduction in paw edema volume (Fig. 20A). In the cotton pellet induced-granuloma test used as a chronic model of inflammation, all tested compounds demonstrated clear anti-inflammatory activity of a magnitude equal or superior to reference compounds (Fig. 20B). Specifically, compounds (7 and 8) showed a significant increase in inhibition of granuloma weight in comparison to celecoxib.

3. Inhibition of monocyte-to-macrophage differentiation assay

In order to further evaluate the anti-inflammatory potential of the compounds, we assessed their effect on inhibition on monocyte recruitment and subsequent activation into macrophages. For this purpose, we utilized the PMA-induced THP-1 differentiation assay as a typical *in vitro* model of this process (Sakamoto et al., 2001). We tested the inhibitory effects of the compounds on monocyte differentiation into pro-inflammatory M1 macrophages, using PMA and LPS consecutively for THP-1 stimulation (Genin, Clement, Fattaccioli, Raes, & Michiels, 2015) (Fig. 20C). The effects of these dual inhibitors were compared to diclofenac as a reference compound. The range of concentrations used for the assay was shown not to induce any cytotoxicity on THP-1 cells (Fig. 20D). As shown in Fig. 20E, pre-incubation of THP-1 monocytes with any of the three compounds inhibited their differentiation into M1 macrophages in a concentration-dependent manner, with 4 and 7 demonstrating higher potency compared to diclofenac.

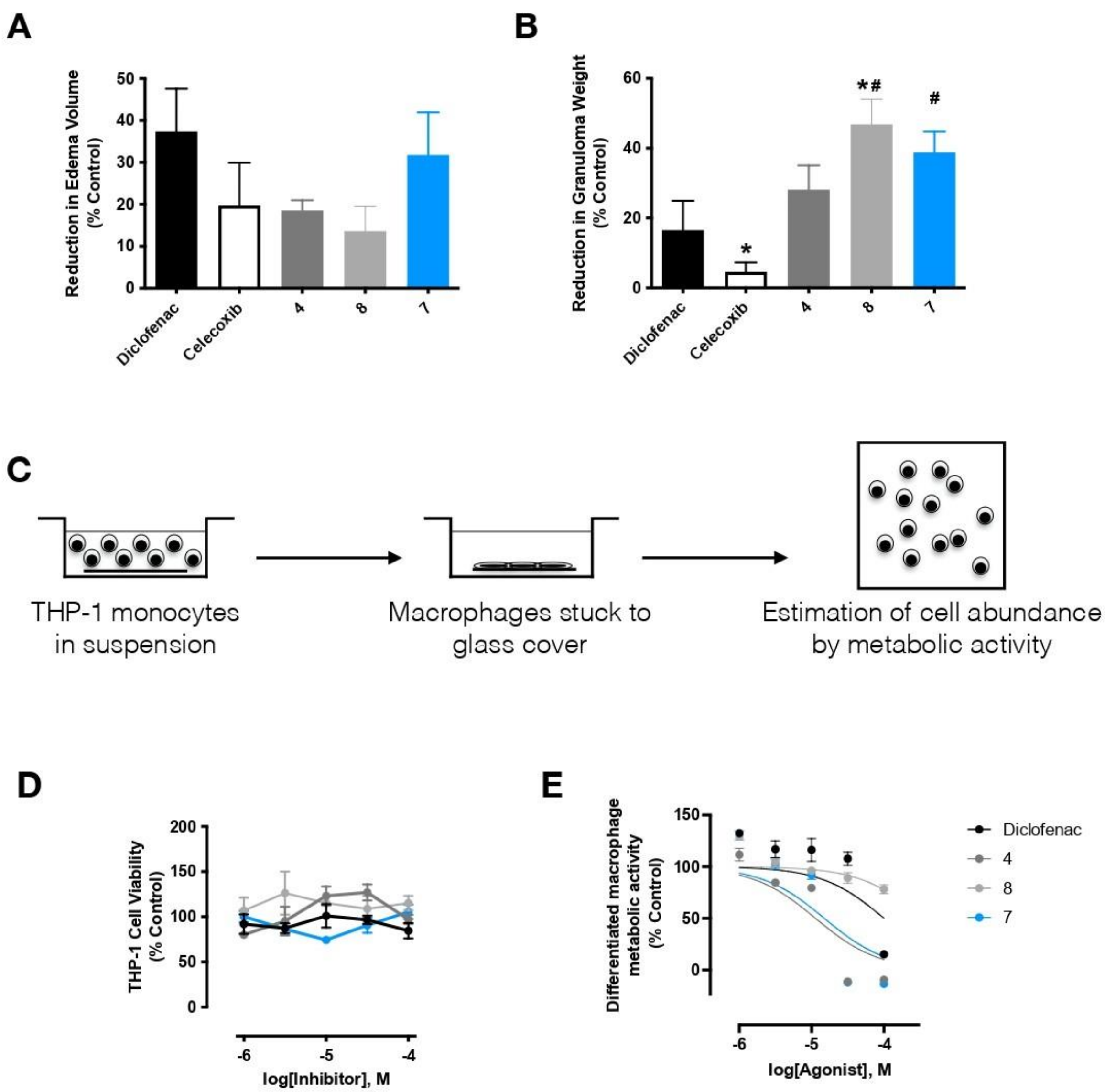

Figure 20. **COX-2/15-LOX dual-targeting compounds demonstrated potential anti-inflammatory properties**. *In vivo* anti-inflammatory activities of compounds (4, 7, 8) in; A, formalin-induced rat paw edema assay (model of acute inflammation) (A) and in cotton pellet induced granuloma test (model of chronic inflammation) (B). C, a schematic representation for monocyte-to-macrophage differentiation assay; D, THP-1 cell viability at the different drug concentrations used for the assay; E, concentration-dependent inhibition of monocyte differentiation into macrophage in response to sequential stimulation with PMA and LPS. Data presented are mean ± SEM. Statistical significance was assessed by one-way ANOVA followed by Tukey multiple comparisons test. * and # denote P-values < 0.05 vs. diclofenac and celecoxib, respectively.

4. *IL-1β Expression*

Previous studies have demonstrated an association between 15-LOX activation and cytokine production in multiple cell lines (Abrial et al., 2015; C. Liu et al., 2009; L. Zhang et al., 2014). In particular, 15-LOX and its metabolites were shown to induce the production of a number of proinflammatory cytokines in macrophages, including tumor necrosis factor-α (TNF-α), IL-1β, IL-6, IL-12, and monocyte chemo-attractant protein-1 (Middleton, Rubinstein, & Pure, 2006; Y. Wen et al., 2007). The produced IL-1β causes further activation of a signaling pathway leading to the enhancement of phospholipase A2-dependent arachidonate release and metabolism in a positive feedback loop (Walters et al., 2011). Interestingly, 15-LOX expression in macrophages also contributes to atherosclerosis progression, via enhancing lipid accumulation and cytokine production (Magnusson et al., 2012). Furthermore, a body of evidence has proposed a role for COX-2 in increasing the production of the pro-inflammatory cytokine IL-1β. PGE2, a major COX-2 metabolite, enhanced NLRP3 inflammasome-dependent IL-1β production in macrophages through enhancing cAMP levels (Hua et al., 2015; Park et al., 2004). In this context, various studies demonstrated that COX-2 inhibition abolished the expression of IL-1β (da Silva et al., 2018; Y. Liu et al., 2018). In an attempt to provide a pathophysiological context for the dual COX-2/15-LOX inhibition, we tested the effect of our hybrid compounds on IL-1β expression in THP-1 monocytes challenged with PMA and LPS (Fig. 21A). PMA/LPS treatment exhibited a marked increase in IL-1β production when compared to untreated control. Such an increase in IL-1β expression was significantly attenuated in cells treated with our compounds.

N. COX-2/15-LOX dual-targeting compounds' anti-inflammatory properties are linked to their ability to induce apoptosis of M1 macrophages

Although our dual COX-2/15-LOX inhibitors did not demonstrate cytotoxic effects on THP-1 monocytes up to the highest concentration used (100 μM), 4 and 7 tended to slightly decrease PMA/LPS-stimulated THP-1 (M1 macrophages) cell viability (Fig. 21B). In view of the enhanced inhibitory effects of the compounds on M1 macrophages, such an observation proposed a possible cell death mechanism induced by our dual inhibitors. Therefore, we examined the protein expression and activity of caspase-3, a key regulator of apoptosis. Our hybrid compounds attenuated the protein expression of non-cleaved procaspase-3, hence suggesting an enhanced cleavage of procaspase-3 into its active form caspase-3 (Fig. 21A). Consistently, these dual inhibitors also produced a significant enhancement of caspase-3 activity in PMA/LPS-induced THP-1 monocytes (Fig. 21C).

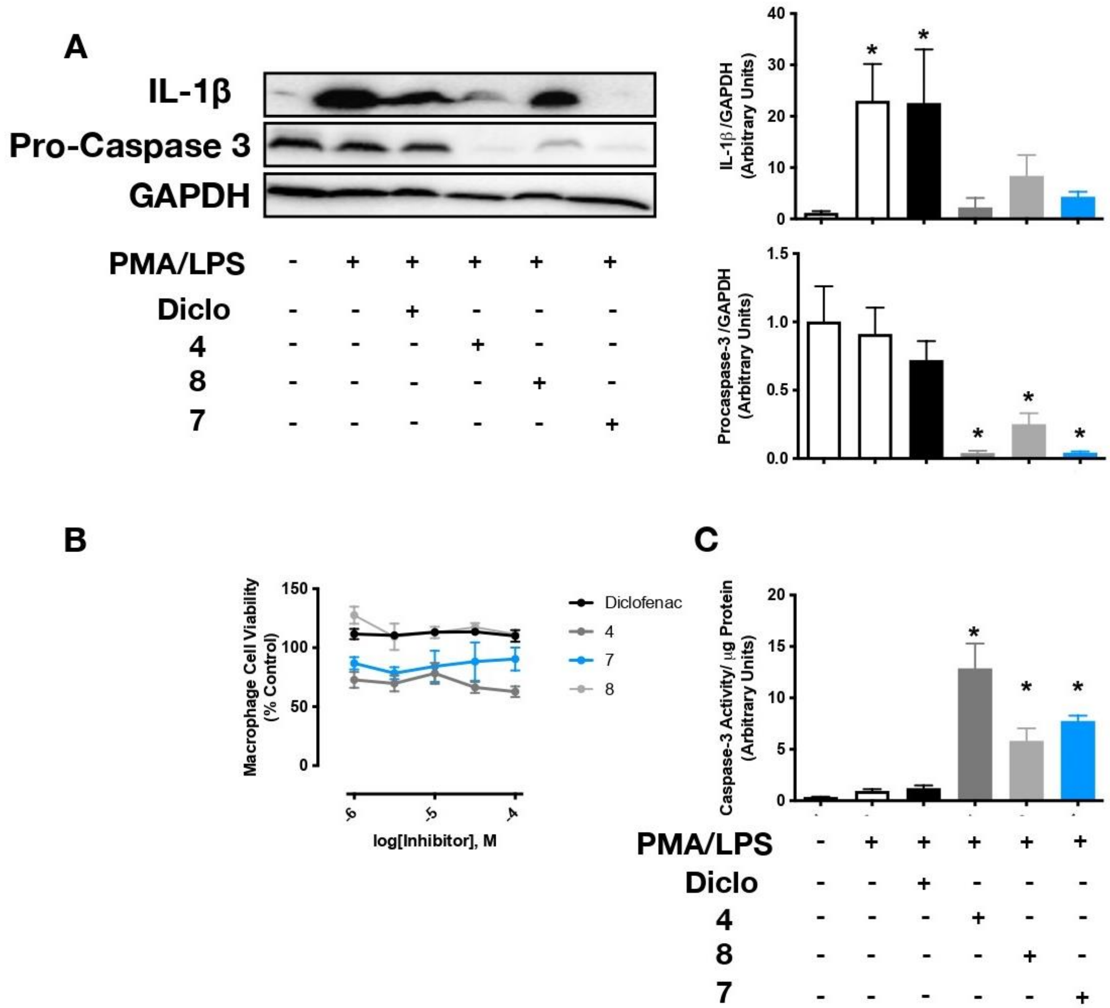

Figure 21. **The effect of selected compounds on IL-1β expression and apoptotic changes in M1 macrophages.** A, representative blots for IL-1β and procaspase-3 (left) and the quantified protein expression levels for IL-1β and procaspase-3 (right); B, M1 macrophage viability at the different drug concentrations; C, increased caspase-3 activity in M1 macrophages treated with different compounds. Data presented are mean ± SEM. Statistical significance was assessed by one-way ANOVA followed by Tukey multiple comparisons test. * and # denote P-values < 0.05 vs. untreated control and PMA/LPS differentiated macrophages, respectively.

O. Triple-targeting compounds exhibit significant COX-2 and 15-LOX inhibitory activities

1. In vitro COX-1 and COX-2 inhibitory assay

As summarized in **Table 3**; all synthesized compounds, with the exception of compound **5f**, were more potent COX-2 inhibitors than the two reference drugs diclofenac and indomethacin. They also showed higher SI than two reference drugs diclofenac and indomethacin. Although they showed lower COX-2 inhibition in comparison to celecoxib, they operated within the same range of sub-micromolar activity.

All compounds inhibited COX-1 in concentrations that are at least one order of magnitude higher than that experienced with COX-2, which highlights the selectivity displayed towards COX-2. For triazoles prepared from benzyl azides, we observed that the addition of 4-bromo substitution enhanced both COX-2 inhibitory activity and SI values when compared to the unsubstituted analogs. The thiazolidine-2,4-dione derivative **5b** was slightly more potent than the rhodanine **5a**. It reached about 8 times the activity of diclofenac and 5 times that of indomethacin. Intriguingly, **5b** showed the highest SI value (159) out of all the synthesized compounds in the study, which accounts for almost one half that of celecoxib activity and selectivity towards COX-2.

Within the triazole series prepared from aryl azides, it was noticed that 4-substitution with lipophilic π-deficient or π-rich substituents as was seen with 4-bromo (**5e** and **6e**) and 4-methoxy (**5g** and **6g**) remarkably enhanced both COX-2 inhibitory activity and SI values over the unsubstituted congeners. 4-Bromophenyl triazolyl compounds **5e** and **6e** showed about 4-5 times the inhibitory activity of indomethacin with about 950 times its SI towards COX-2. They reached about 6-8 times the inhibitory activity of diclofenac with about 19 times its SI towards COX-2. 4-Methoxyphenyl triazolyl compounds **5g** and **6g** showed about a 3.5-6 times the inhibitory activity of indomethacin with about 700 and 1260 times its SI towards COX-2, respectively. They reached about 5-8 times the inhibitory activity of diclofenac with about 14 and 25 times its SI towards COX-2, respectively.

On the other hand, 4-substitition with methyl (**5f** and **6f**) and carboxylic functionalities significantly reduced COX-2 inhibitory activity and SI values in comparison to their unsubstituted counterparts. Surprisingly, the novel propargyl rhodanine **4b** showed higher COX-2 inhibitory activity and SI value than that of propargyl thiazolidine-2,4-dione **4a** and was among the most active compounds in the whole study.

Cycloaddition reaction of **4a** and **4b** with 4-substituted phenacyl azides generally enhanced the activity with the highest difference observed with the 4-bromo substituted derivatives **5j** and **6j**. It is noteworthy that rhodanine derivatives demonstrated superiority in both COX-2 inhibitory activity and SI values in comparison to their thiazolidine-2,4-dione counterparts, with the exception of **5a** and **5b**. A general trend was observed that bromo-containing compounds were among the most active within the whole study.

2. *In vitro 15-LOX inhibitory assay*

Compounds that showed the highest *in vitro* COX-2 inhibitory activity (**4b, 5b, 5e, 5g, 5j, 6b, 6e, 6g, 6i** and **6j**) were. *In vitro* 15-LOX enzymatic inhibitory activities are expressed as IC_{50} values of the tested compounds and shown in **Table 3**. All ten compounds showed substantial LOX inhibitory activity with IC_{50} in the range of 3.14-5.92 µM. They operated in the same order of magnitude as NDGA and quercetin. All ten compounds showed superior LOX inhibitory activity to that of NDGA while displaying varying activity when compared to quercetin. Interestingly, the most and least potent derivatives **4b** and **5b** had almost thrice and twice the activity of NDGA, respectively. Additionally, **4b** was more potent than quercetin while **5e** and **5g** were almost equipotent to quercetin. Other compounds appeared in the following descending order of activity; **6i**, **5e**, **6b**, **6j**, **5j**, **6g** and **5b**. Consequently, the above results showed that all ten compounds have promising LOX inhibitory activity.

Table 3: *In vitro* COX-1, COX-2, 15-LOX inhibitory IC_{50} values and COX SI values of synthesized compounds.

Code	Structure	IC_{50} µM[a]			SI
		COX-1	**COX-2**	**15-LOX**	COX-1/ COX-2[b]
Celecoxib		14.8	0.05	-	296
Diclofenac Na		3.9	0.8	-	4.9
Indomethacin		0.039	0.49	-	0.1
6a	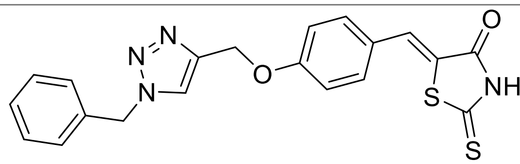	8.4	0.33	-	25.5

5a	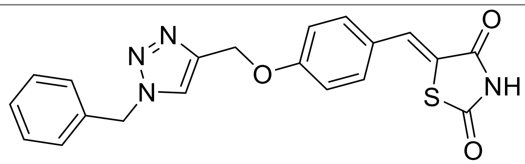	9.4	0.27	-	34.8
6b	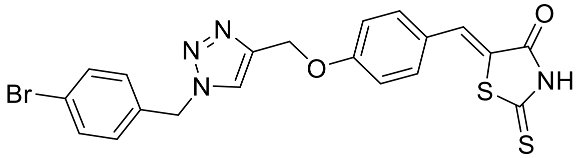	13.4	0.11	4.32	121.8
5b	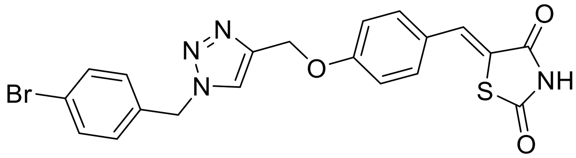	15.9	0.10	5.92	159
6c	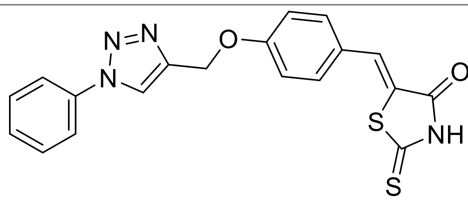	6.4	0.26	-	24.6
5c	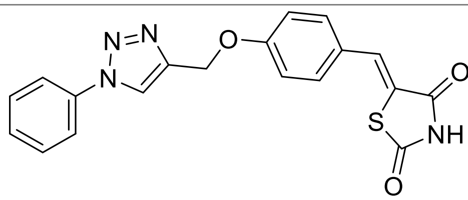	5.9	0.38	-	15.5
6d	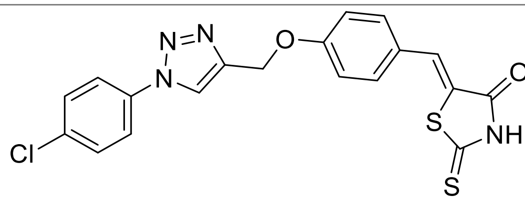	8.6	0.19	-	45.3
5d	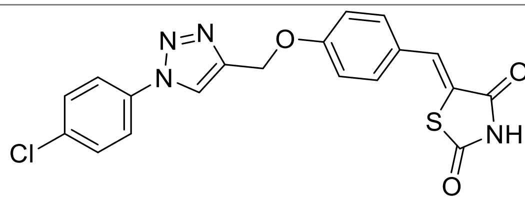	6.9	0.26	-	26.5

6e	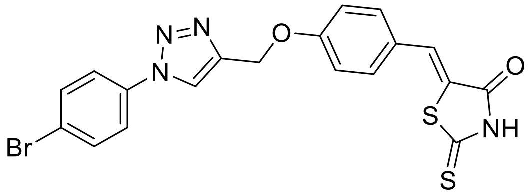	10.5	0.11	3.74	95.5
5e	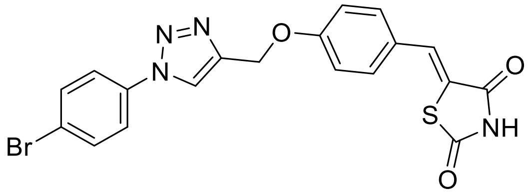	11.6	0.12	4.23	96.7
6f	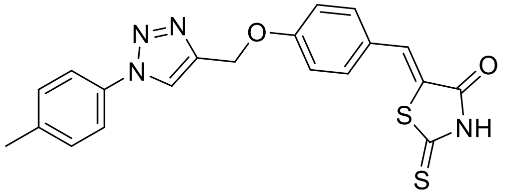	7.4	0.41	-	18.0
5f	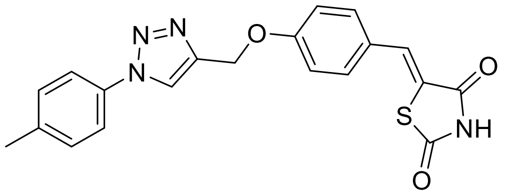	5.9	0.52	-	11.3
6g	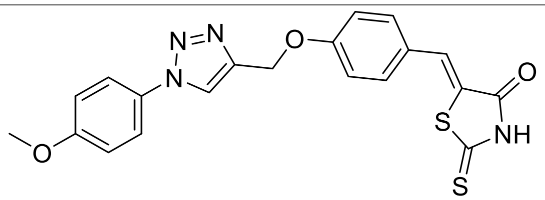	12.6	0.10	5.24	126
5g	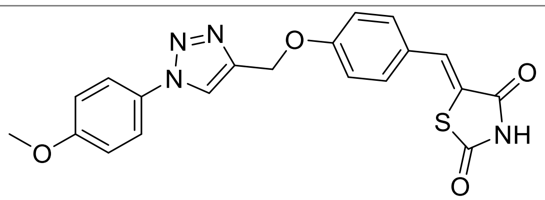	9.8	0.14	3.22	70
6h	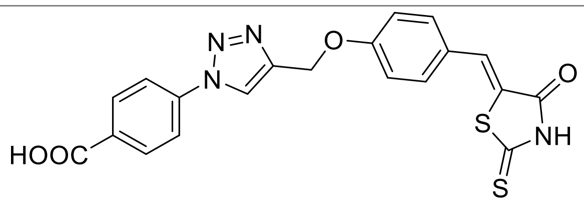	8.2	0.36	-	22.8

5h	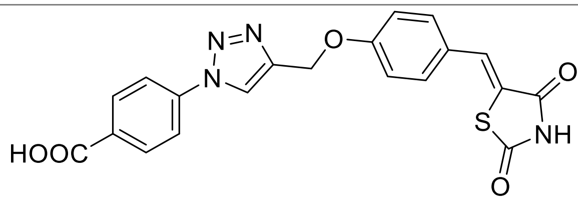	5.9	0.45	-	13.1
6i	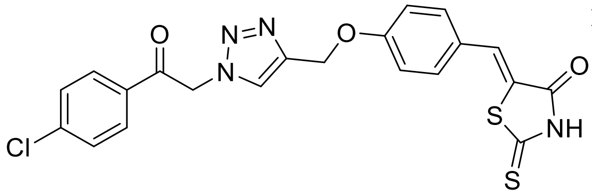	12.4	0.15	4.22	82.7
5i	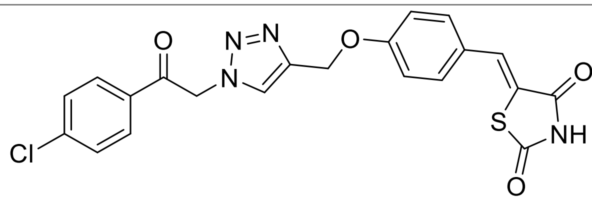	10.9	0.22	-	49.5
6j	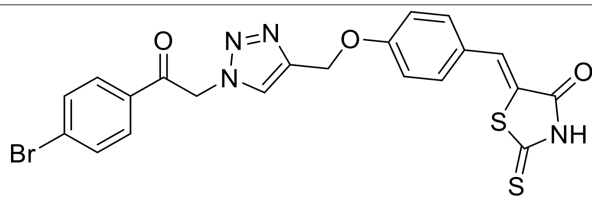	14.9	0.11	4.34	135.5
5j	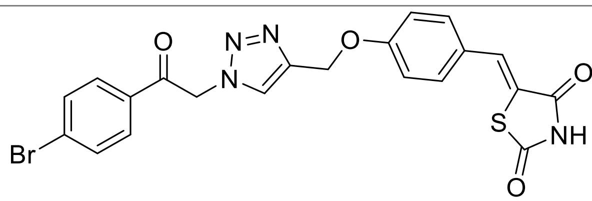	13.6	0.10	4.97	136
4b	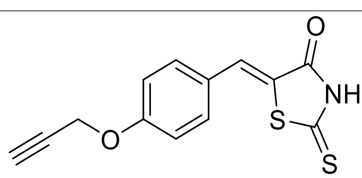	11.6	0.12	3.14	96.7
4a	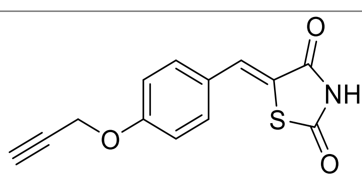	6.9	0.33	-	20.9
NDGA		-	-	10.25	-

Quercetin	-	-	3.27	-

P. Triple-targeting compounds demonstrate selective agonism of PPARγ

1. In vitro glucose uptake using rat hemi-diaphragm model

In order to assess the antidiabetic activity of compounds that showed the highest *in vitro* COX and LOX inhibitory activities (4b, 5b, 5e, 5g, 5j, 6b, 6e, 6g, 6i and 6j), their glucose uptake potential by rat hemi-diaphragm method was measured as previously reported (Kar et al., 2014; B. R. Kumar et al., 2011; Walaas & Walaas, 1952). The glucose content of the working solution was measured, and the glucose uptake was calculated as the difference between the initial and final glucose content at 2 mg of optimized drug concentration. The glucose uptake by rat hemi-diaphragm was measured in mg/dl/45 min. Results of the *in vitro* glucose uptake assay revealed that compounds 4b, 5e, 6g and 6j showed equal or higher glucose uptake than pioglitazone without insulin and significantly higher uptake with insulin. Compounds 5j and 6i showed lower glucose uptake without insulin than pioglitazone but equal or higher uptake with insulin. Interestingly, compounds 5b and 5g showed equal or higher glucose uptake than pioglitazone in an insulin-independent fashion.

2. Immunohistochemical analysis of ligand-stimulated PPARγ nuclear localization

The ability of the synthesized compounds to induce PPARγ nuclear translocation was studied in rat primary adipocytes as described previously (Maresca et al., 2013; Yasmin & Jayaprakash, 2017). Four compounds were selected; 4b & 5e shown to have an insulin-sensitive glucose uptake effect comparable to pioglitazone, and 5b & 5g shown to have a significant insulin-independent glucose uptake. The effect of a 3-hour exposure to 10 μM concentration of each of those compounds on the nuclear localization of PPARγ in rat adipocytes was compared to that of an equivalent concentration of pioglitazone. Figure 17 shows representative micrographs of control and treated adipocytes. Untreated controls (exposed to an equivalent volume of DMSO as the vehicle) showed diffuse cytosolic PPARγ staining. Adipocytes treated with pioglitazone or the selected test compounds showed redistribution of PPARγ staining that is superimposed with nuclear staining as depicted in the fluorescence intensity profiles along the line scans showed in Figure 22. This is suggestive of the ability of the selected compounds to induce PPARγ nuclear translocation similar to pioglitazone. The confirmation of PPARγ nuclear translocation together with insulin-independent glucose uptake of compounds 5b & 5g raise the possibility of selective targeting of signaling pathways.

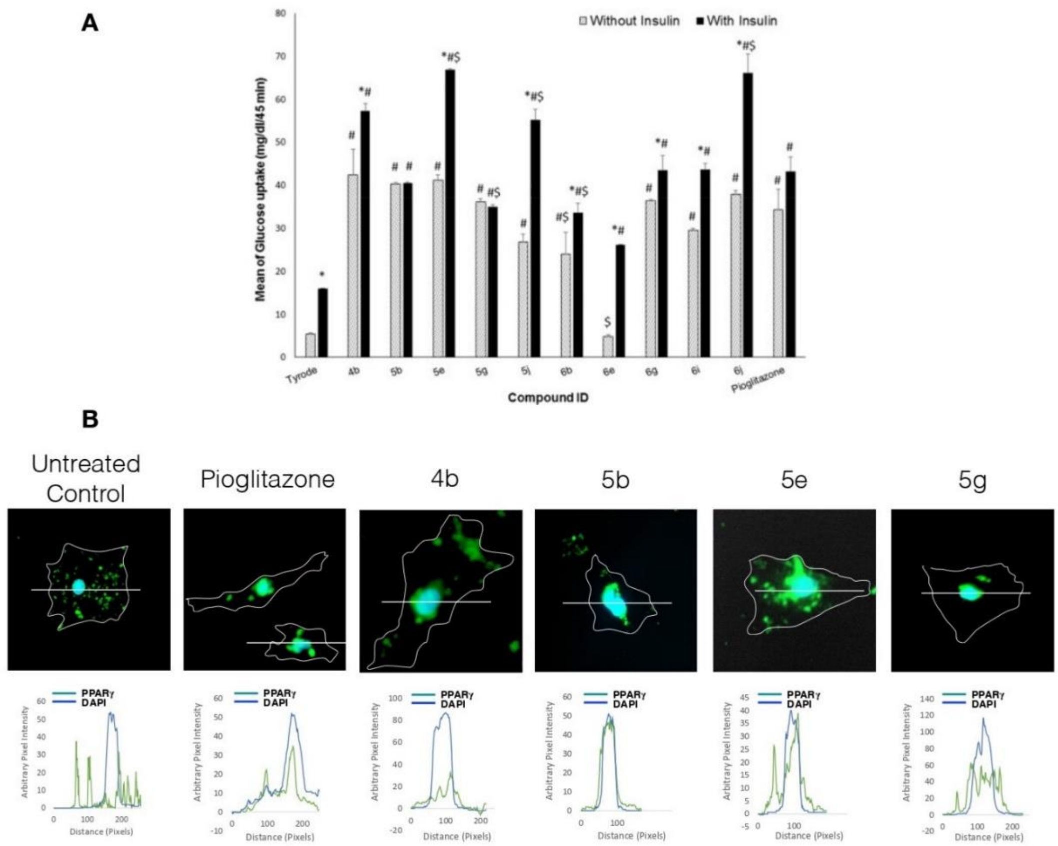

Figure 22. **Triple-targeting compounds exhibit selective PPARγ agonism.** A, *in vitro* glucose uptake activity of the most active compounds both in absence and presence of insulin using rat hemi-diaphragm model. Data represented are mean ± SD of three replicates. Statistical analysis was performed using two-way ANOVA followed by Sidak post hoc test. *P*-values < 0.05 was considered significant. * denotes significance vs. the corresponding effect of each compound in absence of insulin, # denotes significance vs. the corresponding arm of tyrode exposure, while $ denotes significance vs. the corresponding arm of pioglitazone treatment; B, immunofluorescent staining of PPARγ in untreated rat primary adipocytes and those exposed to 10 μM of pioglitazone and different test compounds for 3 hours. Phase contrast cell contours are delineated in white. Nuclei were stained with DAPI. The corresponding graphs show staining intensity for PPARγ (green) and DAPI (blue) along the scan line indicated on the corresponding micrographs.

Q. Triple-targeting compounds exhibit partial PPARγ agonism

1. PPARγ functional reporter gene assay

The effect of the selected compounds showing PPARγ nuclear translocation on its transcriptional activity was assessed using a functional gene reporter assay (Kojo et al., 2003). Human embryonic kidney (HEK293) cells transiently transfected with two components: 1) a hybrid receptor comprising the N-terminal Gal4 DNA binding domain fused to the ligand binding domain of human PPARγ and 2) reporter Renilla luciferase gene functionally linked to the Gal4 upstream activation sequence. The transfected HEK293 cells were exposed to different concentrations of pioglitazone, 4b, 5b, 5e, and 5g for 24 hours. Luciferase activity was measured and compared to basal activity in cells treated with the vehicle (DMSO). As shown in Figure 18A, at the highest concentration (10 μM), pioglitazone showed a 6-fold increase in luciferase activity compared to vehicle. At the same concentration, the tested compounds showed a 2-3-fold increase, with transcriptional activity of 25-45% that of pioglitazone. Based on the transcriptional response, a partial PPARγ agonistic activity can be assumed for the tested compounds.

2. Structure determination of compound 4b bound to PPARγ

Although the biological activity of 4b was confirmed by multiple lines of evidences (molecular then cellular and finally *in vivo*), we wanted to rule out any skepticism about its proven biological activity and exclude the presence of any assay artifacts. Hence, we determined the X-ray crystal structure of compound 4b in complex with the PPARγ ligand binding domain (LBD) which will give us the chance to probe its binding mode and detect specific binding interactions (Fig. 18B). Coordinates and structure factors were deposited in the Protein Data Bank under accession code 6E5A. Two subunits per asymmetric unit were found and both subunits were found bound to 4b in a similar manner. The overall fold of PPARγ was similar to most other observed structures, for example the 4b bound structure displays an RMSD to the rivoglitazone bound structure (PDB:5U5L) of 0.48Å (over 512 Cα atoms), signifying that the binding of compound 4b does not induce major conformational changes as compared to other TZD based compounds. Compound 4b is located in the LBD with the ring systems of the compound located between H3 and the beta-sheet region and the carbon tail inserted into the hydrophobic patch below the AF2 region. 4b makes only one hydrogen bond to PPARγ, via its non-protonated nitrogen atom to the protonated nitrogen backbone atom of Ser342 (3.0Å). All other contacts are hydrophobic and Van der Waals interactions. The double ring system of compound 4b sits between H3 and the beta sheet region making these contacts with Ile281 (H3), Ile341 side chain (beta-sheet), the non-polar portion of Ser342 side chain (beta-sheet), the non-polar portion of Arg288 side chain (H3), Leu353 side chain (H6), and the side chain of Met364 (H7). The carbon tail of 4b makes hydrophobic interactions with H6 and H7 which include those to the side chain of Met364, the side chain of Phe363 (H7), the side chain of Phe360 (H7), and the side chain of Leu353 (H6) as shown in Figure 23B.

A

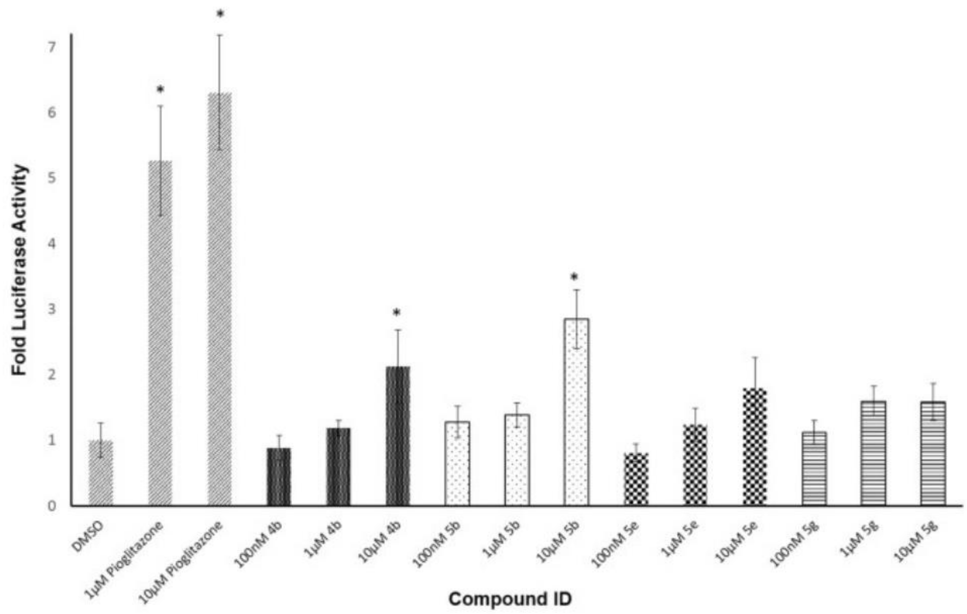

B

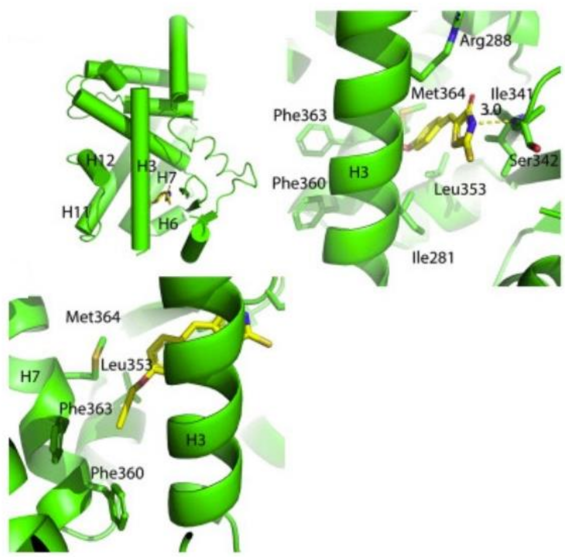

Figure 23. **Triple-targeting compounds exhibit partial PPARγ agonism.** A, graphical representation of the increased PPARγ-mediated transcriptional activity following treatment with different concentrations of pioglitazone and selected synthetic compounds. Results are expressed as fold change compared to luciferase activity in vehicle-treated cells. Data presented are mean ± SEM. Luciferase activity values were compared to vehicle with One-way ANOVA followed by Dunett Multiple Comparisons test. * denotes a P-value < 0.05 vs. DMSO treated cells; B, Binding mode of 4b to PPARγ as determined by X-ray crystallography (PDB accession code 6E5A). PPARγ is shown in green ribbons, compound 4b is shown in yellow sticks, and residues of PPARγ within 3.5Å of the ligand are depicted as green sticks. 1) Overview of the entire PPARγ LBD bound to 4b. 2) Interactions of 4b

with the beta-sheet and H3 region. 3) Interactions of the carbon tail of 4b with residues of the hydrophobic pocket formed by H7, and H3.

R. Triple-targeting compounds manifest potent anti-inflammatory potential

1. In vivo anti-inflammatory activity

Formalin-induced rat paw edema protocol as an acute inflammation model was used to test the *in vivo* anti-inflammatory activity of the four most active compounds **(4b, 5e and 5g)**. Intriguingly, all tested compounds with the exception of **4b** showed equivalent inhibitory effect to celecoxib and diclofenac (Fig. 24A). Additionally**, 4b** demonstrated a statistically significant higher potency compared to celecoxib.

2. Inhibition of monocyte to macrophage differentiation

We anticipated that the three compounds (4b, 5e, and 5g) that showed dual COX-2 and 15-LOX inhibitory activities together with PPARγ partial agonistic activities, would maintain a similar, if not enhanced, activity against THP-1 monocyte differentiation into macrophages. Towards this end, we used the PMA-induced THP-1 differentiation assay as an accepted *in vitro* model of this process (Sakamoto et al., 2001). The effects of these compounds in the assay were compared to diclofenac and pioglitazone as reference compounds. Diclofenac produced a concentration-dependent inhibition of the differentiation process yielding an IC50 value close to that previously reported in a similar assay (Moussa et al., 2018). Surprisingly, pioglitazone did not produce an appreciable inhibition of PMA-induced monocyte differentiation up to 300 μM concentration. While 5g produced effects similar to pioglitazone, 5e showed effects close to that of diclofenac (Fig. 24B). 4b appeared to be more potent than diclofenac in inhibiting this process. Yet, it is worth mentioning that this assay measures the differentiation of monocytes into adherent macrophages with no indication of potential differences in differential polarization, if any. Thus, a negative result might not completely rule out the beneficial effect of PPARγ agonistic activity represented by pioglitazone.

3. IL-1β and TNF-α expression and 20-HETE production assay

Previous literature consistently showed that 15-LOX activation is associated with increased cytokine production in variety of cell types (Abrial et al., 2015; C. Liu et al., 2009; L. Zhang et al., 2014). Specifically, both the addition of 15-LOX arachidonate metabolites or their de novo synthesis in monocytes triggered cytokine production in macrophages, including tumor necrosis factor-α (TNF-α), interleukin-1β (IL-1β), IL-6, and monocyte chemo-attractant protein-1 (Y. Wen et al., 2007). Moreover, the produced IL-1β contributes to further stimulation of signaling pathways leading to the enhancement of phospholipase A2-mediated arachidonate release and metabolism in a positive feedback loop (Walters et al., 2011). We attempted to provide a pathophysiological context for the 15-LOX inhibitory action of our hybrid compounds. We examined the effect of the three compounds (4b, 5e & 5g) on TNF-α and IL-1β production in THP-1 monocytes differentiated into macrophages by PMA, and activated by a lipopolysaccharide (LPS) challenge. Compared to the negative control, LPS-treated macrophages showed massive increases in both TNF-α and IL-1β production (Fig. 24C). The increase in both cytokines' expression was greatly attenuated in cells treated with our compounds. As well, we tested the effect of these compounds on the 20-hydroxyeicosatetraenoic acid (20-HETE) production in these cells as a general indicator of arachidonate metabolism. The concentration of 20-HETE produced in the conditioned medium of PMA-differentiated THP-1 monocytes that were challenged with LPS was measured by enzyme-linked immunosorbent assay (ELISA). 20-HETE production increased following LPS challenge compared to untreated controls. Cells treated with our compounds showed reduced 20-HETE production indicating a possible decrease in arachidonic acid release possibly as a result of the interruption of the IL-1β positive feedback loop (Fig. 24D).

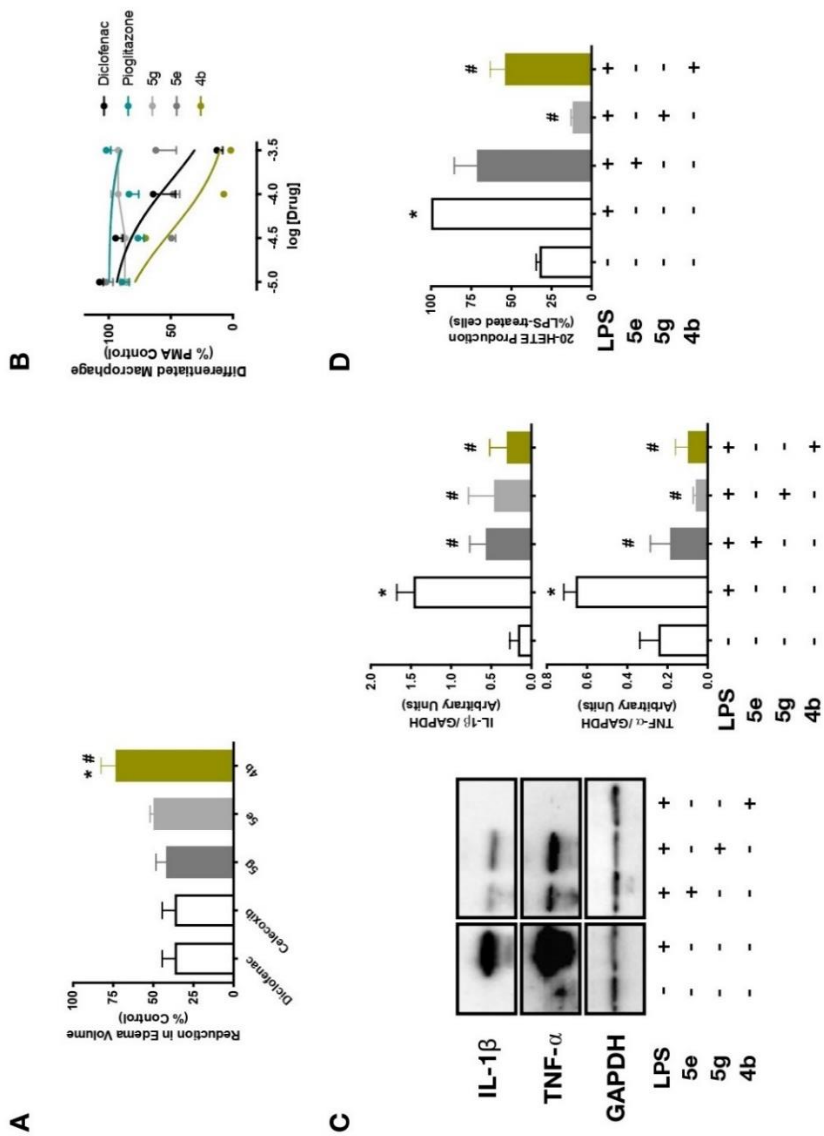

Figure 24. **Triple-targeting compounds exhibit anti-inflammatory properties.** A, Graphical representation of *in vivo* anti-inflammatory activities of selected compounds in formalin-induced rat paw edema bioassay (acute inflammation model). B, inhibition of monocyte-to-macrophage differentiation by diclofenac, pioglitazone, and the selected synthetic compounds. Results are represented as percentage macrophage metabolic activity of the PMA control at different exposure concentrations. C, representative western blotting of IL-1β, TNF-α, and GAPDH from THP-1 cells exposed to different treatment conditions

(left). The bar graphs summarize the quantification of three separate experiments (right). D, 20-HETE concentration in the conditioned medium of THP-1 cells exposed to the indicated treatment conditions. Concentration is normalized to the values measured in untreated cells challenged with LPS. Results presented are Mean ± SD. Statistical significance was measured by one-way ANOVA followed by Tukey Multiple Comparisons *post hoc* test. * denotes significance vs. celecoxib in the *in vivo* anti-inflammatory assay. * denotes a P-value < 0.05 vs. untreated control while # denotes a P-value < 0.05 vs. LPS-challenged cells in western blots.

S. *Ex vivo* exposure of rat aortic rings to PA as a model for lipid-induced ED

Myobath experiments were conducted on thoracic aortic rings obtained from control rats groups. Increasing concentrations of PE produced higher aortic contraction in control aortic rings pre-incubated with 800 μM PA (Fig. 25B). Indeed, the increased sensitivity of PA-exposed vessels to the contractile effect of PE was demonstrated as a reduced EC50 (increased pEC50) in comparison to the control group (Fig. 25C).

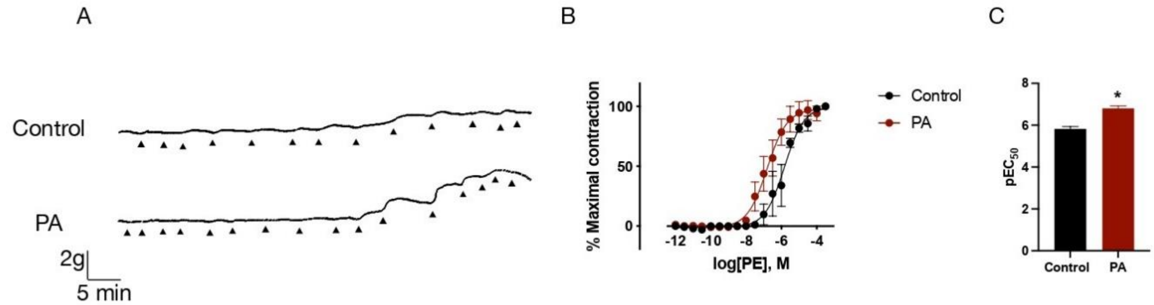

Figure 25. **PE-mediated contractility in control and PA-incubated rings.** A, Representative tracings showing the contractility response to PE on control (top left) and PA incubated aortic rings (bottom left); B, PE concentration-response curve of control and PA group; C, Effective concentration (EC50) of both control and PA-treated groups. Statistical significance was tested by unpaired t-test. * denotes a P-value < 0.05 vs. control rings.

Analysis of endothelium-dependent relaxation showed an impaired ACh-mediated relaxation in rings incubated with 800 μM PA in comparison to control rings. In aortic rings from the control group, ACh induced a maximum relaxation of ~70% of the PE tone at 30 μM concentration, while the PA-incubated aortic ring presented a lower percentage of maximal ACh-mediated relaxation (Fig. 26B). Despite that PA-incubated control aortic rings exhibited an exaggerated response to PE (Fig. 26C), the maximal absolute values of ACh-induced relaxation in the control group remained higher than that of the PA-incubated group (Fig. 26C). Also, PA-treated rings exhibited an enhancement in ROS expression as demonstrated by DHE staining and a reduction in Kir channel expression as shown by western blotting (Fig. 26D).

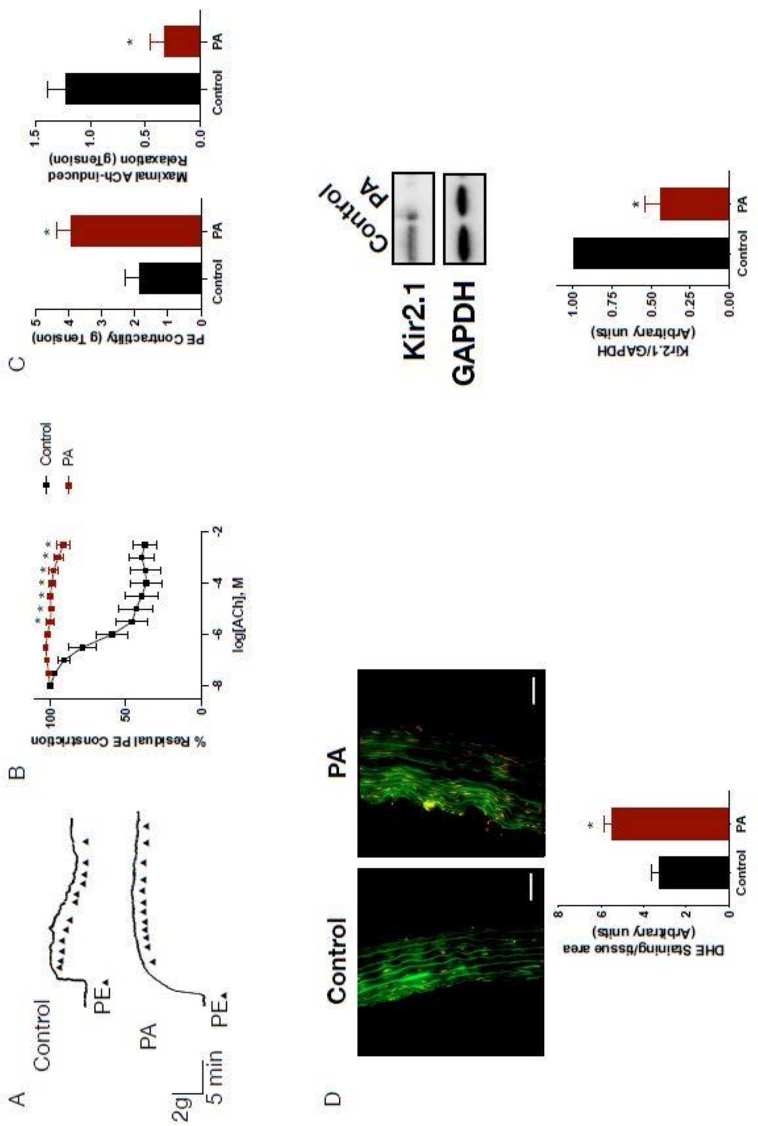

Figure 26. **ACh-mediated endothelium-dependent relaxation of aortic rings from control and PA-incubated aortic rings.** A, Representative tracings showing the relaxant response to ACh in aortic rings pre-constricted with PE from control (top left) and PA incubated aortic rings (bottom left); B, mean normalized ACh-evoked relaxations in presence and absence of PA in aortic rings pre-constricted with PE; C, PE-induced constriction in g tension (left panel) and maximal Ach-induce relaxation in g tension (right panel). D, representative micrographs of DHE staining of control and PA-treated rat aortic rings with the average quantified data. DHE staining appears as red fluorescence on a background of green collagen autofluorescence (left). Scale bars are 40 μm. Representative western blots of Kir2.1 channels in control and PA-treated rings, together with average quantified data normalized to GAPDH (three rats per group, right). Statistical significance was tested by

two-way ANOVA followed by Sidak multiple comparisons tests for B and t-test for C and D. * denotes a P-value < 0.05 vs. control rings.

T. *Ex vivo* evaluation of the effect of MTDLs on the PA-induced endothelial dysfunction

In order to assess understand the potential effect of MTDLs (compounds 4b and 7) on ameliorating PA-induced endothelial damage, we examined the contractile responses of PA-exposed aortic rings following treatment with compounds 4b or 7. Interestingly, concentration-response curves of PE in PA-incubated aortic rings treated with either 4b or 7 showed that only treatment with 4b restored the increased sensitivity to PE to control levels (Fig. 27A), which indeed was reflected on pEC50 values (Fig. 27B). Furthermore, treatment with 4b was able to improve ACh-induced relaxation, which reached about ~80% of the PE tone at 30 μM concentration (Fig. 27D). In contrast, no significant difference was observed in the endothelium-dependent relaxation profile in the PA-incubated vessels treated with compound 7 (Fig. 27D). As such, treatment with 4b produced less PE contractility (nearly 2g tension) when compared to that of the aortic rings treated with PA alone (nearly 4g tension) (Fig. 27E), and restored the absolute value of the maximal ACh-induced relaxation (Fig. 27F).

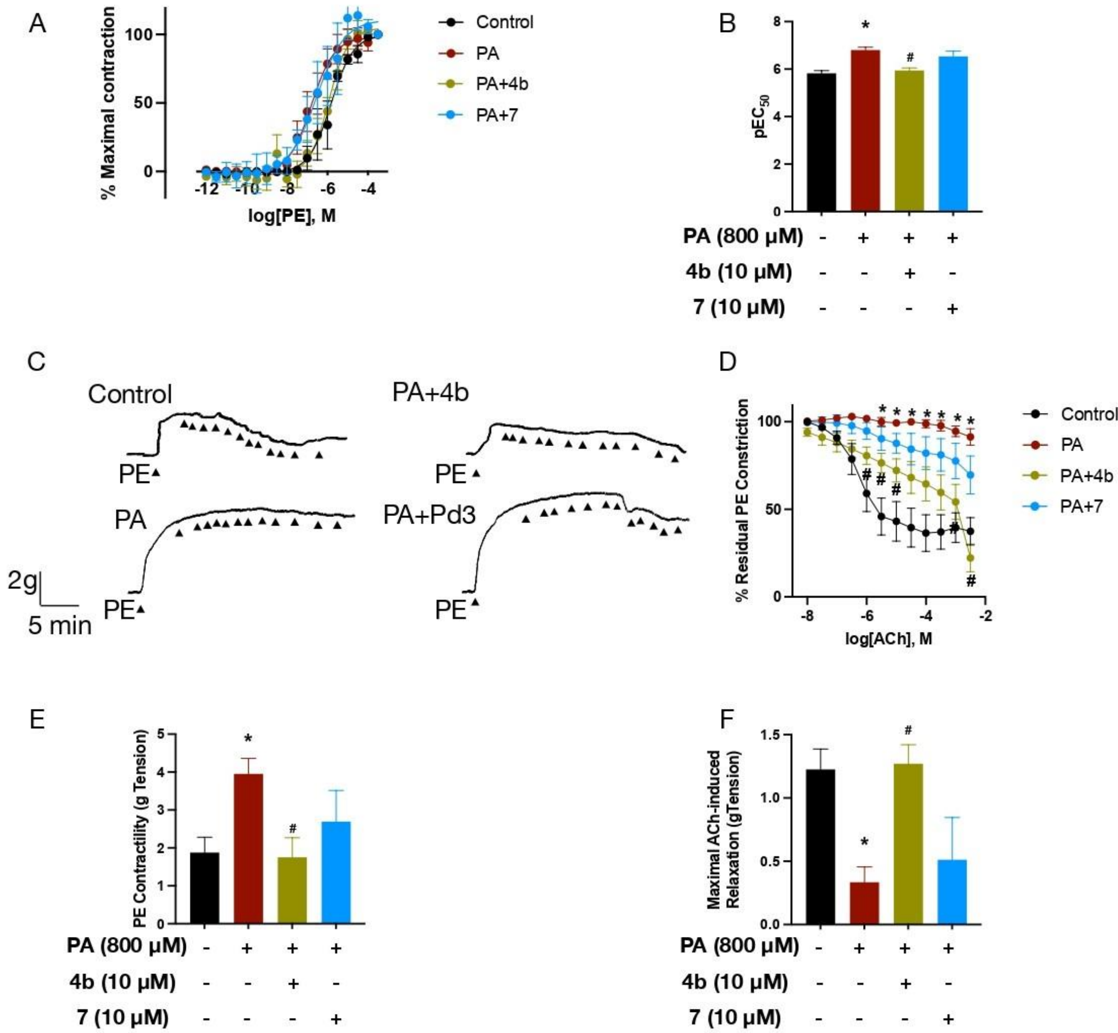

Figure 27. **Ex vivo evaluation of the impact of MTDLs on PA-induced impaired endothelial function**. A, PE concentration-response curve on aortic rings treated with different conditions; B, PE pEC50 values for the different groups; C, representative traces showing the relaxant response to ACh on aortic rings pre-constricted with PE; D, mean normalized ACh-evoked relaxations in aortic rings pre-constricted with PE for the different groups; E, PE-induced constriction in g tension; F, maximal ACh-induced relaxation in g tension. * and # denote a P-value < 0.05 vs. control and PA-exposed rings, respectively. Statistical significance was tested by two-way ANOVA followed by Sidak multiple comparisons tests for D and one-way ANOVA followed by Tukey’s multiple comparisons tests for B, E and F.

U. The effect of MTDLs on endothelium-dependent relaxation Compared to Single Target Compounds

Further experiments were conducted in order to evaluate the beneficial effect of the MTDLs compared to single target compounds, such as the selective COX-2 inhibitor, celecoxib, and pioglitazone, a full PPARγ agonist. Neither the dual-targeting compound 7 nor celecoxib did produce any improvement in ACh-induced relaxation profile in aortic rings pre-constricted with PE (Fig. 28A). However, the addition of pioglitazone demonstrated a significant enhancement of ACh-mediated relaxation, similar to that observed with 4b (Fig. 28B).

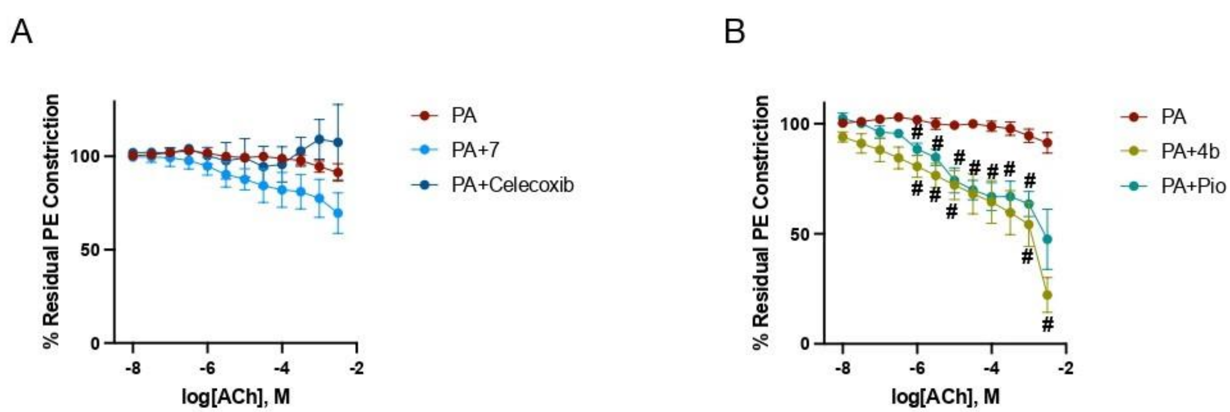

Figure 28. **The effect of single target agents on endothelial dysfunction compared to MTDLs.** Panels A & B, mean normalized ACh-evoked relaxations in aortic rings pre-constricted with PE and incubated with different compounds. # denotes a P-value < 0.05 vs. PA-exposed rings. Statistical significance was tested by two-way ANOVA followed by Sidak multiple comparisons tests for A and B.

V. Evaluation of Kir activity/expression and ROS production as a function of MTDLs treatment

In an attempt to predict the possible enhanced mechanisms accounting for the improved endothelial responses observed with treatment with the triple-targeting compound 4b, we assessed the effect of differential blockade of NO- and EDH-mediated responses on ACh-evoked relaxation in PA-incubated control rings treated with 4b. Interestingly, the addition of L-NAME and BaCl2 significantly attenuated the ACh-induced relaxation (Fig. 29A), indicating that 4b treatment potentially enhanced both endothelial NO and EDH. As such, the effect of 4b on Kir 2.1 channel expression in these tissues was examined (Fig. 29B). Western blotting showed a reduction in protein content of this subunit in aortic tissues of PA-treated aortic rings, with a restoration of expression of Kir 2.1 channel proteins following treatment with 4b. Moreover, DHE staining demonstrated a reduction in ROS production in PA-treated aortic rings in response to treatment with both compounds (Fig. 29C).

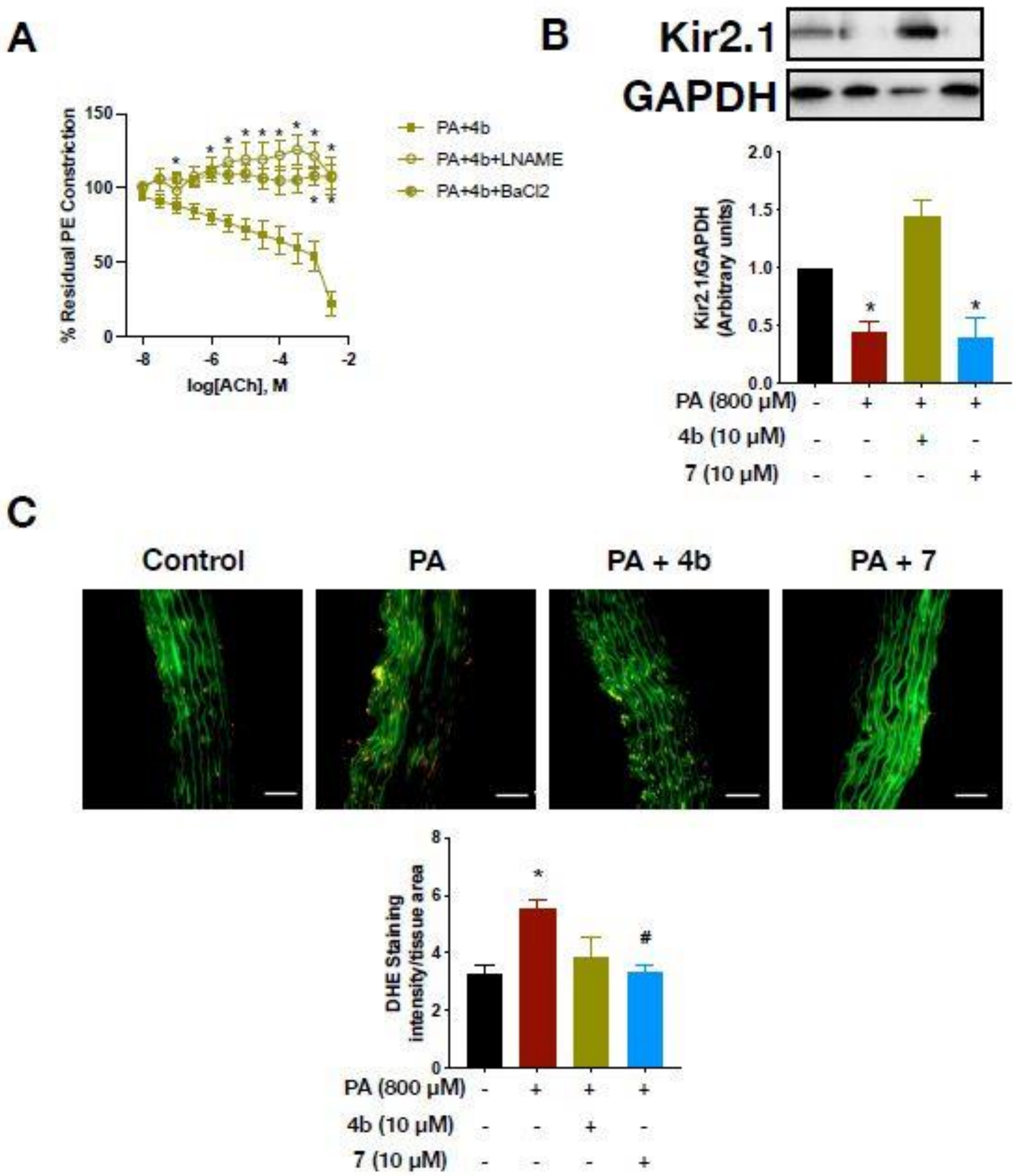

Figure 29. **The impact of MTDLs treatment on components on endothelium mediated relaxation with correlation to inward-rectifier potassium channel expression.** A, mean normalized ACh-evoked relaxation in PA-treated aortic rings pre-incubated with 4b ± endothelial blockers; B, representative western blots showing the change in protein expression of Kir 2.1 channel in PA-incubated aortic rings, and the expression of these channels with the addition of MTDLs (4b and 7). C, representative micrographs of DHE staining of rat aortic rings of different treatments with the average quantified data. DHE staining appears as red fluorescence on a background of green collagen autofluorescence. Scale bars are 40 µm. * denotes a P-value < 0.05 vs PA+4b. Statistical significance was tested by two-way ANOVA followed by Sidak multiple comparisons tests for A.

W. Assessment the effect of MTDLs on endothelium-dependent relaxation in HC-fed rat aortic rings

In order to assess the effect of MTDLs in a state of chronic inflammation, we used aortic rings obtained from HC-fed rats. Myobath experiments showed a significant enhancement of ACh-induced relaxation in HC-fed rat aortic rings treated with compound 4b *ex vivo*. However, the addition of single target compounds such as pioglitazone or celecoxib did not improve ACh-mediated relaxation. (Fig. 30B). Attenuation of the improvement of endothelial function in response to 4b treatment in the presence of $BaCl_2$ indicates that the triple-targeting compound was able to enhance EDH responses that were previously compromised in HC-fed rats (Fig. 30D).

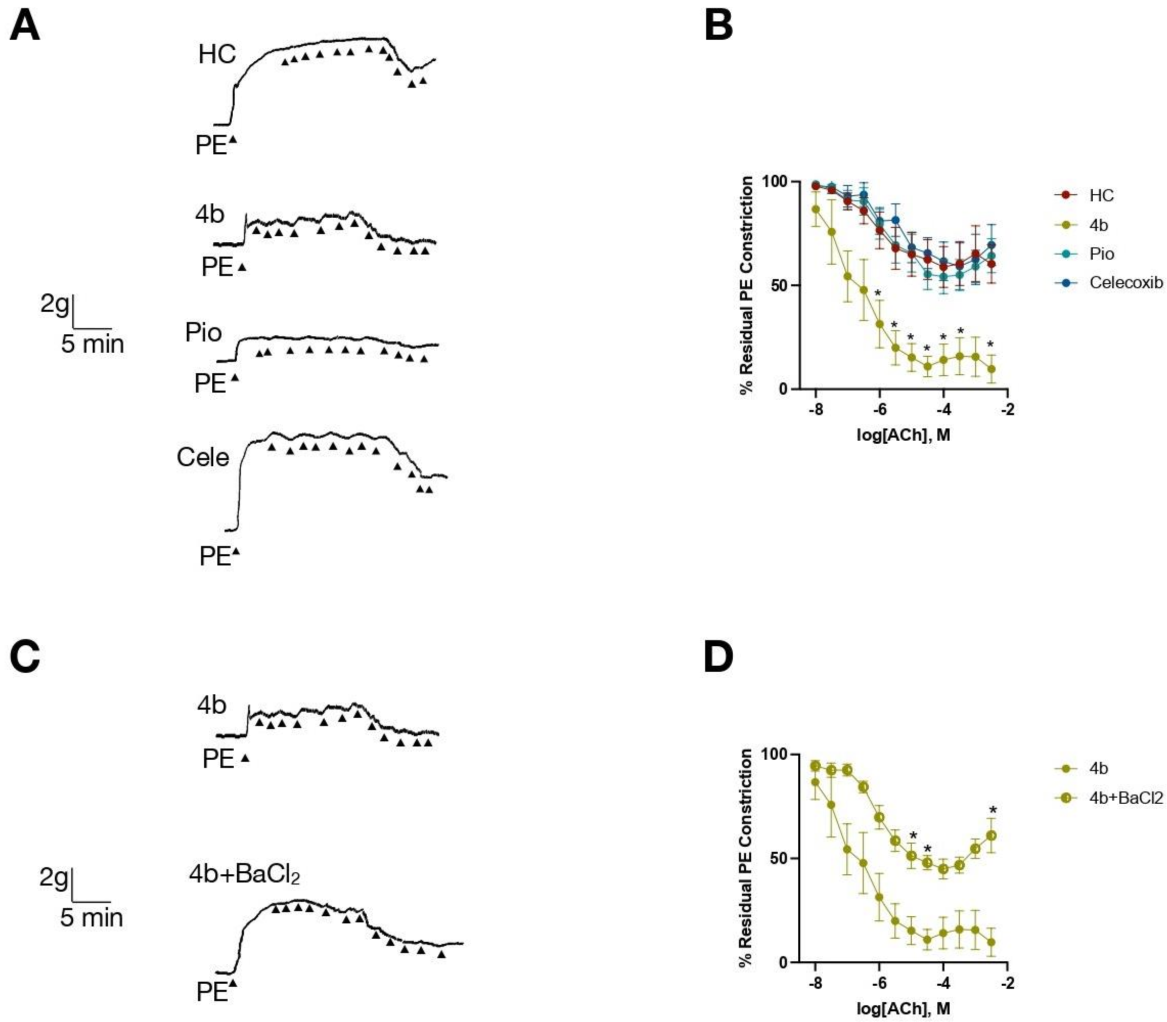

Figure 30. **Assessment of MTDLs effect on endothelium dependent relaxation in HC-fed rat aortic rings.** A and C, representative traces showing the relaxant response to ACh on aortic rings pre-constricted with PE for different groups; B, mean normalized ACh-evoked relaxations in aortic rings pre-constricted with PE for the different groups; D, mean normalized ACh-induced relaxations in aortic rings pre-constricted with PE for 4b, and 4b+BaCl2. * denotes a P-value < 0.05 Vs HC panel B; * denotes a P-value < 0.05 Vs 4b+BaCl2 Statistical significance was tested by two-way ANOVA followed by Sidak multiple comparisons tests for B and D.

CHAPTER V

DISCUSSION

The optimal approach for mitigating diabetic vascular complications remains elusive ("The effect of intensive treatment of diabetes on the development and progression of long-term complications in insulin-dependent diabetes mellitus. The Diabetes Control and Complications Trial Research Group," 1993; Genuth & Ismail-Beigi, 2012; Heller, 2009), especially that a significant proportion of diabetic patients presents with established vascular complications at initial diagnosis (Fowler, 2008). As such, studying the early detrimental mechanisms contributing to ED in the course of diabetes development becomes paramount. In this context, localized perivascular adipose tissue inflammation emerges as a high-yield target for such an intervention (R. Rafeh, A. Viveiros, G. Y. Oudit, & A. F. El-Yazbi, 2020). Nevertheless, presenting as a multi-faceted process with several intertwining and redundant cascades, this inflammatory change together with others triggered downstream pose a considerable challenge.

Towards this end, we used a rat model of mild metabolic challenge allowing a fairly wide window of opportunity to study vascular dysfunction prior to the development of hyperglycemia. To our knowledge, this is the first report to highlight an impairment of Kir channels as the primary cause of endothelial damage during early metabolic alterations, potentially triggered by hypercholesterolemia. Our results also highlight the potential inter-dependence among different endothelium-mediated vasodilatory pathways in producing integrated myoendothelial feedback, whereby a defect in one would be augmented due to a lack of positive interaction with the other.

The rat model used in the present study is a modified form of the high-fat diet animal model, which permits the examination of the development of pathological mechanisms in impaired glucose tolerance and early type II diabetes (Winzell & Ahren, 2004). Our model receives a limited increase in daily calorie intake from fat. Data from previous studies in our laboratory showed that this diet produced stable fasting and random hyperglycemia after 16-20 weeks of treatment (Mohammed A. W. Elkhatib et al., 2019). However, no changes in glucose tolerance, body weight, or blood pressure were observed at 12 weeks (Al-Assi et al., 2018; Mohammed A. W. Elkhatib et al., 2019), thus permitting the study of functional changes occurring in the course of early metabolic alterations without interference from hyperglycemia, impaired glucose tolerance, obesity, or hypertension.

Whereas aortic rings from both control and HC-fed rats had similar vasodilatory responses to the exogenous NO donor sodium nitroprusside, HC-fed-rat aortic tissues showed an impaired ACh-mediated relaxation proposing that the observed defect was likely related to an endothelial, rather than a smooth muscle, dysfunction. This was coupled with an increased initial contraction to 30 μM PE indicating a potential dysfunction in myoendothelial feedback. The persistence of the same defective ACh-mediated relaxation pattern in HC-fed rat tissues in experiments where equi-effective concentrations of PE were used rules out the possibility that the difference in pre-constrictor tone affected the ACh response. While a rich body of literature describes a role for the increased production of endothelin-1, acting through ET_A receptors, in ED observed in diabetes, obesity, and metabolic syndrome (A. K. Harris, Elgebaly, Li, Sachidanandam, & Ergul, 2008; W. Li, Abdul, Ward, & Ergul, 2018; Samsamshariat, Sakhaei, Salehizadeh, Keshvari, & Asgary, 2019; Schinzari, Tesauro, & Cardillo, 2018), this did not appear to be the case in aortic rings from HC rats. *In vitro* exposure to the ET_A receptor antagonist atrasentan did not alter aortic response to ACh. This was similar to previous observations in another animal model of early prediabetes where vascular response was not altered by endothelin-1 (Knudson et al., 2006). Indeed, the above studies citing a role for endothelin-1 in ED in diabetes or obesity reported these findings in advanced disease states with overt hyperglycemia and increased body weight, contrary to the observed phenotype in our rat model. In fact, even studies describing a role for endothelin-1 in impaired flow-mediated dilation in prediabetic patients linked the observed increase in plasma endothelin-1 to post-prandial hyperglycemia (McDonald, Mah, Chitchumroonchokchai, et al., 2019; McDonald, Mah, Dey, et al., 2019), not observed in our model.

We then set to investigate the relative contribution of different EDR mechanisms and the effect of HC-feeding on them. Similar to prior reports of endothelium-mediated vasodilation in conduit arteries (Joannides et al., 1995; H. Shimokawa & Godo, 2016), our results show that NO was the predominant mediator of EDR in aortic rings, but left a residual relaxation that corresponded to the contribution of EDH-type relaxation. EDH-type relaxation is typically described to be initiated by a calcium-triggered endothelial hyperpolarization mediated by SK and IK channel activation, which is followed by further amplification of hyperpolarization through the action of Kir channels (Garland & Dora, 2017). In control aortic rings, the contribution of EDH-type relaxation to the ACh-induced EDR was confirmed in experiments where either SK/IK or Kir channels were blocked significantly attenuating ACh-mediated responses. Although unlikely based on the large difference between the apamin and Tram-34 concentration used and their functional IC_{50} values (Table 1), their lack of effect at the higher ACh concentrations could be due to a competitive relief of channel inhibition. The more pronounced effect of $BaCl_2$ at higher ACh concentrations is in line with previous literature showing a more prominent role for Kir blockade in responses to higher ACh concetrations (Hangaard, Jessen, Kamaev, Aalkjaer, & Matchkov, 2015; McIntyre et al., 2001; Rasmussen, Braunstein, Salomonsson, & Brasen, 2016).

On the other hand, while aortic rings from HC-fed rats appeared to have a relatively intact NO contribution to the reduced EDR, the lack of a residual relaxation, similar to that observed in the control rings, suggested a possible impairment of the EDH-type response. This was further confirmed in experiments using SK/IK and Kir channel blockers. Whereas apamin/tram-34 reduced ACh response at low concentrations to some extent, albeit not as marked as in control tissues; $BaCl_2$ did not alter the ACh effect implicating Kir channel dysfunction in the observed deficit. Significantly, PE-evoked contraction increased in control rings treated with apamin/Tram-34, $BaCl_2$ or L-NAME. This was not the case in rings from HC-fed rats suggesting that EDH impairment attenuated not only the feedback pathway mediated by Kir channels, but also that driven by NO, in a first indication of the interplay between both pathways in our vessel preparation.

To further demonstrate that EDH impairment underlies the endothelial deficit in HC-fed rat aortic rings, we examined the ACh-mediated relaxation following pre-constriction with the thromboxane mimetic, U46619 (Plane & Garland, 1996). PE produces vascular contraction via calcium-sensitization and membrane depolarization and increased cytosolic calcium levels (Plane & Garland, 1996). Under such circumstances, EDH would promote smooth muscle relaxation by opposing the agonist-induced depolarization. On the other hand, U46619-mediated contractions were accompanied by much less depolarization than that observed with PE, thus limiting contribution from EDH-type relaxation (Plane & Garland, 1996). As well, U46619 inhibits intracellular endothelial calcium increase (Ratnayake et al., 2018) potentially interfering with the activation of calcium-dependent potassium channels implicated as an early effector involved in EDH. Moreover, a previous study reported that thromboxane analogues reduced endothelial intercellular communication through gap junctions via increased Cx43 internalization (Ashton et al., 1999), further reducing the likelihood for conduction of EDH into the vascular smooth muscle (VSMC) layer. As such, not only was the ACh-mediated relaxation of the U46619 contractile tone insensitive to $BaCl_2$, but also it was similar in aortic rings from both control and HC-fed rats. Therefore, these results confirm a selective impairment of EDH in aortic rings from HC-fed rats, which did not manifest once this relaxant mechanism was excluded. Of interest though, while initial constrictions to PE were higher in tissues from HC-fed rats, U46619 produced equal contractions in both groups. Indeed, our previous work showed that the nature of vasoconstrictor agent determined the functional components of myoendothelial feedback (Wei et al., 2018).

Kir channels are described as “end-stage amplifiers” of EDH (Sonkusare et al., 2016), owing to their essential role in amplifying hyperpolarization in VSMCs. The negative slope conductance property of the kir2.1 subunit allows Kir channels to respond to the increase in membrane hyperpolarization by enhancing its activity (Jantzi et al., 2006). Thus, we hypothesized that reduced EDH-type relaxation could potentially be attributed to defective Kir channel expression/function. As such, to emphasize the role of dysfunctional Kir channels, we adopted an approach previously used by Smith et al (P. D. Smith et al., 2008) and Allen et al (Allen, Iftinca, Cole, & Plane, 2002), where a non-endothelium triggered hyperpolarization was induced by the application of the K_{ATP} channel opener diazoxide. Smith et al (P. D. Smith et al., 2008) showed that functional Kir channels were able to amplify this hyperpolarization and produce a sustained vasodilation, which was reduced upon pharmacological intervention with $BaCl_2$ or if Kir 2.1 expression was low. This indeed was the case in our experiments where aortic rings from control rats responded by a more profound relaxation to diazoxide compared to rings from HC-fed rats, wherein the response to diazoxide was rendered insensitive to $BaCl_2$ because of the potential deterioration of Kir channel function. Results from western blots demonstrated a downregulation in protein content of Kir2.1 subunit in HC-fed rats, providing a molecular confirmation for the lack of Kir-mediated endothelial relaxing component.

An additional determinant of the vascular response to EDH-type relaxation is myoendothelial gap junctions that provide tight coupling among endothelial cells and VSMCs allowing for a bidirectional gate for electrotonic spread of charge and small molecules (Xavier F. Figueroa, 2004). Given the concluded reduction in myoendothelial feedback in HC-fed rat aortic tissue, suggested by the increased initial PE response and its lack of sensitivity to L-NAME and $BaCl_2$, the effect of gap junction blockade by 18-β-GA on ACh-mediated relaxation was assessed. Congruent with a lack of EDH-type relaxation in HC-fed rat tissue, gap junction blockade did not affect the vasorelaxant response, which was the opposite of observations in control tissue where ACh responses where greatly attenuated. This was despite the observation that Cx43 subunit expression levels increased in aortic tissues from HC-fed rats. Cx43 upregulation is in line with previous literature showing that, while the vascular expression of some connexin subunits (Cx37 and 40) tended to decrease in metabolic disease, Cx43 expression was found to increase (R. A. Alaaeddine et al., 2019). Cx43 is highly expressed in VSMCs and endothelial cells, specifically at the myoendothelial junction (Abed et al., 2014), and is thought to increase in metabolic disturbance as a consequence of increased ERK phosphorylation (Ho et al., 2013), a common observation in the vascular tissue in our rat model (Al-Assi et al., 2018; Mohammed A. W. Elkhatib et al., 2019). Paradoxically, while PE-constricted control tissues exposed to 18-β-GA responded by further constriction possibly due to the interruption of myoendothelial feedback, HC-fed rat aortic segments responded by tone reduction. This observation could be explained by previous evidence linking vascular depolarization to eNOS dysfunction. Previous studies showed that depolarization induced an increased NADPH oxidase-mediated production of ROS leading to impairment of endothelial NO-mediated vasodilation (Oelze et al., 2006; Sohn et al., 2000). Cx43 was consistently implicated in the transfer of ROS across different cell types (Hutnik, Pocrnich, Liu, Laird, & Shao, 2008; Le et al., 2014; Ramachandran, Xie, John, Subramaniam, & Lal, 2007; Raza, Ghoshal, Chockalingam, & Ghosh, 2017; Taniguchi Ishikawa et al., 2012) with protective or detrimental outcomes. The ability of ROS to spread among different vascular cell types across gap junctions was described (Feine et al., 2012) together with their well-documented role in inducing eNOS dysfunction (Ohara, Peterson, & Harrison, 1993a). Thus, it follows that smooth muscle depolarization, produced by PE, when left unopposed by EDH could potentially impair eNOS activity in a manner that is gap junction-dependent. Under such circumstances, gap junction blockade will restore some eNOS activity by interrupting the detrimental outcome of myoendothelial communication. Indeed, this notion was supported by our current observation that tone reduction observed in HC-fed rat tissue following 18-β-GA exposure was abolished in tissues pre-incubated with L-NAME.

To further confirm and reconcile these findings, we assessed whether aortic tissues from HC fed rats showed an increased ROS production and if *in vitro* scavenging of ROS improved the relaxation response to ACh. Indeed, DHE staining showed an increased ROS levels in the smooth muscle layer of HC-fed rat aortic tissues. *In vitro* exposure to the ROS scavenger SOD not only reduced ROS, but also improved ACh-evoked relaxation. This was also associated with a reversal of the tone reduction observed when gap junctions were blocked with 18-β-GA, since ROS no longer flowed into the endothelium and affected NOS function. Conversely, when reduced Kir channel function was simulated in control aortic rings treated with $BaCl_2$, not only did ROS levels increase, but also the tone reduction associated with gap junction blockade was recapitulated providing further support for the role of the interaction between vascular hyperpolarization, ROS production and an integrated myoendothelial feedback. Interestingly, the persistence of DHE staining in smooth muscle layer of HC tissues and $BaCl_2$-treated control tissues after gap junction blockade possibly confirms that ROS production originated in smooth muscle.

To establish a link between these observations and changes occurring *in vivo*, we considered previous evidence describing a reciprocal relationship between Kir channel activity and levels of cholesterol in the microenvironment of the channel (Fang et al., 2006; Maria Sancho & Welsh, 2018). Moreover, a recent study showed that hypercholesterolemia suppressed Kir2.1 channel function and attenuated flow-induced vasodilation (Fancher et al., 2018). Significantly, not only did cholesterol reduction by *in vivo* treatment with atorvastatin improve ACh-evoked relaxation in aortic tissues of HC-fed rats, the sensitivity of these relaxation to $BaCl_2$ was also restored indicating a possible amelioration of Kir channel dysfunction. Indeed, western blotting showed an increase in the expression level of Kir2.1 channel. Along the same lines, vasorelaxation to diazoxide was also improved. It is noteworthy as well that ROS levels in the vascular smooth muscle layer were reduced in HC-fed rats treated with atorvastatin further confirming the proposed model.

Since our rat model is hyperinsulinemic, it could be argued that insulin resistance impairs the PI3K/Akt signaling pathway downstream of insulin receptor (Sowers, 2013; Wheatcroft et al., 2003) possibly reducing Akt-mediated eNOS phosphorylation and eNOS activity leading to the observed endothelial phenotype. However, western blotting showed no difference in the phosphorylation of Akt and eNOS in both groups. Moreover, the improvement in endothelial function observed in atorvastatin-treated HC-fed rats was not associated with an amelioration of hyperinsulinemia. Furthermore, examination of ACh-mediated effects in rat middle cerebral artery, as an example of a microvessel where EDH predominates the endothelial response (Garland & Dora, 2017), confirmed that the attenuated vasodilatory response in vessel segments from HC rats are rather a consequence of Kir channel dysfunction. Moreover, control vessels responded to $BaCl_2$ exposure by a phasic constriction consistent with the blockade of functional Kir channels. This phasic contraction was greatly reduced in cerebral vessel segments from HC-fed rats. Significantly, atorvastatin treatment restored both the $BaCl_2$-sensitive ACh-mediated vasodilation and the phasic contraction to $BaCl_2$ indicating an amelioration of Kir channel function.

Therefore, the present study demonstrates for the first time that early endothelial dysfunction in the course of metabolic disease is a consequence of impaired EDH-type relaxation due to a dysfunctional Kir2.1 channel activity. The endothelial deficit at this stage is further compounded by a potential reduction of eNOS activity resulting from increased production of ROS in vascular smooth muscle accessing the endothelium through gap junctions.

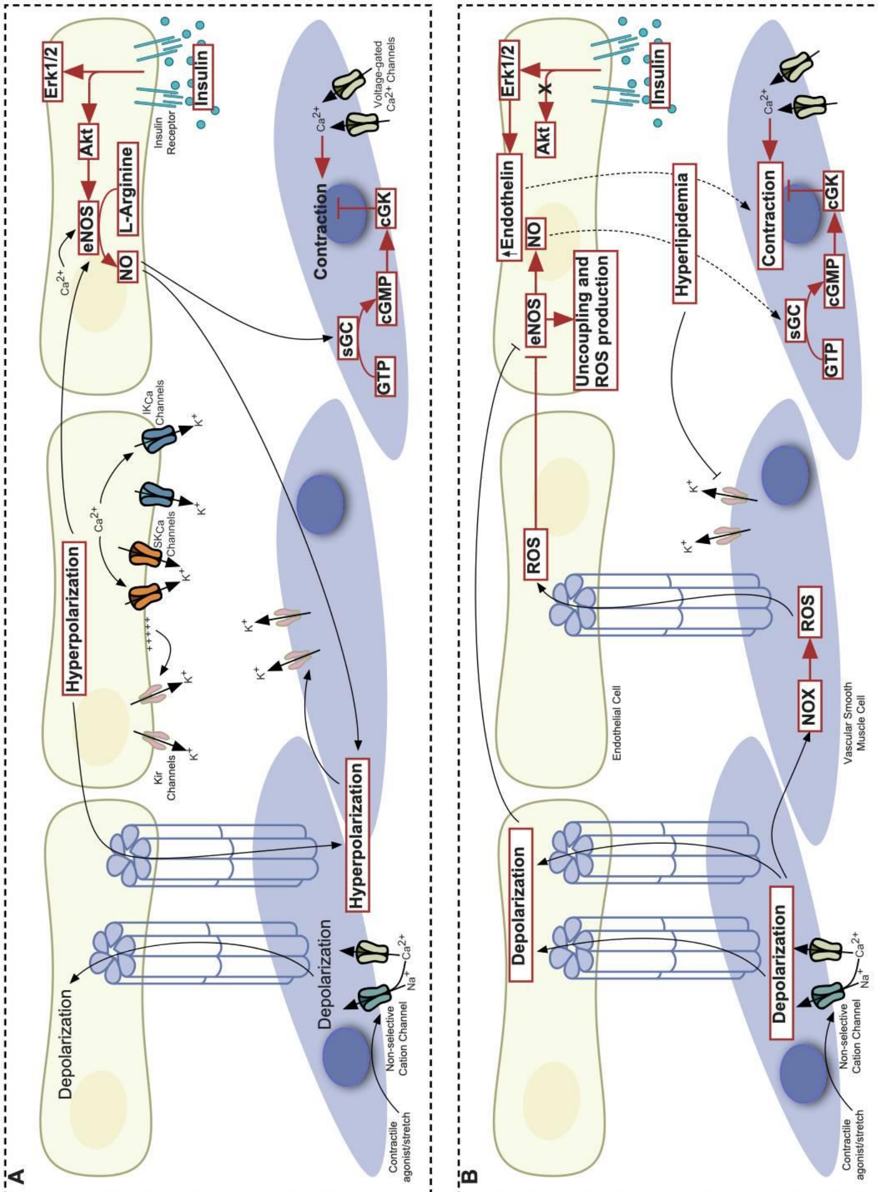

Figure 31. The proposed model of dysfunctional myoendothelial interaction in early metabolic disease. (A) In healthy vessels, stretch/contractile agonists trigger the activation of non-selective cation channels and voltage-dependent calcium channels in the VSMC layer, causing depolarization and an increase in intracellular calcium, activation of myosin light chain kinase (MLCK), phosphorylation of myosin and consequent vasoconstriction. VSMC depolarization is transmitted to the endothelial layer by myoendothelial gap junctions, which together with the flow/agonist-mediated response trigger a local burst of calcium in the endothelium activating two vasorelaxant mechanisms: (1) EDH: activation of SK_{Ca}/IK_{Ca}

channels by calcium results in a local hyperpolarization, which is in turn amplified via the negative slope conductance property of Kir channels, spreading to neighboring cells via myoendothelial gap junctions and opposing the depolarizing current in the VSMCs, and (2) NO-mediated response where eNOS is activated by calcium-dependent or Akt-mediated pathways. NO then diffuses to the VSMCs and activates sGC, leading to an increase in cGMP and consequent relaxation mediated by cGMP-dependent protein kinase (cGK). Both pathways act synergistically in an integrated endothelial response where NO might contribute to the hyperpolarization response in the vascular wall and EDH potentiates and maintains the activity of eNOS by opposing the VSMC-driven depolarization. (B) In early metabolic disease, insulin resistance triggers a biased activation of $Erk_{1/2}$-dependent pathway producing endothelin-1, with reduced Akt-mediated signaling resulting in decreased NO production. Moreover, hypercholesterolemia suppresses Kir channel function and expression, hence attenuating the hyperpolarization currents. In more advanced disease states, IK_{Ca} and SK_{Ca} channel function/expression is compromised as well. This leaves the depolarization originating in the VSMC layer unopposed. This prevailing depolarization gains access to the endothelial layer potentially due to increased Cx43 expression, further decreasing the activity of eNOS and NO availability. eNOS impairment likely occurs as a consequence of depolarization-evoked production of ROS potentially via NADPH oxidase (NOX) activation. Moreover, eNOS uncoupling can also contribute to ROS production further compromising vascular function.

In this context, Kir2 channels are found within lipid-rich domains of the cell membrane (lipid rafts) (Levitan, 2009). Hence, they are widely known to exhibit lipid-binding sites in their cytosolic domains, allowing these channels to be regulated by different lipid modulators (Rosenhouse-Dantsker, Epshtein, & Levitan, 2014). As previously mentioned, the dominant effect of cholesterol on Kir2 channels was shown to cause inhibition of channel function, with kir2.1 and 2.2 being the most sensitive to cholesterol (Romanenko et al., 2004). Conversely, interaction of kir2 channels with phosphatidylinositol 4,5-bisphosphate (PIP2), despite being a minor lipid constituent of the cell membrane, led to stabilization of the channels in the open state (Enkvetchakul, Jeliazkova, & Nichols, 2005). However, changes in Kir2.1 channels cannot be attributed to a simple interaction with cholesterol, as previous studies have provided evidence that diet-induced ED may occur independent of perturbations of cholesterol levels. In high fat diet (HFD)-fed Wistar rats, the reduction in EDR and EDH responses of mesenteric arteries was not associated with cholesterol elevation (Gerber et al., 1999). Although the atorvastatin-induced restoration of Kir channels observed in the present study may be explained by the ability of statins to liberate Kir channels from the inhibitory effects of cholesterol, previous findings have proposed that rosuvastatin is able to reverse EDH-type relaxation, independent of their ability to reduce plasma cholesterol levels, which is suggestive of the possibility of involvement of more complex mechanisms and additional players (Cameron, Cotter, Inkster, & Nangle, 2003). In fact, statin therapy was previously shown to induce a reduction in plasma FFAs concentrations, independent of the extent of reduction in plasma low-density lipoprotein cholesterol level (Sahebkar et al., 2016). Interestingly, FFAs, which are enriched in western diets, are presented as an important link between metabolic disease, insulin resistance and cardiovascular complications (Boden, 2008). A strong body of evidence has illustrated a role for FFAs in inducing vascular and endothelial changes as well as adipose tissue inflammation in metabolic disease.

The pro-inflammatory phenotype acquired by adipose tissue in response to hyperinsulinemia is considered as a key contributor to cardiovascular complications (Fitzgibbons & Czech, 2014). Alterations in the cytokine and adipokine profile of PVAT has been proposed to drive vascular derangements, thus providing a context for the vascular dysfunction observed in early metabolic impairment (Yudkin, Eringa, & Stehouwer, 2005). Importantly, the inflammatory and oxidative microenvironment of adipose tissue culminates in the progression endothelial dysfunction in response to insulin resistance (Gil-Ortega et al., 2014; Ketonen et al., 2010). In fact, the hyperinsulinemia, observed in the rat model used in this study, was previously shown to induce adipose tissue inflammation through triggering adipocyte hypertrophy (Pedersen et al., 2015), in line with our findings demonstrating the presence of hypertrophied PVAT and visceral white adipose tissue in HC-fed rats. In the absence of signs of systemic inflammation (M. A. W. Elkhatib et al., 2019), we tested for the presence of localized PVAT inflammation, that may underlie the reported endothelial defects. The inflammatory profile PVAT was evident from the upregulation of protein expression levels of IL-1β. Such an inflammatory response in adipose tissue is thought to be a result of hypertrophy, to accommodate the increased caloric intake causing a reduction of the interstitial oxygen tension (Y. S. Lee et al., 2014). In addition to adipose hypertrophy, PVAT from HC rats exhibited an enhanced HIF-1α expression, indicative of PVAT hypoxia, which in turn, can trigger upregulation and activation of NF-κB, known to mediate the production of inflammatory cytokines, including IL-1β (Scortegagna et al., 2008). Macrophage infiltration and increased polarization towards an M1 phenotype, confirmed by flow cytometry results, is also thought to further accentuate the inflammatory state of adipose tissue (Morris et al., 2011). Our findings also reported additional manifestations of AT impairment, namely reduced PPAR-γ expression (M. Chattopadhyay et al., 2018).

In contrary to PVAT, the inflammatory and hypoxia phenotype was found absent in visceral white adipose tissue, despite the observed adipocyte hypertrophy. This disparity in sensitivity to inflammation between PVAT and visceral white adipose pools in response to metabolic stress can be attributed to the unique characteristics of each adipose tissue depot (M. J. Lee, Wu, & Fried, 2013). Hence, PVAT, which combines properties of both brown and white adipose tissue, exhibits a higher expression of UCP-1 (Hildebrand, Stumer, & Pfeifer, 2018). Knowing that UCP-1 increases mitochondrial energy dissipation in the form of heat in what is known as non-shivering thermogenesis, its expression level is linked to an enhanced oxygen consumption (K. Schneider et al., 2016; Shabalina et al., 2013; Vijgen et al., 2013). Hence, PVAT depot could become more sensitive to changes in oxygen tension as a result of early adipocyte hypertrophy when compared to visceral white adipose depot. The hypoxic state can also be exacerbated in cases of selective insulin resistance in adipose tissue, where UCP-1 was also shown to be upregulated (Guerra et al., 2001). This is in line with our current findings demonstrating an upregulation of UCP-1 expression in HC-fed rats, while white visceral adipose tissue manifested no UCP-1 expression, congruent with a lack of change in HIF-1α.

Surprisingly, some of the key changes leading to adipose tissue inflammation, including adipose tissue hypertrophy and UCP-1 upregulation, were previously found to be triggered by elevated levels of FFAs, increasing in abundance following western diets (Fedorenko, Lishko, & Kirichok, 2012; Finucane et al., 2015). Furthermore, macrophage recruitment and the observed phenotypic switch towards pro-inflammatory M1 macrophages is also precipitated by FFAs (K. L. Chan et al., 2015). In a state of insulin resistance, lipolysis is enhanced in adipose tissue, thus driving a surge in FFAs levels, spilling out and affecting neighboring cells, specifically vascular and endothelial layers (Guilherme et al., 2008). Congruent with an insulin-desensitizing role for recruited macrophages (Bing, 2015), the increase in FFAs may exacerbate adipose tissue inflammation and insulin resistance in an autocrine manner. As such, macrophages and adipocytes become involved in a feed-forward vicious cycle, that results in aggravating of inflammation and its detrimental consequences on adjacent vascular cells.

In our attempt to address the multifaceted inflammatory nature of metabolic disorders, we adopted a hybrid pharmacophore approach to design the first-in-class multi-targeting drug ligands (MTDLs) as potential simultaneous COX-2/15-LOX inhibitors and/or PPARγ agonists. In light of the important role of COX and 15-LOX enzymes in normal physiological conditions, MTDLs were designed to selectively target the isoforms that are implicated in chronic inflammatory pathways, namely COX-2 and 15-LOX-1, while maintaining the function of other isoenzymes with a relatively more protective role, such as COX-1 and 15-LOX-2. This will preserve the desired activity while halting possible risks. The triple-targeting compounds were designed to act as partial PPARγ agonists, which would diminish the unfavorable effects of full PPARγ agonism (Berger et al., 2003; Silva et al., 2016). Therefore, maximizing pharmacological benefit and minimizing adverse effects is considered in the preliminary drug design rationale. Plenty of evidence supports the feasibility of the design and biological utility of MTDLs modulating COX-2 and 15-LOX activities. Several studies also demonstrated the possibility of including other targets, the most multilateral of which being PPARγ.

We conducted a series of *in vitro* and *in vivo* experiments to assess the anti-inflammatory actions of our dual-targeting compounds. First, *in vitro* COX inhibition assay data identified seven out of the ten compounds as submicromolar COX-2 inhibitors with

IC50 values ranging from 0.09 to 0.14 µM, compared to 0.05, 0.8 and 0.49 µM for the reference drugs celecoxib, diclofenac sodium and indomethacin, respectively. In addition, these compounds displayed relatively weak COX-1 inhibitory activities (6.45-14.02 µM). Moreover, six compounds showed reasonable selectivity indices (COX-1/2) of 80-114. 15-LOX inhibitory activities of the test compounds were also assessed. Interestingly, five compounds exerted substantial activities with IC50 values spanning from 1.96 to 3.52 µM, compared to 3.34 µM for the reference quercetin. Afterwards, three of the most active compounds (4, 7, and 8) were chosen for further biological evaluation. Biological screening results indicated that all compounds showed a significant *in vivo* anti-inflammatory activity, equivalent to that of celecoxib and diclofenac in the acute inflammatory model. In the chronic model, compounds (7, 8) displayed superior anti-inflammatory activity, when compared to diclofenac and celecoxib. As expected, two of these compounds (4, 7) demonstrated potent inhibitory effects on monocyte-to-macrophage differentiation, an important and early step in the inflammatory process, with more selective ability to inhibit differentiation into the pro-inflammatory M1 polarization. Moreover, COX-2/15-LOX inhibitory effects of three compounds (4, 7, 8) were manifested by attenuating IL-1β production in M1 macrophages. Interestingly, these compounds also showed apoptotic effects on M1 macrophages, a mechanism that further augments their anti-inflammatory activity.

We also presented the evaluation of novel triazolyl-thiazolidinedione/rhodanine hybrids as potential simultaneous COX-2/LOX inhibitors and PPARγ partial agonists. Most of the synthesized hybrids showed micromolar inhibitory activities towards COX-2 and 15-

LOX in *in vitro* assays. *In vitro* glucose uptake assay identified compounds 4b, 5e as stronger glucose uptake inducers than pioglitazone in the presence and absence of insulin, and compounds 5b, 5g as equal or higher glucose uptake inducers in an insulin-independent fashion, which raises the possibility of selective targeting of PPARγ signaling pathways. Immunohistochemical analysis of ligand-stimulated PPARγ nuclear localization confirmed the ability of compounds 4b, 5b, 5e and 5g to induce PPARγ nuclear translocation, similar to pioglitazone. Moreover, PPARγ functional reporter gene assay confirmed the partial agonistic activity of the latter 4 compounds towards PPARγ. X-ray crystallography of compound 4b with PPARγ showed its binding outside AF2 part of LBD, which is the part responsible for the full activation of PPARγ and hence complete recruitment of downstream signaling molecules. Instead, it managed to pursue other hydrophobic interactions with residues in H3, H6 and H7 parts of LBD via its phenyl ring and propargyl tail. Also, a key hydrogen bonding interaction with Ser342 in beta sheet was observed. We believe that the presence of only one carbonyl group in rhodanine part of 4b probably changed its ability to bind to AF2 and hence might be partly responsible for its partial agonistic activity. Another part of the partial agonistic activity could be attributed to the hydrophobic interactions, especially those of the propargylic tail. Three compounds with the most favorable properties (4b, 5e & 5g) were chosen for further biological evaluation. While compounds 5e and 5g showed equivalent inhibitory effect to the reference drugs, compound 4b demonstrated a statistically significant higher potency compared to celecoxib in formalin-induced rat paw edema assay. Compounds 5e and 4b were capable to inhibit monocyte to macrophage differentiation, which is a pivotal and early step in inflammatory response. As expected, the most potent 15-LOX inhibitors, 4b, 5e & 5g reduced inflammatory cytokine production and arachidonate metabolism in a human macrophage model challenged by PMA and LPS.

In order to assess the role of MTDLs in halting the observed endothelial impairment in metabolic disease, we used an *ex vivo* model of lipid-induced endothelial dysfunction, where control aortic rings were exposed to palmitic acid, being one of the major FFAs elevated in diabetic individuals (Prescott et al., 1999). This approach was previously used by another study investigating the effect of palmitate on endothelial function, whereby *ex vivo* treatment of aortic rings with palmitate attenuated acetylcholine-mediated relaxation in a concentration-dependent manner (Z. Gao et al., 2014). These results are consistent with our findings demonstrating an increased sensitivity to PE and a decrease in endothelium-dependent relaxation in PA-treated rings, accompanied by a reduction in the expression of Kir channels and an enhancement in ROS expression. As such, this *ex vivo* model is able to recapitulate the endothelial changes reported in the *in vivo* HC-fed rat model, possibly induced by chronic low-grade adipose tissue inflammation.

Plenty of studies highlighted inflammation as a possible mechanism underlying the detrimental effects of FFAs on endothelial function (Kim et al., 2005; K. Liu et al., 2012; Xing et al., 2019). In fact, the inflammatory phenotype induced by FFAs can be aggravated by the close proximity of the inflamed PVAT acting as an ongoing source of FFAs in insulin resistance (Guilherme et al., 2008). Accumulating evidence illustrated a critical role for alterations in the three inflammatory mediators, COX-2, 15-LOX, and PPARγ in the progression of endothelial dysfunction, being a hallmark of atherosclerotic cardiovascular diseases occurring in metabolic disease (discussed in the introduction). Hence, for the purpose of assessing the effectiveness of MTDLs in ameliorating endothelial dysfunction, *in vitro* vascular reactivity experiments were conducted on PA-incubated aortic rings that were pretreated with compounds 4b and 7. The triple target compound 4b, was able to reverse the enhanced sensitivity to PE induced by PA. Also, although both compounds seem to enhance ACh-dependent relaxation, a significant change was only produced by 4b. Along these lines, 4b was able to reduce PE contractility and enhance maximal ACh-induced relaxation. Altogether, these results show that only the triple-targeting compound exhibited a benefit in reducing PA-induced impairment in endothelium-dependent relaxation.

In order to investigate the relative contribution of different targets in alleviating PA-induced ED, we compared the effect of incubation of PA-treated rings with single targeting compounds such as celecoxib and pioglitazone; the selective COX-2 inhibitor, and PPARγ full agonist, respectively. While the treatment with either celecoxib or compound 7 did not produce a significant change in ACh-mediated relaxation, pioglitazone was able to induce a remarkable improvement in the response to ACh. Therefore, these findings highlight the importance of PPARγ as an anti-inflammatory target in counteracting FFA-induced ED.

To assess the underlying mechanism for 4b induced improvement of ED, we added blockers of the two endothelial mechanisms: L-NAME to block NO mechanisms and BaCl2 to block EDH, both of which produced significant attenuation of ACh-dependent relaxation. The reduction due to L-NAME is expected, due to the critical role of NO in the EDR. Interestingly, the reduction due to BaCl2 led us to think of an alternative possible player that was restored by 4b. In-line with these findings, western blotting showed that 4b was able to restore the expression of Kir2.1 channels, congruent with a reduction in ROS expression.

Plenty of evidence demonstrates that atherosclerosis is a major component of cardiovascular diseases that are characterized by a chronic inflammatory state. Given the chronic state of inflammation that drives metabolic disorders and cardiovascular diseases, several lines of evidence highlighted the contribution of inflammatory mediators in the etiology of vascular dysfunction (Castellon & Bogdanova, 2016). We assessed whether these compounds can enhance the endothelial responses in HC-fed rats that demonstrate a chronic state of low-grade perivascular adipose inflammation. Whereas the treatment with single-targeting compounds failed to enhance endothelium-dependent relaxation, only treatment with the triple-targeting compound was able to induce a significant change in ACh-mediated relaxation, further emphasizing the importance of shooting more than one target to address the different layers of the metabolic disease.

In this context, the ability of our anti-inflammatory MTDLs to reverse PA-induced alterations in EDH-responses raises the possibility of interference of inflammatory pathways in the reduction of Kir channels expression/activity observed as a result of caloric excess. Being associated with lipid rafts (Levitan, 2009), the function of Kir2 channels is negatively modulated by caveolin-1 (Cav1), the major constituent of caveolae, which form the smooth invaginations in the lipid rafts of the plasma membrane (H. Han et al., 2014). Although it was strongly believed that cholesterol depletion modifies Kir channel function via disrupting caveolae, this notion was previously negated (H. Han et al., 2014), suggesting the possible involvement of other modulators that trigger Cav1-dependent Kir silencing. Interestingly, FFAs and TNF-α were proposed as active inducers of Cav1 expression in endothelial cells (L. Wang, Lim, Toborek, & Hennig, 2008; Zheng et al., 2009). In particular, the effect of these mediators on the expression of inflammatory markers, most importantly COX-2, was shown to be reduced by Cav1 silencing (L. Wang et al., 2008). In another study, ERK/NF-κB-dependent upregulation of COX-2 by FFAs was found to be mediated by Cav1 in endothelial cells (Zheng et al., 2009). As such, adipose tissue inflammation demonstrated in our HC-fed model, being associated with enhanced TNF-α and FFAs production, may trigger an increase in the expression of endothelial Cav1 and downstream inflammatory mediators, with their potentially deleterious effects on Kir channels.

A potential limitation of this study is the lack of direct evidence on the link between the MTDLs mechanism and the EDH pathway. Further studies should be conducted to elucidate the possible mechanism for the MTDLs-evoked enhancement of Kir channel expression. Furthermore, the possibility of potential adverse effects with the use of MTDLs must be assessed through *in vivo* evaluation. While the available literature shows various levels of biological screening ranging from cellular and molecular assays to *in vivo* anti-inflammatory assays, a structured translational effort is still required to support the adoption of rationally designed molecules in this category into clinical investigation. Our results showed particularly FFA-induced ED, however, future research is required to address the involvement of other lipid mediators in endothelial dysfunction, such as the effects of cholesterol on the endothelial cells.

REFERENCES

Abdelall, E. K., & Kamel, G. M. (2016). Synthesis of new thiazolo-celecoxib analogues as dual cyclooxygenase-2/15-lipoxygenase inhibitors: Determination of regio-specific different pyrazole cyclization by 2D NMR. *Eur J Med Chem, 118*, 250-258. doi:10.1016/j.ejmech.2016.04.049

Abed, A., Dussaule, J. C., Boffa, J. J., Chatziantoniou, C., & Chadjichristos, C. E. (2014). Connexins in renal endothelial function and dysfunction. *Cardiovasc Hematol Disord Drug Targets, 14*(1), 15-21. Retrieved from http://www.ncbi.nlm.nih.gov/pubmed/24720461

Abrial, C., Grassin-Delyle, S., Salvator, H., Brollo, M., Naline, E., & Devillier, P. (2015). 15-Lipoxygenases regulate the production of chemokines in human lung macrophages. *Br J Pharmacol, 172*(17), 4319-4330. doi:10.1111/bph.13210

Afonine, P. V., Grosse-Kunstleve, R. W., Echols, N., Headd, J. J., Moriarty, N. W., Mustyakimov, M., . . . Adams, P. D. (2012). Towards automated crystallographic structure refinement with phenix.refine. *Acta Crystallogr D Biol Crystallogr, 68*(Pt 4), 352-367. doi:10.1107/S0907444912001308

Afonine, P. V., Moriarty, N. W., Mustyakimov, M., Sobolev, O. V., Terwilliger, T. C., Turk, D., . . . Adams, P. D. (2015). FEM: feature-enhanced map. *Acta Crystallogr D Biol Crystallogr, 71*(Pt 3), 646-666. doi:10.1107/S1399004714028132

Ahlqvist, E., van Zuydam, N. R., Groop, L. C., & McCarthy, M. I. (2015). The genetics of diabetic complications. *Nat Rev Nephrol, 11*(5), 277-287. doi:10.1038/nrneph.2015.37

Ahmad, R., Al-Roub, A., Kochumon, S., Akther, N., Thomas, R., Kumari, M., . . . Rosen, E. D. (2018). The Synergy between Palmitate and TNF-alpha for CCL2 Production Is Dependent on the TRIF/IRF3 Pathway: Implications for Metabolic Inflammation. *J Immunol, 200*(10), 3599-3611. doi:10.4049/jimmunol.1701552

Al-Assi, O., Ghali, R., Mroueh, A., Kaplan, A., Mougharbil, N., Eid, A. H., . . . El-Yazbi, A. F. (2018). Cardiac Autonomic Neuropathy as a Result of Mild Hypercaloric Challenge in Absence of Signs of Diabetes: Modulation by Antidiabetic Drugs. *Oxid Med Cell Longev, 2018*, 9389784. doi:10.1155/2018/9389784

Alaaeddine, R., El-khateeb, M., Saad, E. I., Fouad, H. H., El-Sabban, M., Plane, F., & El-Yazbi, A. F. (2018). Endothelial Dysfunction as a result of Hypercaloric Intake: Underlying Mechanism in Absence of Hyperglycemia. *The FASEB Journal, 32*(1_supplement), 837.832-837.832. doi:10.1096/fasebj.2018.32.1_supplement.837.2

Alaaeddine, R. A., Mroueh, A., Gust, S., Eid, A. H., Plane, F., & El-Yazbi, A. F. (2019). Impaired cross-talk between NO and hyperpolarization in myoendothelial feedback: a novel therapeutic target in early endothelial dysfunction of metabolic disease. *Curr Opin Pharmacol, 45*, 33-41. doi:10.1016/j.coph.2019.03.007

Alarcon, G., Roco, J., Medina, M., Medina, A., Peral, M., & Jerez, S. (2018). High fat diet-induced metabolically obese and normal weight rabbit model shows early vascular dysfunction: mechanisms involved. *Int J Obes (Lond), 42*(9), 1535-1543. doi:10.1038/s41366-018-0020-6

Allen, T., Iftinca, M., Cole, W. C., & Plane, F. (2002). Smooth muscle membrane potential modulates endothelium-dependent relaxation of rat basilar artery via myo-endothelial gap junctions. *J Physiol, 545*(Pt 3), 975-986. Retrieved from http://www.ncbi.nlm.nih.gov/pubmed/12482900

AlZaim, I., Hammoud, S. H., Al-Koussa, H., Ghazi, A., Eid, A. H., & El-Yazbi, A. F. (2020). Adipose Tissue Immunomodulation: A Novel Therapeutic Approach in Cardiovascular and Metabolic Diseases. *Front Cardiovasc Med, 7*, 602088. doi:10.3389/fcvm.2020.602088

American Diabetes, A. (2017). Standards of Medical Care in Diabetes. *40 Suppl 1*.

American Diabetes Association. (2020). Standards of Medical Care in Diabetes. *The Journal of Clinical and Applied Research and Education, 43*, S1-S212. Retrieved from https://care.diabetesjournals.org/content/diacare/suppl/2019/12/20/43.Supplement_1.DC1/Standards_of_Care_2020.pdf

Arner, E., Westermark, P. O., Spalding, K. L., Britton, T., Ryden, M., Frisen, J., . . . Arner, P. (2010). Adipocyte turnover: relevance to human adipose tissue morphology. *Diabetes, 59*(1), 105-109. doi:10.2337/db09-0942

Ashton, A. W., Yokota, R., John, G., Zhao, S., Suadicani, S. O., Spray, D. C., & Ware, J. A. (1999). Inhibition of endothelial cell migration, intercellular communication, and vascular tube formation by thromboxane A(2). *J Biol Chem, 274*(50), 35562-35570.

Balakumar, M., Raji, L., Prabhu, D., Sathishkumar, C., Prabu, P., Mohan, V., & Balasubramanyam, M. (2016). High-fructose diet is as detrimental as high-fat diet in the induction of insulin resistance and diabetes mediated by hepatic/pancreatic endoplasmic reticulum (ER) stress. *Mol Cell Biochem, 423*(1-2), 93-104.

Baldan, A., Ferronato, S., Olivato, S., Malerba, G., Scuro, A., Veraldi, G. F., . . . Gomez-Lira, M. (2014). Cyclooxygenase 2, toll-like receptor 4 and interleukin 1beta mRNA expression in atherosclerotic plaques of type 2 diabetic patients. *Inflamm Res, 63*(10), 851-858. doi:10.1007/s00011-014-0759-8

Bassaganya-Riera, J., Misyak, S., Guri, A. J., & Hontecillas, R. (2009). PPAR gamma is highly expressed in F4/80(hi) adipose tissue macrophages and dampens adipose-tissue inflammation. *Cell Immunol, 258*(2), 138-146. doi:10.1016/j.cellimm.2009.04.003

Beloqui, O., Paramo, J. A., Orbe, J., Benito, A., Colina, I., Monasterio, A., & Diez, J. (2005). Monocyte cyclooxygenase-2 overactivity: a new marker of subclinical atherosclerosis in asymptomatic subjects with cardiovascular risk factors? *Eur Heart J, 26*(2), 153-158. doi:10.1093/eurheartj/ehi016

Berger, J. P., Akiyama, T. E., & Meinke, P. T. (2005). PPARs: therapeutic targets for metabolic disease. *Trends Pharmacol Sci, 26*(5), 244-251. doi:10.1016/j.tips.2005.03.003

Berger, J. P., Petro, A. E., Macnaul, K. L., Kelly, L. J., Zhang, B. B., Richards, K., . . . Moller, D. E. (2003). Distinct properties and advantages of a novel peroxisome proliferator-activated protein [gamma] selective modulator. *Mol Endocrinol, 17*(4), 662-676. doi:10.1210/me.2002-0217

Billaud, M., Lohman, A. W., Johnstone, S. R., Biwer, L. A., Mutchler, S., & Isakson, B. E. (2014). Regulation of cellular communication by signaling microdomains in the blood vessel wall. *Pharmacol Rev, 66*(2), 513-569. doi:10.1124/pr.112.007351

Bing, C. (2015). Is interleukin-1beta a culprit in macrophage-adipocyte crosstalk in obesity? *Adipocyte, 4*(2), 149-152. doi:10.4161/21623945.2014.979661

Boden, G. (2008). Obesity and free fatty acids. *Endocrinol Metab Clin North Am, 37*(3), 635-646, viii-ix. doi:10.1016/j.ecl.2008.06.007

Boden, G. (2009). Endoplasmic reticulum stress: another link between obesity and insulin resistance/inflammation? *Diabetes, 58*(3), 518-519. doi:10.2337/db08-1746

Boden, G., Duan, X., Homko, C., Molina, E. J., Song, W., Perez, O., . . . Merali, S. (2008). Increase in endoplasmic reticulum stress-related proteins and genes in adipose tissue of obese, insulin-resistant individuals. *Diabetes, 57*(9), 2438-2444. doi:10.2337/db08-0604

Bolick, D. T., Orr, A. W., Whetzel, A., Srinivasan, S., Hatley, M. E., Schwartz, M. A., & Hedrick, C. C. (2005). 12/15-lipoxygenase regulates intercellular adhesion molecule-1 expression and monocyte adhesion to endothelium through activation of RhoA and nuclear factor-kappaB. *Arterioscler Thromb Vasc Biol, 25*(11), 2301-2307. doi:10.1161/01.ATV.0000186181.19909.a6

Bolick, D. T., Srinivasan, S., Whetzel, A., Fuller, L. C., & Hedrick, C. C. (2006). 12/15 lipoxygenase mediates monocyte adhesion to aortic endothelium in apolipoprotein E-deficient mice through activation of RhoA and NF-kappaB. *Arterioscler Thromb Vasc Biol, 26*(6), 1260-1266. doi:10.1161/01.ATV.0000217909.09198.d6

Bolognesi, M. L., Banzi, R., Bartolini, M., Cavalli, A., Tarozzi, A., Andrisano, V., . . . Melchiorre, C. (2007). Novel class of quinone-bearing polyamines as multi-target-directed ligands to combat Alzheimer's disease. *J Med Chem, 50*(20), 4882-4897. doi:10.1021/jm070559a

Bolotina, V. M., Najibi, S., Palacino, J. J., Pagano, P. J., & Cohen, R. A. (1994). Nitric oxide directly activates calcium-dependent potassium channels in vascular smooth muscle. *Nature, 368*(6474), 850-853. doi:10.1038/368850a0

Bonato, J. M., Bassani, T. B., Milani, H., Vital, M., & de Oliveira, R. M. W. (2018). Pioglitazone reduces mortality, prevents depressive-like behavior, and impacts hippocampal neurogenesis in the 6-OHDA model of Parkinson's disease in rats. *Exp Neurol, 300*, 188-200. doi:10.1016/j.expneurol.2017.11.009

Brahler, S., Kaistha, A., Schmidt, V. J., Wolfle, S. E., Busch, C., Kaistha, B. P., . . . Kohler, R. (2009). Genetic deficit of SK3 and IK1 channels disrupts the endothelium-derived hyperpolarizing factor vasodilator pathway and causes hypertension. *Circulation, 119*(17), 2323-2332. doi:10.1161/CIRCULATIONAHA.108.846634

Brakemeier, S., Eichler, I., Knorr, A., Fassheber, T., Kohler, R., & Hoyer, J. (2003). Modulation of Ca2+-activated K+ channel in renal artery endothelium in situ by nitric oxide and reactive oxygen species. *Kidney Int, 64*(1), 199-207. doi:10.1046/j.1523-1755.2003.00051.x

Brash, A. R. (1999). Lipoxygenases: occurrence, functions, catalysis, and acquisition of substrate. *J Biol Chem, 274*(34), 23679-23682. doi:10.1074/jbc.274.34.23679

Briscoe, C. P., Tadayyon, M., Andrews, J. L., Benson, W. G., Chambers, J. K., Eilert, M. M., . . . Muir, A. I. (2003). The orphan G protein-coupled receptor GPR40 is activated by medium and long chain fatty acids. *J Biol Chem, 278*(13), 11303-11311. doi:10.1074/jbc.M211495200

Brookheart, R. T., Michel, C. I., & Schaffer, J. E. (2009). As a matter of fat. *Cell Metab, 10*(1), 9-12. doi:10.1016/j.cmet.2009.03.011

Buettner, R., Scholmerich, J., & Bollheimer, L. C. (2007). High-fat diets: modeling the metabolic disorders of human obesity in rodents. *Obesity (Silver Spring), 15*(4), 798-808. doi:10.1038/oby.2007.608

Cameron, N., Cotter, M., Inkster, M., & Nangle, M. (2003). Looking to the future: diabetic neuropathy and effects of rosuvastatin on neurovascular function in diabetes models. *Diabetes Res Clin Pract, 61 Suppl 1*, S35-39. doi:10.1016/s0168-8227(03)00123-2

Castellon, X., & Bogdanova, V. (2016). Chronic Inflammatory Diseases and Endothelial Dysfunction. *Aging Dis, 7*(1), 81-89. doi:10.14336/AD.2015.0803

Chadha, N., Bahia, M. S., Kaur, M., & Silakari, O. (2015). Thiazolidine-2,4-dione derivatives: programmed chemical weapons for key protein targets of various pathological conditions. *Bioorg Med Chem, 23*(13), 2953-2974. doi:10.1016/j.bmc.2015.03.071

Chakrabarti, S. K., Cole, B. K., Wen, Y., Keller, S. R., & Nadler, J. L. (2009). 12/15-lipoxygenase products induce inflammation and impair insulin signaling in 3T3-L1 adipocytes. *Obesity (Silver Spring), 17*(9), 1657-1663. doi:10.1038/oby.2009.192

Chan, K. L., Pillon, N. J., Sivaloganathan, D. M., Costford, S. R., Liu, Z., Theret, M., . . . Klip, A. (2015). Palmitoleate Reverses High Fat-induced Proinflammatory Macrophage Polarization via AMP-activated Protein Kinase (AMPK). *J Biol Chem, 290*(27), 16979-16988. doi:10.1074/jbc.M115.646992

Chan, P. C., Hsiao, F. C., Chang, H. M., Wabitsch, M., & Hsieh, P. S. (2016). Importance of adipocyte cyclooxygenase-2 and prostaglandin E2-prostaglandin E receptor 3 signaling in the development of obesity-induced adipose tissue inflammation and insulin resistance. *FASEB J, 30*(6), 2282-2297. doi:10.1096/fj.201500127

Chan, P. C., Liao, M. T., & Hsieh, P. S. (2019). The Dualistic Effect of COX-2-Mediated Signaling in Obesity and Insulin Resistance. *Int J Mol Sci, 20*(13). doi:10.3390/ijms20133115

Chan, P. C., Wu, T. N., Chen, Y. C., Lu, C. H., Wabitsch, M., Tian, Y. F., & Hsieh, P. S. (2018). Targetted inhibition of CD74 attenuates adipose COX-2-MIF-mediated M1 macrophage polarization and retards obesity-related adipose tissue inflammation and insulin resistance. *Clin Sci (Lond), 132*(14), 1581-1596. doi:10.1042/CS20180041

Chang, L., Milton, H., Eitzman, D. T., & Chen, Y. E. (2013). Paradoxical roles of perivascular adipose tissue in atherosclerosis and hypertension. *Circ J, 77*(1), 11-18. doi:10.1253/circj.cj-12-1393

Chang, L., Zhao, X., Garcia-Barrio, M., Zhang, J., & Eugene Chen, Y. (2018). MitoNEET in Perivascular Adipose Tissue Prevents Arterial Stiffness in Aging Mice. *Cardiovasc Drugs Ther, 32*(5), 531-539. doi:10.1007/s10557-018-6809-7

Chatterjee, T. K., Stoll, L. L., Denning, G. M., Harrelson, A., Blomkalns, A. L., Idelman, G., . . . Weintraub, N. L. (2009). Proinflammatory phenotype of perivascular adipocytes: influence of high-fat feeding. *Circ Res, 104*(4), 541-549. doi:10.1161/CIRCRESAHA.108.182998

Chattopadhyay, M., Mukherjee, S., Chatterjee, S. K., Chattopadhyay, D., Das, S., Majumdar, S. S., . . . Bhattarcharya, S. (2018). Impairment of energy sensors, SIRT1 and AMPK, in lipid induced inflamed adipocyte is regulated by Fetuin A. *Cell Signal, 42*, 67-76. doi:10.1016/j.cellsig.2017.10.005

Chattopadhyay, R., Dyukova, E., Singh, N. K., Ohba, M., Mobley, J. A., & Rao, G. N. (2014). Vascular endothelial tight junctions and barrier function are disrupted by 15(S)-hydroxyeicosatetraenoic acid partly via protein kinase C epsilon-mediated zona occludens-1 phosphorylation at threonine 770/772. *J Biol Chem, 289*(6), 3148-3163. doi:10.1074/jbc.M113.528190

Chen, C., Peng, S., Chen, F., Liu, L., Li, Z., Zeng, G., & Huang, Q. (2017). Protective effects of pioglitazone on vascular endothelial cell dysfunction induced by high glucose via inhibition of IKKalpha/beta-NFkappaB signaling mediated by PPARgamma in vitro. *Can J Physiol Pharmacol, 95*(12), 1480-1487. doi:10.1139/cjpp-2016-0574

Chen, Q. H., Rao, P. N., & Knaus, E. E. (2006). Synthesis and biological evaluation of a novel class of rofecoxib analogues as dual inhibitors of cyclooxygenases (COXs) and lipoxygenases (LOXs). *Bioorg Med Chem, 14*(23), 7898-7909. doi:10.1016/j.bmc.2006.07.047

Chen, X., Liu, L., Palacios, G., Gao, J., Zhang, N., Li, G., . . . Lv, H. (2010). Plasma metabolomics reveals biomarkers of the atherosclerosis. *J Sep Sci, 33*(17-18), 2776-2783. doi:10.1002/jssc.201000395

Chinetti, G., Griglio, S., Antonucci, M., Torra, I. P., Delerive, P., Majd, Z., . . . Staels, B. (1998). Activation of proliferator-activated receptors alpha and gamma induces apoptosis of human monocyte-derived macrophages. *J Biol Chem, 273*(40), 25573-25580. doi:10.1074/jbc.273.40.25573

Chittiboyina, A. G., Mizuno, C. S., Desai, P. V., Patny, A., Kurtz, T. W., Pershadsingh, H. A., . . . Avery, M. A. (2009). Design, synthesis, and docking studies of novel telmisartan–glitazone hybrid analogs for the treatment of metabolic syndrome. *Medicinal chemistry research, 18*(7), 589-610. doi:10.1007/s00044-008-9152-x

Cho, K. W., Morris, D. L., & Lumeng, C. N. (2014). Flow cytometry analyses of adipose tissue macrophages. *Methods Enzymol, 537*, 297-314. doi:10.1016/B978-0-12-411619-1.00016-1

Choe, S. S., Huh, J. Y., Hwang, I. J., Kim, J. I., & Kim, J. B. (2016). Adipose Tissue Remodeling: Its Role in Energy Metabolism and Metabolic Disorders. *Front Endocrinol (Lausanne), 7*, 30. doi:10.3389/fendo.2016.00030

Choi, J. H., Park, J. G., Jeon, H. J., Kim, M. S., Lee, M. R., Lee, M. N., . . . Oh, G. T. (2011). 5-(4-Hydroxy-2,3,5-trimethylbenzylidene) thiazolidine-2,4-dione attenuates atherosclerosis possibly by reducing monocyte recruitment to the lesion. *Exp Mol Med, 43*(8), 471-478. doi:10.3858/emm.2011.43.8.053

Cinti, S., Mitchell, G., Barbatelli, G., Murano, I., Ceresi, E., Faloia, E., . . . Obin, M. S. (2005). Adipocyte death defines macrophage localization and function in adipose tissue of obese mice and humans. *J Lipid Res, 46*(11), 2347-2355. doi:10.1194/jlr.M500294-JLR200

Cipollone, F., & Fazia, M. L. (2006). COX-2 and atherosclerosis. *J Cardiovasc Pharmacol, 47 Suppl 1*, S26-36. doi:10.1097/00005344-200605001-00006

Cohen, R. A., Plane, F., Najibi, S., Huk, I., Malinski, T., & Garland, C. J. (1997). Nitric oxide is the mediator of both endothelium-dependent relaxation and hyperpolarization of the rabbit carotid artery. *Proc Natl Acad Sci U S A, 94*(8), 4193-4198.

Cole, B. K., Kuhn, N. S., Green-Mitchell, S. M., Leone, K. A., Raab, R. M., Nadler, J. L., & Chakrabarti, S. K. (2012). 12/15-Lipoxygenase signaling in the endoplasmic reticulum stress response. *Am J Physiol Endocrinol Metab, 302*(6), E654-665. doi:10.1152/ajpendo.00373.2011

Cole, B. K., Morris, M. A., Grzesik, W. J., Leone, K. A., & Nadler, J. L. (2012). Adipose tissue-specific deletion of 12/15-lipoxygenase protects mice from the consequences of a high-fat diet. *Mediators Inflamm, 2012*, 851798. doi:10.1155/2012/851798

Curry, S. L., Cogar, S. M., & Cook, J. L. (2005). Nonsteroidal antiinflammatory drugs: a review. *J Am Anim Hosp Assoc, 41*(5), 298-309. doi:10.5326/0410298

da Silva, D. P. B., Florentino, I. F., da Silva, D. M., Lino, R. C., Cardoso, C. S., Moreira, L. K. S., . . . Costa, E. A. (2018). Molecular docking and pharmacological/toxicological assessment of a new compound designed from celecoxib and paracetamol by molecular hybridization. *Inflammopharmacology, 26*(5), 1189-1206. doi:10.1007/s10787-018-0516-7

Dai, L., Bhargava, P., Stanya, K. J., Alexander, R. K., Liou, Y. H., Jacobi, D., . . . Lee, C. H. (2017). Macrophage alternative activation confers protection against lipotoxicity-induced cell death. *Mol Metab, 6*(10), 1186-1197. doi:10.1016/j.molmet.2017.08.001

de Kreutzenberg, S. V., Puato, M., Kiwanuka, E., Del Prato, S., Pauletto, P., Pasini, L., . . . Avogaro, A. (2003). Elevated non-esterified fatty acids impair nitric oxide independent vasodilation, in humans: evidence for a role of inwardly rectifying potassium channels. *Atherosclerosis, 169*(1), 147-153. doi:10.1016/s0021-9150(03)00153-9

De Silva, T. M., Li, Y., Kinzenbaw, D. A., Sigmund, C. D., & Faraci, F. M. (2018). Endothelial PPARgamma (Peroxisome Proliferator-Activated Receptor-gamma) Is Essential for Preventing Endothelial Dysfunction With Aging. *Hypertension, 72*(1), 227-234. doi:10.1161/HYPERTENSIONAHA.117.10799

de Wit, C., Roos, F., Bolz, S. S., Kirchhoff, S., Kruger, O., Willecke, K., & Pohl, U. (2000). Impaired conduction of vasodilation along arterioles in connexin40-deficient mice. *Circ Res, 86*(6), 649-655. Retrieved from http://www.ncbi.nlm.nih.gov/pubmed/10747000

Dlugosova, K., Weismann, P., Bernatova, I., Sotnikova, R., Slezak, J., & Okruhlicova, L. (2009). Omega-3 fatty acids and atorvastatin affect connexin 43 expression in the aorta of hereditary hypertriglyceridemic rats. *Can J Physiol Pharmacol, 87*(12), 1074-1082. doi:10.1139/Y09-104

Dobrian, A. D., Huyck, R. W., Glenn, L., Gottipati, V., Haynes, B. A., Hansson, G. I., . . . Nadler, J. L. (2018). Activation of the 12/15 lipoxygenase pathway accompanies metabolic decline in db/db pre-diabetic mice. *Prostaglandins Other Lipid Mediat, 136*, 23-32. doi:10.1016/j.prostaglandins.2018.03.003

Dobrian, A. D., Lieb, D. C., Cole, B. K., Taylor-Fishwick, D. A., Chakrabarti, S. K., & Nadler, J. L. (2011). Functional and pathological roles of the 12- and 15-lipoxygenases. *Prog Lipid Res, 50*(1), 115-131. doi:10.1016/j.plipres.2010.10.005

Dobrian, A. D., Lieb, D. C., Ma, Q., Lindsay, J. W., Cole, B. K., Ma, K., . . . Nadler, J. L. (2010). Differential expression and localization of 12/15 lipoxygenases in adipose tissue in human obese subjects. *Biochem Biophys Res Commun, 403*(3-4), 485-490. doi:10.1016/j.bbrc.2010.11.065

Donath, M. Y., Dalmas, E., Sauter, N. S., & Boni-Schnetzler, M. (2013). Inflammation in obesity and diabetes: islet dysfunction and therapeutic opportunity. *Cell Metab, 17*(6), 860-872. doi:10.1016/j.cmet.2013.05.001

Edwards G, D. K., Gardener MJ, Garland CJ, Weston AH. (1998). K+ is an endothelium-derived hyperpolarizing factor in rat arteries. *Nature, 396*, 269-272.

Edwards, G., Feletou, M., & Weston, A. H. (2010). Endothelium-derived hyperpolarising factors and associated pathways: a synopsis. *Pflugers Arch, 459*(6), 863-879. doi:10.1007/s00424-010-0817-1

The effect of intensive treatment of diabetes on the development and progression of long-term complications in insulin-dependent diabetes mellitus. The Diabetes Control and Complications Trial Research Group. (1993). *N Engl J Med, 329*(14), 977-986. doi:10.1056/nejm199309303291401

Eid, A. H., El-Yazbi, A. F., Zouein, F., Arredouani, A., Ouhtit, A., Rahman, M. M., . . . Abou-Saleh, H. (2018). Inositol 1,4,5-Trisphosphate Receptors in Hypertension. *Front Physiol, 9*, 1018. doi:10.3389/fphys.2018.01018

El-Mas, M. M., El-Gowelli, H. M., Abd-Elrahman, K. S., Saad, E. I., Abdel-Galil, A. G., & Abdel-Rahman, A. A. (2011). Pioglitazone abrogates cyclosporine-evoked hypertension via rectifying abnormalities in vascular endothelial function. *Biochem Pharmacol, 81*(4), 526-533. doi:10.1016/j.bcp.2010.11.013

El-Yazbi, A. F., & Abd-Elrahman, K. S. (2017). ROK and Arteriolar Myogenic Tone Generation: Molecular Evidence in Health and Disease. *Front Pharmacol, 8*, 87. doi:10.3389/fphar.2017.00087

El-Yazbi, A. F., Abd-Elrahman, K. S., & Moreno-Dominguez, A. (2015). PKC-mediated cerebral vasoconstriction: Role of myosin light chain phosphorylation versus actin cytoskeleton reorganization. *Biochem Pharmacol, 95*(4), 263-278. doi:10.1016/j.bcp.2015.04.011

Elkhatib, M. A. W., Mroueh, A., Rafeh, R. W., Sleiman, F., Fouad, H., Saad, E. I., . . . El-Yazbi, A. F. (2019). Amelioration of perivascular adipose inflammation reverses vascular dysfunction in a model of non-obese prediabetic metabolic challenge: Potential role of anti-diabetic drugs. *Translational Research, In Press*. doi:10.1016/j.trsl.2019.07.009

Elkhatib, M. A. W., Mroueh, A., Rafeh, R. W., Sleiman, F., Fouad, H., Saad, E. I., . . . El-Yazbi, A. F. (2019). Amelioration of perivascular adipose inflammation reverses vascular dysfunction in a model of nonobese prediabetic metabolic challenge: potential role of antidiabetic drugs. *Transl Res, 214*, 121-143. doi:10.1016/j.trsl.2019.07.009

Elliott, S. S., Keim, N. L., Stern, J. S., Teff, K., & Havel, P. J. (2002). Fructose, weight gain, and the insulin resistance syndrome. *Am J Clin Nutr, 76*(5), 911-922. doi:10.1093/ajcn/76.5.911

Emsley, P., Lohkamp, B., Scott, W. G., & Cowtan, K. (2010). Features and development of Coot. *Acta Crystallogr D Biol Crystallogr, 66*(Pt 4), 486-501. doi:10.1107/S0907444910007493

Engin, A. B. (2017). Adipocyte-Macrophage Cross-Talk in Obesity. *Adv Exp Med Biol, 960*, 327-343. doi:10.1007/978-3-319-48382-5_14

Enkvetchakul, D., Jeliazkova, I., & Nichols, C. G. (2005). Direct modulation of Kir channel gating by membrane phosphatidylinositol 4,5-bisphosphate. *J Biol Chem, 280*(43), 35785-35788. doi:10.1074/jbc.C500355200

Esser, N., L'Homme, L., De Roover, A., Kohnen, L., Scheen, A. J., Moutschen, M., . . . Paquot, N. (2013). Obesity phenotype is related to NLRP3 inflammasome activity and immunological profile of visceral adipose tissue. *Diabetologia, 56*(11), 2487-2497. doi:10.1007/s00125-013-3023-9

Evans, B. E., Rittle, K. E., Bock, M. G., DiPardo, R. M., Freidinger, R. M., Whitter, W. L., . . . et al. (1988). Methods for drug discovery: development of potent, selective, orally effective cholecystokinin antagonists. *J Med Chem, 31*(12), 2235-2246. doi:10.1021/jm00120a002

Evert, A. B., Boucher, J. L., Cypress, M., Dunbar, S. A., Franz, M. J., Mayer-Davis, E. J., . . . American Diabetes, A. (2013). Nutrition therapy recommendations for the management of adults with diabetes. *Diabetes Care, 36*(11), 3821-3842. doi:10.2337/dc13-2042

Fancher, I. S., Ahn, S. J., Adamos, C., Osborn, C., Oh, M. J., Fang, Y., . . . Levitan, I. (2018). Hypercholesterolemia-Induced Loss of Flow-Induced Vasodilation and Lesion Formation in Apolipoprotein E-Deficient Mice Critically Depend on Inwardly Rectifying K(+) Channels. *J Am Heart Assoc, 7*(5). doi:10.1161/JAHA.117.007430

Fang, Y., Mohler, E. R., 3rd, Hsieh, E., Osman, H., Hashemi, S. M., Davies, P. F., . . . Levitan, I. (2006). Hypercholesterolemia suppresses inwardly rectifying K+ channels in aortic endothelium in vitro and in vivo. *Circ Res, 98*(8), 1064-1071. doi:10.1161/01.RES.0000218776.87842.43

Fedorenko, A., Lishko, P. V., & Kirichok, Y. (2012). Mechanism of fatty-acid-dependent UCP1 uncoupling in brown fat mitochondria. *Cell, 151*(2), 400-413. doi:10.1016/j.cell.2012.09.010

Feine, I., Pinkas, I., Salomon, Y., & Scherz, A. (2012). Local oxidative stress expansion through endothelial cells--a key role for gap junction intercellular communication. *PLoS One, 7*(7), e41633. doi:10.1371/journal.pone.0041633

Feletou, M., & Vanhoutte, P. M. (2009). EDHF: an update. *Clin Sci (Lond), 117*(4), 139-155. doi:10.1042/CS20090096

Fernyhough, M. E., Vierck, J. L., Hausman, G. J., Mir, P. S., Okine, E. K., & Dodson, M. V. (2004). Primary adipocyte culture: adipocyte purification methods may lead to a new understanding of adipose tissue growth and development. *Cytotechnology, 46*(2-3), 163-172. doi:10.1007/s10616-005-2602-0

Figueroa, X. F., & Duling, B. R. (2009). Gap junctions in the control of vascular function. *Antioxid Redox Signal, 11*(2), 251-266. doi:10.1089/ars.2008.2117

Finucane, O. M., Lyons, C. L., Murphy, A. M., Reynolds, C. M., Klinger, R., Healy, N. P., . . . Roche, H. M. (2015). Monounsaturated fatty acid-enriched high-fat diets impede adipose NLRP3 inflammasome-mediated IL-1beta secretion and insulin resistance despite obesity. *Diabetes, 64*(6), 2116-2128. doi:10.2337/db14-1098

Fitzgibbons, T. P., & Czech, M. P. (2014). Epicardial and perivascular adipose tissues and their influence on cardiovascular disease: basic mechanisms and clinical associations. *J Am Heart Assoc, 3*(2), e000582. doi:10.1161/JAHA.113.000582

Fleischhacker, E., Esenabhalu, V. E., Spitaler, M., Holzmann, S., Skrabal, F., Koidl, B., . . . Graier, W. F. (1999). Human diabetes is associated with hyperreactivity of vascular smooth muscle cells due to altered subcellular Ca2+ distribution. *Diabetes, 48*(6), 1323-1330. doi:10.2337/diabetes.48.6.1323

Forbes, J. M., & Cooper, M. E. (2013). Mechanisms of diabetic complications. *Physiol Rev, 93*(1), 137-188. doi:10.1152/physrev.00045.2011

Fowler, M. J. (2008). Microvascular and Macrovascular Complications of Diabetes. *Clinical Diabetes, 26*(2), 77-82. doi:10.2337/diaclin.26.2.77

Fratantonio, D., Cimino, F., Molonia, M. S., Ferrari, D., Saija, A., Virgili, F., & Speciale, A. (2017). Cyanidin-3-O-glucoside ameliorates palmitate-induced insulin resistance by modulating IRS-1 phosphorylation and release of endothelial derived vasoactive factors. *Biochim Biophys Acta Mol Cell Biol Lipids, 1862*(3), 351-357. doi:10.1016/j.bbalip.2016.12.008

Gao, Y. J., Lu, C., Su, L. Y., Sharma, A. M., & Lee, R. M. (2007). Modulation of vascular function by perivascular adipose tissue: the role of endothelium and hydrogen peroxide. *Br J Pharmacol, 151*(3), 323-331. doi:10.1038/sj.bjp.0707228

Gao, Z., Zhang, H., Liu, J., Lau, C. W., Liu, P., Chen, Z. Y., . . . Huang, Y. (2014). Cyclooxygenase-2-dependent oxidative stress mediates palmitate-induced impairment of endothelium-dependent relaxations in mouse arteries. *Biochem Pharmacol, 91*(4), 474-482. doi:10.1016/j.bcp.2014.08.009

Garcia-Alonso, V., Titos, E., Alcaraz-Quiles, J., Rius, B., Lopategi, A., Lopez-Vicario, C., . . . Claria, J. (2016). Prostaglandin E2 Exerts Multiple Regulatory Actions on Human Obese Adipose Tissue Remodeling, Inflammation, Adaptive Thermogenesis and Lipolysis. *PLoS One, 11*(4), e0153751. doi:10.1371/journal.pone.0153751

Gargiulo, S., Rossin, D., Testa, G., Gamba, P., Staurenghi, E., Biasi, F., . . . Leonarduzzi, G. (2018). Up-regulation of COX-2 and mPGES-1 by 27-hydroxycholesterol and 4-hydroxynonenal: A crucial role in atherosclerotic plaque instability. *Free Radic Biol Med, 129*, 354-363. doi:10.1016/j.freeradbiomed.2018.09.046

Garland, C. J., & Dora, K. A. (2017). EDH: endothelium-dependent hyperpolarization and microvascular signalling. *Acta Physiol (Oxf), 219*(1), 152-161. doi:10.1111/apha.12649

Garland, C. J., & McPherson, G. A. (1992). Evidence that nitric oxide does not mediate the hyperpolarization and relaxation to acetylcholine in the rat small mesenteric artery. *Br J Pharmacol, 105*(2), 429-435.

Genin, M., Clement, F., Fattaccioli, A., Raes, M., & Michiels, C. (2015). M1 and M2 macrophages derived from THP-1 cells differentially modulate the response of cancer cells to etoposide. *BMC Cancer, 15*, 577. doi:10.1186/s12885-015-1546-9

Genuth, S., & Ismail-Beigi, F. (2012). Clinical Implications of the ACCORD Trial. *The Journal of Clinical Endocrinology & Metabolism, 97*(1), 41-48. doi:10.1210/jc.2011-1679

Gerber, R. T., Holemans, K., O'Brien-Coker, I., Mallet, A. I., van Bree, R., Van Assche, F. A., & Poston, L. (1999). Cholesterol-independent endothelial dysfunction in virgin and pregnant rats fed a diet high in saturated fat. *J Physiol, 517 (Pt 2)*, 607-616. doi:10.1111/j.1469-7793.1999.0607t.x

Gianfrancesco, M. A., Dehairs, J., L'Homme, L., Herinckx, G., Esser, N., Jansen, O., . . . Legrand-Poels, S. (2019). Saturated fatty acids induce NLRP3 activation in human macrophages through K(+) efflux resulting from phospholipid saturation and Na, K-ATPase disruption. *Biochim Biophys Acta Mol Cell Biol Lipids, 1864*(7), 1017-1030. doi:10.1016/j.bbalip.2019.04.001

Gil-Ortega, M., Condezo-Hoyos, L., Garcia-Prieto, C. F., Arribas, S. M., Gonzalez, M. C., Aranguez, I., . . . Fernandez-Alfonso, M. S. (2014). Imbalance between pro and anti-oxidant mechanisms in perivascular adipose tissue aggravates long-term high-fat diet-derived endothelial dysfunction. *PLoS One, 9*(4), e95312. doi:10.1371/journal.pone.0095312

Gimbrone, M. A., Jr., & Garcia-Cardena, G. (2016). Endothelial Cell Dysfunction and the Pathobiology of Atherosclerosis. *Circ Res, 118*(4), 620-636. doi:10.1161/CIRCRESAHA.115.306301

Giraldez-Garcia, C., Sangros, F. J., Diaz-Redondo, A., Franch-Nadal, J., Serrano, R., Diez, J., . . . Group, P. S. (2015). Cardiometabolic Risk Profiles in Patients With Impaired Fasting Glucose and/or Hemoglobin A1c 5.7% to 6.4%: Evidence for a Gradient According to Diagnostic Criteria: The PREDAPS Study. *Medicine (Baltimore), 94*(44), e1935. doi:10.1097/MD.0000000000001935

Gradel, A. K. J., Salomonsson, M., Sorensen, C. M., Holstein-Rathlou, N. H., & Jensen, L. J. (2018). Long-term diet-induced hypertension in rats is associated with reduced expression and function of small artery SKCa, IKCa, and Kir2.1 channels. *Clin Sci (Lond), 132*(4), 461-474. doi:10.1042/CS20171408

Grizelj, I., Cavka, A., Bian, J. T., Szczurek, M., Robinson, A., Shinde, S., . . . Phillips, S. A. (2015). Reduced flow-and acetylcholine-induced dilations in visceral compared to subcutaneous adipose arterioles in human morbid obesity. *Microcirculation, 22*(1), 44-53. doi:10.1111/micc.12164

Guerra, C., Navarro, P., Valverde, A. M., Arribas, M., Brüning, J., Kozak, L. P., . . . Benito, M. (2001). Brown adipose tissue–specific insulin receptor knockout shows diabetic phenotype without insulin resistance. *J Clin Invest, 108*(8), 1205-1213.

Guilherme, A., Virbasius, J. V., Puri, V., & Czech, M. P. (2008). Adipocyte dysfunctions linking obesity to insulin resistance and type 2 diabetes. *Nat Rev Mol Cell Biol, 9*(5), 367-377. doi:10.1038/nrm2391

Han, H., Rosenhouse-Dantsker, A., Gnanasambandam, R., Epshtein, Y., Chen, Z., Sachs, F., . . . Levitan, I. (2014). Silencing of Kir2 channels by caveolin-1: cross-talk with cholesterol. *J Physiol, 592*(18), 4025-4038. doi:10.1113/jphysiol.2014.273177

Han, L., Shen, W. J., Bittner, S., Kraemer, F. B., & Azhar, S. (2017). PPARs: regulators of metabolism and as therapeutic targets in cardiovascular disease. Part II: PPAR-beta/delta and PPAR-gamma. *Future Cardiol, 13*(3), 279-296. doi:10.2217/fca-2017-0019

Hangaard, L., Jessen, P. B., Kamaev, D., Aalkjaer, C., & Matchkov, V. V. (2015). Extracellular Calcium-Dependent Modulation of Endothelium Relaxation in Rat

Mesenteric Small Artery: The Role of Potassium Signaling. *Biomed Res Int, 2015*. doi:10.1155/2015/758346
Harris, A. K., Elgebaly, M. M., Li, W., Sachidanandam, K., & Ergul, A. (2008). Effect of chronic endothelin receptor antagonism on cerebrovascular function in type 2 diabetes. *Am J Physiol Regul Integr Comp Physiol, 294*(4), R1213-1219. doi:10.1152/ajpregu.00885.2007
Harris, S. G., Padilla, J., Koumas, L., Ray, D., & Phipps, R. P. (2002). Prostaglandins as modulators of immunity. *Trends Immunol, 23*(3), 144-150. doi:10.1016/s1471-4906(01)02154-8
Hasan, A., Akhter, N., Al-Roub, A., Thomas, R., Kochumon, S., Wilson, A., . . . Ahmad, R. (2019). TNF-alpha in Combination with Palmitate Enhances IL-8 Production via The MyD88- Independent TLR4 Signaling Pathway: Potential Relevance to Metabolic Inflammation. *Int J Mol Sci, 20*(17). doi:10.3390/ijms20174112
Hatley, M. E., Srinivasan, S., Reilly, K. B., Bolick, D. T., & Hedrick, C. C. (2003). Increased production of 12/15 lipoxygenase eicosanoids accelerates monocyte/endothelial interactions in diabetic db/db mice. *J Biol Chem, 278*(28), 25369-25375. doi:10.1074/jbc.M301175200
Hazarika, A., Kalita, H., Chandra Boruah, D., Chandra Kalita, M., & Devi, R. (2016). Pathophysiology of metabolic syndrome: The onset of natural recovery on withdrawal of a high-carbohydrate, high-fat diet. *Nutrition, 32*(10), 1081-1091. doi:10.1016/j.nut.2016.03.005
He, J., Liu, H., Zhong, J., Guo, Z., Wu, J., Zhang, H., . . . Cheng, C. (2018). Bexarotene protects against neurotoxicity partially through a PPARgamma-dependent mechanism in mice following traumatic brain injury. *Neurobiol Dis, 117*, 114-124. doi:10.1016/j.nbd.2018.06.003
Heller, S. R. (2009). A Summary of the ADVANCE Trial. *Diabetes Care, 32*(suppl 2), S357-S361. doi:10.2337/dc09-S339
Henkel, J., Klauder, J., Statz, M., Wohlenberg, A. S., Kuipers, S., Vahrenbrink, M., & Puschel, G. P. (2021). Enhanced Palmitate-Induced Interleukin-8 Formation in Human Macrophages by Insulin or Prostaglandin E2. *Biomedicines, 9*(5). doi:10.3390/biomedicines9050449
Hidalgo, M. A., Carretta, M. D., & Burgos, R. A. (2021). Long Chain Fatty Acids as Modulators of Immune Cells Function: Contribution of FFA1 and FFA4 Receptors. *Front Physiol, 12*, 668330. doi:10.3389/fphys.2021.668330
Hildebrand, S., Stumer, J., & Pfeifer, A. (2018). PVAT and Its Relation to Brown, Beige, and White Adipose Tissue in Development and Function. *Front Physiol, 9*, 70. doi:10.3389/fphys.2018.00070
Ho, C. F., Chan, K. W., Yeh, H. I., Kuo, J., Liu, H. J., & Wang, C. Y. (2013). Ketone bodies upregulate endothelial connexin 43 (Cx43) gap junctions. *Vet J, 198*(3), 696-701. doi:10.1016/j.tvjl.2013.09.069
Holm, L. J., Mønsted, M. Ø., Haupt-Jorgensen, M., & Buschard, K. (2020). PPARs and the Development of Type 1 Diabetes. *PPAR Research, 2020*, 6198628. doi:10.1155/2020/6198628
Hopkins, A. L. (2008). Network pharmacology: the next paradigm in drug discovery. *Nature Chemical Biology, 4*(11), 682-690. doi:10.1038/nchembio.118

Hotamisligil, G. S. (2006). Inflammation and metabolic disorders. *Nature, 444*(7121), 860-867. doi:10.1038/nature05485

Hsieh, P. S., Jin, J. S., Chiang, C. F., Chan, P. C., Chen, C. H., & Shih, K. C. (2009). COX-2-mediated inflammation in fat is crucial for obesity-linked insulin resistance and fatty liver. *Obesity (Silver Spring), 17*(6), 1150-1157. doi:10.1038/oby.2008.674

Hua, K. F., Chou, J. C., Ka, S. M., Tasi, Y. L., Chen, A., Wu, S. H., . . . Lin, C. H. (2015). Cyclooxygenase-2 regulates NLRP3 inflammasome-derived IL-1beta production. *J Cell Physiol, 230*(4), 863-874. doi:10.1002/jcp.24815

Huang, Y., Cai, X., Mai, W., Li, M., & Hu, Y. (2016). Association between prediabetes and risk of cardiovascular disease and all cause mortality: systematic review and meta-analysis. *BMJ, 355*, i5953. doi:10.1136/bmj.i5953

Hussein, H. A., Moghimi, A., & Roohbakhsh, A. (2019). Anticonvulsant and ameliorative effects of pioglitazone on cognitive deficits, inflammation and apoptosis in the hippocampus of rat pups exposed to febrile seizure. *Iran J Basic Med Sci, 22*(3), 267-276. doi:10.22038/ijbms.2019.35056.8339

Hutnik, C. M. L., Pocrnich, C. E., Liu, H., Laird, D. W., & Shao, Q. (2008). The Protective Effect of Functional Connexin43 Channels on a Human Epithelial Cell Line Exposed to Oxidative Stress. *Investigative Ophthalmology & Visual Science, 49*(2), 800-806. doi:10.1167/iovs.07-0717

Ichioka, M., Suganami, T., Tsuda, N., Shirakawa, I., Hirata, Y., Satoh-Asahara, N., . . . Ogawa, Y. (2011). Increased expression of macrophage-inducible C-type lectin in adipose tissue of obese mice and humans. *Diabetes, 60*(3), 819-826. doi:10.2337/db10-0864

Inoguchi, T., Li, P., Umeda, F., Yu, H. Y., Kakimoto, M., Imamura, M., . . . Nawata, H. (2000). High glucose level and free fatty acid stimulate reactive oxygen species production through protein kinase C--dependent activation of NAD(P)H oxidase in cultured vascular cells. *Diabetes, 49*(11), 1939-1945. doi:10.2337/diabetes.49.11.1939

Jacob, S., Laury-Kleintop, L., & Lanza-Jacoby, S. (2008). The select cyclooxygenase-2 inhibitor celecoxib reduced the extent of atherosclerosis in apo E-/- mice. *J Surg Res, 146*(1), 135-142. doi:10.1016/j.jss.2007.04.040

Jantzi, M. C., Brett, S. E., Jackson, W. F., Corteling, R., Vigmond, E. J., & Welsh, D. G. (2006). Inward rectifying potassium channels facilitate cell-to-cell communication in hamster retractor muscle feed arteries. *Am J Physiol Heart Circ Physiol, 291*(3), H1319-1328. doi:10.1152/ajpheart.00217.2006

Ji, X. X., Ji, X. J., Li, Q. Q., Lu, X. X., & Luo, L. (2018). Rosiglitazone Reduces Apoptosis and Inflammation in Lipopolysaccharide-Induced Human Umbilical Vein Endothelial Cells. *Med Sci Monit, 24*, 6200-6207. doi:10.12659/MSM.910036

Jo, J., Gavrilova, O., Pack, S., Jou, W., Mullen, S., Sumner, A. E., . . . Periwal, V. (2009). Hypertrophy and/or Hyperplasia: Dynamics of Adipose Tissue Growth. *PLoS Comput Biol, 5*(3), e1000324. doi:10.1371/journal.pcbi.1000324

Joannides, R., Haefeli, W. E., Linder, L., Richard, V., Bakkali, E. H., Thuillez, C., & Lüscher, T. F. (1995). Nitric oxide is responsible for flow-dependent dilatation of human peripheral conduit arteries in vivo. *Circulation, 91*(5), 1314-1319.

Johnson, T. D., Marrelli, S. P., Steenberg, M. L., Childres, W. F., & Bryan, R. M., Jr. (1998). Inward rectifier potassium channels in the rat middle cerebral artery. *Am J Physiol, 274*(2 Pt 2), R541-547. Retrieved from http://www.ncbi.nlm.nih.gov/pubmed/9486315

Josephine A. Wright, T. R., and David L. Becker. (2011). Connexins and Diabetes. *Cardiology Research and Practice, 2012*, 8.

Kabsch, W. (2010). Xds. *Acta Crystallogr D Biol Crystallogr, 66*(Pt 2), 125-132. doi:10.1107/S0907444909047337

Kaminskyy, D., Kryshchyshyn, A., & Lesyk, R. (2017). 5-Ene-4-thiazolidinones - An efficient tool in medicinal chemistry. *Eur J Med Chem, 140*, 542-594. doi:10.1016/j.ejmech.2017.09.031

Kar, K., Krithika, U., Mithuna, Basu, P., Santhosh Kumar, S., Reji, A., & Prashantha Kumar, B. R. (2014). Design, synthesis and glucose uptake activity of some novel glitazones. *Bioorg Chem, 56*, 27-33. doi:10.1016/j.bioorg.2014.05.006

Katsuki, S., Arnold, W., Mittal, C., & Murad, F. (1977). Stimulation of guanylate cyclase by sodium nitroprusside, nitroglycerin and nitric oxide in various tissue preparations and comparison to the effects of sodium azide and hydroxylamine. *J Cyclic Nucleotide Res, 3*(1), 23-35. Retrieved from http://www.ncbi.nlm.nih.gov/pubmed/14978

Kaur, G., Devi, M., Kumari, A., Devi, R., & Banerjee, B. (2018). One-Pot Pseudo Five Component Synthesis of Biologically Relevant 1, 2, 6-Triaryl-4-arylamino-piperidine-3-ene-3-carboxylates: A Decade Update. *ChemistrySelect, 3*(34), 9892-9910.

Keegan, A., Walbank, H., Cotter, M. A., & Cameron, N. E. (1995). Chronic vitamin E treatment prevents defective endothelium-dependent relaxation in diabetic rat aorta. *Diabetologia, 38*(12), 1475-1478. doi:10.1007/bf00400609

Kerr, P. M., Wei, R., Tam, R., Sandow, S. L., Murphy, T. V., Ondrusova, K., . . . Plane, F. (2015). Activation of endothelial IKCa channels underlies NO-dependent myoendothelial feedback. *Vascul Pharmacol, 74*, 130-138. doi:10.1016/j.vph.2015.09.001

Ketonen, J., Shi, J., Martonen, E., & Mervaala, E. (2010). Periadventitial adipose tissue promotes endothelial dysfunction via oxidative stress in diet-induced obese C57Bl/6 mice. *Circ J, 74*(7), 1479-1487. doi:10.1253/circj.cj-09-0661

Kiec-Wilk, B., Czech, U., Janczarska, K., Knapp, A., Goralska, J., Cialowicz, U., . . . Dembinska-Kiec, A. (2012). Connexin 43 and metabolic effect of fatty acids in stressed endothelial cells. *Genes Nutr, 7*(2), 257-263. doi:10.1007/s12263-011-0247-5

Kim, F., Tysseling, K. A., Rice, J., Pham, M., Haji, L., Gallis, B. M., . . . Raines, E. W. (2005). Free fatty acid impairment of nitric oxide production in endothelial cells is mediated by IKKbeta. *Arterioscler Thromb Vasc Biol, 25*(5), 989-994. doi:10.1161/01.ATV.0000160549.60980.a8

Kimmoun, A., Louis, H., Al Kattani, N., Delemazure, J., Dessales, N., Wei, C., . . . Levy, B. (2015). beta1-Adrenergic Inhibition Improves Cardiac and Vascular Function in Experimental Septic Shock. *Crit Care Med, 43*(9), e332-340. doi:10.1097/ccm.0000000000001078

Kinouchi, T., Kitazato, K. T., Shimada, K., Yagi, K., Tada, Y., Matsushita, N., . . . Nagahiro, S. (2018). Treatment with the PPARgamma Agonist Pioglitazone in the Early Post-ischemia Phase Inhibits Pro-inflammatory Responses and Promotes Neurogenesis Via the Activation of Innate- and Bone Marrow-Derived Stem Cells in Rats. *Transl Stroke Res, 9*(3), 306-316. doi:10.1007/s12975-017-0577-8

Knudson, J. D., Rogers, P. A., Dincer, U. D., Bratz, I. N., Araiza, A. G., Dick, G. M., & Tune, J. D. (2006). Coronary vasomotor reactivity to endothelin-1 in the prediabetic metabolic syndrome. *Microcirculation, 13*(3), 209-218. doi:10.1080/10739680600556894

Kochumon, S., Wilson, A., Chandy, B., Shenouda, S., Tuomilehto, J., Sindhu, S., & Ahmad, R. (2018). Palmitate Activates CCL4 Expression in Human Monocytic Cells via TLR4/MyD88 Dependent Activation of NF-kappaB/MAPK/ PI3K Signaling Systems. *Cell Physiol Biochem, 46*(3), 953-964. doi:10.1159/000488824

Kohler, R., Olivan-Viguera, A., & Wulff, H. (2016). Endothelial Small- and Intermediate-Conductance K Channels and Endothelium-Dependent Hyperpolarization as Drug Targets in Cardiovascular Disease. *Adv Pharmacol, 77*, 65-104. doi:10.1016/bs.apha.2016.04.002

Kojo, H., Fukagawa, M., Tajima, K., Suzuki, A., Fujimura, T., Aramori, I., . . . Nishimura, S. (2003). Evaluation of human peroxisome proliferator-activated receptor (PPAR) subtype selectivity of a variety of anti-inflammatory drugs based on a novel assay for PPAR delta(beta). *J Pharmacol Sci, 93*(3), 347-355. doi:10.1254/jphs.93.347

Kuhn, H., Banthiya, S., & van Leyen, K. (2015). Mammalian lipoxygenases and their biological relevance. *Biochim Biophys Acta, 1851*(4), 308-330. doi:10.1016/j.bbalip.2014.10.002

Kuhn, H., Walther, M., & Kuban, R. J. (2002). Mammalian arachidonate 15-lipoxygenases structure, function, and biological implications. *Prostaglandins Other Lipid Mediat, 68-69*, 263-290. doi:10.1016/s0090-6980(02)00035-7

Kuhnlein, H. V., & Receveur, O. (1996). Dietary change and traditional food systems of indigenous peoples. *Annu Rev Nutr, 16*, 417-442. doi:10.1146/annurev.nu.16.070196.002221

Kumar, B. R., Soni, M., Kumar, S. S., Singh, K., Patil, M., Baig, R. B., & Adhikary, L. (2011). Synthesis, glucose uptake activity and structure-activity relationships of some novel glitazones incorporated with glycine, aromatic and alicyclic amine moieties via two carbon acyl linker. *Eur J Med Chem, 46*(3), 835-844. doi:10.1016/j.ejmech.2010.12.019

Kumar, D., Goand, U. K., Gupta, S., Shankar, K., Varshney, S., Rajan, S., . . . Gaikwad, A. N. (2018). Saroglitazar reduces obesity and associated inflammatory consequences in murine adipose tissue. *Eur J Pharmacol, 822*, 32-42. doi:10.1016/j.ejphar.2018.01.002

Kundumani-Sridharan, V., Dyukova, E., Hansen, D. E., 3rd, & Rao, G. N. (2013). 12/15-Lipoxygenase mediates high-fat diet-induced endothelial tight junction disruption and monocyte transmigration: a new role for 15(S)-hydroxyeicosatetraenoic acid in endothelial cell dysfunction. *J Biol Chem, 288*(22), 15830-15842. doi:10.1074/jbc.M113.453290

Kurian, M. M., Berwick, Z. C., & Tune, J. D. (2011). Contribution of IKCa channels to the control of coronary blood flow. *Exp Biol Med (Maywood), 236*(5), 621-627. doi:10.1258/ebm.2011.010351

Kwak, B. R., Mulhaupt, F., Veillard, N., Gros, D. B., & Mach, F. (2002). Altered pattern of vascular connexin expression in atherosclerotic plaques. *Arterioscler Thromb Vasc Biol, 22*(2), 225-230. Retrieved from http://www.ncbi.nlm.nih.gov/pubmed/11834520

Lawson, D., Mehta, J., Nichols, W., Mehta, P., & Donnelly, W. (1990). Superoxide radical-mediated endothelial injury and vasoconstriction of rat thoracic aortic rings. *The Journal of laboratory and clinical medicine, 115*(5), 541-548.

Le, H. T., Sin, W. C., Lozinsky, S., Bechberger, J., Vega, J. L., Guo, X. Q., . . . Naus, C. C. (2014). Gap Junction Intercellular Communication Mediated by Connexin43 in Astrocytes Is Essential for Their Resistance to Oxidative Stress. *Journal of Biological Chemistry, 289*(3), 1345-1354. doi:10.1074/jbc.M113.508390

Lee, H. S., Yun, S. J., Ha, J. M., Jin, S. Y., Ha, H. K., Song, S. H., . . . Bae, S. S. (2019). Prostaglandin D2 stimulates phenotypic changes in vascular smooth muscle cells. *Exp Mol Med, 51*(11), 1-10. doi:10.1038/s12276-019-0330-3

Lee, J., Bae, E. H., Ma, S. K., & Kim, S. W. (2016). Altered Nitric Oxide System in Cardiovascular and Renal Diseases. *Chonnam Med J, 52*(2), 81-90. doi:10.4068/cmj.2016.52.2.81

Lee, M. J., Wu, Y., & Fried, S. K. (2013). Adipose tissue heterogeneity: implication of depot differences in adipose tissue for obesity complications. *Mol Aspects Med, 34*(1), 1-11. doi:10.1016/j.mam.2012.10.001

Lee, W.-Y., Lee, C.-Y., Kim, Y.-S., & Kim, C.-E. (2019). The Methodological Trends of Traditional Herbal Medicine Employing Network Pharmacology. *Biomolecules, 9*(8), 362. doi:10.3390/biom9080362

Lee, Y. S., Kim, J. W., Osborne, O., Oh, D. Y., Sasik, R., Schenk, S., . . . Olefsky, J. M. (2014). Increased adipocyte O2 consumption triggers HIF-1alpha, causing inflammation and insulin resistance in obesity. *Cell, 157*(6), 1339-1352. doi:10.1016/j.cell.2014.05.012

Legrand-Poels, S., Esser, N., L'Homme, L., Scheen, A., Paquot, N., & Piette, J. (2014). Free fatty acids as modulators of the NLRP3 inflammasome in obesity/type 2 diabetes. *Biochem Pharmacol, 92*(1), 131-141. doi:10.1016/j.bcp.2014.08.013

Levitan, I. (2009). Cholesterol and Kir channels. *IUBMB Life, 61*(8), 781-790. doi:10.1002/iub.192

Li, H., Horke, S., & Förstermann, U. (2014). Vascular oxidative stress, nitric oxide and atherosclerosis. *Atherosclerosis, 237*(1), 208-219.

Li, L., Li, J., Yi, J., Liu, H., & Lei, H. (2018). Dose-Effect of Irbesartan on Cyclooxygenase-2 and Matrix Metalloproteinase-9 Expression in Rabbit Atherosclerosis. *J Cardiovasc Pharmacol, 71*(2), 82-94. doi:10.1097/FJC.0000000000000544

Li, W., Abdul, Y., Ward, R., & Ergul, A. (2018). Endothelin and diabetic complications: a brain-centric view. *Physiol Res, 67*(Supplementum 1), S83-s94.

Linares, I., Farrokhi, K., Echeverri, J., Kaths, J. M., Kollmann, D., Hamar, M., . . . Selzner, N. (2018). PPAR-gamma activation is associated with reduced liver ischemia-

reperfusion injury and altered tissue-resident macrophages polarization in a mouse model. *PLoS One*, *13*(4), e0195212. doi:10.1371/journal.pone.0195212
Liu, C., Xu, D., Liu, L., Schain, F., Brunnstrom, A., Bjorkholm, M., . . . Sjoberg, J. (2009). 15-Lipoxygenase-1 induces expression and release of chemokines in cultured human lung epithelial cells. *Am J Physiol Lung Cell Mol Physiol, 297*(1), L196-203. doi:10.1152/ajplung.00036.2008
Liu, K., Zhao, W., Gao, X., Huang, F., Kou, J., & Liu, B. (2012). Diosgenin ameliorates palmitate-induced endothelial dysfunction and insulin resistance via blocking IKKbeta and IRS-1 pathways. *Atherosclerosis, 223*(2), 350-358. doi:10.1016/j.atherosclerosis.2012.06.012
Liu, R., Diao, J., He, S., Li, B., Fei, Y., Li, Y., & Fang, W. (2018). XQ-1H protects against ischemic stroke by regulating microglia polarization through PPARgamma pathway in mice. *Int Immunopharmacol, 57*, 72-81. doi:10.1016/j.intimp.2018.02.014
Liu, Y., Duan, C., Chen, H., Wang, C., Liu, X., Qiu, M., . . . Yang, J. (2018). Inhibition of COX-2/mPGES-1 and 5-LOX in macrophages by leonurine ameliorates monosodium urate crystal-induced inflammation. *Toxicol Appl Pharmacol, 351*, 1-11. doi:10.1016/j.taap.2018.05.010
Liu, Y., Xie, A., Singh, A. K., Ehsan, A., Choudhary, G., Dudley, S., . . . Feng, J. (2015). Inactivation of Endothelial Small/Intermediate Conductance of Calcium-Activated Potassium Channels Contributes to Coronary Arteriolar Dysfunction in Diabetic Patients. *J Am Heart Assoc, 4*(8), e002062. doi:10.1161/JAHA.115.002062
Lozano, I., Van der Werf, R., Bietiger, W., Seyfritz, E., Peronet, C., Pinget, M., . . . Dal, S. (2016a). High-fructose and high-fat diet-induced disorders in rats: impact on diabetes risk, hepatic and vascular complications. *Nutr Metab (Lond), 13*, 15. doi:10.1186/s12986-016-0074-1
Lozano, I., Van der Werf, R., Bietiger, W., Seyfritz, E., Peronet, C., Pinget, M., . . . Dal, S. (2016b). High-fructose and high-fat diet-induced disorders in rats: impact on diabetes risk, hepatic and vascular complications. *Nutr Metab (Lond), 13*. doi:10.1186/s12986-016-0074-1
Lu, C. H., Hung, Y. J., & Hsieh, P. S. (2016). Additional effect of metformin and celecoxib against lipid dysregulation and adipose tissue inflammation in high-fat fed rats with insulin resistance and fatty liver. *Eur J Pharmacol, 789*, 60-67. doi:10.1016/j.ejphar.2016.07.012
Lu, Y., Qian, L., Zhang, Q., Chen, B., Gui, L., Huang, D., . . . Chen, L. (2013). Palmitate induces apoptosis in mouse aortic endothelial cells and endothelial dysfunction in mice fed high-calorie and high-cholesterol diets. *Life Sci, 92*(24-26), 1165-1173. doi:10.1016/j.lfs.2013.05.002
Lumeng, C. N., Bodzin, J. L., & Saltiel, A. R. (2007). Obesity induces a phenotypic switch in adipose tissue macrophage polarization. *J Clin Invest, 117*(1), 175-184. doi:10.1172/JCI29881
Luo, W., Xu, Q., Wang, Q., Wu, H., & Hua, J. (2017). Effect of modulation of PPAR-gamma activity on Kupffer cells M1/M2 polarization in the development of non-alcoholic fatty liver disease. *Sci Rep, 7*, 44612. doi:10.1038/srep44612
Magnusson, L. U., Lundqvist, A., Karlsson, M. N., Skalen, K., Levin, M., Wiklund, O., . . . Hulten, L. M. (2012). Arachidonate 15-lipoxygenase type B knockdown leads to

reduced lipid accumulation and inflammation in atherosclerosis. *PLoS One, 7*(8), e43142. doi:10.1371/journal.pone.0043142

Makino A1, P. O., Suarez J, Yuan JX, Dillmann WH. (2008). Downregulation of connexin40 is associated with coronary endothelial cell dysfunction in streptozotocin-induced diabetic mice. *Am J Physiol Cell Physiol., 295*(1).

Mao, Y., Luo, W., Zhang, L., Wu, W., Yuan, L., Xu, H., . . . Shen, Y. H. (2017). STING-IRF3 Triggers Endothelial Inflammation in Response to Free Fatty Acid-Induced Mitochondrial Damage in Diet-Induced Obesity. *Arterioscler Thromb Vasc Biol, 37*(5), 920-929. doi:10.1161/ATVBAHA.117.309017

Maresca, V., Flori, E., Camera, E., Bellei, B., Aspite, N., Ludovici, M., . . . Picardo, M. (2013). Linking alphaMSH with PPARgamma in B16-F10 melanoma. *Pigment Cell Melanoma Res, 26*(1), 113-127. doi:10.1111/j.1755-148X.2012.01042.x

Martens, F. M., Rabelink, T. J., op 't Roodt, J., de Koning, E. J., & Visseren, F. L. (2006). TNF-alpha induces endothelial dysfunction in diabetic adults, an effect reversible by the PPAR-gamma agonist pioglitazone. *Eur Heart J, 27*(13), 1605-1609. doi:10.1093/eurheartj/ehl079

Martinez-Orgado, J., Gonzalez, R., Alonso, M. J., & Marin, J. (1999). Nitric oxide-dependent and -independent mechanisms in the relaxation elicited by acetylcholine in fetal rat aorta. *Life Sci, 64*(4), 269-277.

Marx, N., Duez, H., Fruchart, J. C., & Staels, B. (2004). Peroxisome proliferator-activated receptors and atherogenesis: regulators of gene expression in vascular cells. *Circ Res, 94*(9), 1168-1178. doi:10.1161/01.RES.0000127122.22685.0A

Mashima, R., & Okuyama, T. (2015). The role of lipoxygenases in pathophysiology; new insights and future perspectives. *Redox Biol, 6,* 297-310. doi:10.1016/j.redox.2015.08.006

Matesanz, N., Jewhurst, V., Trimble, E. R., McGinty, A., Owens, D., Tomkin, G. H., & Powell, L. A. (2012). Linoleic acid increases monocyte chemotaxis and adhesion to human aortic endothelial cells through protein kinase C- and cyclooxygenase-2-dependent mechanisms. *J Nutr Biochem, 23*(6), 685-690. doi:10.1016/j.jnutbio.2011.03.020

Mateu, A., Ramudo, L., Manso, M. A., & De Dios, I. (2015). Cross-talk between TLR4 and PPARgamma pathways in the arachidonic acid-induced inflammatory response in pancreatic acini. *Int J Biochem Cell Biol, 69,* 132-141. doi:10.1016/j.biocel.2015.10.022

Matsumoto, T., Kobayashi, S., Ando, M., Watanabe, S., Iguchi, M., Taguchi, K., & Kobayashi, T. (2017). Impaired endothelium-derived hyperpolarization-type relaxation in superior mesenteric arteries isolated from female Otsuka Long-Evans Tokushima Fatty rats. *Eur J Pharmacol, 807*, 151-158. doi:10.1016/j.ejphar.2017.03.062

McCoy, A. J. (2007). Solving structures of protein complexes by molecular replacement with Phaser. *Acta Crystallogr D Biol Crystallogr, 63*(Pt 1), 32-41. doi:10.1107/S0907444906045975

McDonald, J. D., Mah, E., Chitchumroonchokchai, C., Dey, P., Labyk, A. N., Villamena, F. A., . . . Bruno, R. S. (2019). Dairy milk proteins attenuate hyperglycemia-induced impairments in vascular endothelial function in adults with prediabetes by limiting increases in glycemia and oxidative stress that reduce nitric oxide bioavailability. *J Nutr Biochem, 63*, 165-176. doi:10.1016/j.jnutbio.2018.09.018

McDonald, J. D., Mah, E., Dey, P., Olmstead, B. D., Sasaki, G. Y., Villamena, F. A., & Bruno, R. S. (2019). Dairy milk, regardless of fat content, protects against postprandial hyperglycemia-mediated impairments in vascular endothelial function in adults with prediabetes by limiting oxidative stress responses that reduce nitric oxide bioavailability. *J Nutr Biochem, 63*, 129-139. doi:10.1016/j.jnutbio.2018.10.002

McIntyre, C. A., Buckley, C. H., Jones, G. C., Sandeep, T. C., Andrews, R. C., Elliott, A. I., . . . Hadoke, P. W. (2001). Endothelium-derived hyperpolarizing factor and potassium use different mechanisms to induce relaxation of human subcutaneous resistance arteries. *Br J Pharmacol, 133*(6), 902-908. doi:10.1038/sj.bjp.0704143

McNally, P. G., Watt, P. A. C., Rimmer, T., Burden, A. C., Hearnshaw, J. R., & Thurston, H. (1994). Impaired Contraction and Endothelium-Dependent Relaxation in Isolated Resistance Vessels from Patients with Insulin-Dependent Diabetes Mellitus. *Clinical Science, 87*(1), 31-36. doi:10.1042/cs0870031

Meng, Q. Q., Feng, Z. C., Zhang, X. L., Hu, L. Q., Wang, M., Zhang, H. F., & Li, S. M. (2019). PPAR-gamma Activation Exerts an Anti-inflammatory Effect by Suppressing the NLRP3 Inflammasome in Spinal Cord-Derived Neurons. *Mediators Inflamm, 2019*, 6386729. doi:10.1155/2019/6386729

Metz, J. T., & Hajduk, P. J. (2010). Rational approaches to targeted polypharmacology: creating and navigating protein-ligand interaction networks. *Curr Opin Chem Biol, 14*(4), 498-504. doi:10.1016/j.cbpa.2010.06.166

Metzner, J., Popp, L., Marian, C., Schmidt, R., Manderscheid, C., Renne, C., . . . Niederberger, E. (2007). The effects of COX-2 selective and non-selective NSAIDs on the initiation and progression of atherosclerosis in ApoE-/- mice. *J Mol Med (Berl), 85*(6), 623-633. doi:10.1007/s00109-007-0162-9

Meyers, R. O., Lambert, J. D., Hajicek, N., Pourpak, A., Kalaitzis, J. A., & Dorr, R. T. (2009). Synthesis, characterization, and anti-melanoma activity of tetra-O-substituted analogs of nordihydroguaiaretic acid. *Bioorg Med Chem Lett, 19*(16), 4752-4755. doi:10.1016/j.bmcl.2009.06.063

Middleton, M. K., Rubinstein, T., & Pure, E. (2006). Cellular and molecular mechanisms of the selective regulation of IL-12 production by 12/15-lipoxygenase. *J Immunol, 176*(1), 265-274. doi:10.4049/jimmunol.176.1.265

Miller, A. W., Hoenig, M. E., & Ujhelyi, M. R. (1998). Mechanisms of Impaired Endothelial Function Associated With Insulin Resistance. *J Cardiovasc Pharmacol Ther, 3*(2), 125-134. doi:10.1177/107424849800300205

Mishra, N., Panda, R., Mishra, G., Rajakumar, V., Kumar, S., & Tejonidhi, K. (2011). Screening of anti-inflammatory activity and dose selection of Mollugo pentaphylla by using cotton pellet induced. *International Journal of Pharmacy & Life Sciences, 2*(6).

Mistry, D. K., & Garland, C. J. (1998). Nitric oxide (NO)-induced activation of large conductance Ca2+-dependent K+ channels (BK(Ca)) in smooth muscle cells isolated from the rat mesenteric artery. *Br J Pharmacol, 124*(6), 1131-1140. doi:10.1038/sj.bjp.0701940

Miyamoto, J., Hasegawa, S., Kasubuchi, M., Ichimura, A., Nakajima, A., & Kimura, I. (2016). Nutritional Signaling via Free Fatty Acid Receptors. *Int J Mol Sci, 17*(4), 450. doi:10.3390/ijms17040450

Moreno-Dominguez, A., El-Yazbi, A. F., Zhu, H. L., Colinas, O., Zhong, X. Z., Walsh, E. J., . . . Cole, W. C. (2014). Cytoskeletal reorganization evoked by Rho-associated kinase- and protein kinase C-catalyzed phosphorylation of cofilin and heat shock protein 27, respectively, contributes to myogenic constriction of rat cerebral arteries. *J Biol Chem, 289*(30), 20939-20952. doi:10.1074/jbc.M114.553743

Morphy, R., & Rankovic, Z. (2005). Designed multiple ligands. An emerging drug discovery paradigm. *J Med Chem, 48*(21), 6523-6543. doi:10.1021/jm058225d

Morris, D. L., Singer, K., & Lumeng, C. N. (2011). Adipose tissue macrophages: phenotypic plasticity and diversity in lean and obese states. *Current opinion in clinical nutrition and metabolic care, 14*(4), 341-346. doi:10.1097/MCO.0b013e328347970b

Moussa, G., Alaaeddine, R., Alaeddine, L. M., Nassra, R., Belal, A. S. F., Ismail, A., . . . Hazzaa, A. (2018). Novel click modifiable thioquinazolinones as anti-inflammatory agents: Design, synthesis, biological evaluation and docking study. *Eur J Med Chem, 144*, 635-650. doi:10.1016/j.ejmech.2017.12.065

Mudau, M., Genis, A., Lochner, A., & Strijdom, H. (2012). Endothelial dysfunction: the early predictor of atherosclerosis. *Cardiovasc J Afr, 23*(4), 222-231. doi:10.5830/CVJA-2011-068

Mukohda, M., Stump, M., Ketsawatsomkron, P., Hu, C., Quelle, F. W., & Sigmund, C. D. (2016). Endothelial PPAR-gamma provides vascular protection from IL-1beta-induced oxidative stress. *Am J Physiol Heart Circ Physiol, 310*(1), H39-48. doi:10.1152/ajpheart.00490.2015

Mullican, M. D., Wilson, M. W., Connor, D. T., Kostlan, C. R., Schrier, D. J., & Dyer, R. D. (1993). Design of 5-(3,5-di-tert-butyl-4-hydroxyphenyl)-1,3,4-thiadiazoles, -1,3,4-oxadiazoles, and -1,2,4-triazoles as orally-active, nonulcerogenic antiinflammatory agents. *J Med Chem, 36*(8), 1090-1099. doi:10.1021/jm00060a017

Muniyappa, R., Montagnani, M., Koh, K. K., & Quon, M. J. (2007). Cardiovascular actions of insulin. *Endocr Rev, 28*(5), 463-491. doi:10.1210/er.2007-0006

Musser, J. B., Bentley, T. B., Griffith, S., Sharma, P., Karaian, J. E., & Mongan, P. D. (2004). Hemorrhagic shock in swine: nitric oxide and potassium sensitive adenosine triphosphate channel activation. *Anesthesiology, 101*(2), 399-408.

Naim, M. J., Alam, M. J., Ahmad, S., Nawaz, F., Shrivastava, N., Sahu, M., & Alam, O. (2017). Therapeutic journey of 2,4-thiazolidinediones as a versatile scaffold: An insight into structure activity relationship. *Eur J Med Chem, 129*, 218-250. doi:10.1016/j.ejmech.2017.02.031

Nunemaker, C. S., Chen, M., Pei, H., Kimble, S. D., Keller, S. R., Carter, J. D., . . . Nadler, J. L. (2008). 12-Lipoxygenase-knockout mice are resistant to inflammatory effects of obesity induced by Western diet. *Am J Physiol Endocrinol Metab, 295*(5), E1065-1075. doi:10.1152/ajpendo.90371.2008

Odegaard, J. I., Ricardo-Gonzalez, R. R., Goforth, M. H., Morel, C. R., Subramanian, V., Mukundan, L., . . . Chawla, A. (2007). Macrophage-specific PPARgamma controls alternative activation and improves insulin resistance. *Nature, 447*(7148), 1116-1120. doi:10.1038/nature05894

Oelze, M., Warnholtz, A., Faulhaber, J., Wenzel, P., Kleschyov, A. L., Coldewey, M., . . . Munzel, T. (2006). NADPH oxidase accounts for enhanced superoxide production and impaired endothelium-dependent smooth muscle relaxation in BKbeta1-/- mice. *Arterioscler Thromb Vasc Biol, 26*(8), 1753-1759. doi:10.1161/01.ATV.0000231511.26860.50

Ohara, Y., Peterson, T. E., & Harrison, D. G. (1993a). Hypercholesterolemia increases endothelial superoxide anion production. *J Clin Invest, 91*(6), 2546-2551. doi:10.1172/JCI116491

Ohara, Y., Peterson, T. E., & Harrison, D. G. (1993b). Hypercholesterolemia increases endothelial superoxide anion production. *J Clin Invest, 91*(6), 2546-2551. doi:10.1172/JCI116491

Oyama, Y., Kawasaki, H., Hattori, Y., & Kanno, M. (1986). Attenuation of endothelium-dependent relaxation in aorta from diabetic rats. *Eur J Pharmacol, 132*(1), 75-78. doi:https://doi.org/10.1016/0014-2999(86)90013-0

Oyamada, M., Oyamada, Y., & Takamatsu, T. (2005). Regulation of connexin expression. *Biochim Biophys Acta, 1719*(1-2), 6-23. doi:10.1016/j.bbamem.2005.11.002

Ozaki, M., Kawashima, S., Yamashita, T., Hirase, T., Namiki, M., Inoue, N., . . . Yokoyama, M. (2002). Overexpression of endothelial nitric oxide synthase accelerates atherosclerotic lesion formation in apoE-deficient mice. *J Clin Invest, 110*(3), 331-340. doi:10.1172/JCI15215

Park, Y. G., Kang, S. K., Noh, S. H., Park, K. K., Chang, Y. C., Lee, Y. C., & Kim, C. H. (2004). PGE2 induces IL-1beta gene expression in mouse osteoblasts through a cAMP-PKA signaling pathway. *Int Immunopharmacol, 4*(6), 779-789. doi:10.1016/j.intimp.2004.03.003

Pedersen, D. J., Guilherme, A., Danai, L. V., Heyda, L., Matevossian, A., Cohen, J., . . . Czech, M. P. (2015). A major role of insulin in promoting obesity-associated adipose tissue inflammation. *Mol Metab, 4*(7), 507-518. doi:10.1016/j.molmet.2015.04.003

Peng, J., Wang, K., Xiang, W., Li, Y., Hao, Y., & Guan, Y. (2019). Rosiglitazone polarizes microglia and protects against pilocarpine-induced status epilepticus. *CNS Neurosci Ther, 25*(12), 1363-1372. doi:10.1111/cns.13265

Petrosino, M., Lori, L., Pasquo, A., Lori, C., Consalvi, V., Minicozzi, V., . . . Chiaraluce, R. (2017). Single-Nucleotide Polymorphism of PPARgamma, a Protein at the Crossroads of Physiological and Pathological Processes. *Int J Mol Sci, 18*(2). doi:10.3390/ijms18020361

Pickkers, P., Dorresteijn, M. J., Bouw, M. P., van der Hoeven, J. G., & Smits, P. (2006). In vivo evidence for nitric oxide-mediated calcium-activated potassium-channel activation during human endotoxemia. *Circulation, 114*(5), 414-421. doi:10.1161/CIRCULATIONAHA.105.590232

Pieper, G. M., & Gross, G. J. (1988). Oxygen free radicals abolish endothelium-dependent relaxation in diabetic rat aorta. *American Journal of Physiology-Heart and Circulatory Physiology, 255*(4), H825-H833. doi:10.1152/ajpheart.1988.255.4.H825

Pillon, N. J., Azizi, P. M., Li, Y. E., Liu, J., Wang, C., Chan, K. L., . . . Klip, A. (2015). Palmitate-induced inflammatory pathways in human adipose microvascular endothelial cells promote monocyte adhesion and impair insulin transcytosis. *Am J Physiol Endocrinol Metab, 309*(1), E35-44. doi:10.1152/ajpendo.00611.2014

Pirat, C., Farce, A., Lebegue, N., Renault, N., Furman, C., Millet, R., . . . Chavatte, P. (2012). Targeting peroxisome proliferator-activated receptors (PPARs): development of modulators. *J Med Chem, 55*(9), 4027-4061. doi:10.1021/jm101360s

Pires Gouvea, D., Vasconcellos, F. A., Dos Anjos Berwaldt, G., Neto, A. C., Fischer, G., Sakata, R. P., . . . Cunico, W. (2016). 2-Aryl-3-(2-morpholinoethyl)thiazolidin-4-ones: Synthesis, anti-inflammatory in vivo, cytotoxicity in vitro and molecular docking studies. *Eur J Med Chem, 118*, 259-265. doi:10.1016/j.ejmech.2016.04.028

Plane, F., & Garland, C. J. (1993). Differential effects of acetylcholine, nitric oxide and levcromakalim on smooth muscle membrane potential and tone in the rabbit basilar artery. *Br J Pharmacol, 110*(2), 651-656.

Plane, F., & Garland, C. J. (1996). Influence of contractile agonists on the mechanism of endothelium-dependent relaxation in rat isolated mesenteric artery. *Br J Pharmacol, 119*(2), 191-193. Retrieved from http://www.ncbi.nlm.nih.gov/pubmed/8886397

Plane, F., Johnson, R., Kerr, P., Wiehler, W., Thorneloe, K., Ishii, K., . . . Cole, W. (2005). Heteromultimeric Kv1 channels contribute to myogenic control of arterial diameter. *Circ Res, 96*(2), 216-224. doi:10.1161/01.RES.0000154070.06421.25

Pober, J. S., & Sessa, W. C. (2007). Evolving functions of endothelial cells in inflammation. *Nat Rev Immunol, 7*(10), 803-815. doi:10.1038/nri2171

Poledne, R., Malinska, H., Kubatova, H., Fronek, J., Thieme, F., Kauerova, S., & Lesna, I. K. (2019). Polarization of Macrophages in Human Adipose Tissue is Related to the Fatty Acid Spectrum in Membrane Phospholipids. *Nutrients, 12*(1). doi:10.3390/nu12010008

Poudyal, H., Lemonakis, N., Efentakis, P., Gikas, E., Halabalaki, M., Andreadou, I., . . . Brown, L. (2017). Hydroxytyrosol ameliorates metabolic, cardiovascular and liver changes in a rat model of diet-induced metabolic syndrome: Pharmacological and metabolism-based investigation. *Pharmacol Res, 117*, 32-45. doi:10.1016/j.phrs.2016.12.002

Prescott, J., Owens, D., Collins, P., Johnson, A., & Tomkin, G. H. (1999). The fatty acid distribution in low density lipoprotein in diabetes. *Biochim Biophys Acta, 1439*(1), 110-116. doi:10.1016/s1388-1981(99)00082-7

Proschak, E., Stark, H., & Merk, D. (2019). Polypharmacology by Design: A Medicinal Chemist's Perspective on Multitargeting Compounds. *J Med Chem, 62*(2), 420-444. doi:10.1021/acs.jmedchem.8b00760

Rafeh, R., Viveiros, A., Oudit, Gavin Y., & El-Yazbi, Ahmed F. (2020). Targeting perivascular and epicardial adipose tissue inflammation: therapeutic opportunities for cardiovascular disease. *Clinical Science, 134*(7), 827-851. doi:10.1042/cs20190227

Rafeh, R., Viveiros, A., Oudit, G. Y., & El-Yazbi, A. F. (2020). Targeting perivascular and epicardial adipose tissue inflammation: therapeutic opportunities for cardiovascular disease. *Clin Sci (Lond), 134*(7), 827-851. doi:10.1042/CS20190227

Rajapaksha, H., Bhatia, H., Wegener, K., Petrovsky, N., & Bruning, J. B. (2017). X-ray crystal structure of rivoglitazone bound to PPARgamma and PPAR subtype selectivity of TZDs. *Biochim Biophys Acta Gen Subj, 1861*(8), 1981-1991. doi:10.1016/j.bbagen.2017.05.008

Ramachandran, S., Xie, L.-H., John, S. A., Subramaniam, S., & Lal, R. (2007). A novel role for connexin hemichannel in oxidative stress and smoking-induced cell injury. *PLoS One, 2*(8), e712-e712. doi:10.1371/journal.pone.0000712

Ramsay, R. R., Popovic-Nikolic, M. R., Nikolic, K., Uliassi, E., & Bolognesi, M. L. (2018). A perspective on multi-target drug discovery and design for complex diseases. *Clin Transl Med, 7*(1), 3. doi:10.1186/s40169-017-0181-2

Rand, V. E., & Garland, C. J. (1992). Endothelium-dependent relaxation to acetylcholine in the rabbit basilar artery: importance of membrane hyperpolarization. *Br J Pharmacol, 106*(1), 143-150.

Rasmussen, K. M., Braunstein, T. H., Salomonsson, M., & Brasen, J. C. (2016). Contribution of K(+) channels to endothelium-derived hypolarization-induced renal vasodilation in rats in vivo and in vitro. *468*(7), 1139-1149. doi:10.1007/s00424-016-1805-x

Rastelli, G., & Pinzi, L. (2015). Computational polypharmacology comes of age. *Front Pharmacol, 6*(157). doi:10.3389/fphar.2015.00157

Ratnayake, M., Wilson, C., Lee, M. D., Girkin, J. M., Saunter, C. M., & McCarron, J. G. (2018). Complex Interactions of excitatory and inhibitory stimuli in the vascular endothelium. *The FASEB Journal, 32*(1_supplement), 843.845-843.845. doi:10.1096/fasebj.2018.32.1_supplement.843.5

Raval, M., Frank, P. G., Laury-Kleintop, L., Yan, G., & Lanza-Jacoby, S. (2010). Celecoxib combined with atorvastatin prevents progression of atherosclerosis. *J Surg Res, 163*(2), e113-122. doi:10.1016/j.jss.2010.03.011

Raza, A., Ghoshal, A., Chockalingam, S., & Ghosh, S. S. (2017). Connexin-43 enhances tumor suppressing activity of artesunate via gap junction-dependent as well as independent pathways in human breast cancer cells. *Sci Rep, 7*(1), 7580. doi:10.1038/s41598-017-08058-y

Reddy, A. S., & Zhang, S. (2013). Polypharmacology: drug discovery for the future. *Expert Rev Clin Pharmacol, 6*(1), 41-47. doi:10.1586/ecp.12.74

Reeves, P. G., Nielsen, F. H., & Fahey, G. C., Jr. (1993). AIN-93 purified diets for laboratory rodents: final report of the American Institute of Nutrition ad hoc writing committee on the reformulation of the AIN-76A rodent diet. *J Nutr, 123*(11), 1939-1951. doi:10.1093/jn/123.11.1939

Ricciotti, E., & FitzGerald, G. A. (2011). Prostaglandins and inflammation. *Arterioscler Thromb Vasc Biol, 31*(5), 986-1000. doi:10.1161/ATVBAHA.110.207449

Ricote, M., Li, A. C., Willson, T. M., Kelly, C. J., & Glass, C. K. (1998). The peroxisome proliferator-activated receptor-gamma is a negative regulator of macrophage activation. *Nature, 391*(6662), 79-82. doi:10.1038/34178

Rival, Y., Puech, L., Taillandier, T., Beneteau, N., Rouquette, A., Lestienne, F., . . . Junquero, D. (2009). PPAR activators and COX inhibitors selectively block cytokine-induced COX-2 expression and activity in human aortic smooth muscle cells. *Eur J Pharmacol, 606*(1-3), 121-129. doi:10.1016/j.ejphar.2009.01.010

Rocha, M. L., Kihara, A. H., Davel, A. P., Britto, L. R., Rossoni, L. V., & Bendhack, L. M. (2008). Blood pressure variability increases connexin expression in the vascular smooth muscle of rats. *Cardiovasc Res, 80*(1), 123-130. doi:10.1093/cvr/cvn178

Rocha, R. M., Barra, G. B., Rosa, E. C., Garcia, E. C., Amato, A. A., & Azevedo, M. F. (2015). Prevalence of the rs1801282 single nucleotide polymorphism of the PPARG gene in patients with metabolic syndrome. *Arch Endocrinol Metab, 59*(4), 297-302. doi:10.1590/2359-3997000000086

Roghani-Dehkordi, F., & Roghani, M. (2016). The vasorelaxant effect of simvastatin in isolated aorta from diabetic rats. *ARYA Atheroscler, 12*(2), 104-108. Retrieved from http://www.ncbi.nlm.nih.gov/pubmed/27429631

Romanenko, V. G., Fang, Y., Byfield, F., Travis, A. J., Vandenberg, C. A., Rothblat, G. H., & Levitan, I. (2004). Cholesterol sensitivity and lipid raft targeting of Kir2.1 channels. *Biophys J, 87*(6), 3850-3861. doi:10.1529/biophysj.104.043273

Rosenhouse-Dantsker, A., Epshtein, Y., & Levitan, I. (2014). Interplay Between Lipid Modulators of Kir2 Channels: Cholesterol and PIP2. *Comput Struct Biotechnol J, 11*(19), 131-137. doi:10.1016/j.csbj.2014.09.007

Rubio-Navarro, A., Guerrero-Hue, M., Martin-Fernandez, B., Cortegano, I., Olivares-Alvaro, E., de Las Heras, N., . . . Moreno, J. A. (2016). Phenotypic Characterization of Macrophages from Rat Kidney by Flow Cytometry. *J Vis Exp*(116). doi:10.3791/54599

Rudnicki, M., Tripodi, G. L., Ferrer, R., Bosca, L., Pitta, M. G., Pitta, I. R., & Abdalla, D. S. (2016). New thiazolidinediones affect endothelial cell activation and angiogenesis. *Eur J Pharmacol, 782*, 98-106. doi:10.1016/j.ejphar.2016.04.038

Ruffino, J. S., Davies, N. A., Morris, K., Ludgate, M., Zhang, L., Webb, R., & Thomas, A. W. (2016). Moderate-intensity exercise alters markers of alternative activation in circulating monocytes in females: a putative role for PPARgamma. *Eur J Appl Physiol, 116*(9), 1671-1682. doi:10.1007/s00421-016-3414-y

Sadeghian, H., & Jabbari, A. (2016). 15-Lipoxygenase inhibitors: a patent review. *Expert Opin Ther Pat, 26*(1), 65-88. doi:10.1517/13543776.2016.1113259

Sadik, C. D., Sies, H., & Schewe, T. (2003). Inhibition of 15-lipoxygenases by flavonoids: structure-activity relations and mode of action. *Biochem Pharmacol, 65*(5), 773-781. doi:10.1016/s0006-2952(02)01621-0

Saeedi, P., Petersohn, I., Salpea, P., Malanda, B., Karuranga, S., Unwin, N., . . . Committee, I. D. F. D. A. (2019). Global and regional diabetes prevalence estimates for 2019 and projections for 2030 and 2045: Results from the International Diabetes Federation Diabetes Atlas, 9(th) edition. *Diabetes Res Clin Pract, 157*, 107843. doi:10.1016/j.diabres.2019.107843

Sahebkar, A., Simental-Mendia, L. E., Pedone, C., Ferretti, G., Nachtigal, P., Bo, S., . . . Watts, G. F. (2016). Statin therapy and plasma free fatty acids: a systematic review and meta-analysis of controlled clinical trials. *Br J Clin Pharmacol, 81*(5), 807-818. doi:10.1111/bcp.12854

Sakamoto, H., Aikawa, M., Hill, C. C., Weiss, D., Taylor, W. R., Libby, P., & Lee, R. T. (2001). Biomechanical strain induces class a scavenger receptor expression in human monocyte/macrophages and THP-1 cells: a potential mechanism of increased atherosclerosis in hypertension. *Circulation, 104*(1), 109-114. doi:10.1161/hc2701.091070

Samsamshariat, S. Z. A., Sakhaei, F., Salehizadeh, L., Keshvari, M., & Asgary, S. (2019). Relationship between Resistin, Endothelin-1, and Flow-Mediated Dilation in Patient with and without Metabolic Syndrome. *Adv Biomed Res, 8*, 16. doi:10.4103/abr.abr_126_18

Sanchez-Tejeda, J. F., Sanchez-Ruiz, J. F., Salazar, J. R., & Loza-Mejia, M. A. (2020). A Definition of "Multitargeticity": Identifying Potential Multitarget and Selective Ligands Through a Vector Analysis. *Front Chem, 8*, 176. doi:10.3389/fchem.2020.00176

Sancho, M., Fabris, S., Hald, B. O., Brett, S. E., Sandow, S. L., Poepping, T. L., & Welsh, D. G. (2019). Membrane Lipid-KIR2.x Channel Interactions Enable Hemodynamic Sensing in Cerebral Arteries. *Arterioscler Thromb Vasc Biol, 39*(6), 1072-1087. doi:10.1161/atvbaha.119.312493

Sancho, M., & Welsh, D. G. (2018). Cerebral Vascular KIR2.x Channels are Distinctly Regulated by Membrane Lipids and Hemodynamic Forces. *The FASEB Journal, 32*(1_supplement), 705.707-705.707. doi:10.1096/fasebj.2018.32.1_supplement.705.7

Sandow, S. L., & Hill, C. E. (2000). Incidence of myoendothelial gap junctions in the proximal and distal mesenteric arteries of the rat is suggestive of a role in endothelium-derived hyperpolarizing factor-mediated responses. *Circ Res, 86*(3), 341-346.

Santin, J. R., Uchoa, F. D., Lima Mdo, C., Rabello, M. M., Machado, I. D., Hernandes, M. Z., . . . Farsky, S. H. (2013). Chemical synthesis, docking studies and biological effects of a pan peroxisome proliferator-activated receptor agonist and cyclooxygenase inhibitor. *Eur J Pharm Sci, 48*(4-5), 689-697. doi:10.1016/j.ejps.2012.12.029

Schach, C., Resch, M., Schmid, P. M., Riegger, G. A., & Endemann, D. H. (2014). Type 2 diabetes: increased expression and contribution of IKCa channels to vasodilation in small mesenteric arteries of ZDF rats. *Am J Physiol Heart Circ Physiol, 307*(8), H1093-1102. doi:10.1152/ajpheart.00240.2013

Schauberger, E., Peinhaupt, M., Cazares, T., & Lindsley, A. W. (2016). Lipid Mediators of Allergic Disease: Pathways, Treatments, and Emerging Therapeutic Targets. *Curr Allergy Asthma Rep, 16*(7), 48. doi:10.1007/s11882-016-0628-3

Schinzari, F., Tesauro, M., & Cardillo, C. (2018). Increased endothelin-1-mediated vasoconstrictor tone in human obesity: effects of gut hormones. *Physiol Res, 67*(Supplementum 1), S69-s81.

Schneider, C., & Pozzi, A. (2011). Cyclooxygenases and lipoxygenases in cancer. *Cancer Metastasis Rev, 30*(3-4), 277-294. doi:10.1007/s10555-011-9310-3

Schneider, I., & Bucar, F. (2005). Lipoxygenase inhibitors from natural plant sources. Part 1: Medicinal plants with inhibitory activity on arachidonate 5-lipoxygenase and 5-lipoxygenase[sol]cyclooxygenase. *Phytother Res, 19*(2), 81-102. doi:10.1002/ptr.1603

Schneider, K., Valdez, J., Nguyen, J., Vawter, M., Galke, B., Kurtz, T. W., & Chan, J. Y. (2016). Increased Energy Expenditure, Ucp1 Expression, and Resistance to Diet-induced Obesity in Mice Lacking Nuclear Factor-Erythroid-2-related Transcription Factor-2 (Nrf2). *J Biol Chem, 291*(14), 7754-7766. doi:10.1074/jbc.M115.673756

Schwingshackl, L., & Hoffmann, G. (2012). Monounsaturated fatty acids and risk of cardiovascular disease: synopsis of the evidence available from systematic reviews and meta-analyses. *Nutrients, 4*(12), 1989-2007. doi:10.3390/nu4121989

Scortegagna, M., Cataisson, C., Martin, R. J., Hicklin, D. J., Schreiber, R. D., Yuspa, S. H., & Arbeit, J. M. (2008). HIF-1alpha regulates epithelial inflammation by cell autonomous NFkappaB activation and paracrine stromal remodeling. *Blood, 111*(7), 3343-3354. doi:10.1182/blood-2007-10-115758

Sears, D. D., Miles, P. D., Chapman, J., Ofrecio, J. M., Almazan, F., Thapar, D., & Miller, Y. I. (2009). 12/15-lipoxygenase is required for the early onset of high fat diet-induced adipose tissue inflammation and insulin resistance in mice. *PLoS One, 4*(9), e7250. doi:10.1371/journal.pone.0007250

Secor, J. D., Fligor, S. C., Tsikis, S. T., Yu, L. J., & Puder, M. (2021). Free Fatty Acid Receptors as Mediators and Therapeutic Targets in Liver Disease. *Front Physiol, 12*, 656441. doi:10.3389/fphys.2021.656441

Shabalina, I. G., Petrovic, N., de Jong, J. M., Kalinovich, A. V., Cannon, B., & Nedergaard, J. (2013). UCP1 in brite/beige adipose tissue mitochondria is functionally thermogenic. *Cell Rep, 5*(5), 1196-1203. doi:10.1016/j.celrep.2013.10.044

Shahid, M., Hornberg, J., Superti-Furga, G., Young, M., Keiser, M., Mason, J., . . . Dancey, J. (2012). *Designing multi-target drugs*: Royal Society of Chemistry.

Shaligram, S., Sangüesa, G., Akther, F., Alegret, M., Laguna, J. C., & Rahimian, R. (2018). Differential effects of high consumption of fructose or glucose on mesenteric arterial function in female rats. *J Nutr Biochem, 57*, 136-144. doi:10.1016/j.jnutbio.2018.03.021

Shao, L. (2009). Network Systems Underlying Traditional Chinese Medicine Syndrome and Herb Formula. *Current Bioinformatics, 4*(3), 188-196. doi:http://dx.doi.org/10.2174/157489309789071129

Shaquiquzzaman, M., Verma, G., Marella, A., Akhter, M., Akhtar, W., Khan, M. F., . . . Alam, M. M. (2015). Piperazine scaffold: A remarkable tool in generation of diverse pharmacological agents. *Eur J Med Chem, 102*, 487-529. doi:10.1016/j.ejmech.2015.07.026

Sheng, J. Z., & Braun, A. P. (2007). Small- and intermediate-conductance Ca2+-activated K+ channels directly control agonist-evoked nitric oxide synthesis in human vascular endothelial cells. *Am J Physiol Cell Physiol, 293*(1), C458-467. doi:10.1152/ajpcell.00036.2007

Sheng, J. Z., Ella, S., Davis, M. J., Hill, M. A., & Braun, A. P. (2009). Openers of SKCa and IKCa channels enhance agonist-evoked endothelial nitric oxide synthesis and arteriolar vasodilation. *FASEB J, 23*(4), 1138-1145. doi:10.1096/fj.08-120451

Shi, H., Kokoeva, M. V., Inouye, K., Tzameli, I., Yin, H., & Flier, J. S. (2006). TLR4 links innate immunity and fatty acid-induced insulin resistance. *J Clin Invest, 116*(11), 3015-3025. doi:10.1172/JCI28898

Shimokawa, H., & Godo, S. (2016). Diverse Functions of Endothelial NO Synthases System: NO and EDH. *J Cardiovasc Pharmacol, 67*(5), 361-366. doi:10.1097/FJC.0000000000000348

Shimokawa, H., Yasutake, H., Fujii, K., Owada, M. K., Nakaike, R., Fukumoto, Y., . . . Takeshita, A. (1996). The Importance of the Hyperpolarizing Mechanism Increases as the Vessel Size Decreases in Endothelium-Dependent Relaxations in Rat Mesenteric Circulation. *J Cardiovasc Pharmacol, 28*(5), 703-711. Retrieved from https://journals.lww.com/cardiovascularpharm/Fulltext/1996/11000/The_Importance_of_the_Hyperpolarizing_Mechanism.14.aspx

Silva, J. C., Cesar, F. A., de Oliveira, E. M., Turato, W. M., Tripodi, G. L., Castilho, G., . . . Abdalla, D. S. (2016). New PPARgamma partial agonist improves obesity-induced metabolic alterations and atherosclerosis in LDLr(-/-) mice. *Pharmacol Res, 104*, 49-60. doi:10.1016/j.phrs.2015.12.010

Sindhu, S., Akhter, N., Wilson, A., Thomas, R., Arefanian, H., Al Madhoun, A., . . . Ahmad, R. (2020). MIP-1alpha Expression Induced by Co-Stimulation of Human Monocytic Cells with Palmitate and TNF-alpha Involves the TLR4-IRF3 Pathway and Is Amplified by Oxidative Stress. *Cells, 9*(8). doi:10.3390/cells9081799

Sindhu, S., Al-Roub, A., Koshy, M., Thomas, R., & Ahmad, R. (2016). Palmitate-Induced MMP-9 Expression in the Human Monocytic Cells is Mediated through the TLR4-MyD88 Dependent Mechanism. *Cell Physiol Biochem, 39*(3), 889-900. doi:10.1159/000447798

Sindhu, S., Kochumon, S., Shenouda, S., Wilson, A., Al-Mulla, F., & Ahmad, R. (2019). The Cooperative Induction of CCL4 in Human Monocytic Cells by TNF-alpha and Palmitate Requires MyD88 and Involves MAPK/NF-kappaB Signaling Pathways. *Int J Mol Sci, 20*(18). doi:10.3390/ijms20184658

Singh, N. K., & Rao, G. N. (2019). Emerging role of 12/15-Lipoxygenase (ALOX15) in human pathologies. *Prog Lipid Res, 73*, 28-45. doi:10.1016/j.plipres.2018.11.001

Smith, P. D., Brett, S. E., Luykenaar, K. D., Sandow, S. L., Marrelli, S. P., Vigmond, E. J., & Welsh, D. G. (2008). KIR channels function as electrical amplifiers in rat vascular smooth muscle. *J Physiol, 586*(4), 1147-1160. doi:10.1113/jphysiol.2007.145474

Smith, W. L., DeWitt, D. L., & Garavito, R. M. (2000). Cyclooxygenases: structural, cellular, and molecular biology. *Annu Rev Biochem, 69*, 145-182. doi:10.1146/annurev.biochem.69.1.145

Sohn, H. Y., Keller, M., Gloe, T., Morawietz, H., Rueckschloss, U., & Pohl, U. (2000). The small G-protein Rac mediates depolarization-induced superoxide formation in human endothelial cells. *J Biol Chem, 275*(25), 18745-18750. doi:10.1074/jbc.M000026200

Song, Y., Connor, D. T., Doubleday, R., Sorenson, R. J., Sercel, A. D., Unangst, P. C., . . . Dyer, R. D. (1999). Synthesis, structure-activity relationships, and in vivo evaluations of substituted di-tert-butylphenols as a novel class of potent, selective, and orally active cyclooxygenase-2 inhibitors. 1. Thiazolone and oxazolone series. *J Med Chem, 42*(7), 1151-1160. doi:10.1021/jm9805081

Song, Y. S., Lee, D. H., Yu, J. H., Oh, D. K., Hong, J. T., & Yoon, D. Y. (2016). Promotion of adipogenesis by 15-(S)-hydroxyeicosatetraenoic acid. *Prostaglandins Other Lipid Mediat, 123*, 1-8. doi:10.1016/j.prostaglandins.2016.02.001

Sonkusare, S. K., Dalsgaard, T., Bonev, A. D., & Nelson, M. T. (2016). Inward rectifier potassium (Kir2.1) channels as end-stage boosters of endothelium-dependent vasodilators. *J Physiol, 594*(12), 3271-3285. doi:10.1113/JP271652

Sowers, R. M. a. J. R. (2013). Role of Insulin Resistance in Endothelial Dysfunction. *Rev Endocr Metab Disord., 14*(1).

Steinberg, H. O., Paradisi, G., Hook, G., Crowder, K., Cronin, J., & Baron, A. D. (2000). Free fatty acid elevation impairs insulin-mediated vasodilation and nitric oxide production. *Diabetes, 49*(7), 1231-1238. doi:10.2337/diabetes.49.7.1231

Steinberg, H. O., Tarshoby, M., Monestel, R., Hook, G., Cronin, J., Johnson, A., . . . Baron, A. D. (1997). Elevated circulating free fatty acid levels impair endothelium-dependent vasodilation. *J Clin Invest, 100*(5), 1230-1239. doi:10.1172/JCI119636

Stienstra, R., Duval, C., Keshtkar, S., van der Laak, J., Kersten, S., & Muller, M. (2008). Peroxisome proliferator-activated receptor gamma activation promotes infiltration of alternatively activated macrophages into adipose tissue. *J Biol Chem, 283*(33), 22620-22627. doi:10.1074/jbc.M710314200

Subramaniam, G., Achike, F. I., & Mustafa, M. R. (2009). Characterizing the mechanisms of insulin vasodilatation of normal and streptozotocin-induced diabetic rat aorta. *J Cardiovasc Pharmacol, 53*(4), 333-340. doi:10.1097/FJC.0b013e31819fd4a7

Subramanium, P. (2015). Evaluation of anti-inflammatory and analgesic activities of methanolic leaf extract of the endangered tree species, Hildegardia populifolia (Roxb.) Schott and Endl. *International Journal of Green Pharmacy (IJGP), 9*(2), 125-130.

Suganami, T., Nishida, J., & Ogawa, Y. (2005). A paracrine loop between adipocytes and macrophages aggravates inflammatory changes: role of free fatty acids and tumor necrosis factor alpha. *Arterioscler Thromb Vasc Biol, 25*(10), 2062-2068. doi:10.1161/01.ATV.0000183883.72263.13

Suganami, T., Tanimoto-Koyama, K., Nishida, J., Itoh, M., Yuan, X., Mizuarai, S., . . . Ogawa, Y. (2007). Role of the Toll-like receptor 4/NF-kappaB pathway in saturated fatty acid-induced inflammatory changes in the interaction between adipocytes and macrophages. *Arterioscler Thromb Vasc Biol, 27*(1), 84-91. doi:10.1161/01.ATV.0000251608.09329.9a

Sultana, C., Shen, Y., Rattan, V., & Kalra, V. K. (1996). Lipoxygenase metabolites induced expression of adhesion molecules and transendothelial migration of monocyte-like HL-60 cells is linked to protein kinase C activation. *J Cell Physiol, 167*(3), 477-487. doi:10.1002/(SICI)1097-4652(199606)167:3<477::AID-JCP12>3.0.CO;2-1

Sun, L., Xu, Y.-W., Han, J., Liang, H., Wang, N., & Cheng, Y. (2015). 12/15-Lipoxygenase metabolites of arachidonic acid activate PPARγ: a possible neuroprotective effect in ischemic brain. *Journal of lipid research, 56*(3), 502-514. doi:10.1194/jlr.M053058

Surwit, R. S., Kuhn, C. M., Cochrane, C., McCubbin, J. A., & Feinglos, M. N. (1988). Diet-induced type II diabetes in C57BL/6J mice. *Diabetes, 37*(9), 1163-1167. Retrieved from http://www.ncbi.nlm.nih.gov/pubmed/3044882

Tang, F., Zhang, Q., Nie, Z., Yao, S., & Chen, B. (2009). Sample preparation for analyzing traditional Chinese medicines. *TrAC Trends in Analytical Chemistry, 28*(11), 1253-1262. doi:https://doi.org/10.1016/j.trac.2009.09.004

Taniguchi Ishikawa, E., Gonzalez-Nieto, D., Ghiaur, G., Dunn, S. K., Ficker, A. M., Murali, B., . . . Cancelas, J. A. (2012). Connexin-43 prevents hematopoietic stem cell senescence through transfer of reactive oxygen species to bone marrow stromal cells. *Proceedings of the National Academy of Sciences, 109*(23), 9071-9076. doi:10.1073/pnas.1120358109

Tare, M., Parkington, H. C., Coleman, H. A., Neild, T. O., & Dusting, G. J. (1990). Hyperpolarization and relaxation of arterial smooth muscle caused by nitric oxide derived from the endothelium. *Nature, 346*(6279), 69-71. doi:10.1038/346069a0

Taylor, P. D., McCarthy, A. L., Thomas, C. R., & Poston, L. (1992). Endothelium-dependent relaxation and noradrenaline sensitivity in mesenteric resistance arteries of streptozotocin-induced diabetic rats. *Br J Pharmacol, 107*(2), 393-399. doi:10.1111/j.1476-5381.1992.tb12757.x

Tchkonia, T., Thomou, T., Zhu, Y., Karagiannides, I., Pothoulakis, C., Jensen, M. D., & Kirkland, J. L. (2013). Mechanisms and metabolic implications of regional differences among fat depots. *Cell Metab, 17*(5), 644-656. doi:10.1016/j.cmet.2013.03.008

Tep-areenan, P., Wetchasit, P., & Sawasdee, P. (2015). Extracted Anaxagorea luzonensis A. Gray Restored Impairment of Endothelium-Dependent Vasorelaxation Induced by Homocysteine Thiolactone in Rat Aortic Rings. *J Med Assoc Thai, 98 Suppl 10*, S31-37.

Thakali, K., Galligan, J. J., Fink, G. D., Gariepy, C. E., & Watts, S. W. (2008). Pharmacological endothelin receptor interaction does not occur in veins from ET(B) receptor deficient rats. *Vascul Pharmacol, 49*(1), 6-13. doi:10.1016/j.vph.2008.03.005

Thijssen, M. A., & Mensink, R. P. (2005). Fatty acids and atherosclerotic risk. *Handb Exp Pharmacol*(170), 165-194. doi:10.1007/3-540-27661-0_5

Tokutome, M., Matoba, T., Nakano, Y., Okahara, A., Fujiwara, M., Koga, J. I., . . . Egashira, K. (2019). Peroxisome proliferator-activated receptor-gamma targeting nanomedicine promotes cardiac healing after acute myocardial infarction by skewing monocyte/macrophage polarization in preclinical animal models. *Cardiovasc Res, 115*(2), 419-431. doi:10.1093/cvr/cvy200

van Haperen, R., de Waard, M., van Deel, E., Mees, B., Kutryk, M., van Aken, T., . . . de Crom, R. (2002). Reduction of blood pressure, plasma cholesterol, and atherosclerosis by elevated endothelial nitric oxide. *J Biol Chem, 277*(50), 48803-48807. doi:10.1074/jbc.M209477200

van Herpen, N. A., & Schrauwen-Hinderling, V. B. (2008). Lipid accumulation in non-adipose tissue and lipotoxicity. *Physiol Behav, 94*(2), 231-241. doi:10.1016/j.physbeh.2007.11.049

Vanheel, B., Van de Voorde, J., & Leusen, I. (1994). Contribution of nitric oxide to the endothelium-dependent hyperpolarization in rat aorta. *J Physiol, 475*(2), 277-284. doi:10.1113/jphysiol.1994.sp020068

Vanhoutte, P. M., Boulanger, C. M., & Mombouli, J. V. (1995). Endothelium-derived relaxing factors and converting enzyme inhibition. *Am J Cardiol, 76*(15), 3E-12E. Retrieved from http://www.ncbi.nlm.nih.gov/pubmed/7484885

Vanhoutte, P. M., Shimokawa, H., Feletou, M., & Tang, E. H. (2017). Endothelial dysfunction and vascular disease - a 30th anniversary update. *Acta Physiol (Oxf), 219*(1), 22-96. doi:10.1111/apha.12646

Vasamsetti, S. B., Karnewar, S., Kanugula, A. K., Thatipalli, A. R., Kumar, J. M., & Kotamraju, S. (2015). Metformin inhibits monocyte-to-macrophage differentiation via AMPK-mediated inhibition of STAT3 activation: potential role in atherosclerosis. *Diabetes, 64*(6), 2028-2041. doi:10.2337/db14-1225

Vijgen, G. H., Sparks, L. M., Bouvy, N. D., Schaart, G., Hoeks, J., van Marken Lichtenbelt, W. D., & Schrauwen, P. (2013). Increased oxygen consumption in human adipose

tissue from the "brown adipose tissue" region. *J Clin Endocrinol Metab, 98*(7), E1230-1234. doi:10.1210/jc.2013-1348
Walaas, E., & Walaas, O. (1952). Effect of insulin on rat diaphragm under anaerobic conditions. *J Biol Chem, 195*(1), 367-373. Retrieved from https://www.ncbi.nlm.nih.gov/pubmed/14938388
Waldron, G. J., & Garland, C. J. (1994). Contribution of both nitric oxide and a change in membrane potential to acetylcholine-induced relaxation in the rat small mesenteric artery. *Br J Pharmacol, 112*(3), 831-836.
Walters, J. N., Bickford, J. S., Beachy, D. E., Newsom, K. J., Herlihy, J. D., Peck, M. V., . . . Nick, H. S. (2011). cPLA(2)alpha gene activation by IL-1beta is dependent on an upstream kinase pathway, enzymatic activation and downstream 15-lipoxygenase activity: a positive feedback loop. *Cell Signal, 23*(12), 1944-1951. doi:10.1016/j.cellsig.2011.07.002
Wang, D., & Dubois, R. N. (2010). Eicosanoids and cancer. *Nat Rev Cancer, 10*(3), 181-193. doi:10.1038/nrc2809
Wang, L., Chen, Y., Li, X., Zhang, Y., Gulbins, E., & Zhang, Y. (2016). Enhancement of endothelial permeability by free fatty acid through lysosomal cathepsin B-mediated Nlrp3 inflammasome activation. *Oncotarget, 7*(45), 73229-73241. doi:10.18632/oncotarget.12302
Wang, L., Lim, E. J., Toborek, M., & Hennig, B. (2008). The role of fatty acids and caveolin-1 in tumor necrosis factor alpha-induced endothelial cell activation. *Metabolism, 57*(10), 1328-1339. doi:10.1016/j.metabol.2008.01.036
Wang, Q., Su, Y. Y., Li, Y. Q., Zhang, Y. F., Yang, S., Wang, J. L., & Li, H. Y. (2017). Atorvastatin alleviates renal ischemia-reperfusion injury in rats by promoting M1-M2 transition. *Mol Med Rep, 15*(2), 798-804. doi:10.3892/mmr.2016.6074
Wang, X., Cao, Q., Yu, L., Shi, H., Xue, B., & Shi, H. (2016). Epigenetic regulation of macrophage polarization and inflammation by DNA methylation in obesity. *JCI Insight, 1*(19), e87748. doi:10.1172/jci.insight.87748
Wang, Y., Thatcher, S. E., & Cassis, L. A. (2017). Measuring Blood Pressure Using a Noninvasive Tail Cuff Method in Mice. *Methods Mol Biol, 1614*, 69-73. doi:10.1007/978-1-4939-7030-8_6
Wasserman David, H., Wang Thomas, J., & Brown Nancy, J. (2018). The Vasculature in Prediabetes. *Circ Res, 122*(8), 1135-1150. doi:10.1161/CIRCRESAHA.118.311912
Weber, K. J., Sauer, M., He, L., Tycksen, E., Kalugotla, G., Razani, B., & Schilling, J. D. (2018). PPARgamma Deficiency Suppresses the Release of IL-1beta and IL-1alpha in Macrophages via a Type 1 IFN-Dependent Mechanism. *J Immunol, 201*(7), 2054-2069. doi:10.4049/jimmunol.1800224
Wei, R., Lunn, S. E., Tam, R., Gust, S. L., Classen, B., Kerr, P. M., & Plane, F. (2018). Vasoconstrictor stimulus determines the functional contribution of myoendothelial feedback to mesenteric arterial tone. *J Physiol, 596*(7), 1181-1197. doi:10.1113/jp274797
Wei R., K. P., Plane F. . (2014). Relationship between endothelial KCa channels and NO in rat basilar artery. *Jouranl of Vascular Research, 51*(Suppl 2), 41.

Weisberg, S. P., McCann, D., Desai, M., Rosenbaum, M., Leibel, R. L., & Ferrante, A. W., Jr. (2003). Obesity is associated with macrophage accumulation in adipose tissue. *J Clin Invest, 112*(12), 1796-1808. doi:10.1172/JCI19246

Wen, H., Gris, D., Lei, Y., Jha, S., Zhang, L., Huang, M. T., . . . Ting, J. P. (2011). Fatty acid-induced NLRP3-ASC inflammasome activation interferes with insulin signaling. *Nat Immunol, 12*(5), 408-415. doi:10.1038/ni.2022

Wen, Y., Gu, J., Chakrabarti, S. K., Aylor, K., Marshall, J., Takahashi, Y., . . . Nadler, J. L. (2007). The role of 12/15-lipoxygenase in the expression of interleukin-6 and tumor necrosis factor-alpha in macrophages. *Endocrinology, 148*(3), 1313-1322. doi:10.1210/en.2006-0665

Wheatcroft, S. B., Williams, I. L., Shah, A. M., & Kearney, M. T. (2003). Pathophysiological implications of insulin resistance on vascular endothelial function. *Diabet Med, 20*(4), 255-268. Retrieved from http://www.ncbi.nlm.nih.gov/pubmed/12675638

Williams, C. J., Headd, J. J., Moriarty, N. W., Prisant, M. G., Videau, L. L., Deis, L. N., . . . Richardson, D. C. (2018). MolProbity: More and better reference data for improved all-atom structure validation. *Protein Sci, 27*(1), 293-315. doi:10.1002/pro.3330

Winzell, M. S., & Ahren, B. (2004). The high-fat diet-fed mouse: a model for studying mechanisms and treatment of impaired glucose tolerance and type 2 diabetes. *Diabetes, 53 Suppl 3*, S215-219. Retrieved from http://www.ncbi.nlm.nih.gov/pubmed/15561913

Wu, H. M., Ni, X. X., Xu, Q. Y., Wang, Q., Li, X. Y., & Hua, J. (2020). Regulation of lipid-induced macrophage polarization through modulating peroxisome proliferator-activated receptor-gamma activity affects hepatic lipid metabolism via a Toll-like receptor 4/NF-kappaB signaling pathway. *J Gastroenterol Hepatol*. doi:10.1111/jgh.15025

Xavier F. Figueroa, B. E. I., and Brian R. Duling (2004). Connexins: Gaps in Our Knowledge of Vascular Function. *Physiology (Bethesda)*.

Xing, J. H., Li, R., Gao, Y. Q., Wang, M. Y., Liu, Y. Z., Hong, J., . . . Li, L. (2019). NLRP3 inflammasome mediate palmitate-induced endothelial dysfunction. *Life Sci, 239*, 116882. doi:10.1016/j.lfs.2019.116882

Xu, H., Barnes, G. T., Yang, Q., Tan, G., Yang, D., Chou, C. J., . . . Chen, H. (2003). Chronic inflammation in fat plays a crucial role in the development of obesity-related insulin resistance. *J Clin Invest, 112*(12), 1821-1830. doi:10.1172/JCI19451

Xu, H., Wang, Z., Sun, Z., Ni, Y., & Zheng, L. (2018). GATA4 protects against hyperglycemia-induced endothelial dysfunction by regulating NOX4 transcription. *Mol Med Rep, 17*(1), 1485-1492. doi:10.3892/mmr.2017.8062

Yang, H. M., Kim, H. S., Park, K. W., You, H. J., Jeon, S. I., Youn, S. W., . . . Walsh, K. (2004). Celecoxib, a cyclooxygenase-2 inhibitor, reduces neointimal hyperplasia through inhibition of Akt signaling. *Circulation, 110*(3), 301-308. doi:10.1161/01.CIR.0000135467.43430.16

Yang, X., Wang, X., Liu, D., Yu, L., Xue, B., & Shi, H. (2014). Epigenetic regulation of macrophage polarization by DNA methyltransferase 3b. *Mol Endocrinol, 28*(4), 565-574. doi:10.1210/me.2013-1293

Yang, Z., & Ming, X. F. (2006). Recent advances in understanding endothelial dysfunction in atherosclerosis. *Clin Med Res*, *4*(1), 53-65. Retrieved from http://www.ncbi.nlm.nih.gov/pubmed/16595793
Yasmin, S., Capone, F., Laghezza, A., Piaz, F. D., Loiodice, F., Vijayan, V., . . . Lavecchia, A. (2017). Novel Benzylidene Thiazolidinedione Derivatives as Partial PPARgamma Agonists and their Antidiabetic Effects on Type 2 Diabetes. *Sci Rep, 7*(1), 14453. doi:10.1038/s41598-017-14776-0
Yasmin, S., & Jayaprakash, V. (2017). Thiazolidinediones and PPAR orchestra as antidiabetic agents: From past to present. *Eur J Med Chem, 126*, 879-893. doi:10.1016/j.ejmech.2016.12.020
Yeh, H. I., Lu, C. S., Wu, Y. J., Chen, C. C., Hong, R. C., Ko, Y. S., . . . Tsai, C. H. (2003). Reduced expression of endothelial connexin37 and connexin40 in hyperlipidemic mice: recovery of connexin37 after 7-day simvastatin treatment. *Arterioscler Thromb Vasc Biol, 23*(8), 1391-1397. doi:10.1161/01.ATV.0000083508.21989.15
Young, W., Mahboubi, K., Haider, A., Li, I., & Ferreri, N. R. (2000). Cyclooxygenase-2 is required for tumor necrosis factor-alpha- and angiotensin II-mediated proliferation of vascular smooth muscle cells. *Circ Res, 86*(8), 906-914. doi:10.1161/01.res.86.8.906
Yuan, J., Ge, H., Liu, W., Zhu, H., Chen, Y., Zhang, X., . . . Lin, J. (2017). M2 microglia promotes neurogenesis and oligodendrogenesis from neural stem/progenitor cells via the PPARgamma signaling pathway. *Oncotarget, 8*(12), 19855-19865. doi:10.18632/oncotarget.15774
Yudkin, J. S., Eringa, E., & Stehouwer, C. D. (2005). "Vasocrine" signalling from perivascular fat: a mechanism linking insulin resistance to vascular disease. *Lancet, 365*(9473), 1817-1820. doi:10.1016/S0140-6736(05)66585-3
Zhang, L., Li, Y., Chen, M., Su, X., Yi, D., Lu, P., & Zhu, D. (2014). 15-LO/15-HETE mediated vascular adventitia fibrosis via p38 MAPK-dependent TGF-beta. *J Cell Physiol, 229*(2), 245-257. doi:10.1002/jcp.24443
Zhang, P., Xing, X., Hu, C., Yu, H., Dong, Q., Chang, G., . . . Zhang, D. (2016). 15-Lipoxygenase-1 Is Involved in the Effects of Atorvastatin on Endothelial Dysfunction. *Mediators Inflamm, 2016*, 6769032. doi:10.1155/2016/6769032
Zhang, Q.-W., Lin, L.-G., & Ye, W.-C. (2018). Techniques for extraction and isolation of natural products: a comprehensive review. *Chinese Medicine, 13*(1), 20. doi:10.1186/s13020-018-0177-x
Zhang, T., Shao, B., & Liu, G. A. (2017). Rosuvastatin promotes the differentiation of peripheral blood monocytes into M2 macrophages in patients with atherosclerosis by activating PPAR-gamma. *Eur Rev Med Pharmacol Sci, 21*(19), 4464-4471. Retrieved from https://www.ncbi.nlm.nih.gov/pubmed/29077145
Zhang, W., Huai, Y., Miao, Z., Qian, A., & Wang, Y. (2019). Systems Pharmacology for Investigation of the Mechanisms of Action of Traditional Chinese Medicine in Drug Discovery. *Frontiers in pharmacology, 10*(743). doi:10.3389/fphar.2019.00743
Zhang, Y., Zhan, R. X., Chen, J. Q., Gao, Y., Chen, L., Kong, Y., . . . Huang, Q. R. (2015). Pharmacological activation of PPAR gamma ameliorates vascular endothelial insulin resistance via a non-canonical PPAR gamma-dependent nuclear factor-kappa B trans-repression pathway. *Eur J Pharmacol, 754*, 41-51. doi:10.1016/j.ejphar.2015.02.004

Zhang, Y., Zhang, C., Li, H., & Hou, J. (2017). Down-regulation of vascular PPAR-gamma contributes to endothelial dysfunction in high-fat diet-induced obese mice exposed to chronic intermittent hypoxia. *Biochem Biophys Res Commun, 492*(2), 243-248. doi:10.1016/j.bbrc.2017.08.058

Zhao, L. M., Wang, Y., Yang, Y., Guo, R., Wang, N. P., & Deng, X. L. (2014). Metformin Restores Intermediate-Conductance Calcium-Activated K(+) Channel- and Small-Conductance Calcium-Activated K(+) Channel-Mediated Vasodilatation Impaired by Advanced Glycation End Products in Rat Mesenteric Artery. [Corrected]. *Mol Pharmacol, 86*(5), 580-591. doi:10.1124/mol.114.092874

Zheng, Y., Lim, E. J., Wang, L., Smart, E. J., Toborek, M., & Hennig, B. (2009). Role of caveolin-1 in EGCG-mediated protection against linoleic-acid-induced endothelial cell activation. *J Nutr Biochem, 20*(3), 202-209. doi:10.1016/j.jnutbio.2008.02.004

Zhou, J., Jiang, X., He, S., Jiang, H., Feng, F., Liu, W., . . . Sun, H. (2019). Rational Design of Multitarget-Directed Ligands: Strategies and Emerging Paradigms. *J Med Chem, 62*(20), 8881-8914. doi:10.1021/acs.jmedchem.9b00017